AAMRL-TR-87-011

HUMAN JOINT ARTICULATION AND MOTION-RESISTIVE PROPERTIES

ALI E. ENGIN
SHUENN-MUH CHEN

THE OHIO STATE UNIVERSITY
DEPARTMENT OF ENGINEERING MECHANICS
1314 KINNEAR ROAD
COLUMBUS, OH 43212

JANUARY 1987

FINAL REPORT FOR PERIOD SEPTEMBER 1983 - JULY 1986
RF PROJECT 763802/715689
CONTRACT NO. F33615-83-C-0510

Approved for public release; distribution is unlimited.

HARRY G. ARMSTRONG AEROSPACE MEDICAL RESEARCH LABORATORY
HUMAN SYSTEMS DIVISION
AIR FORCE SYSTEMS COMMAND
WRIGHT-PATTERSON AIR FORCE BASE, OHIO 45433-6573

NOTICES

When US Government drawings, specifications, or other data are used for any purpose other than a definitely related Government procurement operation, the Government thereby incurs no responsibility nor any obligation whatsoever, and the fact that the Government may have formulated, furnished, or in any way supplied the said drawings, specifications, or other data, is not to be regarded by implication or otherwise, as in any manner licensing the holder or any other person or corporation, or conveying any rights or permission to manufacture, use, or sell any patented invention that may in any way be related thereto.

Please do not request copies of this report from the Armstrong Aerospace Medical Research Laboratory. Additional copies may be purchased from:

National Technical Information Service
5285 Port Royal Road
Springfield, Virginia 22161

Federal Government agencies and their contractors registered with Defense Technical Information Center should direct requests for copies of this report to:

Defense Technical Information Center
Cameron Station
Alexandria, Virginia 22314

TECHNICAL REVIEW AND APPROVAL

AAMRL-TR-87-011

The voluntary informed consent of the subjects used in this research was obtained as required by Air Force Regulation 169-3.

This report has been reviewed by the Office of Public Affairs (PA) and is releasable to the National Technical Information Service (NTIS). At NTIS, it will be available to the general public, including foreign nations.

This technical report has been reviewed and is approved for publication.

FOR THE COMMANDER

Henning E. von Gierke

HENNING E. VON GIERKE, Dr Ing
Director
Biodynamics and Bioengineering Division
Armstrong Aerospace Medical Research Laboratory

SECURITY CLASSIFICATION OF THIS PAGE

AD-A182 574

REPORT DOCUMENTATION PAGE

1a. REPORT SECURITY CLASSIFICATION: Unclassified	1b. RESTRICTIVE MARKINGS
2a. SECURITY CLASSIFICATION AUTHORITY	3. DISTRIBUTION/AVAILABILITY OF REPORT: Approved for public release; distribution is unlimited.
2b. DECLASSIFICATION/DOWNGRADING SCHEDULE	
4. PERFORMING ORGANIZATION REPORT NUMBER(S)	5. MONITORING ORGANIZATION REPORT NUMBER(S): AAMRL-TR-87-011
6a. NAME OF PERFORMING ORGANIZATION: The Ohio State University Research Foundation; 6b. OFFICE SYMBOL (If applicable)	7a. NAME OF MONITORING ORGANIZATION: HSD, AFSC AAMRL/BBM
6c. ADDRESS (City, State and ZIP Code): 1314 Kinnear Road Columbus OH 43212	7b. ADDRESS (City, State and ZIP Code): Wright-Patterson AFB OH 45433-6573
8a. NAME OF FUNDING/SPONSORING ORGANIZATION: AAMRL; 8b. OFFICE SYMBOL (If applicable): BBM	9. PROCUREMENT INSTRUMENT IDENTIFICATION NUMBER: F33615-83-C-0510
8c. ADDRESS (City, State and ZIP Code): Wright-Patterson AFB OH 45433-6573	10. SOURCE OF FUNDING NOS.

PROGRAM ELEMENT NO.	PROJECT NO.	TASK NO.	WORK UNIT NO.
62202F	7231	23	04

11. TITLE (Include Security Classification): Human Joint Articulation & Motion-Resistive Properties

12. PERSONAL AUTHOR(S): Engin, Ali E. and Chen, Shuenn-Muh

13a. TYPE OF REPORT	13b. TIME COVERED	14. DATE OF REPORT (Yr., Mo., Day)	15. PAGE COUNT
Final	FROM 13Sep83 TO 13Jul86	April 1987	189

16. SUPPLEMENTARY NOTATION: cont'd from pg 1 → Keywords:)

17. COSATI CODES		
FIELD	GROUP	SUB. GR.

18. SUBJECT TERMS (Continue on reverse if necessary and identify by block number): Biomechanics, elbow complex, joint kinematics, joint sinus, joint restoring forces, joint passive forces, hip complex, shoulder complex, sonic digitizer, statistical data base.

19. ABSTRACT (Continue on reverse if necessary and identify by block number)

Three-dimensional joint kinematics and motion resistive properties were measured for the shoulder, hip and elbow joints on ten male volunteers. A sonic three-dimensional spatial digitizing system was used to track multiple targets on adjacent body segments while each of the segments was moved through a maximum voluntary range of motion and also while it was subsequently forced to maximum voluntarily allowable ranges by an external force applicator. The target data were used to reconstruct the segment kinematics, which were then related to the force required to attain a given joint orientation. The final data are provided in a globographic presentation in which equal force values are depicted as contours on a global surface. The resistive forces are expressed as functions of the orientation angles in spherical harmonic

(Continued on reverse)

20. DISTRIBUTION/AVAILABILITY OF ABSTRACT	21. ABSTRACT SECURITY CLASSIFICATION
UNCLASSIFIED/UNLIMITED ☒ SAME AS RPT. ☐ DTIC USERS ☐	Unclassified

22a. NAME OF RESPONSIBLE INDIVIDUAL	22b. TELEPHONE NUMBER (Include Area Code)	22c. OFFICE SYMBOL
INTS KALEPS	513/255-3608	AAMRL/BBM

DD FORM 1473, 83 APR EDITION OF 1 JAN 73 IS OBSOLETE.

SECURITY CLASSIFICATION OF THIS PAGE

A

Block 19 (Abstract) continued.

expansion form. Statistical analyses have been performed on these data to generate both means and variances for the kinematics and resistive force properties. The data have direct applicability to better understanding of the kinematics of human long bone joints; providing preliminary limits for safe joint ranges of motions and forces; and serving as a data base for analytical and mechanical models of the human body.

Cont'd pg A

PREFACE

The research work described in this report was performed for the Modeling and Analysis Branch of the Armstrong Aerospace Medical Research Laboratory at Wright-Patterson Air Force Base under Contract No. F33615-83-C-0510. The research was monitored by Dr. Ints Kaleps, Chief of the Modeling and Analysis Branch, and it was administered by The Ohio State University Research Foundation under Project No. 715689.

The authors also acknowledge the utilization of some of the hardware and software, developed by one of the former graduate students of the senior author, namely, Dr. Richard D. Peindl, in various aspects of the research work presented in this report.

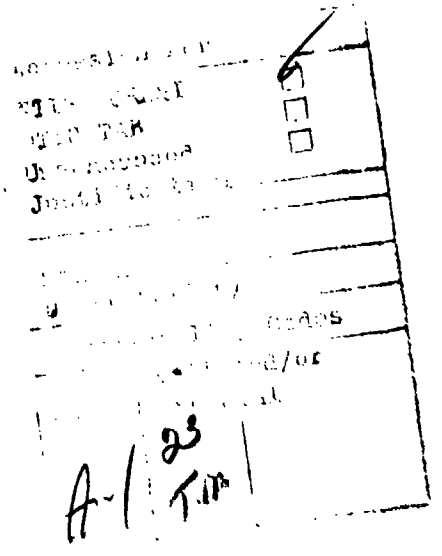

TABLE OF CONTENTS

LIST OF FIGURES

LIST OF FIGURES (continued)

LIST OF FIGURES (continued)

LIST OF FIGURES (continued)

LIST OF FIGURES (continued)

LIST OF TABLES

LIST OF TABLES (continued)

1. INTRODUCTION

1.1 Background

Mathematical modeling and simulation of biomechanical system crash response play an economical and versatile role in the understanding of injury mechanisms. In quantitative gross biodynamic motion studies, cognizant of the high cost of conducting experimental research with human cadavers and/or anthropomorphic dummies, biomechanicians have turned their attention to the utilization of computer-based mathematical models of the total human body since the advent of high speed computer technology. Among these models, the most popular and sophisticated versions are articulated and multisegmented to simulate the total human body as a linked structure made up of rigid bodies. Fig. 1.1 shows a typical three-dimensional model consisting of fifteen segments. Representative three-dimensional models developed in various research centers include six-segment model of UMTRI (formerly called HSRI) (Robbins et al., 1972), twelve-segment models of TTI (Young, 1970) and of UCIN (Huston et al., 1974), and fifteen-segment model of Calspan (Fleck, 1975). With some additional features, the Calspan model is also being used by the U.S. Air Force under the title of Articulated Total Body (ATB) model in aerospace related applications.

In these models, the equations of motion are formulated by using either the Newtonian approach or Lagrange's equations, Euler's rigid body equations, and Lagrange's form of d'Alembert's principle and solved by various methods such as Runge-Kutta or Predictor-Corrector numerical integration scheme. Joints are modeled as either the ball-and-socket type with three degrees of freedom or the hinge type with only one degree of freedom. Resistive force responses beyond the joint stop contour (maximum range of motion) are modeled as one or a combination of the following simple mechanical components: a linear spring, a non-linear spring, a Coulomb friction damper, and a viscous damper. Furthermore, joint properties, i.e., stop contours and resistive force characteristics are estimated and, in some cases, even assumed. A thorough review of both two- and three-dimensional mathematical models simulating biodynamic response of the human body along with the associated experimental validation studies performed, was provided by King and Chou (1976).

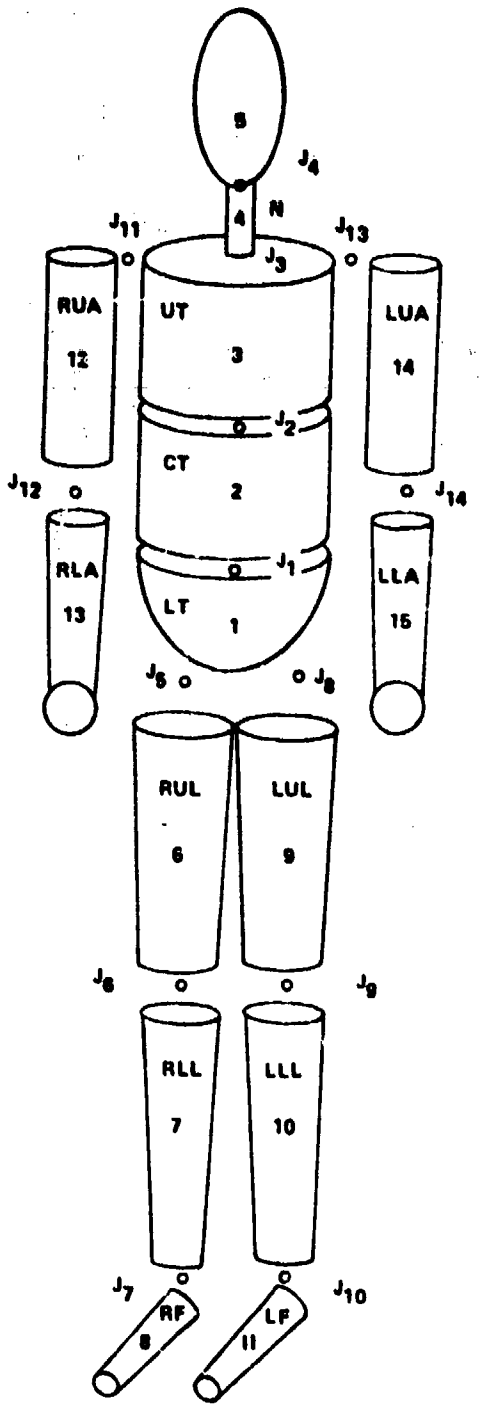

Fig. 1.1 A fifteen-segment model of the total human body

Obviously, the effectiveness of these multisegmented mathematical models in accurately predicting in-vivo biodynamic responses, depends upon the individual segment properties such as center of gravity, moment of inertia, geometry, etc., and more heavily upon the biomechanical joint properties between any two linked segments. In particular, the resistive force properties of the joints play a direct and significant role in the understanding of injury mechanisms as well as in the prediction of injury. Although a number of studies have supplied data for model segment properties (Hatze, 1980; McConville et al., 1980), data on biomechanical joint properties are comparatively sparse (Steindler, 1973) and limited (Engin, 1980; Engin, 1984). Of course, a complete data base for the biomechanical joint properties should undoubtedly include a statistical analysis to account for the intra- and inter-subject variations. The more sound the joint property data base is, the more realistically the multisegmented anthropomorphic dummies and computer-based mathematical total-human-body models can be constructed and formulated.

1.2 Definitions of Joint Sinus and Globographic Representation

Throughout this dissertation, the terms joint sinus and globographic representation (first used by Dempster, 1965) will be repeatedly used in the discussion of joint properties. Since these two terms are not commonly known, let us give their definitions to avoid possible confusion.

Joint Sinus: the maximum range of angular motion permitted by the moving member of a joint while the other member is rigidly fixed. The joint should possess at least two degrees of freedom such that the moving member sweeps out a conical concavity within which the joint structures permit all possible movements.

Globographic representation: a graphical method of representing a joint sinus upon the surface of a globe with meridians and parallels which define a grid pattern of the angular spherical coordinates with respect to a fixed axis system attached to the rigidly fixed member; the center of the globe is positioned at the functional center of the joint.

In this study, we will also use another method to represent a joint sinus, namely, a single-valued functional relationship between the two

spherical angles of the joint sinus. While the globographic representation provides a physically meaningful plot for the joint sinus, the single-valued functional relationship condenses the joint sinus data into a functional expansion form for easy incorporation into the existing three-dimensional multisegmented models of the total human body.

1.3 Scope of Research

The primary goal of this research program is to provide/establish proper biomechanical joint property data/databases pertinent to the human shoulder, hip, and humero-elbow complexes for incorporation into the existing three-dimensional multisegmented models. A recently developed new kinematic data collection methodology by means of sonic emitters and a data analysis technique based on selection of the "most accurate" axis system from an overdeterminate number of sonic emitters on the moving segment (Engin et al., 1984a) were applied and extended. The passive resistive force data were collected by utilizing a three-dimensional multiple-axis force and moment transducer whose calibration and application with sonic emitters was described in a previous work (Engin et al., 1984b). System accuracy of this data acquisition technique was also previously documented by performing:

(1) Error analysis on two types of controlled linear translational motion; a rather high degree of accuracy was attained (Engin et al., 1984a).

(2) Joint sinus simulation tests on a mechanical revoluto-hinge joint; even with high degrees of acoustic blockage, an average of 86.51% of the calculated joint centers fell within 1.46 cm. from the true joint center (Engin and Peindl, 1986).

(3) Forced abduction simulation tests (sweeping-type motions) on the same mechanical revolute-hinge joint; an average of 81.55% of the calculated joint centers fell within less than 0.5 cm. from the true joint center (Engin and Peindl, 1986).

The system accuracy tests described above, demonstrate that the sonic digitizing technique can be employed to perform fairly complicated three-dimensional rigid body kinematic analysis when used in connection with an overdeterminate number of sonic emitters. In this study, the performance of the data acquisition system and efficacy of the associated

data analysis methodology is culminatingly assessed by observing good repeatability of the joint sinus sample means from different runs on ten subjects.

Finally, a statistical data base for the biomechanical joint poperties is established in a systematic way for a special population, namely, the male population of ages 18 thru 32 possessing neither musculoskeletal abnormalities nor any history of trauma in the joints studied herein. Ten subjects were randomly chosen to form the sample with emphasis placed on choosing subjects whose anthropometry approximates the average for the above-defined population. Selected anthropometric measurements of these subjects are given in Appendix A. The sample mean and sample standard deviation as well as the confidence intervals for the population mean and population standard deviation were obtained in a systematic way and were expressed in functional expansion form relative to a locally-defined joint axis system as well as relative to the fixed-body axis system in the form of globographic representation. It is believed that this is the first attempt to establish a statistically meaningful data base for the biomechanical properties of the major human articulating joints for the purposes of incorporation into the multisegmented mathematical models of the total human body.

2. KINEMATICS BY MEANS OF AN OVERDETERMINATE NUMBER OF SONIC EMITTERS

In this chapter, we shall discuss the general approach to studying the three-dimensional kinematics of a typical joint complex, which links two body segments, by means of an overdeterminate number of sonic emitters. The following chapters will apply this methodology to determine the maximum voluntary ranges of motion and passive resistive properties beyond them for the shoulder, hip, and humero-elbow complexes.

2.1 Review of the Sonic Digitizing Technique

Sonic digitizing is the process of converting information on position via sound waves to digital values in a form suitable for data transmission, storage, and processing. The sound waves, which are audible impulses of a specific frequency, are generated by an electrical arc at the tip of the emitter powered by the GP6-3D Sonic Digitizer manufactured by Science Accessories Corporation. "Point" microphone sensors capable of detecting this specific frequency of sonic impulses are used to receive the sound waves. By multiplying the transit time required for a sound wave to reach a microphone sensor with the speed of sound in still air, the sonic digitizer converts the distance from the emitter tip to the "point" microphone sensor (to be referred to as slant range distance) into digital values. These digits are then transmitted to a PDP-11/34 minicomputer for data analysis and storage.

By applying this sonic digitizing principle, a rigid planar rectangular sensor board/assembly with four "point" microphones/sensors (A, B, C, D) arranged at the corners, as shown in Fig. 2.1, was constructed (Engin and Peindl, 1985). The purpose of this set-up is to convert the four slant range distances of a sonic emitter, which defines a point in the 3-D space, into regular Cartesian coordinates suitable for performing kinematic analysis. Note that only three slant range distances are needed for the conversion. The fourth sensor is used for spare purposes. During conversion analysis, the computer program is designed to examine all four slant range distances, select the three smallest, and discard the fourth. In the special case where one of the slant range distances is zero, namely, the sonic emitter is totally blocked from being detected by one of the four microphone sensors, the zero reading is disregarded.

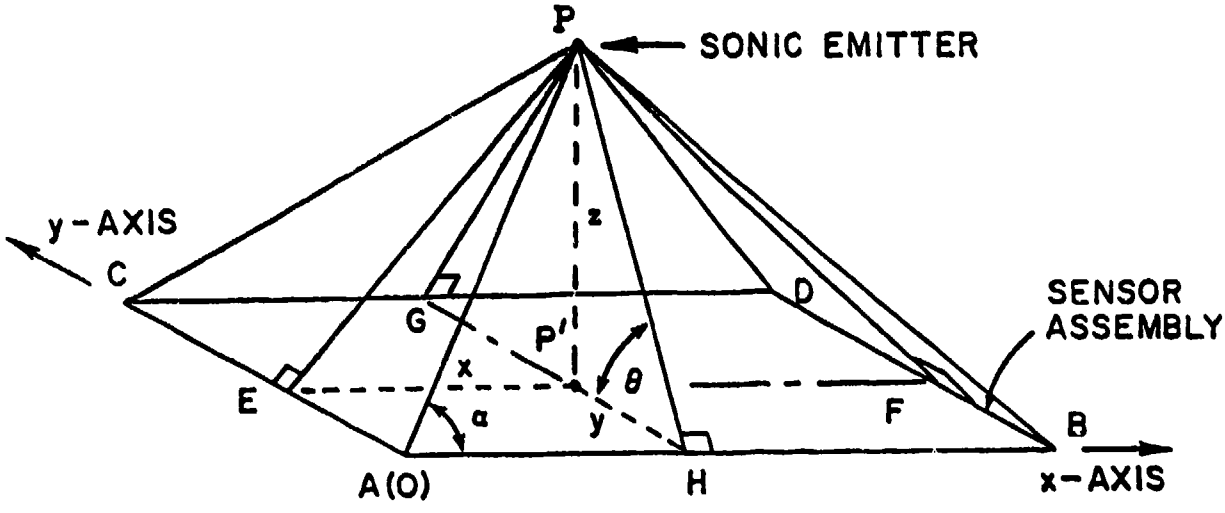

Fig. 2.1 Quantities used to convert slant range distances (PA, PB, PC, PD) to Cartesian coordinates (x, y, z)

With respect to the selected 3-D coordinate system (to be referred to as the sensor assembly axis system) as shown in Fig. 2.1, slant range distances PA, PB, and PC will be used to illustrate the conversion procedure. Applying the law of cosines to triangle APB, we have

$$(PB)^2 = (PA)^2 + (AB)^2 - 2(PA)(AB)\cos\alpha \qquad (2.1.1)$$

where AB = 165 cm. is a calibrated dimension for the sensor assembly. We also note that

$$x = AH = (PA)\cos\alpha \qquad (2.1.2)$$

Therefore,

$$(PB)^2 = (PA)^2 + (AB)^2 - 2(AB)x \qquad (2.1.3)$$

or,

$$x = [(PA)^2 + (AB)^2 - (PB)^2]/2(AB) \qquad (2.1.4)$$

Similarly, by applying the law of cosines to triangle APC, one obtains

$$y = AE = [(PA)^2 + (AC)^2 - (PC)^2]/2(AC) \qquad (2.1.5)$$

where AC = 110 cm. is also a calibrated dimension for the sensor assembly. Finally, one obtains the z coordinate by

$$z = PP' = [(PA)^2 - (x^2 + y^2)]^{1/2} \qquad (2.1.6)$$

In like manner, similar equations for x, y, and z can be written for any combination of three slant range distances.

2.2 Moving Rigid-Body Kinematics and Initialization of a Baseline Data Set

Consider a typical joint complex connecting two body segments. In order to facilitate the relative motion studies between the two body segments, one of them is first rigidly fixed. To each body segment an axis system can then be defined and affixed by mounted sonic emitters. The six degrees of freedom permitted by a general joint complex are completely determined if one point (e.g., the origin of the moving body axis system) on the moving body and the transformation (direction cosine) matrix of the moving-body axis system with respect to the fixed-body axis system are known. The coordinates of this point determine the location (three translational degrees of freedom) and the transformation matrix determines the orientation (three rotational degrees of freedom) of the moving body segment. The orientation can be described in various ways, for example, (1) a set of three successive rotations about the three axes of the fixed-body axis system, (2) three Euler's angles, and (3) a rotation about an arbitrary axis in space. A detailed derivation of the transformation matrices resulting from the above three ways can be found in Suh and Radcliffe (1978).

To define an axis system affixed to a body segment, three noncolinear points (emitters) on or extended from the body segment are needed. Normally, it is desirable to select one of the axes, e.g., the z axis to coincide with the longitudinal axis of the moving body segment and the origin to be a certain point on this axis. We shall refer to

this type of axis systems as the longitudinal (or long-bone) axis systems. However, since the sonic digitizing technique is applied in this study, total and partial acoustic blockage may occur to produce zero and inaccurate readings for one, or two, or even all three sonic emitters used. Note that in defining the fixed-body axis system, this difficulty can always be avoided by adjusting the sensor assembly to an optimal "view" of the three emitters since these emitters are not moving. In the case of the moving body segment, it is desirable to continuously monitor the moving body axis system while performing joint property experiments. As a result, total or partial acoustic blockage becomes inevitable for some "bad" positions where sound waves must travel around the emitters' bases or the moving body segment itself. Therefore, it is necessary to collect redundant data so that zero readings from individual emitters would not affect kinematic analysis. Obviously, we would select the "most accurate" three emitters in cases where more than three emitters produce non-zero readings.

From experimental experience, six emitters are most suitable for the redundancy process. Seven or more emitters would dramatically increase computing time without noticeable improvements in accuracy, while four or five emitters do not provide a sufficient spare. Note that if six emitters are used, a total of 20 ($C(6, 3) = \frac{6!}{3!3!}$) different axis systems can be constructed; if seven emitters are used, a total of 35 ($C(7,3) = \frac{7!}{4!3!}$) different axis systems can be constructed.

It is advantageous to arrange the six sonic emitters circumferentially and more or less equally-spaced around the moving body segment. (In reality, the six emitters are first put on an orthotic cuff which, in turn, is strapped circumferentially to the moving body segment). The advantage is that, by doing so, we have reduced the number of "bad" positions to a minimum and also provided the moving body segment with the largest amount of freedom to reach all allowable ranges of motion. However, such an arrangement of the six emitters makes them unsuitable for direct construction of the longitudinal axis system as normally desired. One way of resolving this inconvenience is to establish the relationship (to be explained later) between the six emitters and the longitudinal axis system directly constructed by three properly positioned emitters before performing kinematic data collection

and analysis. Since this relationship is invariant, i.e., it does not depend upon the orientation/location of the moving body segment or the sensor assembly, its accuracy can be checked against pre-calibrated inter-emitter distances to within 1% of error by adjusting the relative orientation and location between the moving body segment and the sensor assembly to an optimal "view". This procedure is called initialization. The initialized data set, which is reliably accurate, also provides a baseline for the selection of the "most accurate" longitudinal axis systems (will be explained in detail in the next section) for the continuously collected kinematic data whose accuracies are uncontrollable due to partial and/or total acoustic blockage and motion during kinematic data collection. This baseline contains the interrelationships among the six sonic emitters on the moving body. The following explains how the interrelationships among these nine emitters (three for defining the longitudinal axis system, six on the moving body segment) are initialized.

First, the coordinates of the nine emitters are calculated in terms of the sensor assembly axis system. Next, a total of 20 axis systems is defined by calculating the direction cosine matrices A_{is} ($1 \leq i \leq 20$) with respect to the sensor assembly axis system from all possible combinations of any three out of the six moving-body emitters. Note that these axis systems can always be obtained since all the six emitters are arranged in such a way that no three of them are colinear, i.e., three mutually orthogonal unit vectors can always be found. The longitudinal axis system is similarly defined by calculating its direction cosine matrix, $B_{\ell s}$, with respect to the sensor assembly axis system. Next, the transformation (direction cosine) matrix describing the ith axis system relative to the jth axis system ($1 \leq i < j \leq 20$) is then calculated by $A_{ij} = A_{is} A_{sj} = A_{is} A_{js}^{-1} = A_{is} A_{js}^{T}$, where A_{is} and A_{js} are the transformation matrices describing the ith and jth axis systems relative to the sensor assembly axis system, respectively. Note that these 190 ($C(20,2) = \frac{20!}{18!\,2!}$) transformation matrices relating each of the 20 axis systems relative to every other system are an intrinsic geometric property of the six moving-body emitters and are independent of the sensor assembly axis system. Second, the distances between the origins of any two of the 20 axis systems, D_{ij} ($1 \leq i < j \leq 20$) are initialized. Obviously, these 190 scalar quantities are also intrinsic and independent

of the sensor assembly axis system. Third, the coordinates (position vectors) of the origin of the longitudinal axis system with respect to the 20 moving-body axis systems are also initialized by $\vec{J}_i = A_{is} \vec{J}_s$ $(1 \leq i \leq 20)$, where $\vec{J}_s$ is the position vector from the origin of the ith axis system to the origin of the longitudinal axis system expressed in terms of the sensor assembly axis system. Note that these 20 vectors are also intrinsic and independent of the sensor assembly axis system during the initialization process. Last, the transformation matrices of the longitudinal axis system with respect to each of the 20 moving-body axis systems are initialized by $B_{li} = B_{ls} A_{si} = B_{ls} A_{is}^T$ $(1 \leq i \leq 20)$. Note that these 20 matrices are also independent of the sensor assembly axis system. All the initialized data are stored in the computer and retrieved for the selection process and determination of the longitudinal axis system once the "most accurate" moving-body axis system is selected.

2.3 Selection of the "Most Accurate" Axis System on the Moving Body

The initialized data set discussed in the previous section forms a baseline for the selection criterion since these data are obtained in an optimal view of the sensor assembly and their accuracy can be well controlled. However, for a typical kinematic test, with the moving body segment in motion, the accuracy is uncontrollable. Since the initialized data set is independent of the sensor assembly axis system, it can be used for any position and orientation of the moving body segment in selecting the "most accurate" moving-body axis system for determination of the desired longitudinal axis system which conveniently describes the complete kinematics of the moving body segment. The sequential firing rate of the six moving-body emitters is set at 7 records per second, and the motion speed of the moving body segment is maintained at approximately 6° arc/sec. One record is defined as a complete sequential firing of all the six moving-body emitters from which one set of kinematic data with respect to the fixed body axis system is determined through coordinate transformation and vector analyses.

The choice of the "most accurate" axis system on the moving body segment during a kinematic test is made on a record by record basis. For each record of the kinematic data, the coordinates of the six moving-body emitters (assuming that all of them give good readings, i.e., none of

them is totally blocked from sensor view) are first used to obtain the intrinsic matrix interrelationships between any two of the 20 axis systems as described in the initialization process. If there were no errors in the kinematic measurements, and the orthotic cuff remains rigid, then we should obtain the equalities:

$$(A_{ij})_{kinematic} = (A_{ij})_{initial} \text{ , or}$$

$$(A_{ij})_{kinematic} (A_{ij}^T)_{initial} = I \qquad (1 \leq i < j \leq 20) \qquad (2.3.1)$$

and

$$(D_{ij})_{kinematic} = (D_{ij})_{initial} \text{ , or}$$

$$(D_{ij})_{kinematic} - (D_{ij})_{initial} = 0 \qquad (1 \leq i < j \leq 20) \qquad (2.3.2)$$

where I is the 3 x 3 identity matrix. This, however, is not the case for a typical kinematic test due to such factors as motion during data collection, changes in the emitter's orientations with respect to the sensor assembly, or the partial acoustic blockage of individual emitters by the fixed body or the moving body segment itself. Therefore, we obtain the following inequalities:

$$(A_{ij})_{kinematic} (A_{ij}^T)_{initial} = G_{ij} \neq I \qquad (1 \leq i < j \leq 20) \qquad (2.3.3)$$

and

$$(D_{ij})_{kinematic} - (D_{ij})_{initial} = \delta_{ij} \neq 0 \qquad (1 \leq i < j \leq 20) \qquad (2.3.4)$$

where G_{ij} is a general matrix with off-diagonal terms, and δ_{ij} is an apparent dislocation (translational shift) between the origins of the ith and jth axis systems. The general matrix can be considered as a rotation matrix describing an apparent rotational shift between the ith and the jth axis systems from their initialized interrelationship. It should be pointed out that both the dislocation and rotational shift are a relative measure of the errors involved. These errors are not correctable, i.e., we cannot pinpoint the absolute errors. Nevertheless, we have at least a

relative sense of how much they are so that we can always select the "most accurate" data set. Therefore, a good relative indication of the magnitude of the rotational shift is to consider the amount of rotation, γ_{ij}, introduced by G_{ij} about an axis. To calculate γ_{ij}, we notice that the rotation matrix describing a rotation of amount α about an axis whose orientation is specified by the direction cosines of a unit vector $\vec{u} = [u_x, u_y, u_z]$ is (Suh and Radcliffe, 1978)

$$R = \begin{bmatrix} u_x^2(1-\cos\alpha)+\cos\alpha & u_xu_y(1-\cos\alpha)-u_z\sin\alpha & u_xu_z(1-\cos\alpha)+u_y\sin\alpha \\ u_xu_y(1-\cos\alpha)+u_z\sin\alpha & u_y^2(1-\cos\alpha)+\cos\alpha & u_yu_z(1-\cos\alpha)-u_x\sin\alpha \\ u_xu_z(1-\cos\alpha)-u_y\sin\alpha & u_yu_z(1-\cos\alpha)+u_x\sin\alpha & u_z^2(1-\cos\alpha)+\cos\alpha \end{bmatrix} \quad (2.3.5)$$

Summing up the diagonal terms of the matrix R and noting that $u_x^2 + u_y^2 + u_z^2 = 1$, we obtain

$$\alpha = \cos^{-1}[\tfrac{1}{2}(\mathrm{tr}R - 1)] \quad (2.3.6)$$

where trR is the trace of R, i.e., the sum of all the three diagonal terms of the matrix R. Applying this equation to the general matrix G_{ij}, we find

$$\gamma_{ij} = \cos^{-1}\left[\tfrac{1}{2}(\mathrm{tr}\, G_{ij} - 1)\right] = \gamma_{ji} \quad (2.3.7)$$

Since the orthotic cuff is made of rather rigid steel and during the kinematic test there is essentially no force applied on it, we attribute both the translational and rotational shifts to motion during the emitter firing sequence and/or measurement inaccuracies due to partial acoustic blockage.

For each kinematic data record, if one assumes the jth axis system to be accurate, then the ith axis system has obviously introduced both errors, i.e., δ_{ij} and γ_{ij}. If we then calculate, for each axis system, the root mean square error, ε_i, by assuming all the other 19 axis systems are accurate, as

$$\varepsilon_i = \left\{ \sum_{\substack{j=1 \\ j\neq i}}^{20} \left[(\delta_{ij})^2 + (\gamma_{ij})^2 \right] \right\}^{1/2} \qquad (1 \leq i \leq 20) \quad (2.3.8)$$

(Note that, in this equation, γ_{ij} should be thought of as the arc length obtained when γ_{ij} is multiplied by a unit length), the axis system which exhibits the smallest c_i has obviously undergone the least apparent shift (rotational and translational) with respect to all the other axis systems as initialized. From a statistical point of view, this axis system has the highest probability of being the most accurate as compared to the initialized geometry.

For each kinematic data record, the "most accurate" axis system on the moving body segment is then used to calculate the origin and the direction cosine matrix of the longitudinal axis system via the initialized data, i.e., $\vec{J}_i$ and $B_{\ell i}$. Or, stating it in another manner, we are monitoring the desired longitudinal axis system via a versatile medium, i.e., the six emitters on the moving body segment.

3. BIOMECHANICAL PROPERTIES OF THE HUMAN SHOULDER COMPLEX

3.1 Introduction

In multisegmented mathematical models of the total human body, the most complicated and least successfully modeled joint has been the shoulder complex mainly due to the lack of an appropriate biomechanical data base as well as the anatomical complexity of the shoulder region. The term "shoulder complex" refers to the combination of the shoulder joint (the glenohumeral joint) and the shoulder girdle which includes the clavicle and scapula and their articulations. Therefore, in discussing the joint sinus of the shoulder complex, it is more appropriate to use the term "shoulder complex sinus" to designate the range of extreme allowable motion of the humerus with respect to torso. It is important to make this distinction since it is possible to define joint sinuses for various skeletal components of the shoulder complex. An anatomical description and a brief account of studies on the shoulder complex was provided by Engin (1980) and more details can be found in standard text books (Steindler, 1973; Gray's Anatomy, 1973; Norkin and Levangie, 1983); thus they will not be repeated here.

3.2 Determination of the Maximum Voluntary Shoulder Complex Sinus

The basic components of the data acquisition system used in the study are the sonic digitizer, digitizer sensor assembly with four microphones, torso restraint system, and the orthotic arm cuff with sonic emitters as shown in Fig. 3.1. The emitter positioning for the six arm cuff emitters and the three longitudinal-axis-system emitters was provided by Engin et al. (1984a).

The procedure for determination of the shoulder complex sinus involves the following basic steps: (1) immobilizing the body segment (torso) to be treated as the fixed body and defining the fixed body axis system as shown in Fig. 3.2(a), (2) having the subject move the upper arm along the maximal voluntary range of motion (stop contour) and monitor, with respect to the fixed body axis system, the 3-D coordinates of a distal point on the moving body segment; this point on the elbow joint is selected as being on the humeral longitudinal axis at the level of the

Fig. 3.1 Subject in the torso restraint system and the arm cuff with six sonic emitters

humeral condylar maximal width, (3) fitting the 3-D coordinates to a sphere using a least-squares technique, thus establishing a center for the best-fitted sphere and an idealized link length (radius of the sphere), (4) fitting a plane to the same 3-D coordinates using a least-squares technique; the normal to this plane (specified by the spherical coordinates (ϕ_n, θ_n) as shown in Fig. 3.2(b)) establishes the pole of a local joint axis system (z_{jt}-axis) about which the shoulder complex sinus, designated by the spherical coordinates (ϕ, θ) of the vector connecting the center of the sphere with the distal elbow point, can be expressed as a single-valued functional relationship, i.e., $\theta = \theta(\phi)$.

Since the origin of the fixed body axis system is inaccessible, a relative axis locator device (RALD) (Engin et al., 1984) is used to

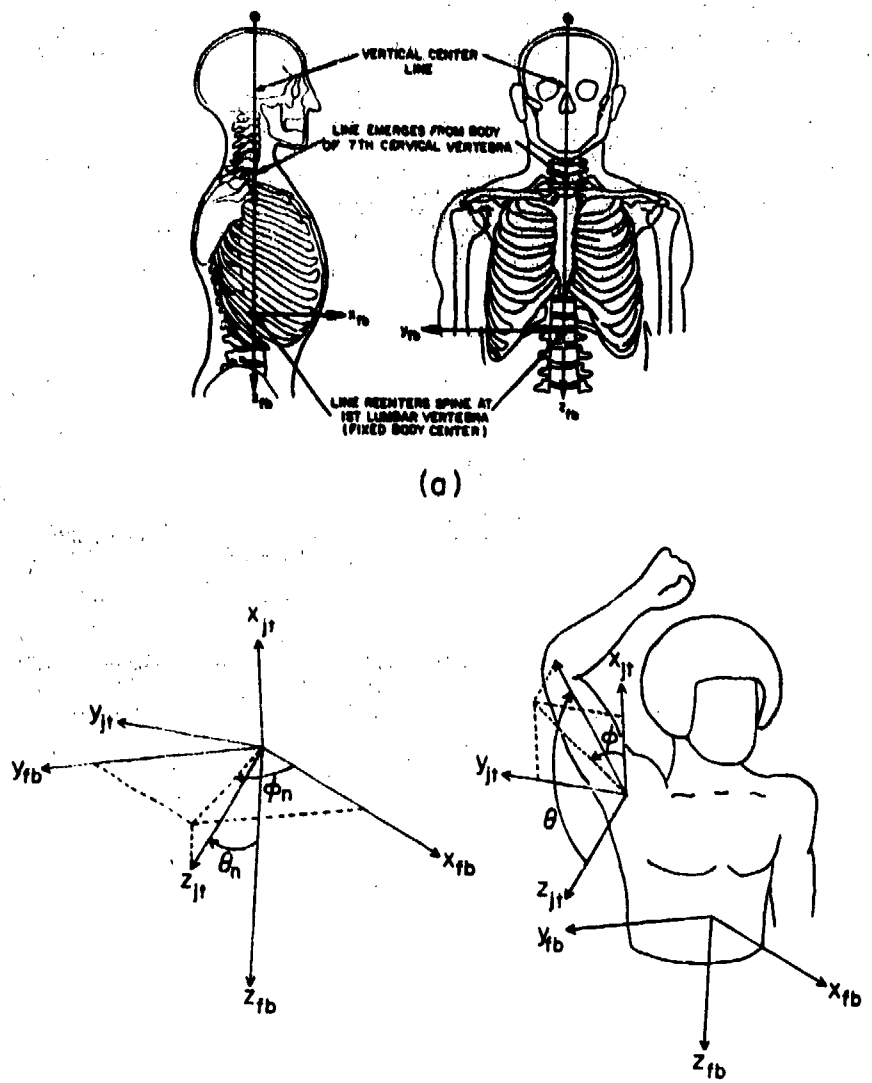

Fig. 3.2 (a) Selected origin and axis system (x_{fb}, y_{fb}, z_{fb}) of the fixed segment (torso).

(b) Relative orientation of the fixed body (x_{fb}, y_{fb}, z_{fb}) and locally-defined joint (x_{jt}, y_{jt}, z_{jt}) axis systems.

locate the origin and define the transformation matrix of the fixed body axis system in terms of the microphone/sensor assembly axis system. The accuracy of these data can always be maintained within 1% of error against pre-calibrated dimensions by adjusting the orientation and location of the microphone/sensor assembly. Of course, this adjustment should also take into account the orientation and/or position of the arm cuff in order to obtain the best kinematic data even though an overdeterminate number of sonic emitters and a "most accurate" selection criterion are used.

Table 3.1 lists the centers and radii of the best-fitted spheres and (ϕ_n, θ_n) as well as their sample means and sample standard deviations for all ten subjects. The mean values for (ϕ_n, θ_n) shall be designated as (ϕ_m, θ_m) and the corresponding joint axis system shall be referred to as the mean joint axis system.

Before the test, each subject was instructed to move his upper arm along its maximum range of motion boundary in a counterclockwise motion as viewed from the sensor assembly. He was also instructed to displace the arm distally along its longitudinal axis as far as possible at all times while circumscribing the joint sinus. Preferred rotation of the upper arm about its longitudinal axis was left up to the discretion of subjects in obtaining the maximal contour. Several sweeps of this type were performed before data were collected so that the subjects could experiment with obtaining the largest possible range of motion. In order to help maintain a constant rate of motion, a large clock with an easily visible second hand was placed in front of the subject. The subject was instructed to imagine his humerus as the second hand, and to synchronize his joint sinus circumscription with the clock's 60 second sweep. In this manner, three test runs (sweeps) were collected for each subject.

To consolidate the enormous volume of experimental raw data into a form readily usable by the multisegmented total-human-body models currently in use, functional expansions for the shoulder complex sinuses are desirable. This is also the reason why we want to represent the shoulder complex sinus in a single-valued functional relationship, i.e., $\theta = \theta(\phi)$, with respect to the locally-defined joint axis system. It will be shown in Section 3.4 that the functional expansions also greatly facilitate the statistical analysis.

Table 3.1 Centers and radii of the best-fitted spheres and (ϕ_n, θ_n) for all ten subjects

SUBJECT NO.	CENTER (cm) x_{fb}	y_{fb}	z_{fb}	RADIUS (cm)	ϕ_n (deg.)	θ_n (deg.)
1	8.85	14.92	-26.97	36.75	57.37	72.24
2	3.30	10.01	-25.25	35.37	56.52	77.32
3	5.45	15.50	-25.76	34.19	55.51	81.61
4	9.67	16.75	-33.67	36.28	59.72	83.20
5	2.53	13.78	-24.77	32.09	58.82	79.53
6	3.78	15.48	-25.39	32.83	62.58	77.86
7	7.10	16.51	-24.68	32.18	59.43	78.87
8	4.51	12.59	-24.94	35.25	57.12	77.90
9	6.88	17.27	-24.62	31.77	60.98	84.31
10	1.88	16.25	-25.85	33.96	64.87	77.93
Sample Mean	5.40	14.91	-26.19	34.07	59.29	79.08
Sample St. Dev.	2.66	2.23	2.72	1.81	2.90	3.42

The following trigonometric polynomial, with ten basis functions, initially proposed by Herron (1974):

$$\theta(\phi) = \sum_{n=1}^{5} \cos^{n-1}\phi\,(C_{2n-1} + C_{2n}\sin\phi) \qquad (3.2.1)$$

will be used for the functional expansions by the method of least-squares. Ten was chosen for the number of basis functions (or coefficients) and determined as the smallest number for which the criterion $e \leq 0.001e_o$ is satisfied, where e is the square sum of curve-fitting errors, 0.001 is the relative tolerance chosen, and e_o is the square sum of the experimental data (θ) values. A detailed discussion of the above criterion can be found in Berztiss (1964). Fig. 3.3 shows a sense of how "well" the expansion of Eq. (3.2.1) fits the raw data for any of the three sinuses taken from the sample.

3.3 Passive Resistive Properties Beyond the Shoulder Complex Sinus

In general, the passive resistive properties in an articulating joint may depend on at least three variables which define the orientation of one segment of the joint with respect to the adjacent one. For example, the three Euler angles, namely, ϕ, θ, and ψ can be used to define the orientation of the upper arm with respect to torso. If we exclude the rotational influence of the upper arm along its long-bone axis with respect to the other two directions, then, the passive resistive properties can be expressed as $f = f(\phi, \theta)$ where ϕ and θ are the spherical coordinates with respect to the local joint axis system defined in Section 3.2.

The basic components of the data acquisition system are shown in Fig. 3.4. The major component of the system is the sonic digitizer and the digitizer sensor assembly. The subject restraint/positioning system was designed so that the subject's torso can be positioned in a wide range of orientations. The force applicator is a hand-maneuvered device which is constrained to motion in a level, horizontal plane by a track-mounted trolley system located overhead. It utilizes a six-component transducer which measures forces and moments in three orthogonal directions. The orientation of the upper arm with respect to torso is monitored by means of the arm cuff with six sonic emitters as was used

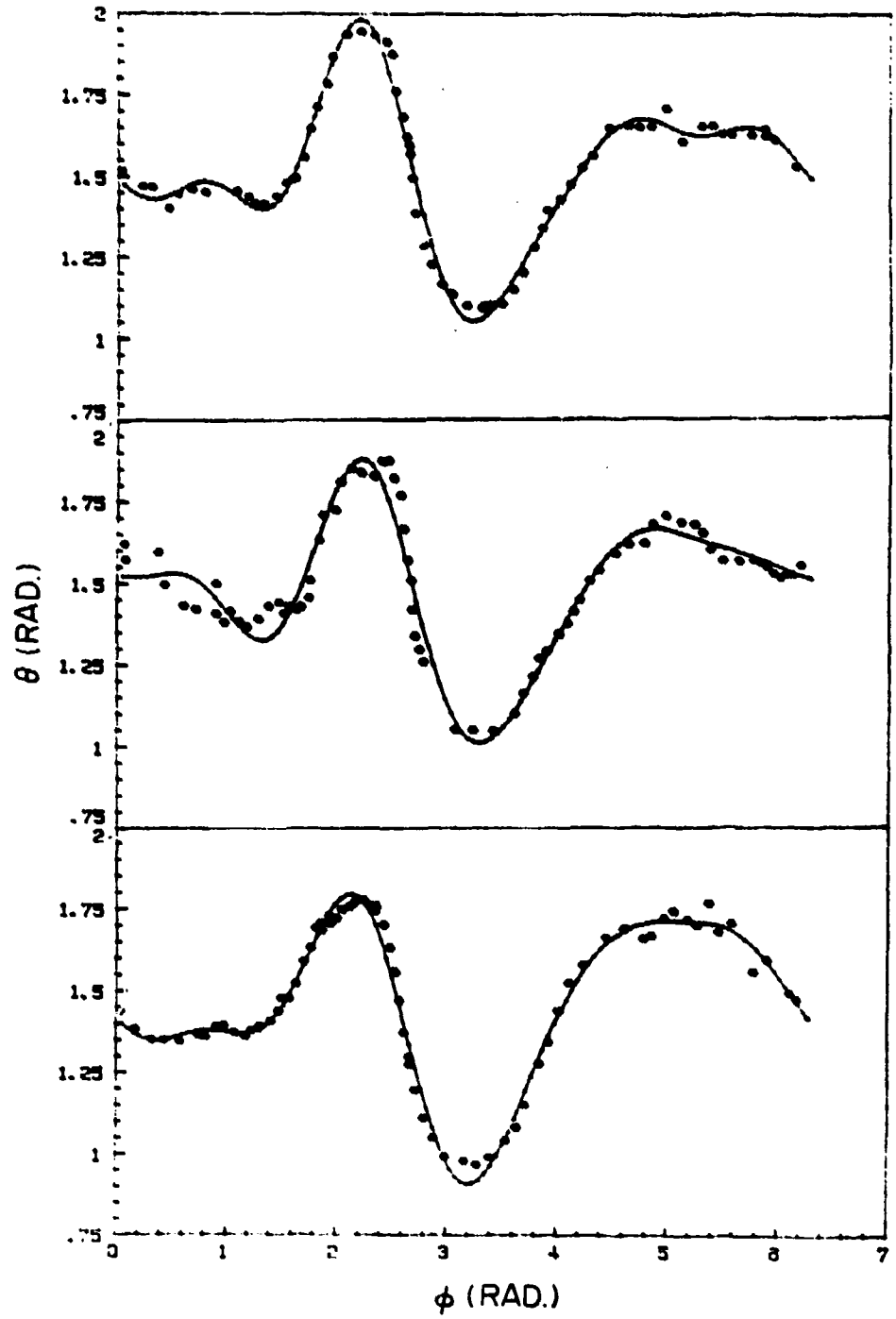

Fig. 3.3 Curve-fitted raw data for joint sinuses of three subjects.

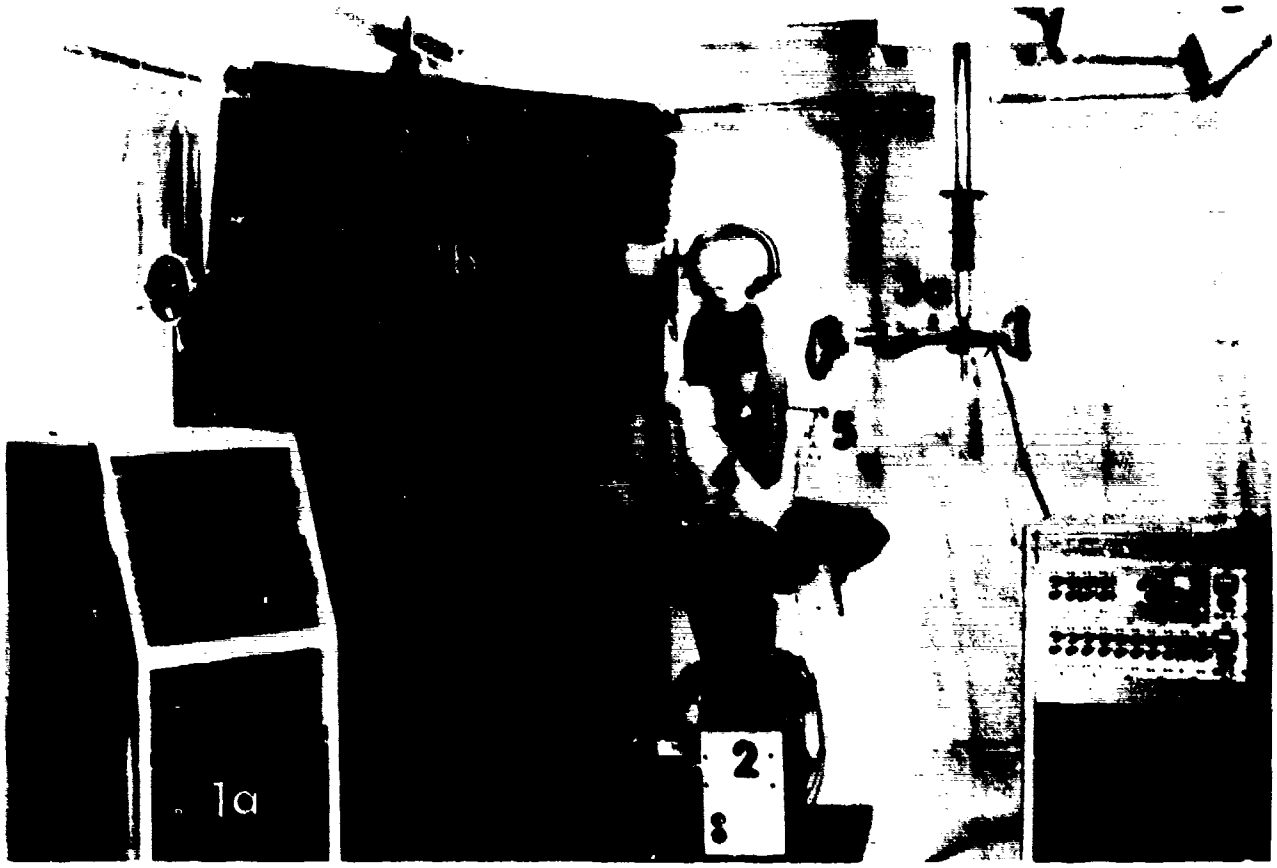

Fig. 3.4 Various components of the data acquisition system. 1) Sonic Digitizer, 2) Subject Restraint/Positioning System, 3a) Force Applicator, 3b) Strain Gage Signal Conditioner/Amplifier, 4) Arm Cuff with Orthotic Shell, 5) Fixed Body Axis Locator Device.

for the shoulder complex sinus tests. This data acquisition system thus enables one to perform a series of tests in which the upper arm is forced c tward in the direction of increasing θ for a constant-ϕ value in the local joint axis system defined by (ϕ_n, θ_n) (refer to Fig. 3.2). Furthermore, forces and moments at the joint due to gravitational loading can be held relatively constant and can be factored out by setting all the bridge ci·cuits of the force-moment transducer to zero at the start of each forced sweep.

The subject is first rotated by an angle $-(90^\circ - \phi_n)$ about the positioning system yaw axis, and then rotated $-(90^\circ - \theta_n)$ about the roll axis. If the subject then extends his upper arm in an orientation

parallel to the pitch axis of the positioning system, his humeral longitudinal axis will be at (ϕ_n, θ_n) with respect to the torso fixed body axis system. The force applicator is then positioned vertically at the same level as the subject's upper arm, and the front of the force transducer is strapped to the subject's arm near the elbow joint. The subject is then asked to move his arm to its maximal position in the constrained plane of motion of the force applicator. The arm is "backed-off" from this position, and this then is the starting location of the forced sweep. The subject's upper arm is then abducted or adducted in a quasi-static manner until the subject experiences discomfort or the upper arm can no longer be displaced (i.e., adduction into the torso occurs). The forced angular velocity, which is the same as the circumscription speed in obtaining the shoulder complex sinus described in Section 3.2, is set at an average of 6° of arc/sec for these tests. During the entire course of each test, the subject is instructed to let his arm hang limply and not to actively (muscularly) resist the motion of the test. The bridge circuits of the force-moment transducer are all set to zero at the start of each test, so that the recorded values during the sweep are departures from this "neutral" force orientation, or stating it in a different manner, they are the passive resistive force values.

With respect to the joint axis system, these forced sweeps take place in a direction of increasing θ, and at an approximately constant-ϕ value. By then rotating the positioning system about its pitch axis, a series of constant-ϕ sweeps are obtained. Each time, the force applicator is vertically positioned at the proper level with the humeral longitudinal axis in a level horizontal plane. In this way the tests are performed as four sub-series with each sub-series discernible by its own experimental set-up configuration. The groupings consist of constant-ϕ sweeps in: 1) the upper-rear quadrant ($0° < \phi < 90°$), 2) the lower-rear quadrant ($90° < \phi < 180°$), 3) lower-front quadrant ($180° < \phi < 270°$) and 4) the upper-front quadrant ($270° < \phi < 360°$).

The data obtained according to the procedure outlined above were analyzed as follows. First, the force and moment vectors obtained from the force applicator data were used to calculate a total moment vector with respect to the instantaneous joint center which is chosen to be the glenohumeral joint center location. Next, a moment arm vector was calculated from the center of the best-fitted sphere (described in

Section 3.2) to the point of force application. Next, the intersection of this vector with a sphere of radius equal to one meter was selected as a "normalized" point of force application. The total moment vector was then resolved into components along the moment arm and perpendicular to the moment arm vector. The component along the position vector (moment arm vector) was then discarded, since it does not serve to restore the moving segment to an orientation within the voluntary shoulder complex sinus. From the remaining moment component and the normalized position vector the resistive force vector was then calculated. Since the moment arm is normalized to one meter, the magnitude of the resistive force vector is the same as that of the resistive moment vector. We shall refer to this magnitude as the passive resistive force (moment) property. Note that this force vector is always tangent to the surface of the selected normal sphere. Fig. 3.5 depicts the vectors and coordinates specified in the analysis.

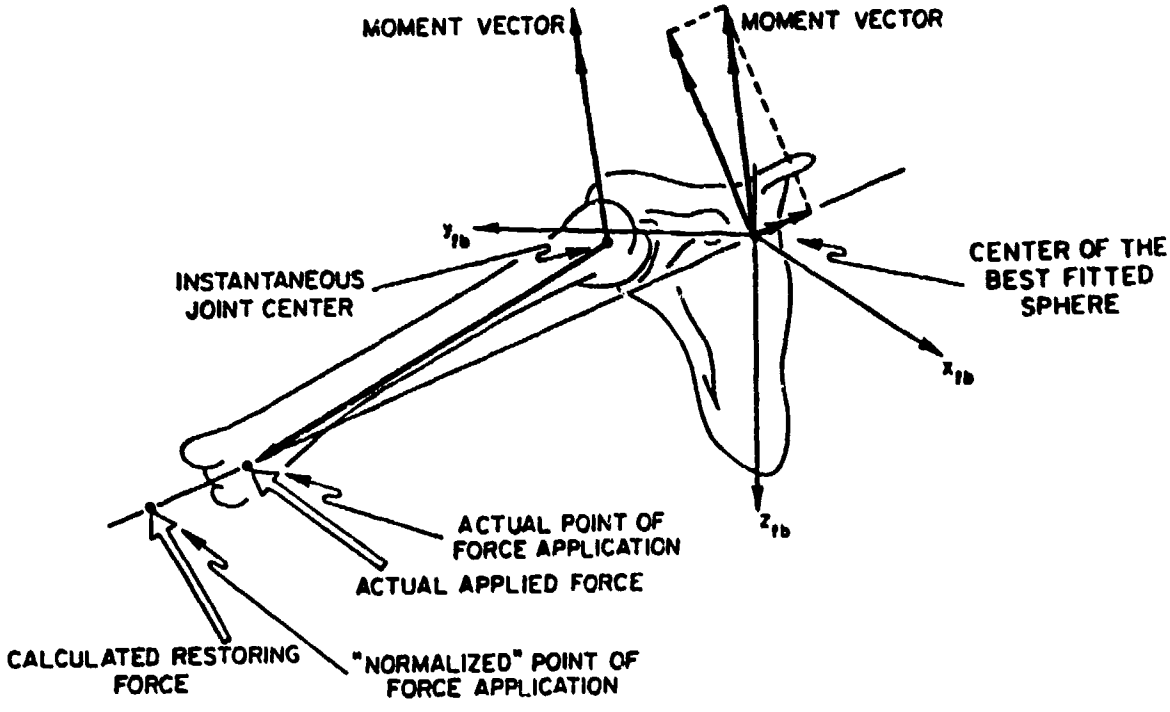

Fig. 3.5 Illustration of the vector quantities used in the calculation of resistive force values.

Finally, to consolidate the vast amount of passive resistive force (moment) data and to facilitate the statistical analysis, the functional expansion $f(\phi, \theta)$ must be established. A variety of basis functions has been investigated by utilizing the GLM (General Linear Model) program of the SAS (Statistical Analysis System) computer package (SAS User's Guide, 1982) of the Instruction and Research Computer Center at The Ohio State University. It was found that the functional expansion

$$\begin{aligned} f(\phi, \theta) = (C_1 &+ C_2\cos\phi + C_3\sin\phi)\theta + (C_4\cos^2\phi + C_5\cos\phi\sin\phi \\ &+ C_6\sin^2\phi)\theta^2 + (C_7\cos^3\phi + C_8\cos^2\phi\sin\phi \\ &+ C_9\cos\phi\sin^2\phi + C_{10}\sin^3\phi)\theta^3 \end{aligned} \tag{3.3.1}$$

provides the best fit. Ten was used for the number of basis functions (or coefficients) and determined as the smallest number for which the following criterion chosen

$$R^2 = 1 - \frac{SSE}{SSTO} \geq 90\% \tag{3.3.2}$$

is satisfied, where

$R^2 (0 \leq R^2 \leq 1)$ which is called the coefficient of multiple determination and measures the proportionate reduction of total variation in f associated with the use of the set of (ϕ, θ) independent variables, SSE is the error (residual) sum of squares or

$$SSE = \sum_{i=1}^{n} [f(\phi_i, \theta_i) - z_i(\phi_i, \theta_i)]^2 \text{, and}$$

SSTO is the total sum of squares, or

$$SSTO = \sum_{i=1}^{n} [z_i(\phi_i, \theta_i) - \bar{z}]^2 \text{, where}$$

n = total number of experimental force (moment) data points collected, $z_i(\phi_i, \theta_i)$ = the experimental force (moment) value collected at the ith point (ϕ_i, θ_i), and

$$\bar{z} = \frac{1}{n} \sum_{i=1}^{n} z_i(\phi_i, \theta_i).$$

A detailed discussion of the R^2 and related regression analysis can be found in Neter, et al. (1985).

Since $\theta(\theta \geq 0)$ measures how far the upper arm departs from the z-axis of the local joint axis system, and ϕ goes from 0 to 2π, we can treat θ as the radial coordinate and ϕ as the angular coordinate in the polar coordinate system (θ, ϕ). The pole is then the z-axis of the local joint axis system . Therefore, if we introduce the following coordinate transformation

$$p = \theta\cos\phi$$
$$q = \theta\sin\phi \qquad (3.3.3)$$

then (p, q) can be regarded as the corresponding rectangular coordinate system. Fig. 3.6 illustrates both coordinate systems and the corresponding four test quadrants. We shall define the combination of these two coordinate systems as the modified joint axis system. Obviously in terms of the modified coordinates, (p, q), the expansion function now becomes

$$f(\phi, \theta) = F(p, q) = C_1\sqrt{p^2+q^2} + C_2p + C_3q + C_4p^2 + C_5pq + C_6q^2 + C_7p^3 + C_8p^2q + C_9pq^2 + C_{10}q^3 \qquad (3.3.4)$$

With the help of the modified joint axis system, a physically meaningful plot can be made for the above expansion function to give us a visual aid to the understanding of the overall resistive force (moment) properties of any articulating joint. Fig. 3.7 shows the constant resistive force (moment) contour map for a subject and Fig. 3.8 shows a corresponding three-dimensional perspective view. Fig. 3.9 illustrates the sense of how "well" the expansion $f(\phi, \theta)$ fits the raw data for several constant-ϕ sweeps.

3.4 Statistical Analysis

Considering the vast quantities of sinus and force data for ten subjects, it would be very cumbersome if one uses a direct statistical analysis technique. It is more desirable to develop a systematic and

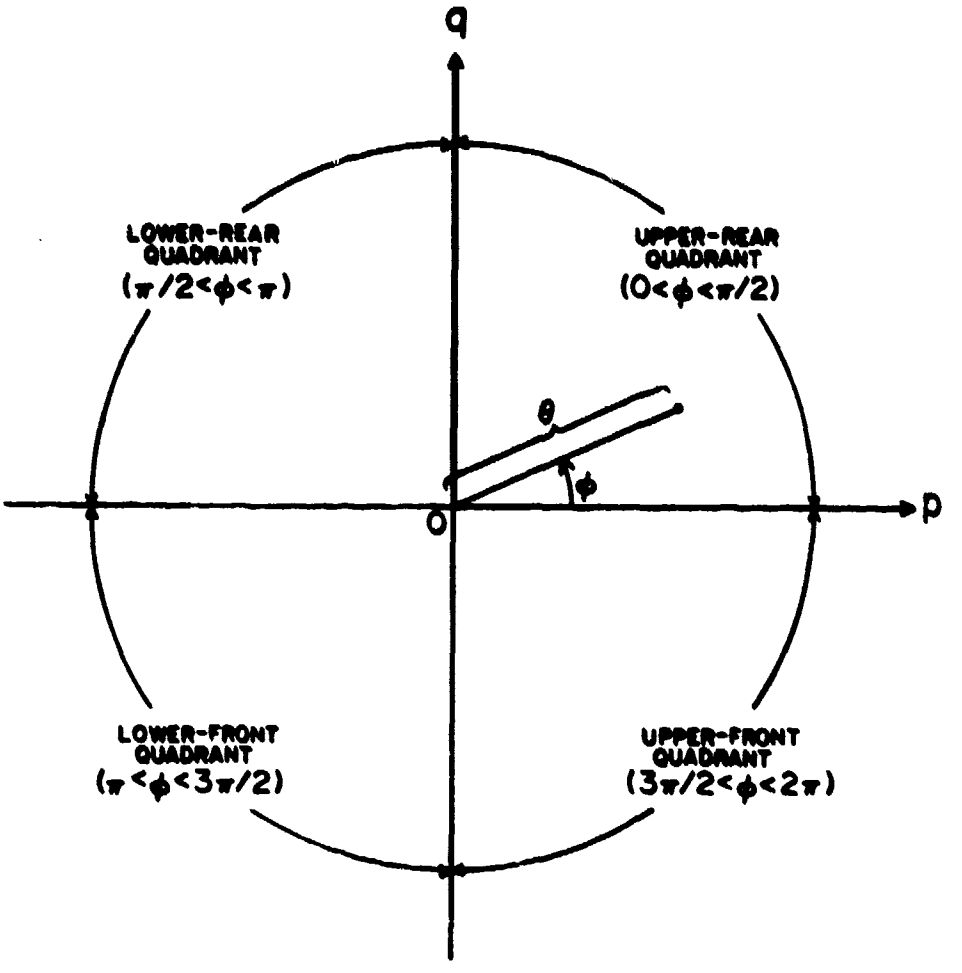

Fig. 3.6 The modified joint axis system and the corresponding four test quadrants.

easily manageable approach to deal with the extensive data. Therefore, Eqs. (3.2.1) and (3.3.1) will be utilized in an appropriate manner to seek for a sample mean, sample variance, and the confidence intervals for the population mean and variance. In this section we shall derive the method in a general sense.

Let $f(\vec{x}) = \sum_{i=1}^{M} C_i \, g_i(\vec{x})$ be a functional expansion (by the method of least squares in this study) for the experimental measurement of a certain quantity f having n independent variables, i.e., $\vec{x} = (x_1, x_2, x_3, \ldots, x_n)$, where $\{g_i(\vec{x}) \mid i = 1, 2, 3, \ldots, M\}$ is a set of mutually independent basis functions, $\{C_i \mid i = 1, 2, 3, \ldots, M\}$ is the

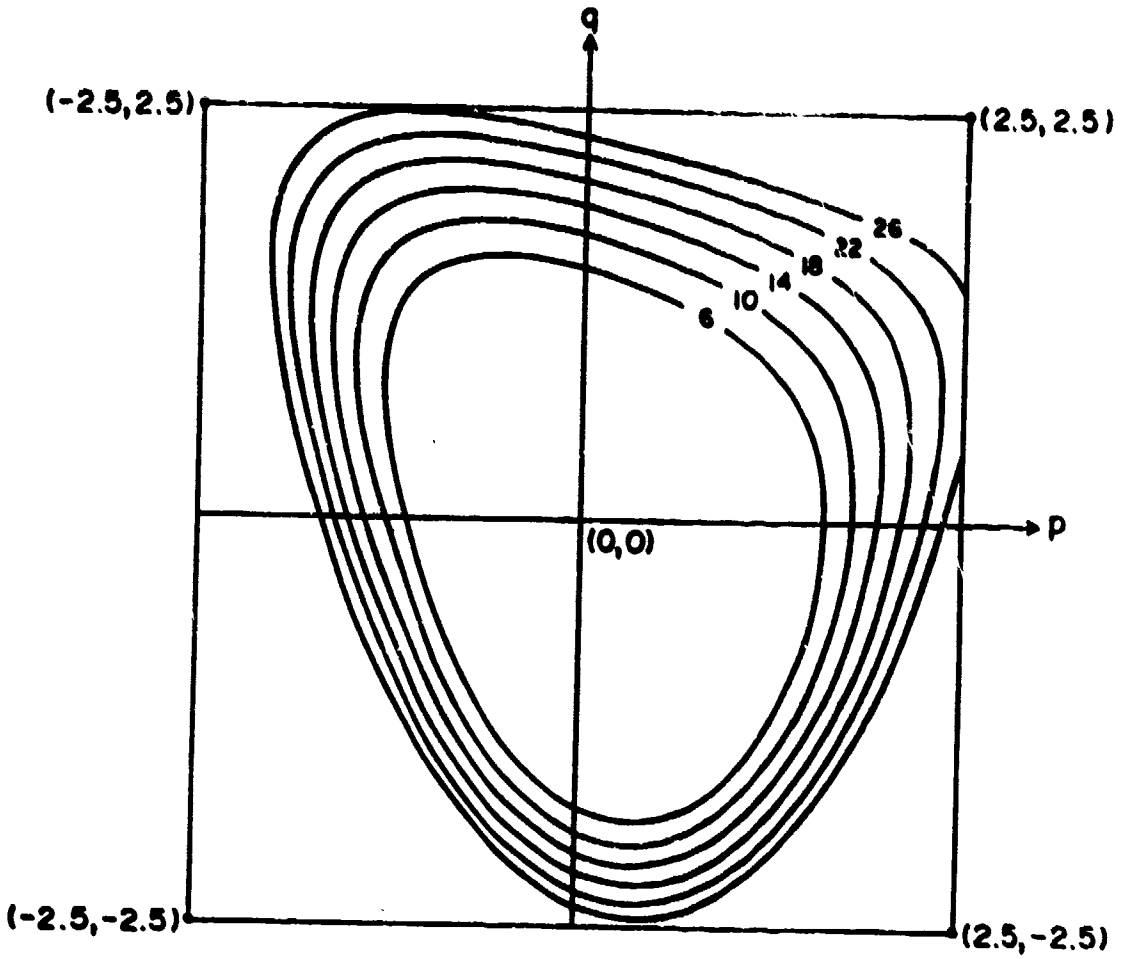

Fig. 3.7 Constant resistive force (moment), in Newtons (Newton-Meters), contour map for a subject in the modified joint axis system, in radians.

corresponding set of independent expansion coefficients, and N is the number of basis functions or coefficients. Consider now the statistics of the quantity f for a chosen population from which we have a random sample of size N. Then, obviously, the coefficients, C_i, become statistically independent random variables, and the non-random basis functions become statistically constant. Furthermore, f is now a linear combination of random variables, and, so, is itself a random variable.

From probability theory, for each $\vec{x}$, the population mean, $\mu_f(\vec{x})$, is

$$\mu_f(\vec{x}) = E[f(\vec{x})] = E[\sum_{i=1}^{N} C_i \, g_i(\vec{x})]$$

$$= \sum_{i=1}^{N} g_i(\vec{x}) \, E[C_i] = \sum_{i=1}^{N} g_i(\vec{x}) \, \mu_{C_i} \qquad (3.4.1)$$

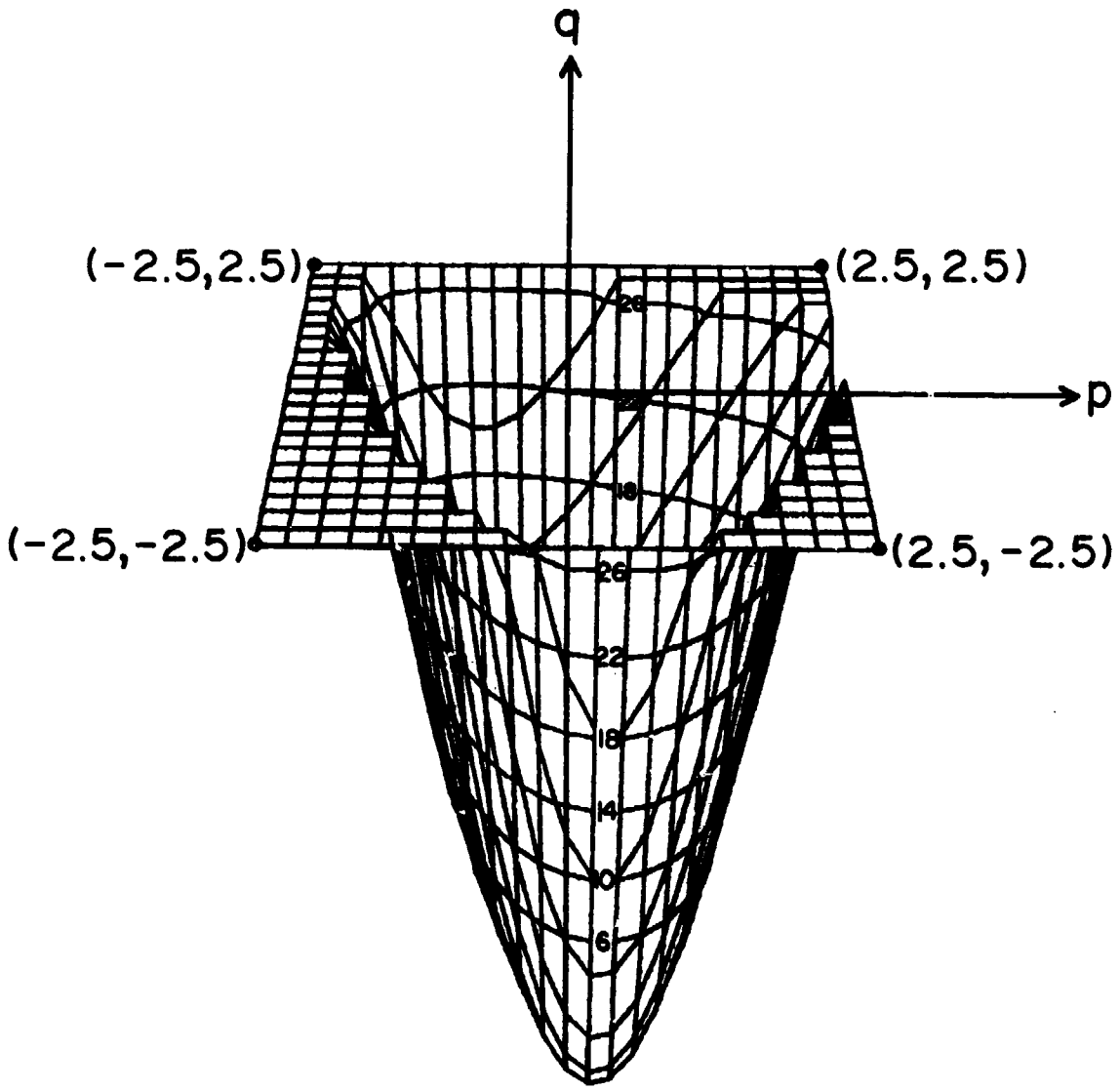

Fig. 3.8 Perspective view of Fig. 3.7.

and the population variance, $\sigma_f^2(\vec{x})$, is

$$\sigma_f^2(\vec{x}) = \text{VAR}[f(\vec{x})] = \text{VAR}[\sum_{i=1}^{M} C_i \, g_i \, (\vec{x})]$$

$$= \sum_{i=1}^{M} g_i^2(\vec{x}) \, \text{VAR}[C_i]$$

$$= \sum_{i=1}^{M} g_i^2(\vec{x}) \, \sigma_{C_i}^2 \qquad (3.4.2)$$

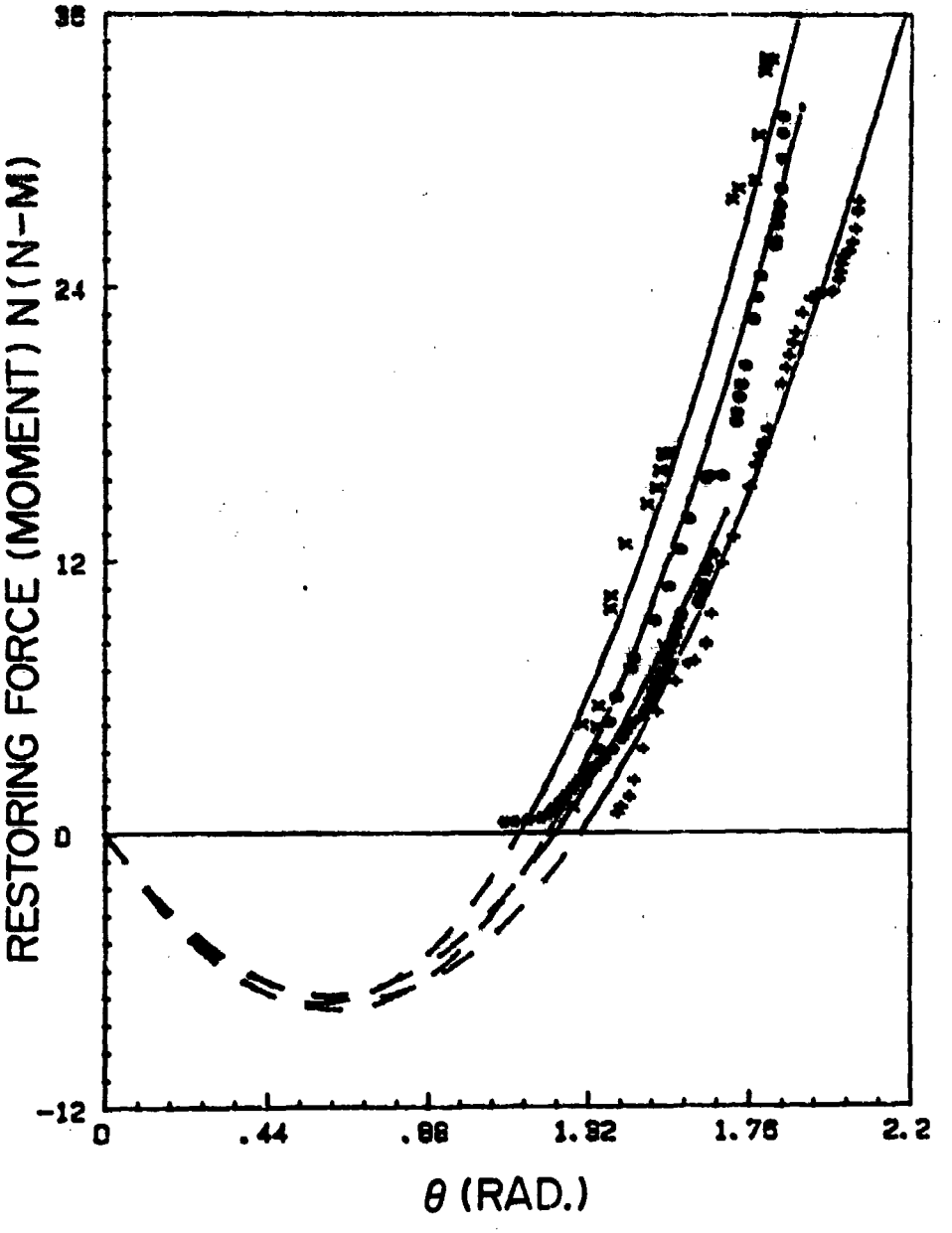

Fig. 3.9 Raw data and fitted curves drawn from $f(\phi, \theta)$ for various constant-ϕ sweeps for the subject mentioned in Fig. 3.7.

where we have utilized

$$\text{COV}[C_i, C_j] = 0 \quad \text{for all } 1 \leq i < j \leq M \tag{3.4.3}$$

since all the coefficients are mutually independent. Note that in Eq. (3.4.1) the operator E stands for the mathematical expectation and in Eq. (3.4.2) the operator VAR for the variance. Therefore, if we know the

population means, μ_{c_i}, and the population variances, $\sigma^2_{c_i}$, for all the M coefficients, we can evaluate the population mean and variance for $f(\vec{x})$.

Sample Mean, $\bar{f}(\vec{x})$, and Sample Variance, $s^2_f(\vec{x})$

Since the population means and variances of the coefficients can rarely be obtained, we seek for statistical estimates, namely, the sample means, $\bar{C}_i$, and sample variances, $S^2_{c_i}$, from the given random sample of size N. From statistical theory, an estimate for μ_{c_i} is

$$\bar{C}_i = \frac{1}{N} \sum_{j=1}^{N} (C_i)_j \qquad (3.4.4)$$

where $(C_i)_j$ stands for the ith coefficient of the jth sample outcome, and an unbiased estimate for $\sigma^2_{c_i}$ is

$$S^2_{c_i} = \frac{1}{N-1} \left\{ \sum_{j=1}^{N} (C_i)^2_j - \frac{1}{N} \left[\sum_{j=1}^{N} (C_i)_j \right]^2 \right\} \qquad (3.4.5)$$

Thus, an estimate for $\mu_f(\vec{x})$ from Eq. (3.4.1) is

$$\bar{f}(\vec{x}) = \sum_{i=1}^{M} g_i(\vec{x})\, \bar{C}_i \qquad (3.4.6)$$

and an unbiased estimate for $\sigma^2_f(\vec{x})$ from Eq. (3.4.2) is

$$S^2_f(\vec{x}) = \sum_{i=1}^{M} g^2_i(\vec{x})\, S^2_{c_i} \qquad (3.4.7)$$

Confidence Interval for $\mu_f(\vec{x})$

From statistical theory, the random variable $\dfrac{\bar{f}(\vec{x}) - \mu_f(\vec{x})}{S_f(\vec{x})/\sqrt{N}}$

has a t-distribution with N-1 degrees of freedom, regardless of the parameter values $\mu_f(\vec{x})$ and $\sigma^2_f(\vec{x})$. Therefore, the confidence interval of $\mu_f(\vec{x})$ can be obtained by

$$\Pr \left\{ -\alpha_\gamma \leq \frac{\bar{f}(\vec{x}) - \mu_f(\vec{x})}{S_f(\vec{x})/\sqrt{N}} \leq \alpha_\gamma \right\} = \gamma \qquad (3.4.8)$$

where Pr is the probability, γ is the confidence level to be chosen, and

α_γ (> 0) is the solution of the equation

$$\int_{\alpha_\gamma}^{\infty} t_{N-1}(z)\, dz = \frac{1-\gamma}{2} \tag{3.4.9}$$

where t_{N-1} is the probability density function of the t-distribution with N-1 degrees of freedom. Rearranging the inequalities, we obtain the confidence interval for $\mu_f(\vec{x})$, at the confidence level γ,

$$\text{CONF}\left\{ \bar{f}(\vec{x}) - \frac{\alpha_\gamma S_f(\vec{x})}{\sqrt{N}} \leq \mu_f(\vec{x}) \leq \bar{f}(\vec{x}) + \frac{\alpha_\gamma S_f(\vec{x})}{\sqrt{N}} \right\} \tag{3.4.10}$$

Confidence Interval for $\sigma_f^2(\vec{x})$

The fact that the random variable $\dfrac{(N-1)\, S_f^2(\vec{x})}{\sigma_f^2(\vec{x})}$ has a χ^2-distribution with N-1 degrees of freedom enables us to have

$$\Pr\left\{ \alpha_\gamma \leq \frac{(N-1)\, S_f^2(\vec{x})}{\sigma_f^2(\vec{x})} \leq \beta_\gamma \right\} = \gamma \tag{3.4.11}$$

where α_γ is the solution of the equation

$$\int_0^{\alpha_\gamma} \chi^2_{N-1}(z)dz = \frac{1-\gamma}{2} \quad , \tag{3.4.12}$$

and β_γ is the solution of the equation

$$\int_{\beta_\gamma}^{\infty} \chi^2_{N-1}(z)dz = \frac{1-\gamma}{2} \quad , \tag{3.4.13}$$

where χ^2_{N-1} is the probability density function of the χ^2-distribution with N-1 degrees of freedom. Rearranging the inequalities, we obtain the confidence interval for $\sigma_f^2(\vec{x})$, at the confidence level γ,

$$\text{CONF}\left\{ \frac{(N-1)\, S_f^2(\vec{x})}{\beta_\gamma} \leq \sigma_f^2(\vec{x}) \leq \frac{(N-1)\, S_f^2(\vec{x})}{\alpha_\gamma} \right\} \tag{3.4.14}$$

3.5 Coordinate Transformations Among the Fixed Body, Individual Joint and Mean Joint Axis Systems

Since we shall utilize the functional expansion forms, Eqs. (3.2.1) and (3.3.1), to perform statistical analysis for the shoulder complex

sinuses and passive resistive properties beyond them, appropriate coordinate systems should be consistently used for the purposes of statistically comparing the coefficients of the data sets for ten subjects. In representing the joint property data in functional expansion form, different coordinate systems used will result in different coefficients although the same basis functions are used. Therefore, it is necessary to perform coordinate transformations for the spherical angles, ϕ and θ, among the fixed body, individual local joint and mean joint axis systems.

The local joint axis system, as shown in Fig. 3.10 is uniquely

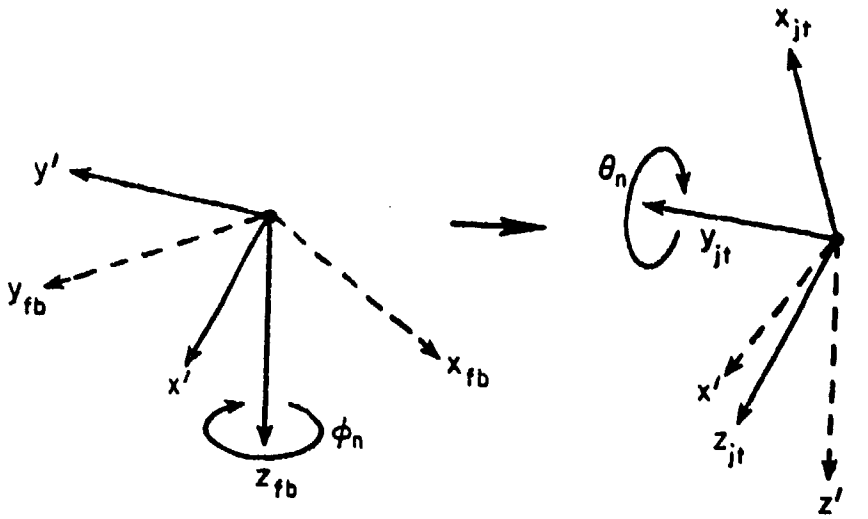

Fig. 3.10 Joint axis system as obtained by two successive rotations, first about the z_{fb}-axis and then about the intermediate (primed) y'-axis from the fixed body axis system.

obtained in this study by first rotating the fixed body axis system by an angle ϕ_n about the z_{fb}-axis and then rotating the intermediate (primed) axis system by an angle θ_n about the y'-axis. The mean joint axis system is obtained in a similar manner with (ϕ_n, θ_n) replaced by (ϕ_m, θ_m). Since the joint sinus with spherical coordinates (ϕ, θ) implies a unit vector with rectangular coordinates $(\sin\theta\cos\phi, \sin\theta\sin\phi, \cos\theta)$, the coordinate transformation from (ϕ_f, θ_f), relative to the fixed body

axis system, to (ϕ_j, θ_j), relative to the joint axis system, can be obtained in the following manner:

$$\begin{bmatrix} \sin\theta_j \cos\phi_j \\ \sin\theta_j \sin\phi_j \\ \cos\theta_j \end{bmatrix}_{jt} = N_{jt/fb} \begin{bmatrix} \sin\theta_f \cos\phi_f \\ \sin\theta_f \sin\phi_f \\ \cos\theta_f \end{bmatrix}_{fb} = \begin{bmatrix} x \\ y \\ z \end{bmatrix}_{jt} \tag{3.5.1}$$

where $N_{jt/fb} = \begin{bmatrix} \cos\theta_n & 0 & -\sin\theta_n \\ 0 & 1 & 0 \\ \sin\theta_n & 0 & \cos\theta_n \end{bmatrix} \begin{bmatrix} \cos\phi_n & \sin\phi_n & 0 \\ -\sin\phi_n & \cos\phi_n & 0 \\ 0 & 0 & 1 \end{bmatrix}$

$$= \begin{bmatrix} \cos\theta_n \cos\phi_n & \cos\theta_n \sin\phi_n & -\sin\theta_n \\ -\sin\phi_n & \cos\phi_n & 0 \\ \sin\theta_n \cos\phi_n & \sin\theta_n \sin\phi_n & \cos\theta_n \end{bmatrix}$$

is the transformation matrix defining the joint axis system relative to the fixed body axis system, and x, y, z can be numerically calculated with (ϕ_n, θ_n) and the joint sinus (ϕ_f, θ_f) specified. Comparing the left and right hand sides of Eq. (3.5.1), we have

$$\begin{cases} \phi_j = \tan^{-1} \dfrac{y}{x} \text{ and} \\ \theta_j = \cos^{-1} z \ . \end{cases} \tag{3.5.2}$$

The coordinate transformation from (ϕ_f, θ_f) to (ϕ_{mj}, θ_{mj}), where mj stands for the mean joint axis system, can be obtained in the same way as above with (ϕ_n, θ_n) replaced by (ϕ_m, θ_m) so that the transformation matrix defining the mean joint axis system relative to the fixed body axis system now becomes

$$M_{mj/fb} = \begin{bmatrix} \cos\theta_m \cos\phi_m & \cos\theta_m \sin\phi_m & -\sin\theta_m \\ -\sin\phi_m & \cos\phi_m & 0 \\ \sin\theta_m \cos\phi_m & \sin\theta_m \sin\phi_m & \cos\theta_m \end{bmatrix}$$

If the joint sinus is given relative to the individual local joint axis system, then the spherical coordinate transformation from (ϕ_j, θ_j) to (ϕ_{mj}, θ_{mj}) can be achieved by noting that

$$\begin{bmatrix} \sin\theta_{mj}\cos\phi_{mj} \\ \sin\theta_{mj}\sin\phi_{mj} \\ \cos\theta_{mj} \end{bmatrix}_{mj} = N_{mj/fb}\, L_{fb/jt} \begin{bmatrix} \sin\theta_j\cos\phi_j \\ \sin\theta_j\sin\phi_j \\ \cos\theta_j \end{bmatrix}_{jt}$$

$$= \begin{bmatrix} X \\ Y \\ Z \end{bmatrix}_{mj} \tag{3.5.3}$$

where $L_{fb/jt} = N^{-1}_{jt/fb} = N^{T}_{jt/fb}$ since $N_{jt/fb}$ is a proper orthogonal matrix, i.e.,

$$N_{jt/fb}\, N^{T}_{jt/fb} = I\ , \tag{3.5.4}$$

and X, Y, Z can be numerically calculated with (ϕ_m, θ_m), (ϕ_n, θ_n) and the joint sinus (ϕ_j, θ_j) specified. Comparing the left and right hand sides of Eq. (3.5.3), we have

$$\begin{cases} \phi_{mj} = \tan^{-1}\dfrac{Y}{X} \text{ and} \\ \theta_{mj} = \cos^{-1} Z\ . \end{cases} \tag{3.5.5}$$

3.6 Statistical Data Base for the Biomechanical Properties of the Human Shoulder Complex

Since each subject has an individual local joint axis system specified by (ϕ_n, θ_n), in statistically comparing the functional expansion coefficients of the joint property data, two different sets of sample means and sample variances can be envisioned and obtained from different points of view:

1. Subject-Based Mean and Variance

Here, we consider each individual local joint axis system, defined

by (ϕ_n, θ_n), as an index attributable to the individual anatomical variations in overall joint articulating structure as well as muscle/ligament orientations, and subjective kinematic behavioral variations in the circumscription mannerism. Then, not to be biased, each individual joint sinus and the resistive force (moment) data should be described by (ϕ_j, θ_j) with respect to the joint axis system of each subject, namely,

$\theta_j = \theta_j(\phi_j)$ for the shoulder complex sinus, and

$F = F(\phi_j, \theta_j)$ for the resistive force (moment).

The functional expansion coefficients obtained from these data are called <u>subject-based coefficients</u>. Furthermore, the population/sample means and variances obtained from the subject-based coefficients will be called subject-based population/sample means and variances, respectively. Obviously, from a statistical point of view, the most appropriate axis system for the subject-based population/sample means and variances is the population/sample mean joint axis system.

2. <u>Space-Based Mean and Variance</u>

In this case, the shoulder complex sinuses and the resistive force (moment) data are described by (ϕ_{mj}, θ_{mj}) with respect to a common mean joint axis system for all subjects, namely,

$\theta_{mj} = \theta_{mj}(\phi_{mj})$ for the shoulder complex sinus, and

$F = F(\phi_{mj}, \theta_{mj})$ for the resistive force (moment).

The functional expansion coefficients obtained from these data are now called <u>space-based coefficients</u>. In addition, the population/sample means and variances obtained from the space-based coefficients will be called space-based population/sample means and variances, respectively.

<u>Maximum Voluntary Shoulder Complex Sinus</u>

Table 3.2 lists the ten subject-based coefficients of the shoulder complex sinuses for all ten subjects. Table 3.3 lists the corresponding

Table 3.2 Subject-based coefficients of the shoulder complex sinuses for all ten subjects

COEFFI-CIENTS		C_1	C_2	C_3	C_4	C_5	C_6	C_7	C_8	C_9	C_{10}
SUBJ. NO.	1	1.59292	-0.10675	-0.24466	-0.36233	0.19558	0.44395	0.49886	0.06685	-0.62262	-0.42877
	2	1.18066	-0.08909	-0.07757	-0.06084	0.11961	0.33650	0.23417	-0.34872	-0.32021	-0.04841
	3	1.42229	-0.05486	-0.18374	-0.15690	0.28160	0.35114	0.34084	-0.26833	-0.30699	-0.12560
	4	1.70121	-0.10321	-0.27100	-0.32562	-0.02313	0.74636	0.45572	0.19442	-0.26271	-0.79351
	5	1.28393	-0.07031	-0.33344	-0.47247	-0.04754	0.67981	0.55630	0.44145	-0.12712	-0.61977
	6	1.57994	-0.09393	-0.33890	-0.37299	0.39152	0.89132	0.55373	0.05622	-0.69396	-0.86106
	7	1.75422	-0.06345	-0.32748	-0.46664	-0.15587	0.63602	0.62553	0.22174	-0.22427	-0.80867
	8	1.53784	-0.12414	-0.26177	-0.41879	0.35225	0.79143	0.50138	0.17251	-0.60433	-0.49631
	9	1.50215	-0.12424	-0.12763	-0.28346	0.47236	0.53337	0.27331	-0.00376	-0.63518	-0.39607
	10	1.43838	-0.09574	-0.29782	-0.01552	0.28790	0.44899	0.51590	-0.44247	-0.49447	-0.12844
Sample Mean		1.49936	-0.09257	-0.24640	-0.29356	0.18743	0.58589	0.45557	0.00899	-0.42918	-0.47066
Sample Variance		0.03112	0.00057	0.00808	0.02666	0.04345	0.03684	0.01685	0.07865	0.04141	0.09062

Table 3.3 Space-based coefficients of the shoulder complex sinuses for all ten subjects

COEFFI-CIENTS		C_1	C_2	C_3	C_4	C_5	C_6	C_7	C_8	C_9	C_{10}
SUBJ. NO.	1	1.18167	-0.13492	-0.10623	-0.04934	0.11099	0.29947	0.22508	-0.37071	-0.30969	0.01536
	2	1.59502	-0.13343	-0.36746	-0.36963	0.18949	0.38560	0.49613	0.09209	-0.61517	-0.36522
	3	1.42535	-0.12051	-0.14047	-0.16509	0.26499	0.37472	0.34033	-0.26402	-0.29337	-0.16580
	4	1.69959	-0.09904	-0.19982	-0.31658	-0.01759	0.76733	0.45691	0.17579	-0.26778	-0.81237
	5	1.28512	-0.07703	-0.32588	-0.47315	-0.05643	0.67388	0.55654	0.43909	-0.11917	-0.61506
	6	1.57365	-0.04192	-0.36103	-0.36639	0.42768	0.91880	0.55155	0.03496	-0.72275	-0.88100
	7	1.75407	-0.06101	-0.33126	-0.46733	-0.15494	0.63562	0.62551	0.22275	-0.22494	-0.80821
	8	1.54165	-0.16045	-0.28826	-0.42410	0.33518	0.79179	0.50885	0.18746	-0.59228	-0.50851
	9	1.50088	-0.09623	-0.03463	-0.28225	0.47499	0.54593	0.27331	-0.00882	-0.63813	-0.40824
	10	1.43259	-0.00208	-0.31430	-0.00739	0.31598	0.45068	0.51082	-0.44820	-0.51794	-0.11297
Sample Mean		1.49896	-0.09266	-0.24693	-0.29213	0.18903	0.58438	0.45450	0.00604	-0.43012	-0.46720
Sample Variance		0.03091	0.00232	0.01395	0.02770	0.04548	0.04255	0.01727	0.08065	0.04394	0.09848

ten space-based coefficients. These two tables also list the sample means and variances for all ten coefficients. Fig. 3.11 shows the best

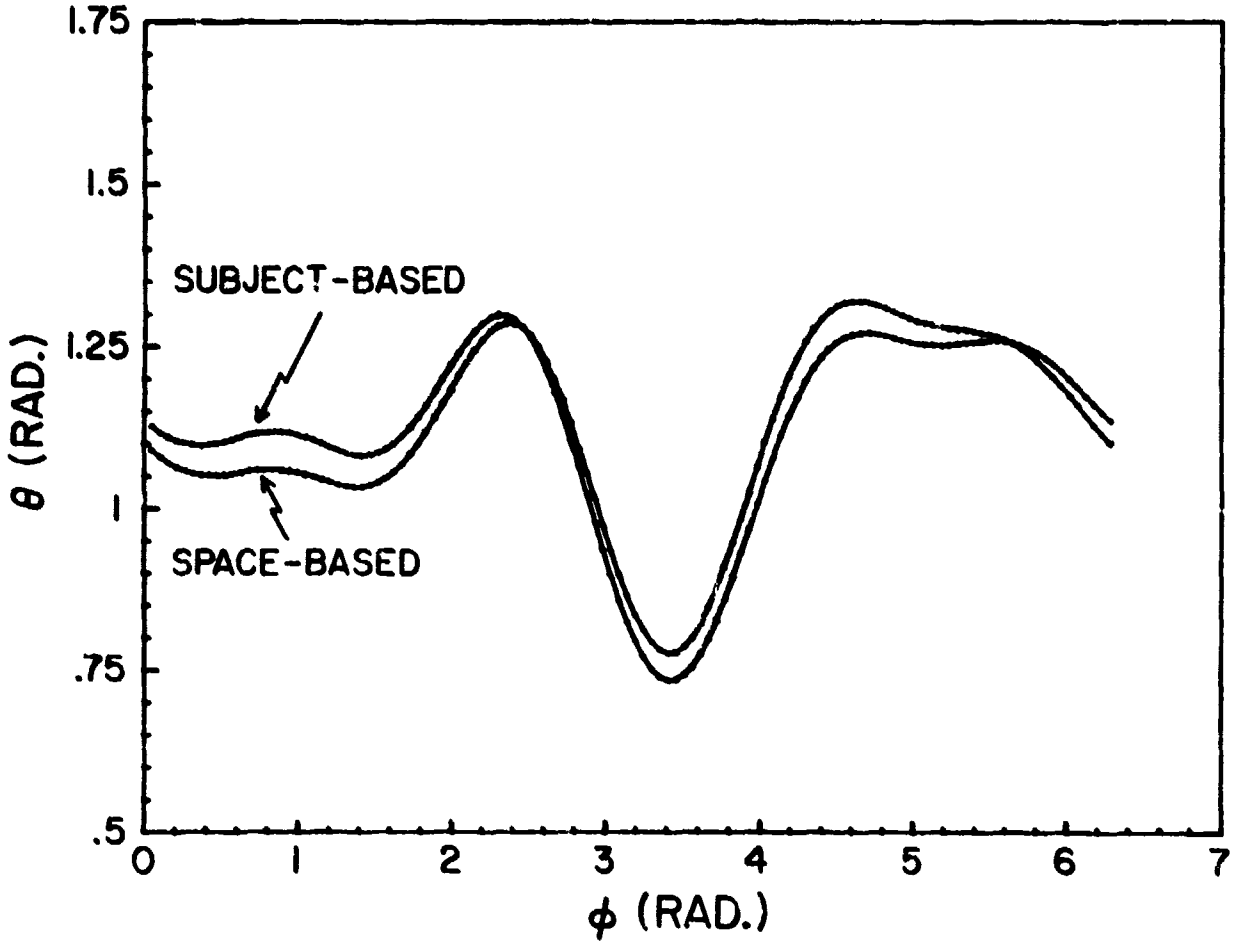

Fig. 3.11 Subject-based and space-based maximum voluntary shoulder complex sinuses for the first subject

fitted curves for both space-based and subject-based sinuses for the first subject who has the $(\phi_n, \theta_n) = (57°.37, 72°.24)$ which depart the most from the mean values $(\phi_m, \theta_m) = (59°.29, 79°.08)$. The more the individual joint axis system deviates from the mean joint axis system, the bigger is the difference between the space-based and the subject-based sinuses.

Now let us apply the results obtained from the statistical analysis developed in Section 3.4 to establish a statistical data base for the shoulder complex sinus. In this case, the functional expansion,

Eq. (3.2.1), has only one independent variable, i.e., ϕ.

From Eq. (3.4.6) one obtains the sample mean

$$\bar{\theta}(\phi) = \sum_{n=1}^{5} \cos^{n-1}\phi \left(\bar{C}_{2n-1} + \bar{C}_{2n} \sin\phi \right) \tag{3.6.1}$$

and from Eq. (3.4.7) the unbiased sample variance

$$s_{\theta}^{2}(\phi) = \sum_{n=1}^{5} \cos^{2(n-1)}\phi \left(s_{C_{2n-1}}^{2} + s_{C_{2n}}^{2} \sin^{2}\phi \right) \tag{3.6.2}$$

Fig. 3.12 displays the least-squares fitted data for the subject-based sinuses of all ten subjects. This figure also shows curves for the sample mean, $\bar{\theta}(\phi)$, and those corresponding to $\bar{\theta}(\phi) \pm s_{\theta}(\phi)$. Fig. 3.13

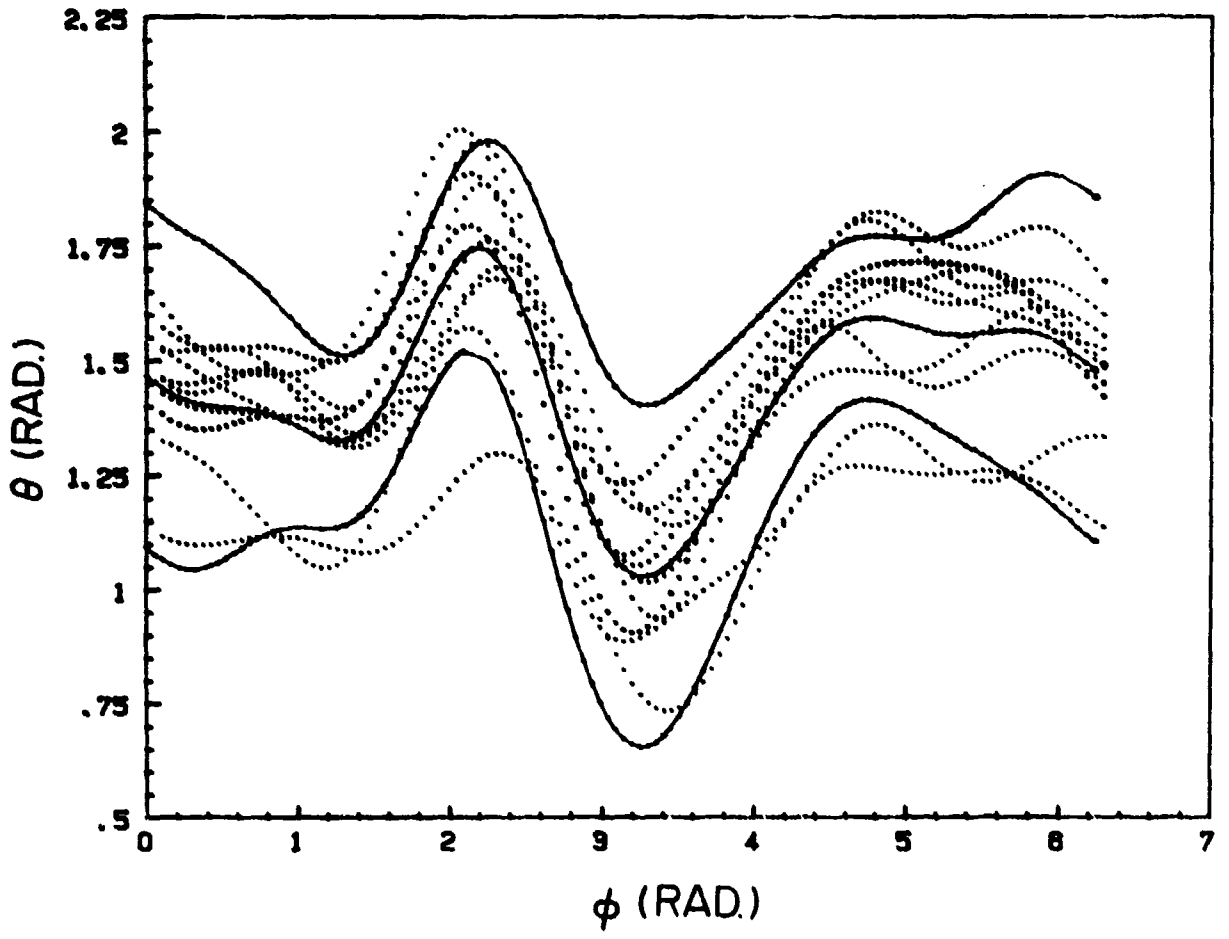

Fig. 3.12 Curve-fitted data for subject-based sinuses of all subjects (dotted curves). Solid curves are for $\bar{\theta}$ and $\bar{\theta} \pm s_{\theta}$.

shows their corresponding globographic representations in the torso-fixed coordinate system, i.e., the spherical coordinates on the globe are referred to the fixed body axis system. Therefore, the coordinates $(\phi_g, \theta_g) = (0^\circ, 90^\circ)$ on the globe corresponds to the emergent point of the x_{fb}-axis, and the coordinates $(\phi_g, \theta_g) = (90^\circ, 90^\circ)$ corresponds to the emergent point of the y_{fb}-axis. Note that, in this case, since each subject's sinus is defined by its own local axis system designated by (ϕ_n, θ_n), from a statistical point of view, the most "appropriate" local axis system for the subject-based $\bar{\theta}(\phi)$ and $s_\theta^2(\phi)$ is the mean joint axis system, designated by the sample mean, (ϕ_m, θ_m), taken from the sample.

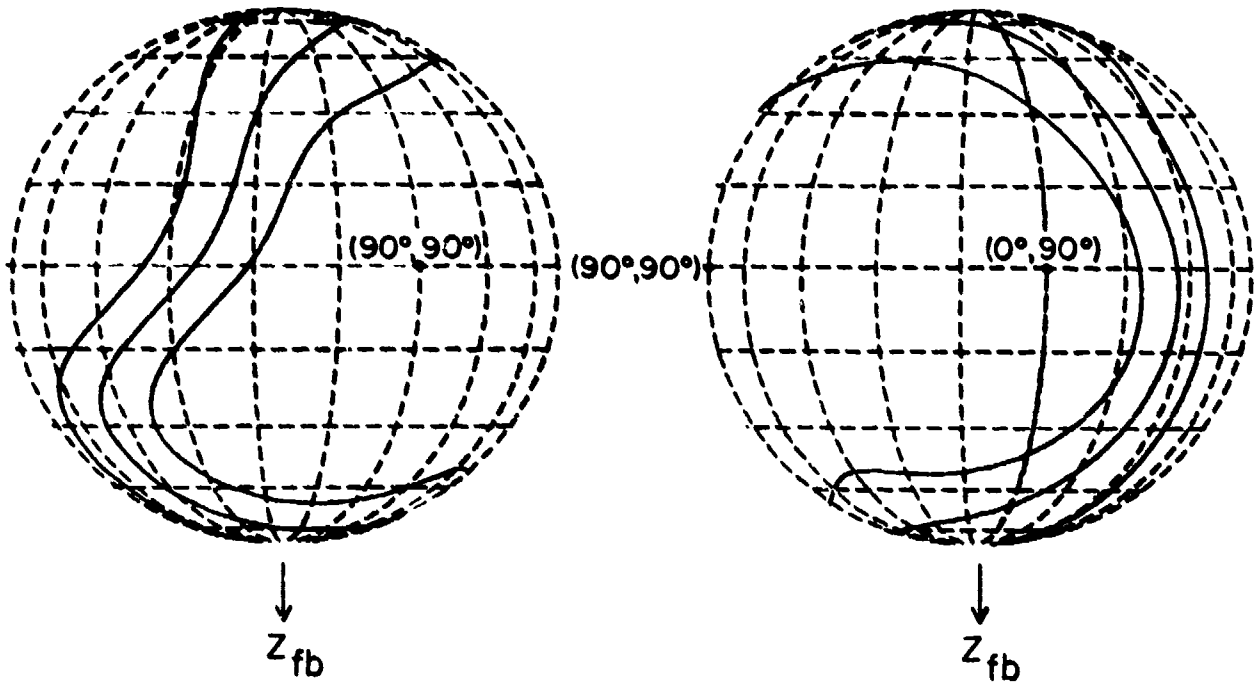

Fig. 3.13 Globographic representations of $\bar{\theta}$ and $\bar{\theta} \pm S_\theta$ (subject-based).

Fig. 3.14 displays the least-squares fitted data for the space-based sinuses for all ten subjects. This figure also shows curves for the sample mean, $\bar{\theta}(\phi)$, and those corresponding to $\bar{\theta}(\phi) \pm S_\theta(\phi)$. Fig. 3.15 shows their corresponding globographic representations. Obviously, in this case, the mean joint axis system should be used for the space-based $\bar{\theta}(\phi)$ and $S_\theta^2(\phi)$, since all the sinuses are represented in this axis system.

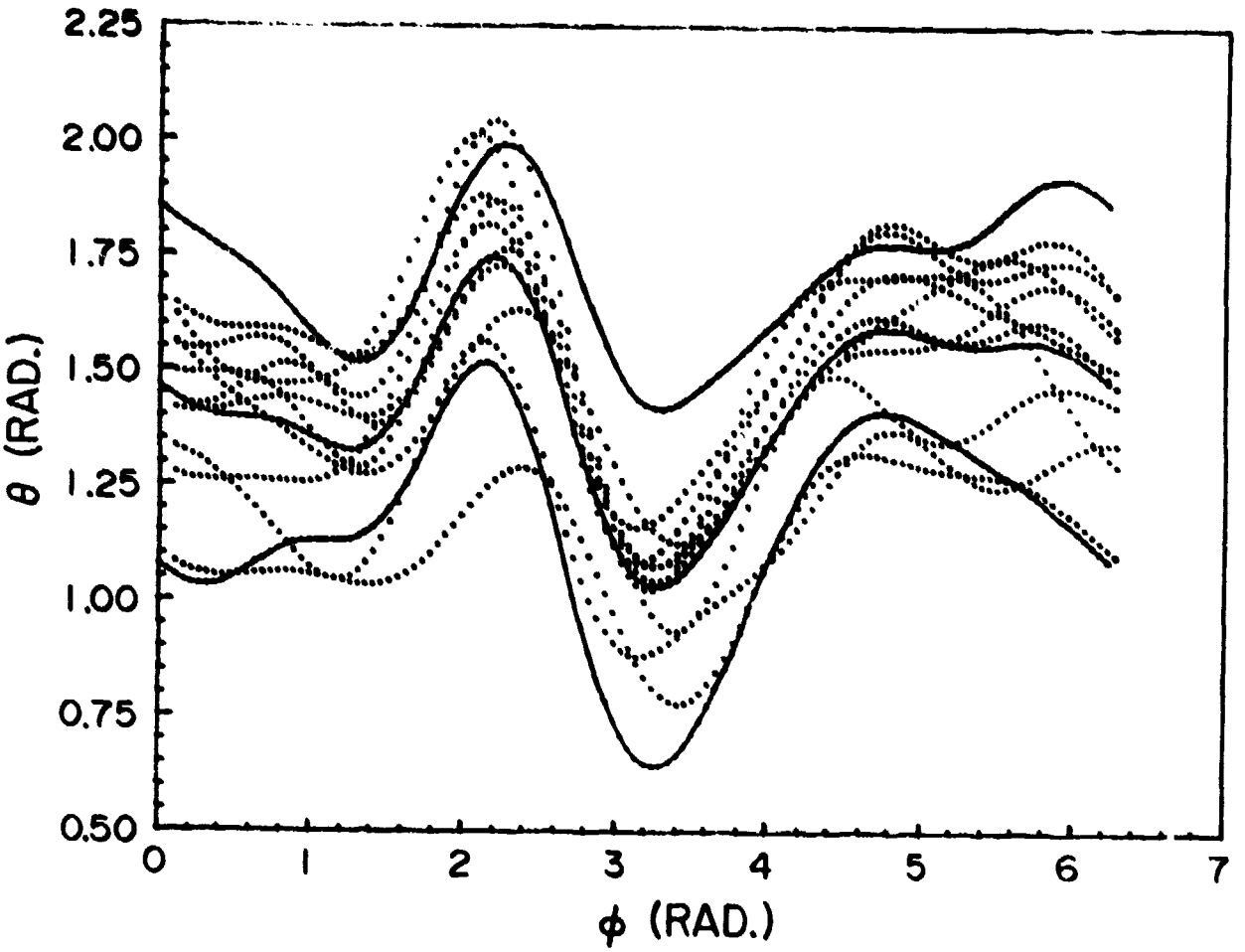

Fig. 3.14 Least-squares fitted data (dotted lines) for the space-based sinuses for all ten subjects. The middle solid curve is the space-based sample mean joint sinus, $\bar{\theta}(\phi)$. The upper and lower solid curves are $\bar{\theta}(\phi) + S_\theta(\phi)$ and $\bar{\theta}(\phi) - S_\theta(\phi)$, respectively.

For the purposes of comparison, Fig. 3.16 displays the sample mean, $\bar{\theta}(\phi)$, and those corresponding to $\bar{\theta}(\phi) \pm S_\theta(\phi)$ for both space based and subject-based sinuses. It should be remarked that, while the space-based and subject-based sinuses may differ significantly for an individual subject, their sample means and, $\bar{\theta}(\phi) \pm S_\theta(\phi)$, may be indiscernible as indicated in Fig. 3.16.

One of the most important ways of testing the ultimate overall performance of the data acquisition system and efficacy of the associated data analysis methodology is good repeatability of sample means and sample standard deviations from <u>different</u> runs made on the same sample. Fig. 3.17 displays the subject-based sample means, and $\bar{\theta} \pm S_\theta$ from three

different runs for all subjects. Rather good repeatability obviously exists if one realizes that most of the deviations arise from the variations during circumscription type of motion by the subjects.

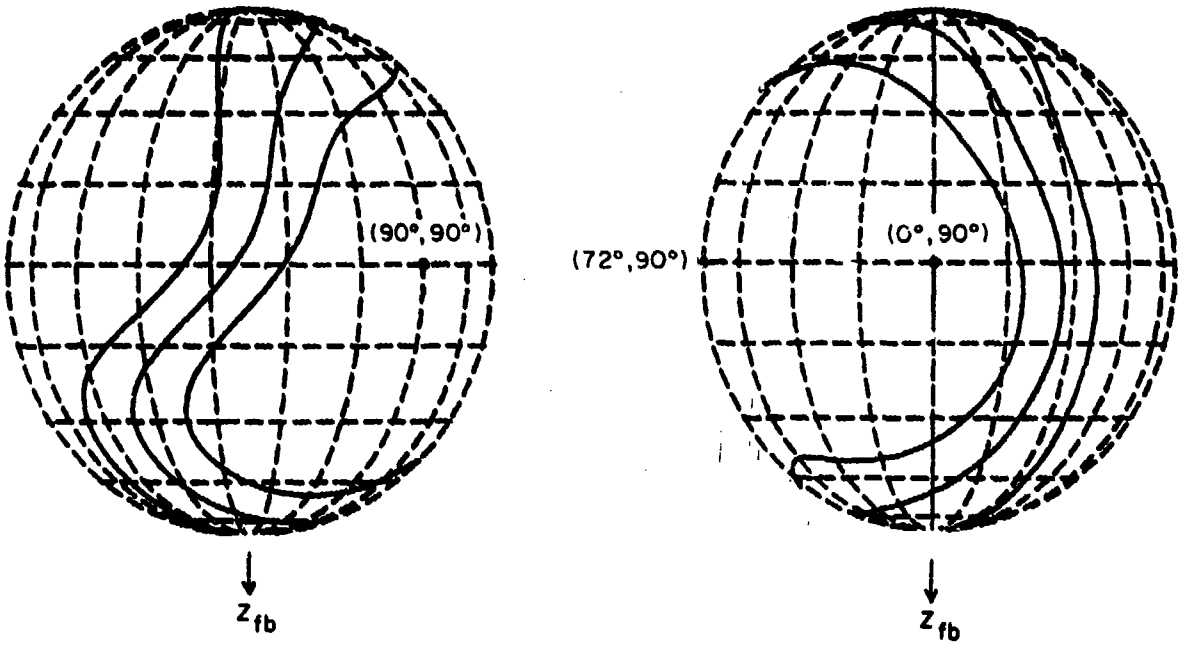

Fig. 3.15 Globographic representations of $\bar{\theta}(\phi)$ and $\bar{\theta}(\phi) \pm S_\theta(\phi)$ (space-based).

For the confidence level of 95%, utilizing Eq. (3.4.8), we obtain from statistical table (Kreyszig, 1972) that,

$$\Pr\left\{ -2.26 \leq \frac{\bar{\theta}(\phi) - \mu_\theta(\phi)}{S_\theta(\phi)/\sqrt{10}} \leq 2.26 \right\} = 95\% \qquad (3.6.3)$$

Rearranging the inequalities, we obtain

$$\Pr\left\{ [\bar{\theta}(\phi) - 0.715\, S_\theta(\phi)] \leq \mu_\theta(\phi) \leq [\bar{\theta}(\phi) + 0.715\, S_\theta(\phi)] \right\} = 95\% \qquad (3.6.4)$$

In other words, we are 95% confident that the population mean $\mu_\theta(\phi)$ is within the interval $[\bar{\theta}(\phi) - 0715S_\theta(\phi),\ \bar{\theta}(\phi) + 0.715S_\theta(\phi)]$ at each value of ϕ.

Fig. 3.18 shows the confidence intervals for both the space-based and subject-based population means for comparison. Fig. 3.19 displays the globographic representation of the confidence interval for the

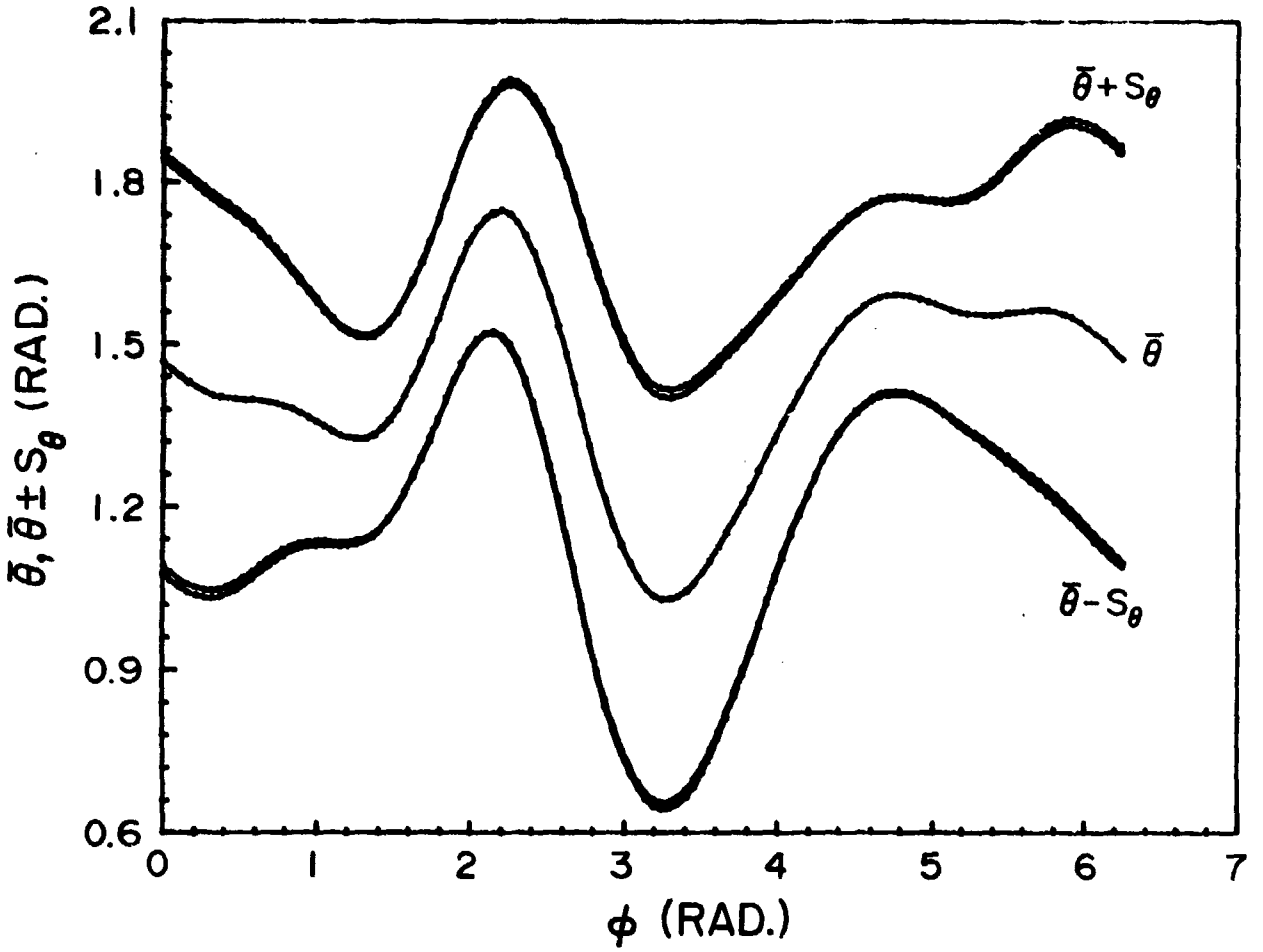

Fig. 3.16 $\bar{\theta}(\phi)$ and $\bar{\theta}(\phi) \pm S_\theta(\phi)$ for both space-based and subject-based sinuses. Note that the two $\bar{\theta}$ curves coincide with each other in this figure.

subject-based population mean, $\mu_\theta(\phi)$.

For the confidence interval of the population variance, from Eq. (3.4.11), we have

$$\Pr\left\{ 2.70 \leq \frac{9\, s_\theta^2(\phi)}{\sigma_\theta^2(\phi)} \leq 19.02 \right\} = 95\% \qquad (3.6.5)$$

with 2.5% of probability on both tails of the χ^2-distribution curve. Rearranging the inequalities, we have

$$\Pr\left\{ 0.473\, s_\theta^2(\phi) \leq \sigma_\theta^2(\phi) \leq 3.33\, s_\theta^2(\phi) \right\} = 95\% \qquad (3.6.6)$$

In other words, we are 95% sure that the population standard deviation $\sigma_\theta(\phi)$ is bracketed by the interval $[0.688S_\theta(\phi), 1.82S_\theta(\phi)]$ at each value

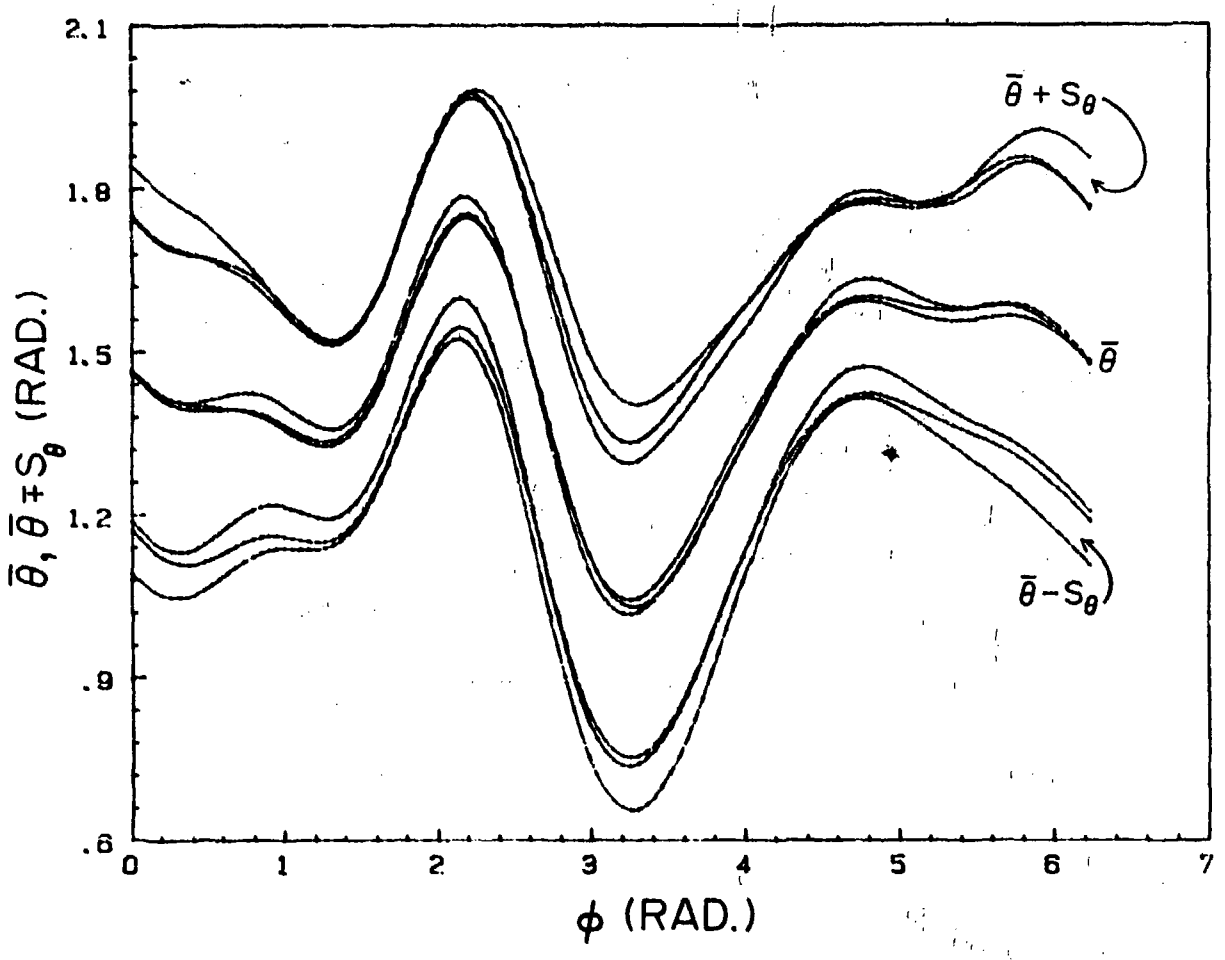

Fig. 3.17 $\bar{\theta}(\phi)$ and $\bar{\theta} \pm S_\theta(\phi)$ for three different runs for all subjects.

of ϕ. Fig. 3.20 shows the plots of this interval as well as $S_\theta(\phi)$ for the subject-based population standard deviation, $\sigma_\theta(\phi)$.

Passive Resistive Force (Moment) Properties

Table 3.4 lists the subject-based coefficients, as well as their sample means and sample variances, for the passive resistive force (moment) data for all ten subjects. Table 3.5 lists the corresponding space-based coefficients.

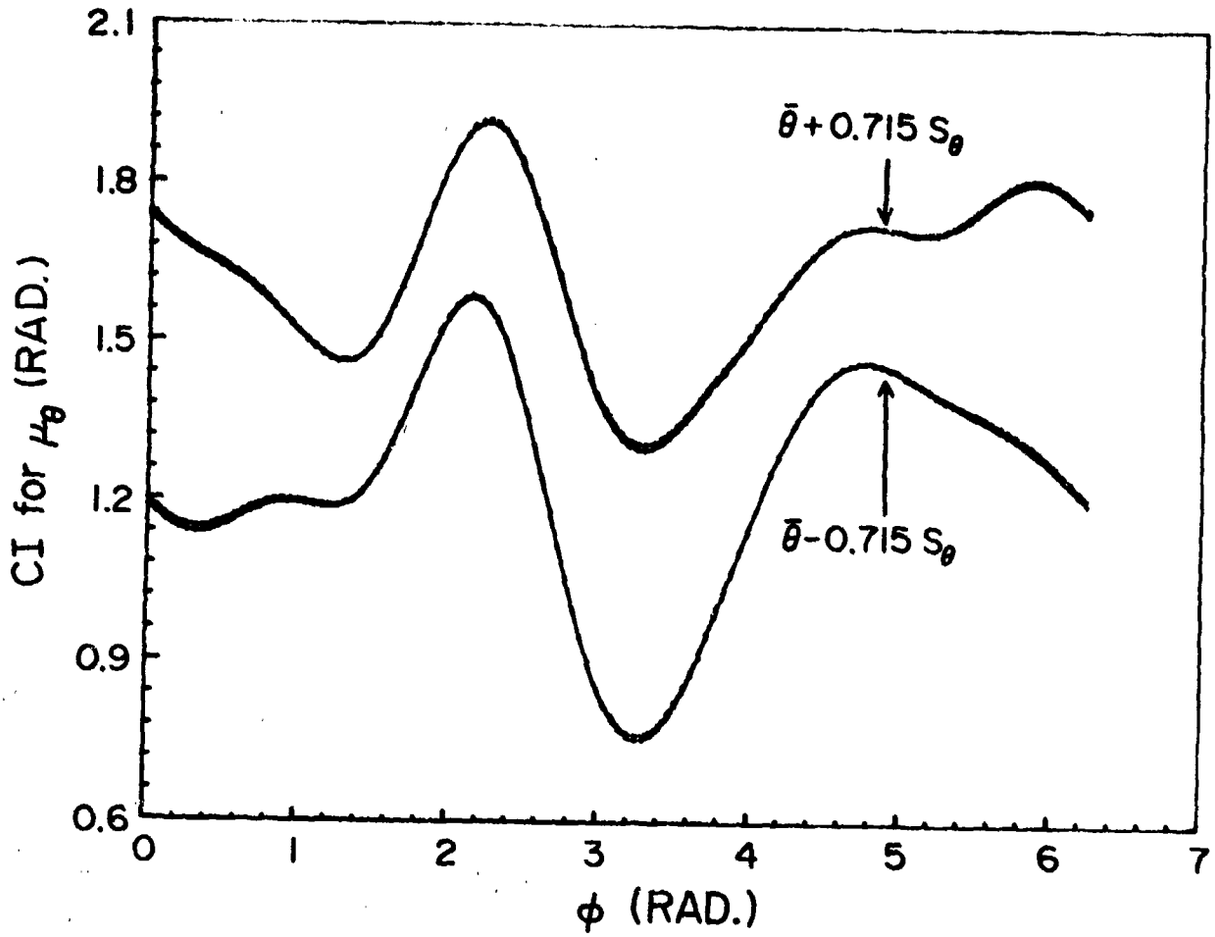

Fig. 3.18 Confidence intervals (CI) for both the space-based and subject-based population means.

From Eq. (3.4.6) one obtains the sample mean

$$\bar{f}(\phi, \theta) = (\bar{C} + \bar{C}_2\cos\phi + \bar{C}_3\sin\phi)\theta + (\bar{C}_4\cos^2\phi + \bar{C}_5\cos\phi\sin\phi + \bar{C}_6\sin^2\phi)\theta^2 + (\bar{C}_7\cos^3\phi + \bar{C}_8\cos^2\phi\sin\phi + \bar{C}_9\cos\phi\sin^2\phi + \bar{C}_{10}\sin^3\phi)\theta^3 \qquad (3.4.7)$$

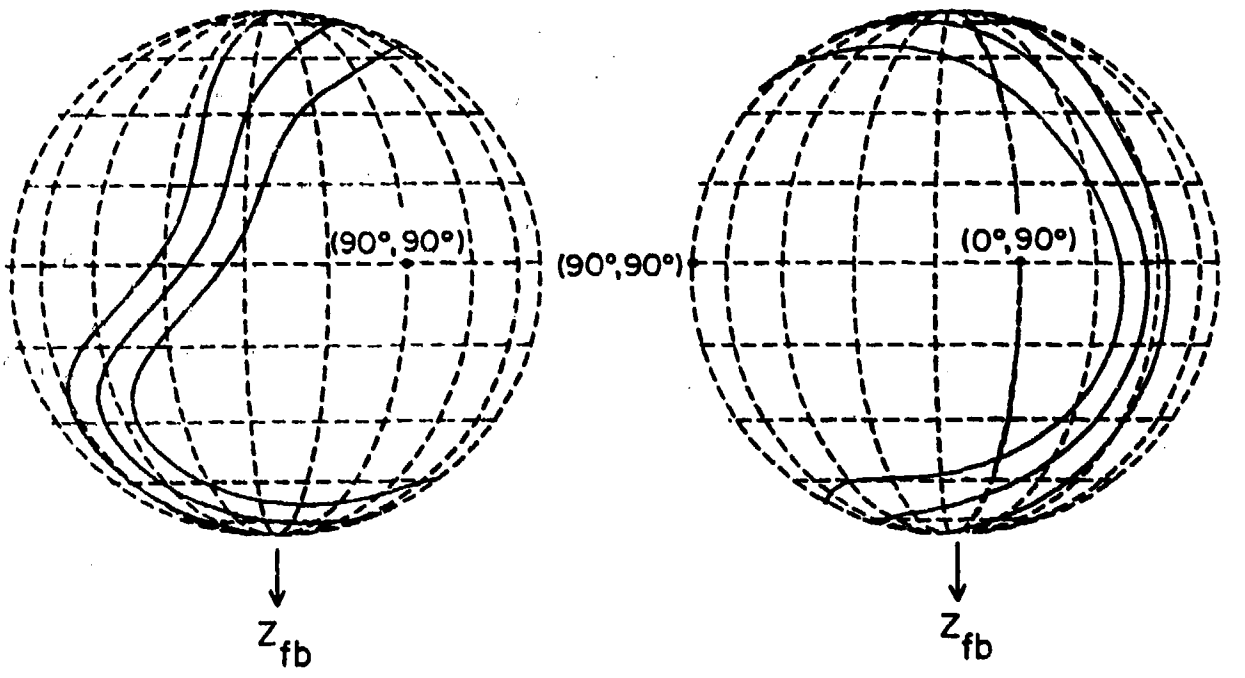

Fig. 3.19 Globographic representations for the sample mean, $\bar{\theta}$, and the 95% Confidence Interval for the subject-based population mean, μ_θ.

and from Eq. (3.4.7) the sample variance

$$S_f^2(\phi, \theta) = (S_{C_1}^2 + S_{C_2}^2 \cos^2\phi + S_{C_3}^2 \sin^2\phi)\theta^2 + (S_{C_4}^2 \cos^4\phi + S_{C_5}^2 \cos^2\phi\sin^2\phi + S_{C_6}^2 \sin^4\phi)\theta^4 + (S_{C_7}^2 \cos^6\phi + S_{C_8}^2 \cos^4\phi\sin^2\phi + S_{C_9}^2 \cos^2\phi\sin^4\phi + S_{C_{10}}^2 \sin^6\phi)\theta^6 \quad . \tag{3.6.8}$$

Note that, in this case, the functional expansion for the force (moment) properties, i.e. Eq. (3.3.1), has two independent variables, ϕ and θ.

Fig. 3.21 shows both the space-based and the subject-based sample means for the passive resistive force (moment) property in the form of a constant contour map. Since the difference between these two contour maps is imperceptible they are shown in two separate figures rather than in a superimposed format.

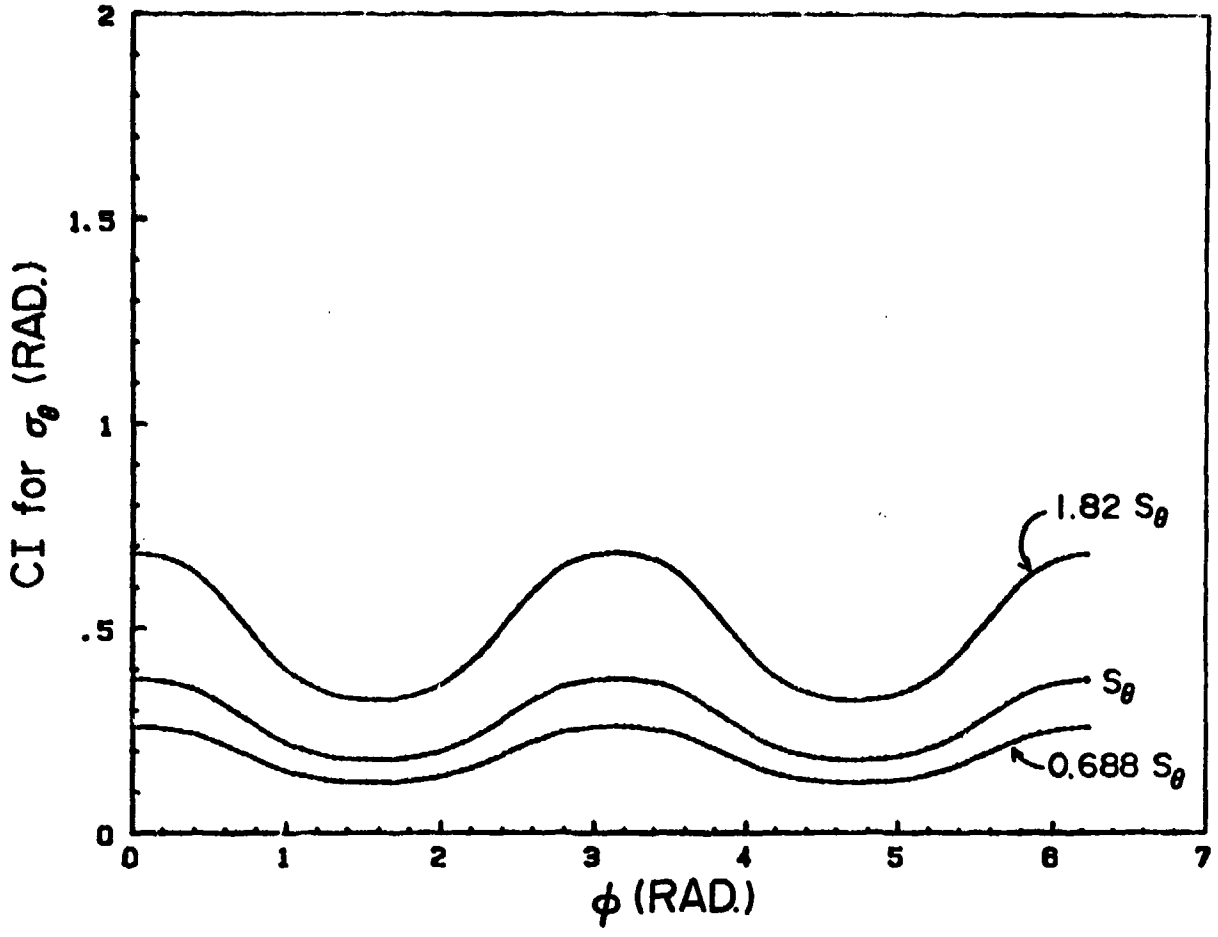

Fig. 3.20 The 95% Confidence Interval (CI) for the population standard deviation, σ_θ. The subject-based sample standard deviation, S_θ, is also shown.

It should be mentioned that the force (moment) data were collected beyond the maximum voluntary sinus up to the point, which will be referred to as the maximum forced sinus, where the subject starts experiencing discomfort or the upper arm can no longer be moved (i.e. adduction into the torso occurs). The raw data for the maximal forced sinus are curve fitted by the same functional expansion used for the maximal voluntary sinus. Table 3.6 lists the subject-based coefficients as well as their sample means and sample variances for the ten subjects' maximal forced sinuses. The statistical analysis procedure is also applied to the maximum forced sinuses. Fig. 3.22, for comparison, displays the space-based as well as the subject-based sample means for the maximal forced sinuses. With the exception of the region $0 < \phi < \frac{\pi}{2}$,

Table 3.4 Subject-based coefficients for the passive resistive force (moment) data for all ten subjects

COEFFICIENTS		C_1	C_2	C_3	C_4	C_5	C_6	C_7	C_8	C_9	C_{10}
SUBJ. NO.	1	-21.36600	-4.80500	-0.72700	22.06600	4.38400	16.55500	0.51300	-4.84200	1.79200	-0.10900
	2	-33.74500	0.23400	5.61000	31.49600	8.40000	22.99200	-3.53400	-8.05100	0.09300	-1.57300
	3	-30.76300	-4.94500	-0.35900	26.06300	7.38400	22.98300	-0.91700	-6.41200	-0.49900	-1.71500
	4	-26.52200	3.19000	5.28400	25.72400	6.65400	17.86100	-3.62800	-6.36300	-2.08500	-1.64000
	5	-15.06400	-2.25400	-4.62300	19.08300	5.13200	12.21000	-3.36300	-2.72200	1.26600	1.03000
	6	-20.32000	-0.93700	8.20800	16.10400	6.94600	16.73100	-1.31900	-3.95400	0.22300	-1.62800
	7	-19.38200	-2.32700	-1.02800	13.51900	2.13400	12.15200	-0.16100	-1.02800	-0.29300	0.34000
	8	-16.09600	-0.92600	4.27800	10.56800	1.66300	12.45500	-0.90400	-1.70600	1.03100	-0.21500
	9	-17.80500	-6.06200	2.62300	17.43000	4.11000	13.35300	0.85200	-2.15800	1.14300	-0.08700
	10	-13.86800	-1.53400	2.86600	14.00700	4.75400	10.54000	-1.21800	-4.11600	-0.56000	-0.46200
Sample Mean		-21.49310	-2.03660	2.21320	19.60600	5.15610	15.78320	-1.36790	-4.13520	0.21110	-0.60590
Sample Variance		45.48725	7.51404	14.91813	43.76720	4.90238	20.00472	2.68291	5.27504	1.31021	0.94889

Table 3.5 Space-based coefficients for the passive resistive force (moment) data for all ten subjects

COEFFI-CIENTS		C_1	C_2	C_3	C_4	C_5	C_6	C_7	C_8	C_9	C_{10}
SUBJ. NO.	1	-21.77200	-0.49800	0.53500	22.69200	3.95200	16.39900	0.39000	-4.08200	1.00600	-0.50400
	2	-35.05500	2.27200	6.50200	32.33400	7.19800	23.12200	-3.86000	-7.05000	0.02700	-1.58800
	3	-31.81800	-5.62700	-0.36800	27.31800	7.13200	22.53100	-1.37600	-5.83300	-0.01000	-1.19700
	4	-24.89000	0.55200	4.36000	25.49800	7.21700	16.86000	-3.60000	-6.66600	-1.48000	-1.30600
	5	-14.96100	-2.44300	-4.64400	19.10400	4.96000	12.10800	-3.39300	-2.63000	1.36600	1.07700
	6	-20.43000	-1.66200	7.41400	15.83900	7.17000	17.24500	-0.87800	-3.88500	0.09300	-1.81800
	7	-19.40200	-2.28600	-1.02700	13.52000	2.14500	12.17000	-0.15300	-1.03400	-0.30000	0.32900
	8	-16.03200	-0.45800	4.93200	10.56600	1.53100	12.35600	-0.96300	-1.71900	1.11200	-0.23700
	9	-17.44700	-8.43000	1.56400	17.05700	4.06400	13.25400	0.89800	-2.46100	1.45700	0.15100
	10	-13.17800	-2.31000	2.13100	13.11400	5.37400	10.94800	-0.69100	-1.43800	-0.94400	-0.69300
Sample Mean		-21.49850	-2.08900	2.13990	19.70420	5.07430	15.69930	-1.36260	-3.97980	0.23270	-0.57860
Sample Variance		51.73908	9.36730	13.86847	49.71848	4.58292	19.00889	2.87292	4.24702	0.98632	0.85544

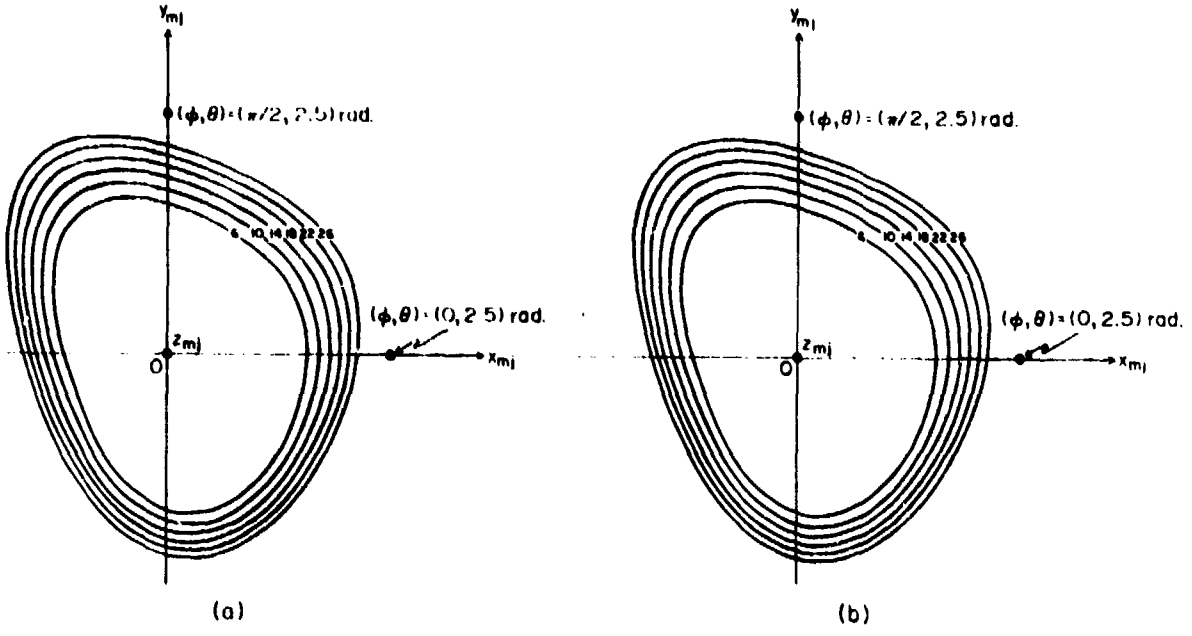

Fig. 3.21 Constant contour maps of (a) space-based and (b) subject-based sample means for the passive resistive force (moment) in Newtons (Newton-Meters).

these two sample means have indistinguishable difference. Finally, Fig. 3.23 shows the globographic representations of the subject-based mean maximal voluntary and mean maximal forced sinuses.

In computing the sample means, we found two different alternatives to represent the individual joint sinus and passive resistive property. For the shoulder complex investigated in this study, it was established that the difference between the subject-based and the space-based sample means is indicernible even though each one possesses a particular anatomical or physical significance. In the next two chapters, for simplicity, we shall adopt the subject-based approach in representing the joint properties for the hip and humero-elbow complexes.

To obtain some physical insights into the nature of the joint property of the human shoulder complex, let us superimpose the three most important results, i.e., the (subject-based) sample means of the passive resistive force (moment), maximum voluntary sinus, and maximum forced sinus, on the same figure as shown in Fig. 3.24. First, several observations concerning the passive resistive properties beyond the

Table 3.6 Subject-based coefficients of the maximum forced sinuses for all ten subjects

COEFFI-CIENTS		C_1	C_2	C_3	C_4	C_5	C_6	C_7	C_8	C_9	C_{10}
SUBJ. NO.	1	1.95847	-0.13361	-0.42477	-0.19760	-0.06931	0.86523	0.71596	-0.33193	-0.38737	-0.80224
	2	2.05970	-0.15205	-0.44746	-0.37028	0.18673	0.71718	0.92062	0.10291	-0.72357	-0.76177
	3	2.02944	0.04465	-0.02249	-0.05501	-0.01525	0.78285	0.27618	-0.60899	-0.21055	-0.43102
	4	2.06142	-0.06659	-0.14934	-0.22026	0.01678	0.23767	0.38708	-0.21028	-0.20828	-0.05278
	5	2.02973	-0.04433	0.13719	-0.42731	-0.17474	-0.30285	-0.07285	-0.11544	-0.30782	1.04693
	6	2.02761	-0.11431	-0.22517	-0.13266	0.09089	-0.30028	0.54808	-0.26533	-0.24242	0.74863
	7	2.14849	-0.12938	0.12166	0.05062	0.06783	0.08645	0.15261	-0.99712	-0.69896	0.21765
	8	1.95496	-0.29534	-0.26107	-0.08081	0.49858	0.42557	0.84891	-0.79603	-0.58480	0.19829
	9	1.83864	-0.15643	0.14464	-0.12550	0.46590	0.16682	-0.31702	-0.41109	-1.26334	-0.78313
	10	1.99501	-0.15882	-0.26241	-0.56146	-0.36536	-0.01707	0.61799	0.20085	0.11311	0.98942
Sample Mean		2.01035	-0.12062	-0.13892	-0.21203	0.07020	0.26616	0.40775	-0.34324	-0.45140	0.03700
Sample Variance		0.00674	0.00784	0.05030	0.03538	0.07038	0.18028	0.16174	0.14207	0.14629	0.52602

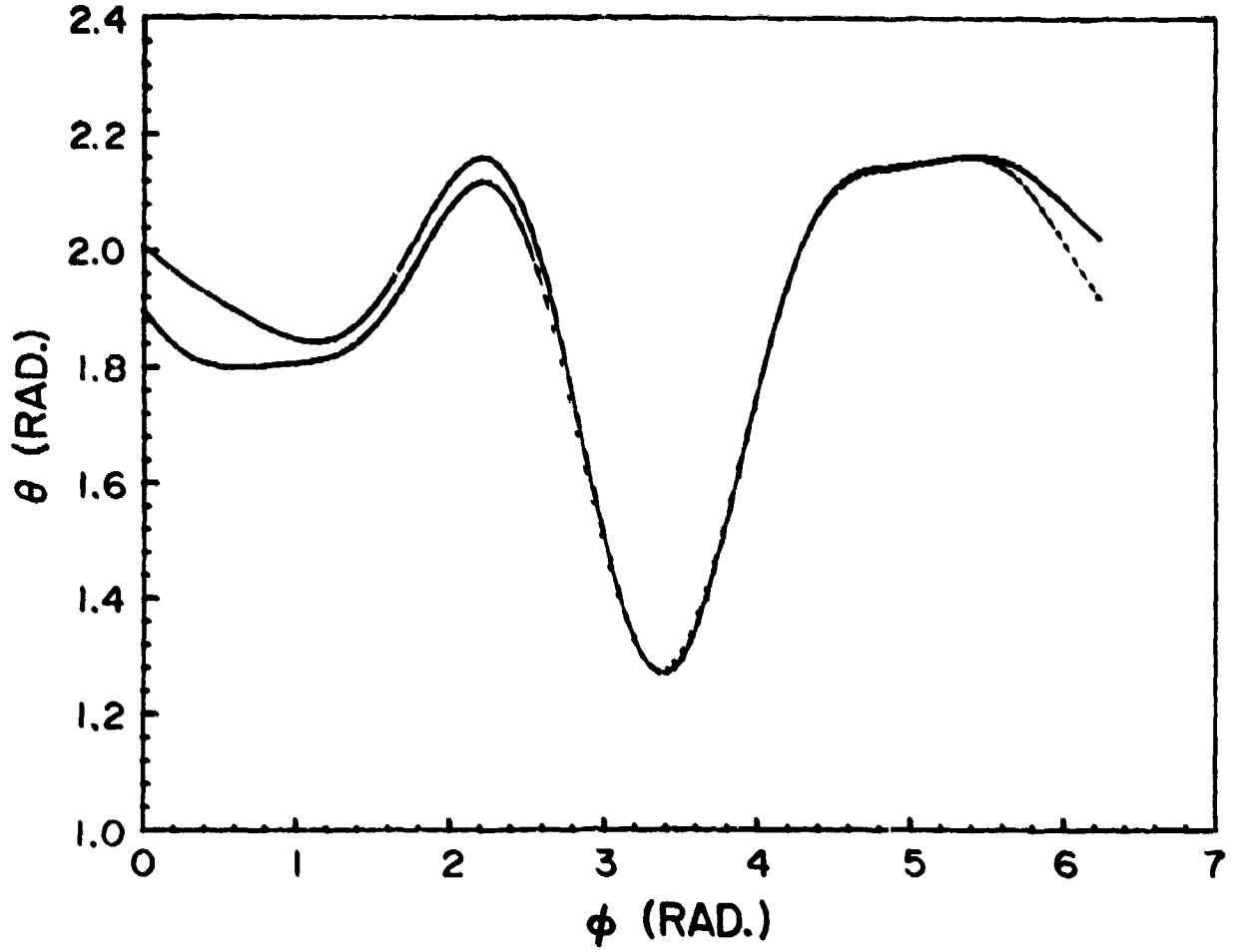

Fig. 3.22 Space-based and subject-based sample means for the maximal forced sinuses.

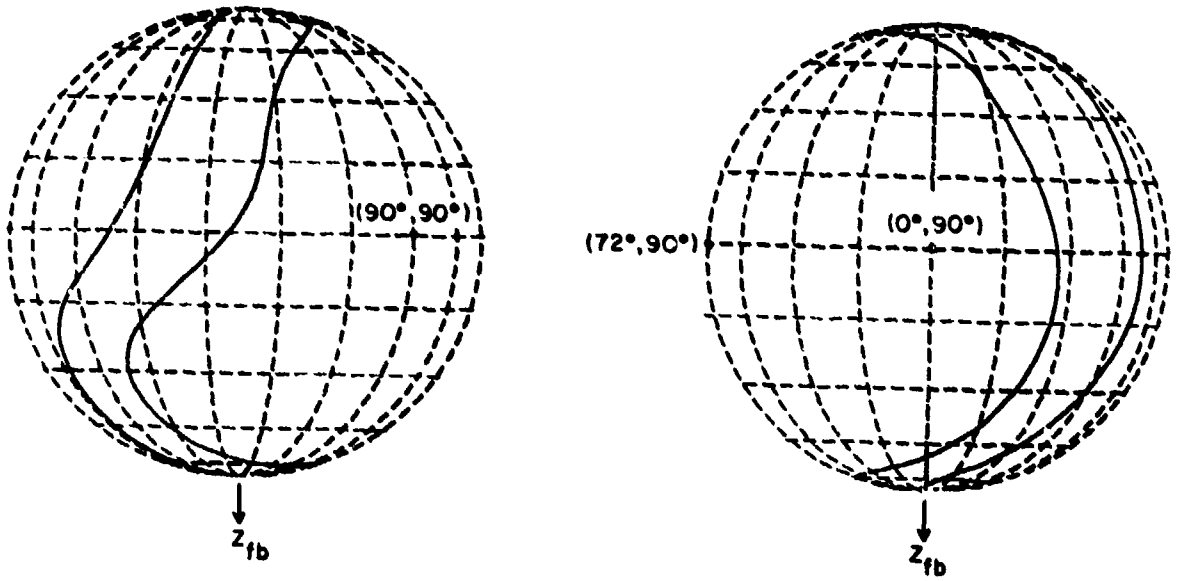

Fig. 3.23 Globographic representations of the subject-based mean maximal voluntary (inner curve) and mean maximal forced (outer curve) sinuses.

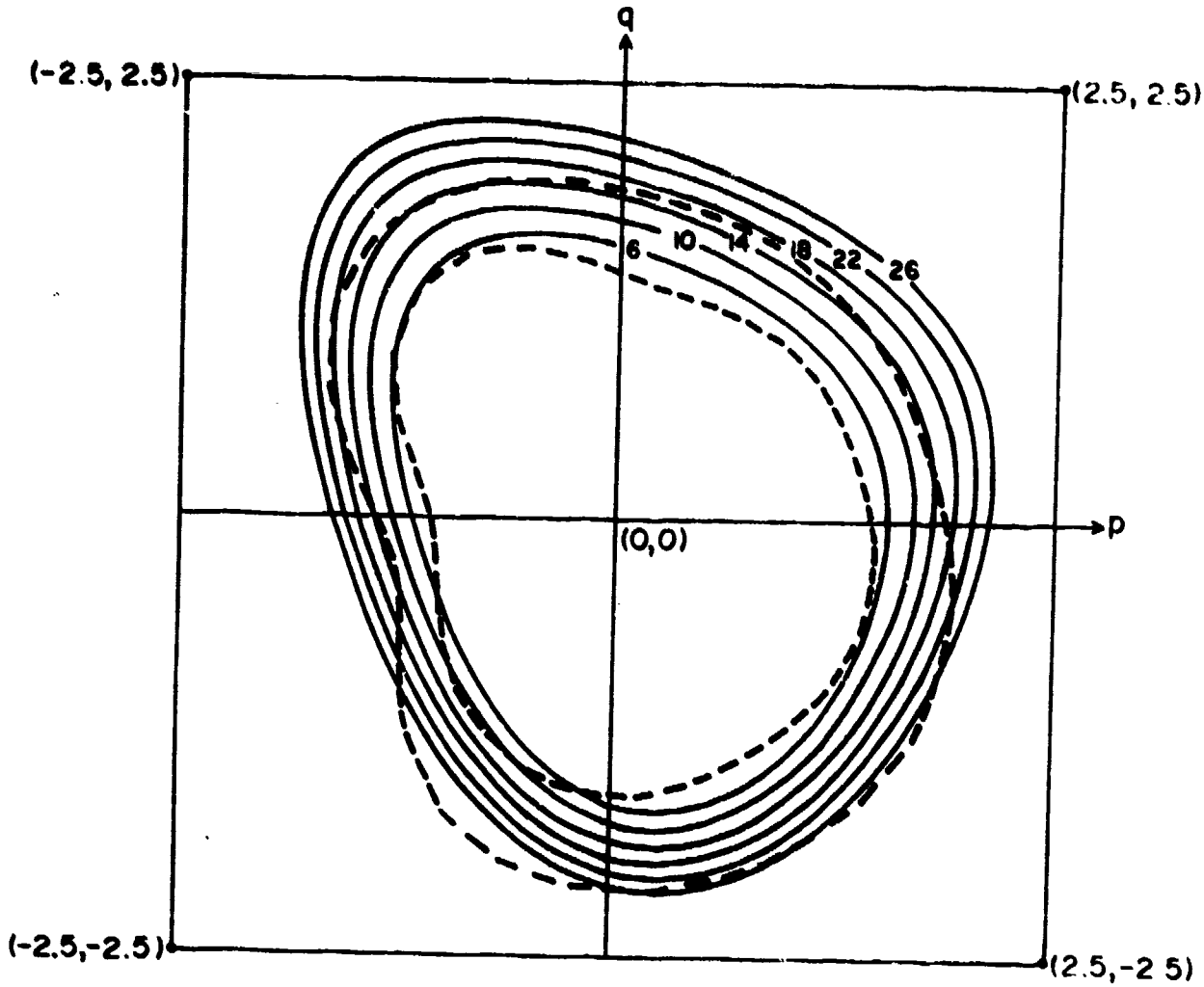

Fig. 3.24 Subject-based sample means of the passive resistive force (moment), maximum voluntary sinus (inner dashed), and maximum forced sinus (outer dashed).

maximal voluntary shoulder complex sinus can be made:

1. The constant resistive force (moment) contours are not simply an outward conformal expansion of the maximal voluntary sinus as one might surmise and adopt to use in currently existing multisegmented total-human-body models.

2. The shoulder complex is least resilient in the two rear quadrants ($0 < \phi < \pi$). In this region, more or less constant

force (moment) values [between 14 and 18 Newtons (Newton-Meters)] were observed to initiate discomfort.

3. The lower front portion ($\pi < \phi < \frac{3}{2}\pi$) of the plot exhibits the most resilient behavior due to adduction of the upper arm into the torso. No real discomfort was observed and the maximal forced sinus in this region is based on the θ values reached as far as possible during the constant-ϕ sweeps for the force (moment) levels which were applied.

4. The upper front region ($\frac{3}{2}\pi < \phi < 2\pi$) exhibits an intermediate (transitional) characteristic in terms of resilience. In this region, discomfort initiates at the force (moment) level of about 26 Newtons (Newton-Meters).

Second, the maximum voluntary and forced sinuses specify the applicable domain of the passive resistive property. The resistive forces (moments) below the maximal voluntary sinus are appreciably lower in magnitude and thus can be neglected. Therefore, the maximal voluntary sinus can be considered as the lower limit of the applicable range for the expansion function $\bar{f}(\phi, \theta)$. In fact, Fig. 3.9 shows that in the neighborhood of the origin (pole), dashed curves indicate both lacking good fit and being outside the applicable domain. In the strict sense, the upper limit is the maximal forced sinus for the applicability of $\bar{f}(\phi, \theta)$. However, the extrapolated values by $\bar{f}(\phi, \theta)$ beyond this upper limit are most likely predictions and can be used up to the point of impending injury for the simulation studies of multisegmented mathematical models.

4. BIOMECHANICAL PROPERTIES OF THE HUMAN HIP COMPLEX

4.1 Introduction

This chapter deals with the in-vivo biomechanical properties of the human hip complex in the sitting position with the torso being fixed. The data so obtained are suitable for simulating a seated pilot as well as an occupant in a car.

The term "hip complex" refers to the combination of the hip joint, pelvis, lumbar spine, and their articulations. Fig. 4.1 shows the principal bones and ligaments of the hip complex. Since the femoral motion, while sitting with torso being fixed, is normally accompanied by lumbar flexion and pelvic tilting, it is more appropriate to use the term "hip complex sinus," rather than "hip joint sinus," to designate the range of extreme allowable motion of the femur with respect to torso. The human hip has been normally modeled as a three-degree-of-freedom ball and socket joint by most researchers (Dempster, 1955; Johnston and Smidt, 1969; Chao et al., 1970; Lamoreux, 1971), although in some cases it has also been simplified by neglecting the axial rotation (Saunders et al., 1953; Paul, 1965). In planar motion studies, it is even assumed as a one-degree-of-freedom revolute (or hinge) joint (Clayson et al., 1966; Beckett and Chang, 1968).

Functionally, unlike the shoulder which has sacrificed stability in favor of mobility, the hip provides essential stability for support of the body as well as a certain degree of mobility. Structurally, the pelvis is more rigid than the rather freely movable scapula. The interplay among the hip joint, pelvis, and lumbar spine is similar to that between the shoulder joint (the glenohumeral joint) and the shoulder girdle which includes the clavicle and the scapula. However, the articulations of the sacroiliac joint and symphysis pubis provide much less mobility than those of the shoulder girdle. Furthermore, the joint capsule, the ligaments, and the muscles have reduced the freedom of the hip joint whose bony structure permits almost as much mobility as is found in the glenohumeral joint. For example, hip hyperextension is practically insignificant mainly due to the ligamentous check of the iliofemoral (Y) ligament. Finally, it should be noted that hip flexion is also dependent upon the amount of knee flexion due to the interaction

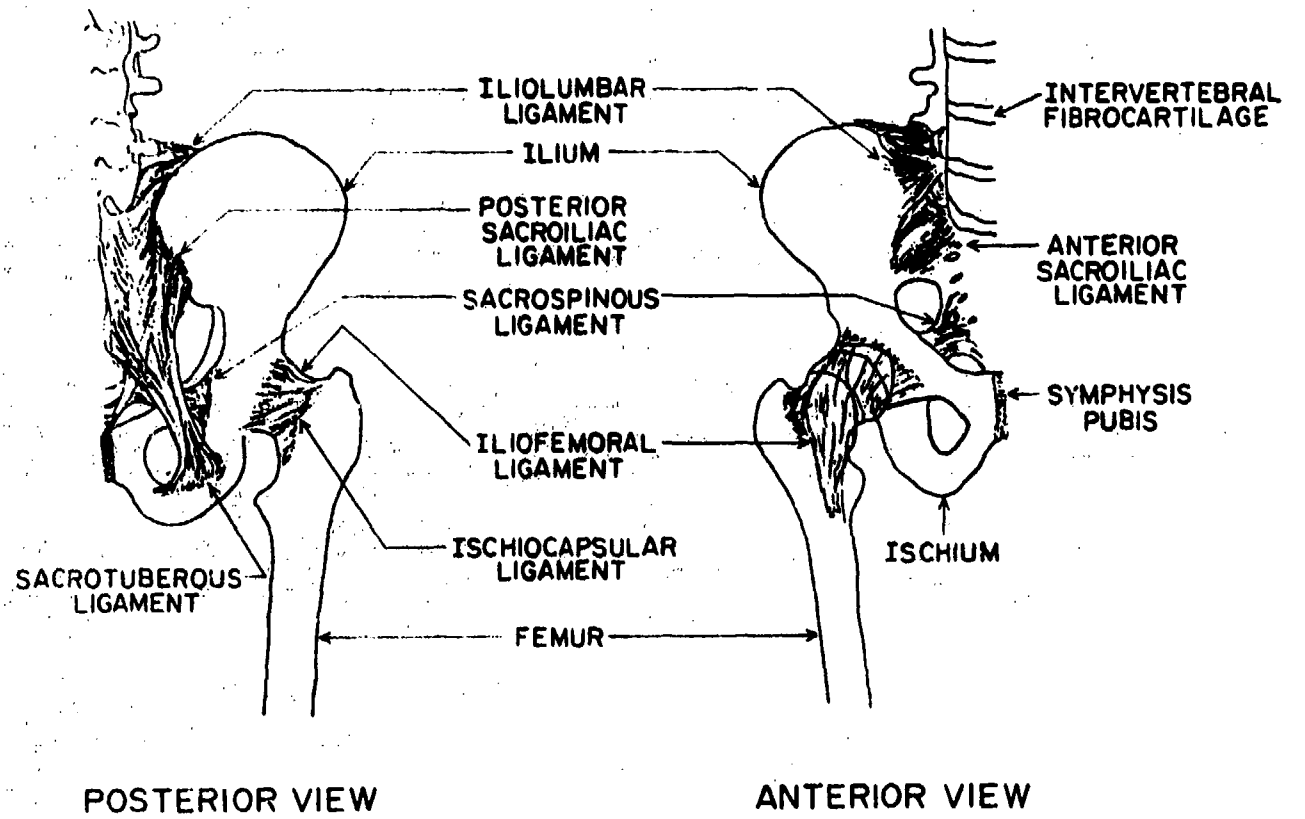

Fig. 4.1 Principal bones and ligaments of the hip complex.

of the two-joint muscles between the hip and knee joints. With the knee in full extension, hip flexion is limited by the hamstrings. More detailed anatomical and kinesiological descriptions are available in standard textbooks (Steindler, 1973; Norkin and Levangie, 1983; Gray's Anatomy, 1973) and, therefore, will not be made here.

4.2 Determination of the Hip Complex Sinus

The major components of the data acquisition system used in this study are the sonic digitizer which is linked with the PDP-11/34 minicomputer, digitizer sensor assembly, torso restraint system, and six sonic emitters mounted on a cylindrical thigh cuff as shown in Fig. 4.2. The thigh cuff is, in turn, attached to an orthotic brace, which is held onto the thigh by three Velcro straps. The front part of the brace is shaped so that the patella can move freely.

Fig. 4.2 Major components of the data acquisitions system. 1) Sonic Digitizer, 2) Digitizer Sensor Assembly, Torso Restraint System, 4) Thigh Cuff with Six Sonic Emitters.

The quantitative determination of the hip complex sinus involves the following basic steps: (1) immobilizing the torso to be treated as the fixed body and defining the fixed body axis system as shown in Fig. 3.2(a), (2) having the subject move the upper leg along the maximal voluntary range of motion and monitor, with respect to the fixed body axis system, the 3-D coordinates of a distal point on the moving body segment; this point (to be referred to as the knee joint reference point) is selected as being on the mechanical axis of the femur at the level of the femoral lateral epicondyle, (3) fitting the knee joint reference point coordinates to a sphere using the least-squares method, thus establishing a center for the best-fitted sphere and an idealized link

length (radius of the sphere), (4) fitting a plane to the same knee joint reference point coordinates to a sphere using the least-squares method; the normal to this plane (specified by the spherical coordinates (ϕ_n, θ_n) as shown in Fig. 4.3) establishes the pole (z_{jt}-axis) of a local joint axis system with respect to which the hip complex sinus, designated by the spherical coordinates (ϕ, θ) of the vector connecting the center of the best-fitted sphere with the knee joint reference point, can be expressed as a single-valued functional relationship, i.e., $\theta = \theta(\phi)$.

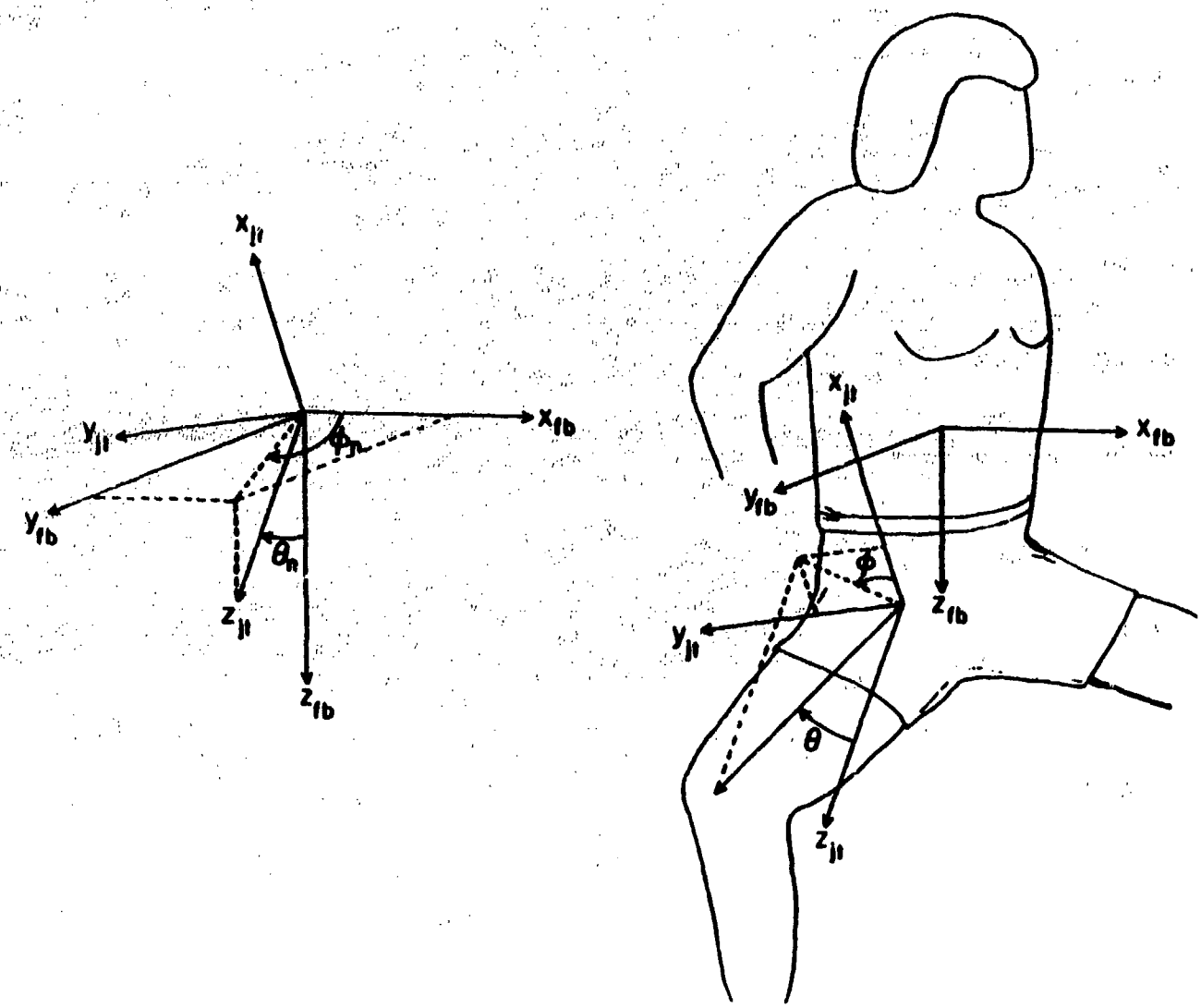

Fig. 4.3 Relative orientation between the fixed body (x_{fb}, y_{fb}, z_{fb}) and locally-defined joint (x_{jt}, y_{jt}, z_{jt}) axis systems.

Since only the knee joint reference point is monitored in this study, only the relationships between this point and the six sonic emitters on the thigh cuff need to be initialized. The calculations are the same as those used for the origin of the longitudinal axis system thoroughly discussed in Section 2.2. However, since the knee joint reference point is inaccessible, two emitters are needed to interpolate it as being located at the center. The emitter positioning for this initialization process is schematically shown in Fig. 4.4.

Before the hip complex sinus test, the subject was instructed to move his upper leg along its maximal voluntary range of motion in a counterclockwise motion as viewed from the sensor assembly. He was also instructed to displace the upper leg distally along its longitudinal axis as far as possible at all times while circumscribing the hip complex sinus. Preferred rotation of the upper leg about its longitudinal axis as well as preferred knee flexion were left up to the discretion of the subject in obtaining the maximal contour. Several sweeps of this type were practiced before data were collected so that the subject could experiment with obtaining the largest possible range of motion. In order to help maintain a constant rate of motion during data collection, a large clock with an easily visible second hand was placed in front of the subject. The subject was instructed to imagine his upper leg as the second hand, and to synchronize his hip complex sinus circumscription with the clock's 60 second sweep.

Table 4.1 lists the centers and radii of the best-fitted spheres and (ϕ_n, θ_n) values of the best-fitted planes for all ten subjects. With respect to each individual local joint axis system, Figs. 4.5-4.7 show the hip complex sinuses for three subjects and their corresponding least-squares fitted functional expansions of Eq. (3.2.1). Figs. 4.8-4.10 display the corresponding globographic representations of these three subjects' functional expansion sinuses with respect to the fixed body axis system.

4.3 Determination of the Passive Resistive Properties

As is the case for the forced tests on the shoulder complex, it is also desirable to perform a series of forced tests in which the upper leg is forced outward in the direction of increasing θ for a constant-ϕ value

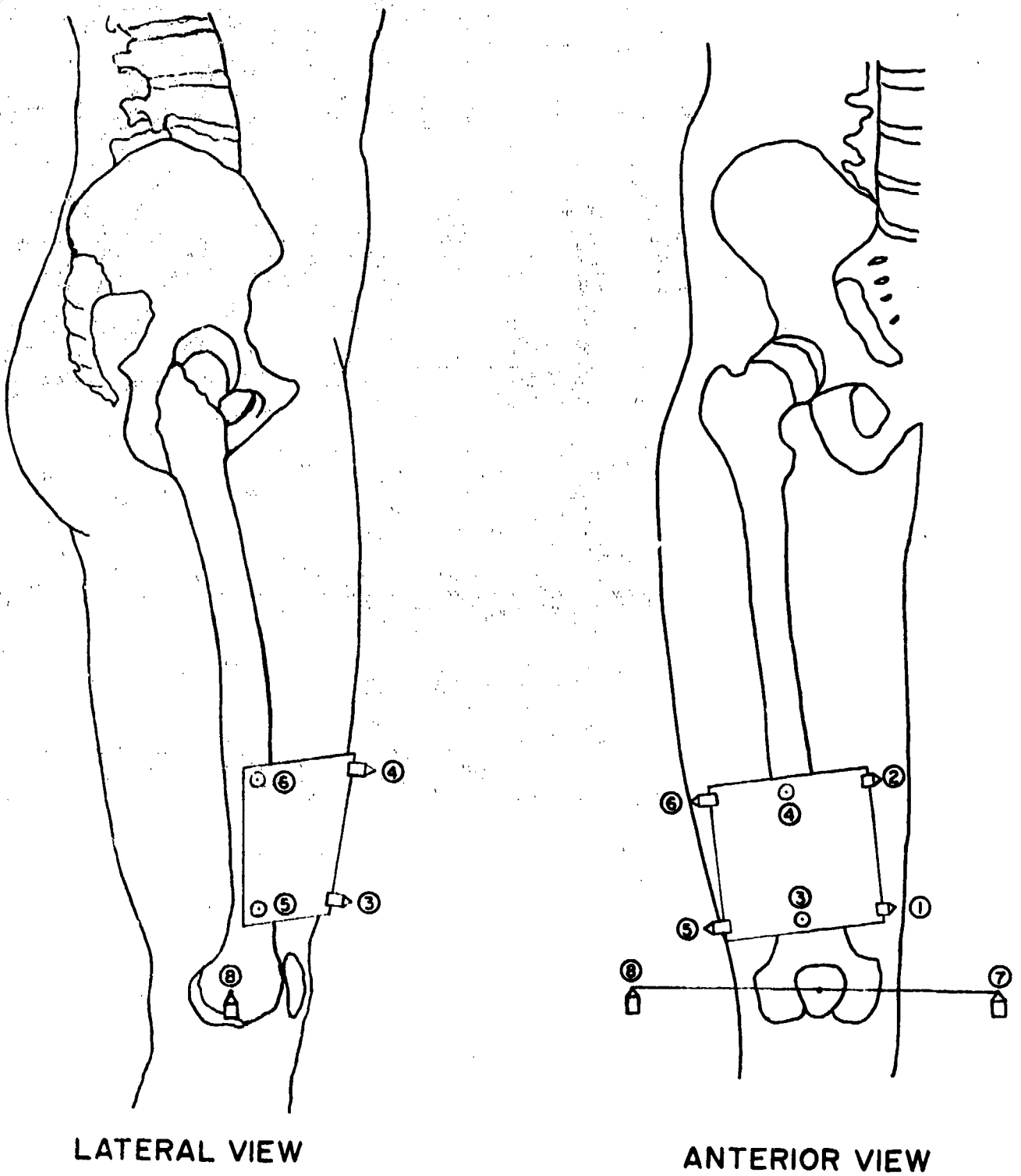

Fig. 4.4 Emitter positioning for initialization process.

Table 4.1 Centers and radii of the best-fitted spheres and and (ϕ_n, θ_n) for all ten subjects.

SUBJECT No.	CENTER (cm) x_{fb}	y_{fb}	z_{fb}	RADIUS (cm)	ϕ_n (deg.)	θ_n (deg.)
1	1.77	6.14	20.85	47.82	47.22	64.85
2	3.63	5.98	27.45	43.76	53.78	52.18
3	5.26	8.49	28.80	47.35	42.37	60.04
4	-0.10	5.64	31.39	45.50	47.06	52.54
5	3.24	5.96	27.57	43.79	55.17	51.40
6	3.93	6.94	26.78	46.61	37.17	52.83
7	-0.50	5.08	29.85	46.81	49.39	53.77
8	3.12	7.01	29.30	47.87	33.46	57.18
9	-1.70	6.26	18.07	50.07	36.78	68.34
10	3.84	4.40	25.16	48.90	34.54	55.35
Sample Mean	2.25	6.19	26.52	46.85	43.19	56.85
Sample St. Dev.	2.28	1.12	4.15	2.04	7.96	5.81

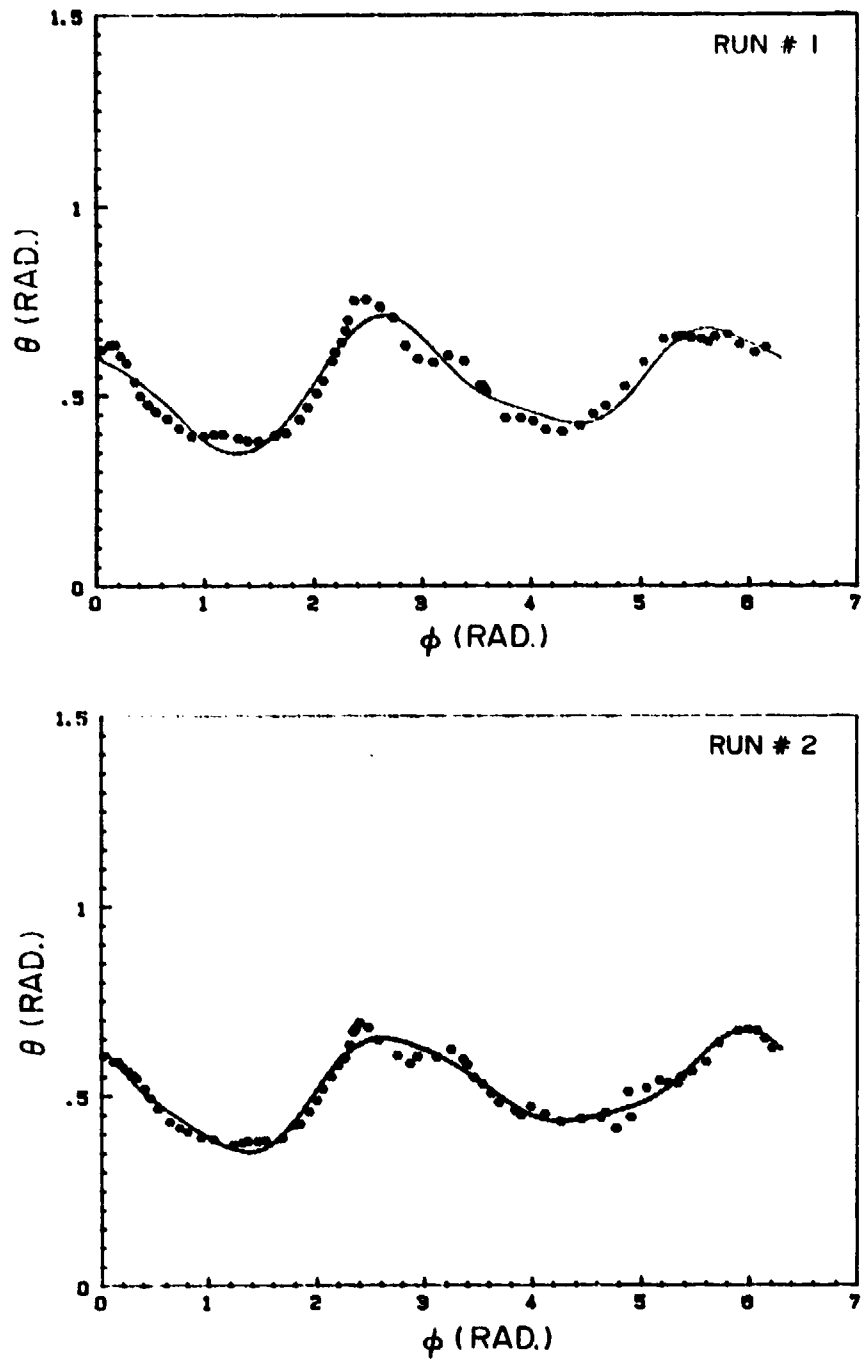

Fig. 4.5 Raw data and the functional expansions of the hip complex sinus for subject No. 1.

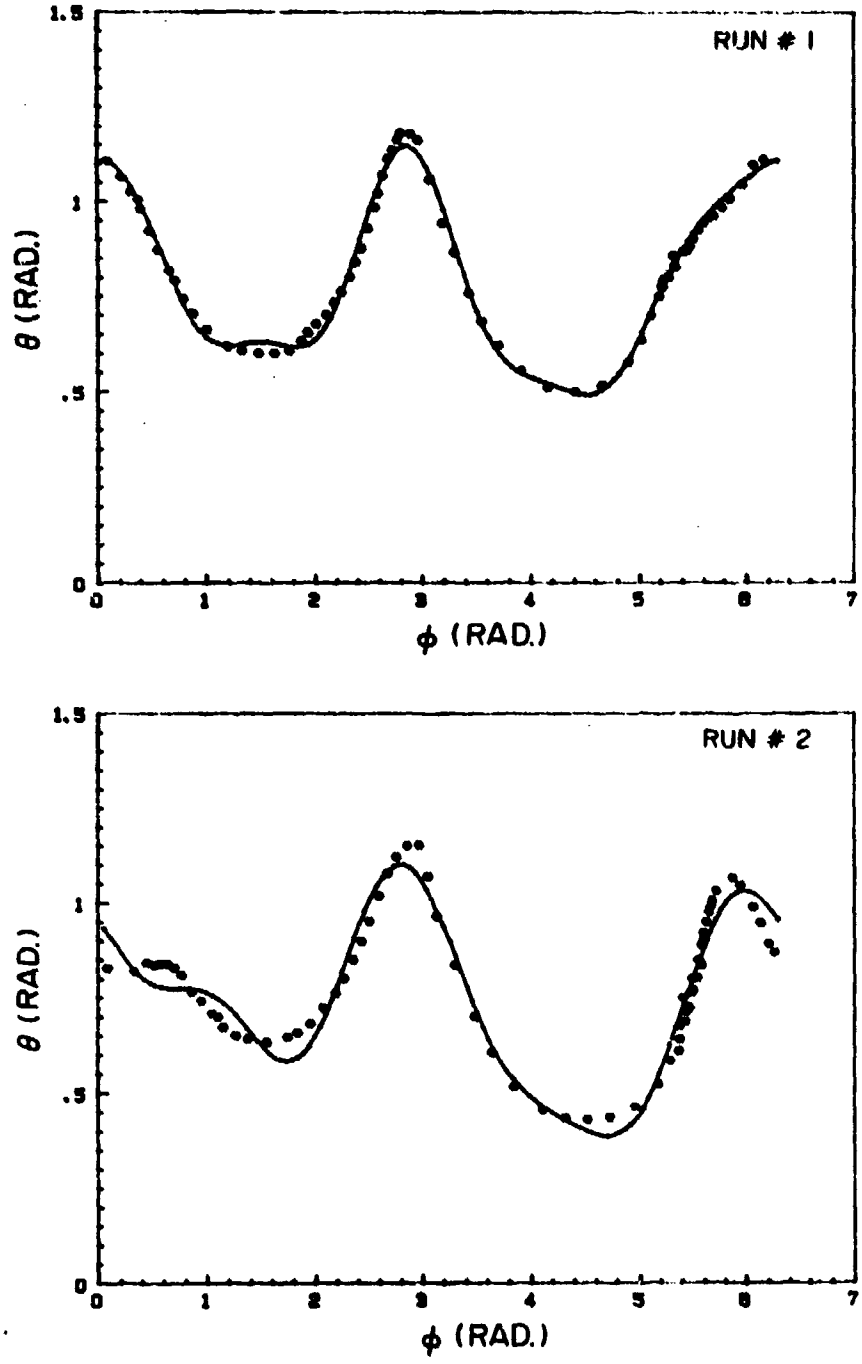

Fig. 4.6 Raw data and the functional expansions of the hip complex sinus for subject No. 2.

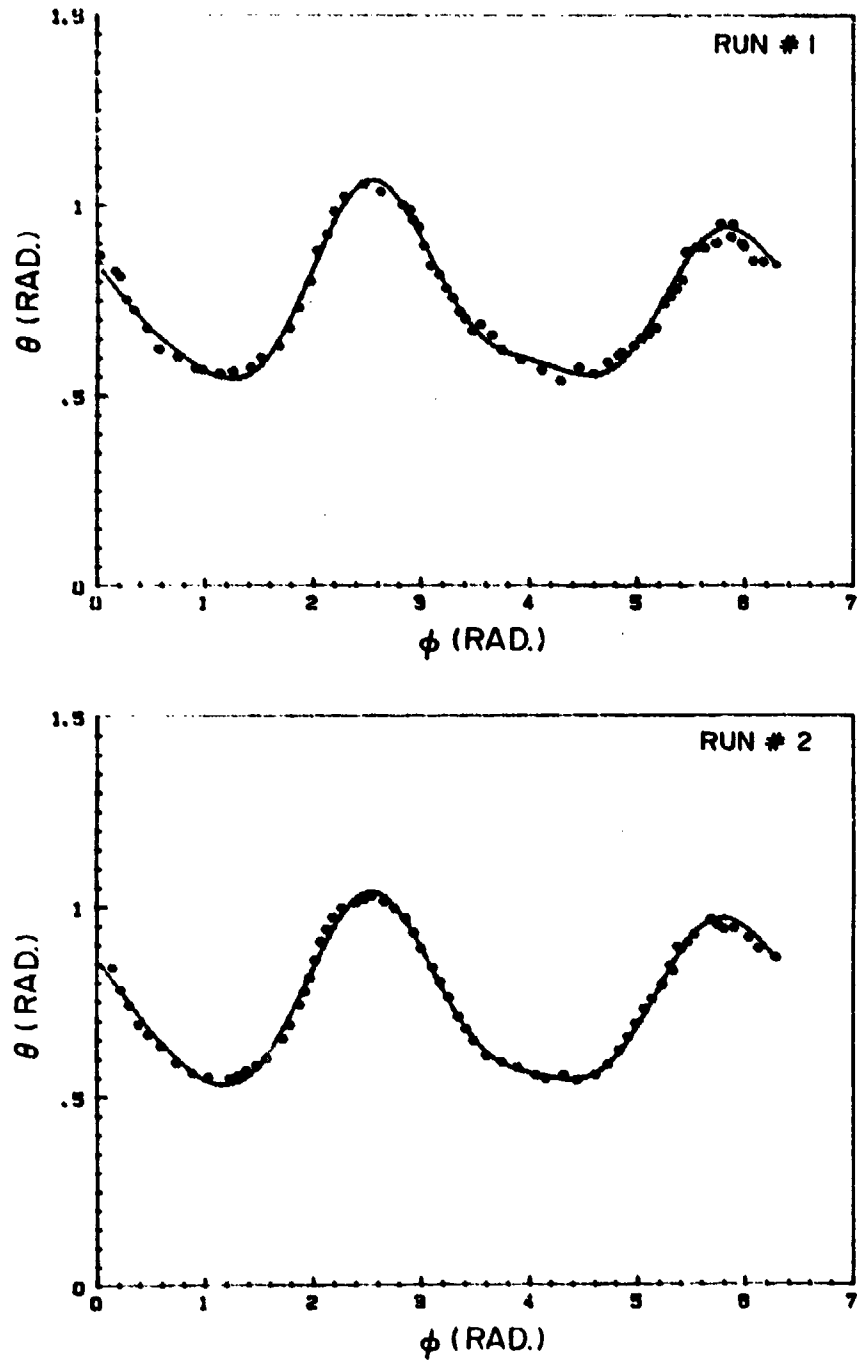

Fig. 4.7 Raw data and the functional expansions of the hip complex sinus for subject No. 3.

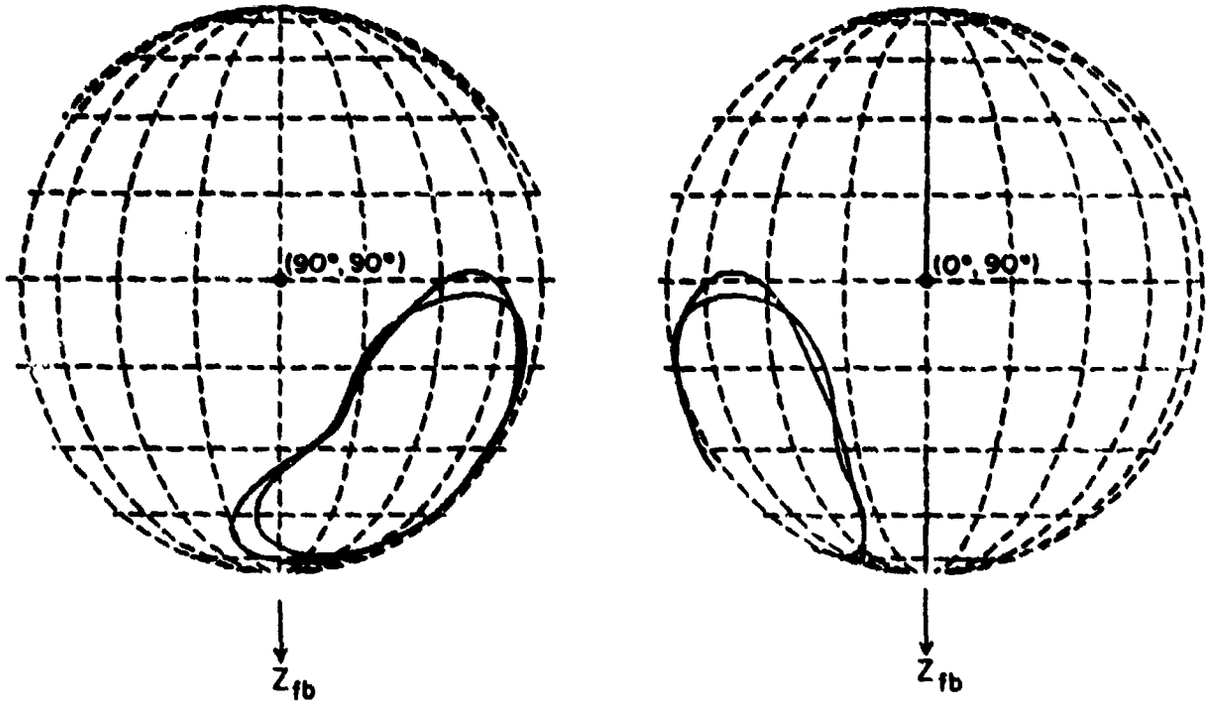

Fig. 4.8 Globographic representations of the hip complex sinuses for subject No. 1.

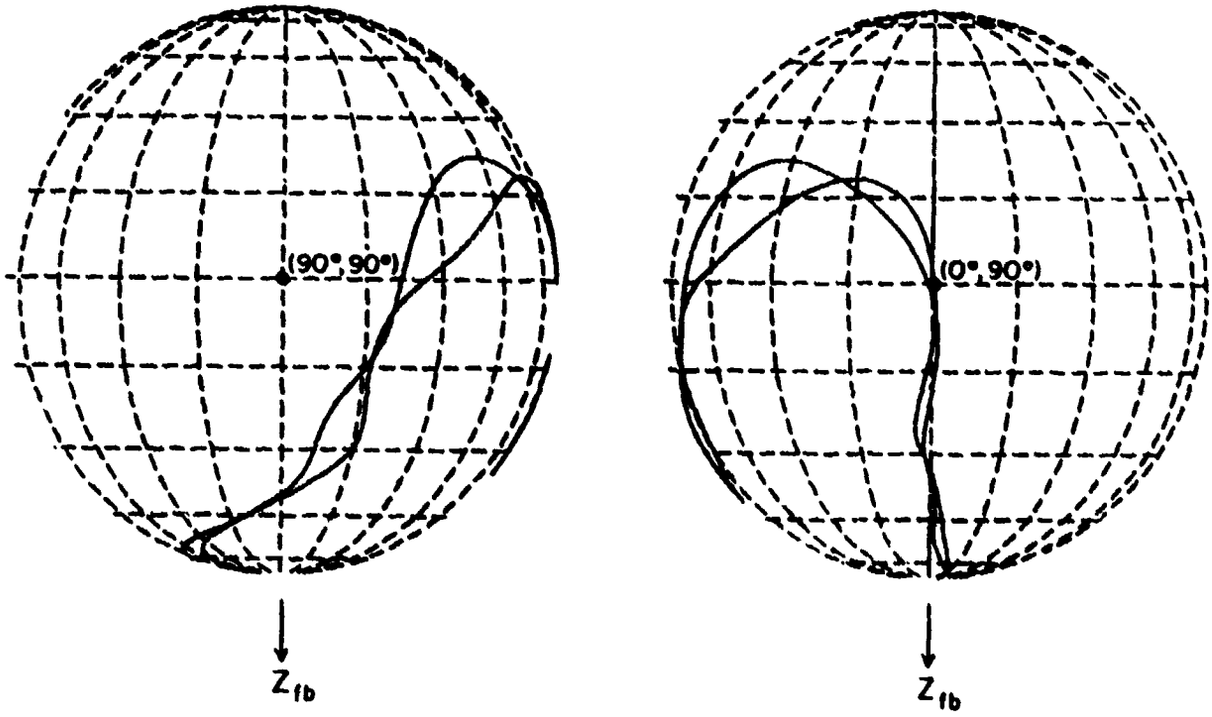

Fig. 4.9 Globographic representations of the hip complex sinuses for subject No. 2.

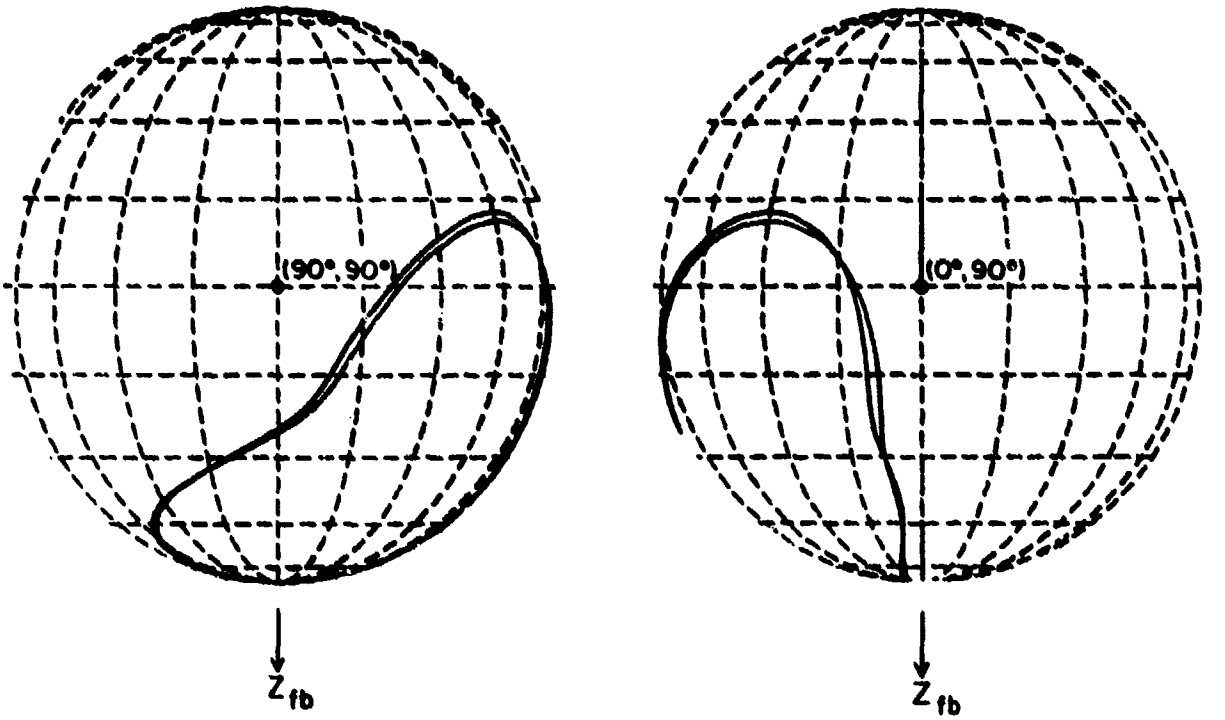

Fig. 4.10 Globographic representations of the hip complex sinuses for subject No. 3.

with respect to the local joint axis system.

For a typical forced kinematic test, the subject's torso is first rotated by an angle - $(90° - \phi_n)$ about the positioning system yaw axis, and then rotated - $(90° - \theta_n)$ about the roll axis. If the subject then extends his upper leg in an orientation parallel to the horizontal pitch axis of the positioning system, the mechanical axis of the femur will be at (ϕ_n, θ_n), i.e., coincide with the z_{jt}-axis with respect to the torso fixed body axis system. To factor out the gravitational loading of the leg, an adjustable pulley-cable system is used to hold the leg with the pulley positioned directly above the hip joint so that the horizontal component of the cable force passes through the hip joint and does not serve to either abduct or adduct the upper leg. The subject is first instructed to move his leg to its maximal voluntary position in the constrained plane of motion of the upper leg. The leg is backed-off from its maximal voluntary position, and this then is the starting orientation of the forced sweep. The force applicator is then positioned vertically

at the same level as the subject's upper leg, and the transducer front is pointed near the knee joint. The subject's upper leg is next abducted or adducted in a quasi-static manner until the subject starts experiencing discomfort or the upper leg can no longer be displaced (e.g., adduction into the torso occurs). During the entire course of each test, the subject is instructed to let his leg hang limply and not to actively (muscularly) resist the motion of the test. The bridge circuits of the force-moment transducer are all set to zero at the start of each test, so that recorded values during the sweep are departures from this "neutral" force-moment orientation, or stating it in a different manner, they are the passive resistive force-moment values.

With respect to the joint axis system, as mentioned earlier, these force sweeps take place in a direction of increasing θ, and at an approximately constant-ϕ value. By then rotating the restraint positioning system about its pitch axis, a series of constant-ϕ sweeps are obtained. In this way the tests are performed as four sub-series with each sub-series discernible by its own experimental set-up configuration as shown in Fig. 4.11. The groupings consist of constant-ϕ sweeps in: 1) the upper-rear quadrant ($0^\circ < \phi < 90^\circ$), 2) the lower-rear quadrant ($90^\circ < \phi < 180^\circ$), 3) the lower-front quadrant ($180^\circ < \phi < 270^\circ$, and 4) the upper-front quadrant ($270^\circ < \phi < 360^\circ$).

The data obtained according to the procedure outlined above are analyzed as follows. First, the force ($\vec{F}$) and moment ($\vec{M}$) vectors obtained from the force applicator transducer are used to calculate a total moment vector with respect to the center of the best-fitted sphere

$$\vec{M}_{total} = \vec{M} + \vec{r} \times \vec{F}$$

where $\vec{r}$ is the moment arm vector from the center of the best-fitted sphere to the point of force application. Next, the total moment vector is resolved into components along and perpendicular to the moment arm vector. The component along the moment arm vector is then discarded, since it does not serve to restore the moving segment to an orientation within the maximal voluntary hip complex sinus. Finally, a "normalized" moment arm vector of unit length, i.e., one meter, along the moment arm vector is used together with the remaining moment component (the passive resistive moment vector) to calculate the passive resistive force vector.

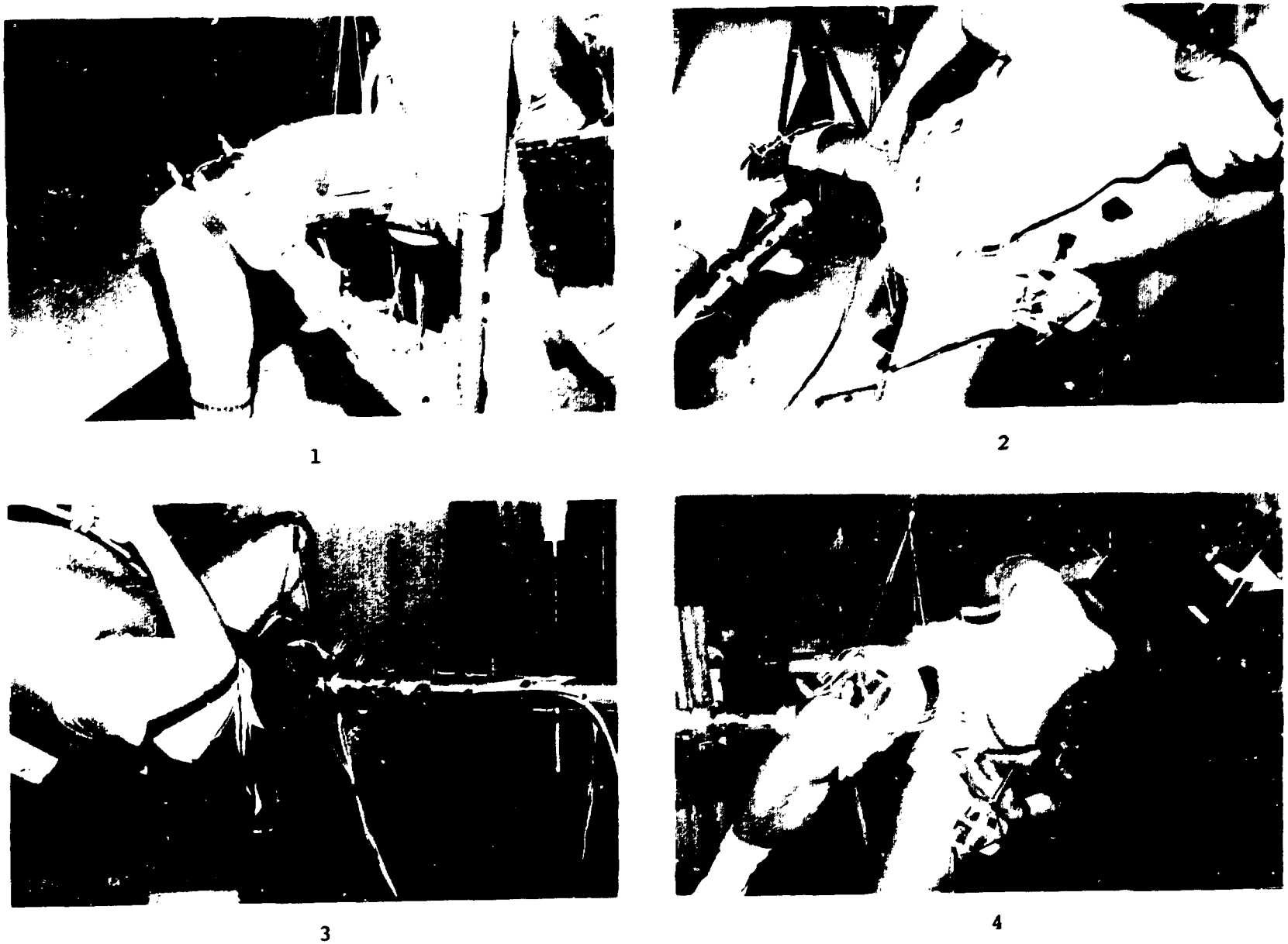

Fig. 4.11 Representative test configurations in each of the four quadrants:
1) upper-rear, 2) lower-rear, 3) lower-front, 4) upper-front

Since the moment arm is normalized to one meter, the magnitude of the resistive force vector is the same as that of the resistive moment vector. We shall refer to this magnitude as the passive resistive force (moment) property, which is assumed to be a function of ϕ and θ in this study with respect to the local joint axis system.

Figs. 4.12-4.14 show the constant resistive force (moment) contour maps for three subjects on the modified joint axis system. Fig. 4.15 displays the "goodness" of the curve fitting for the raw data of several constant-ϕ sweeps for the first subject. In Figs. 4.12-4.14, the respective maximal voluntary hip complex sinuses and maximal forced sinuses are also indicated. Finally, Figs. 4.16-4.18 show the globographic representations of the maximal forced sinuses together with the maximal voluntary sinuses (run No. 1) for the three subjects.

4.4 Statistical Data Base for the Biomechanical Properties of the Human Hip Complex

Since the functional expansions used herein are the same as those used for the shoulder complex, the statistical analysis is the same as presented in Section 3.6; thus it will not be repeated here.

Table 4.2 lists the expansion coefficients of the hip complex sinuses for all ten subjects. This table also lists the sample means and sample variances of the ten coefficients. Fig. 4.19 displays these ten sinuses as well as their sample mean, $\bar{\theta}(\phi)$, and $\bar{\theta}(\phi) \pm S_{\theta}(\phi)$. Fig. 4.20 shows the globographic representations of the latter three. Fig. 4.21 shows the $\bar{\theta}$ and $\bar{\theta} \pm S_{\theta}$ curves for two different runs. Again, this figure reveals good repeatability of the hip complex sinus tests.

For the confidence level of 95%, Fig. 4.22 shows the confidence interval of the population mean, and Fig. 4.23 its corresponding globographic representation.

Table 4.3 lists the expansion coefficients as well as their sample means and sample variances of the passive resistive force (moment) data for all ten subjects. Table 4.4 lists the expansion coefficients of the maximum forced sinuses for all ten subjects. Fig. 4.24 superimposes the sample means of the passive resistive property, the maximum voluntary and forced sinuses. Finally, Fig. 4.25 shows the globographic representations of the sample means of the maximum voluntary and forced sinuses.

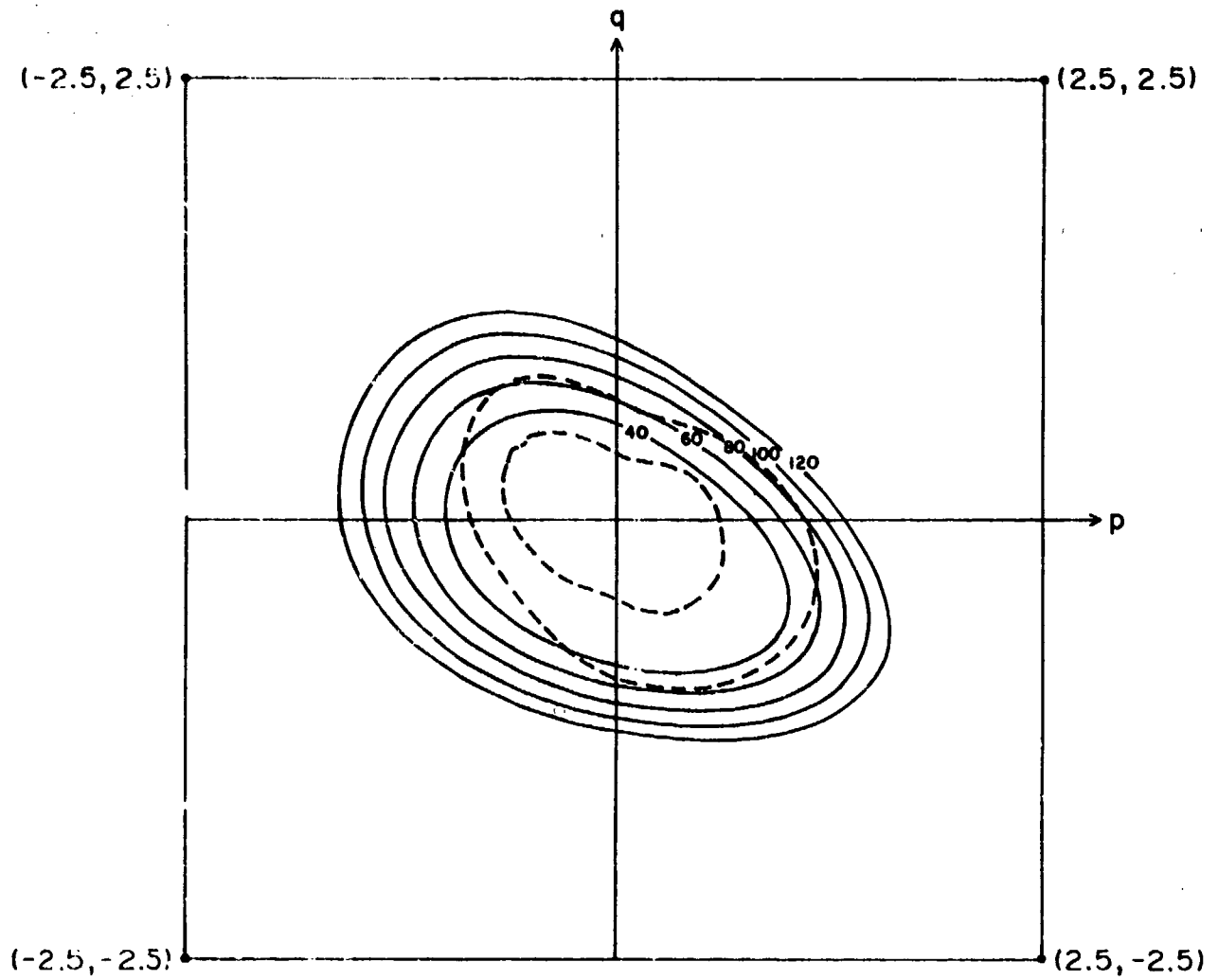

Fig. 4.12 Constant resistive force (moment), in Newtons (Newton-Meters), contour map on the modified joint axis system, in radians, for subject No. 1. The maximal voluntary hip complex sinus (inner dashed) and the maximal forced sinus (outer dashed) are also indicated.

Based on the numerical results shown in Fig. 4.24, several observations and remarks concerning the passive resistive properties of the human hip complex beyond the maximal voluntary sinuses can be made:

1. The constant resistive force (moment) contours are not simply an outward conformal expansion of the maximal voluntary sinus as one might surmise and adopt to use in currently existing multisegmented total-human-body models.

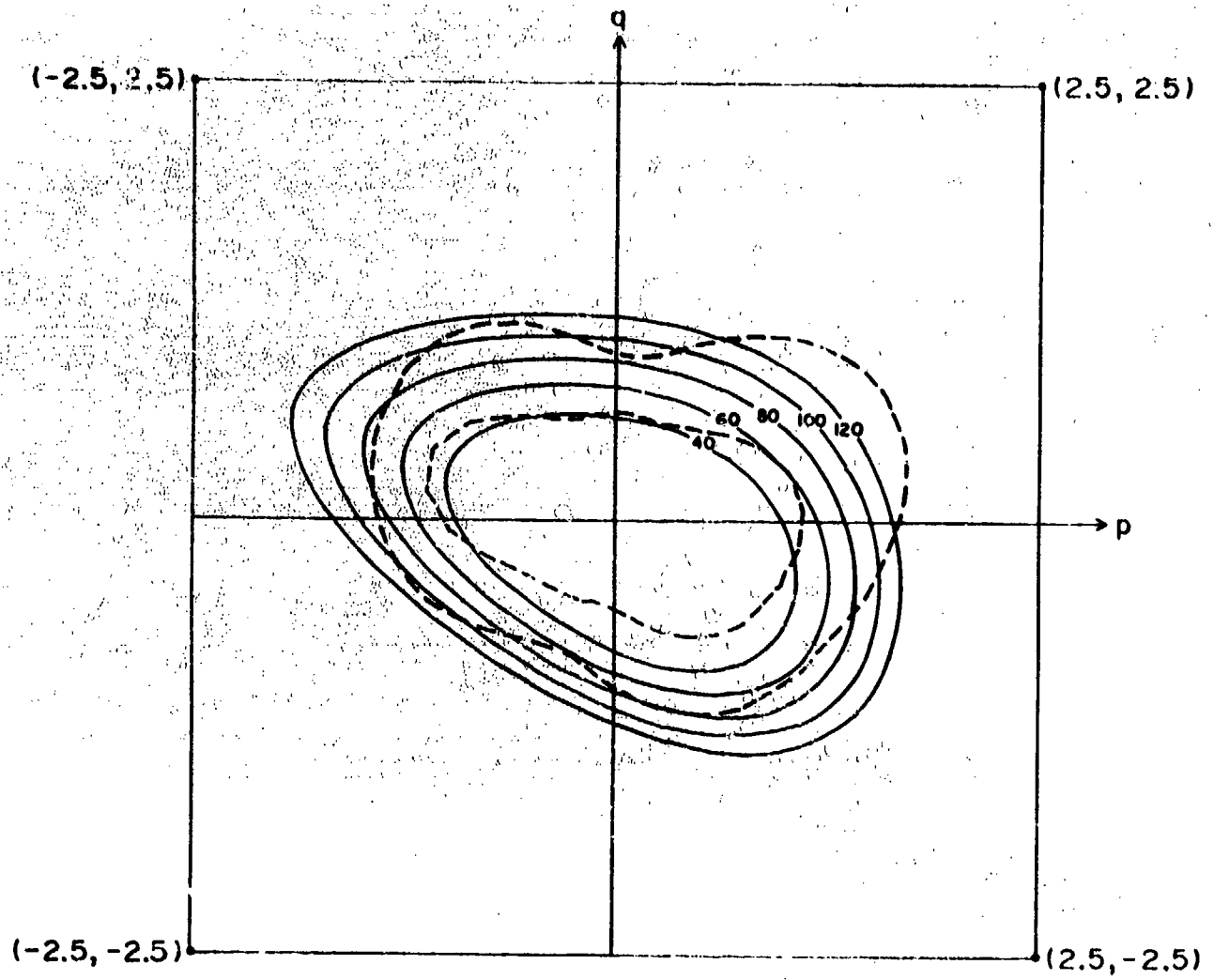

Fig. 4.13 Constant resistive force (moment), in Newtons (Newton-Meters), contour map on the modified joint axis system, in radians, for subject No. 2. The maximal voluntary hip complex sinus (inner dashed) and the maximal forced sinus (outer dashed) are also indicated.

2. The two rear quadrants ($0 < \phi < \pi$) are the most important regions in terms of pain threshold and injury potential. In this region, discomfort was observed at the force (moment) levels of approximately 60 to 80 Newtons (Newton-Meters), which are about 4.5 times those found on the shoulder complex.

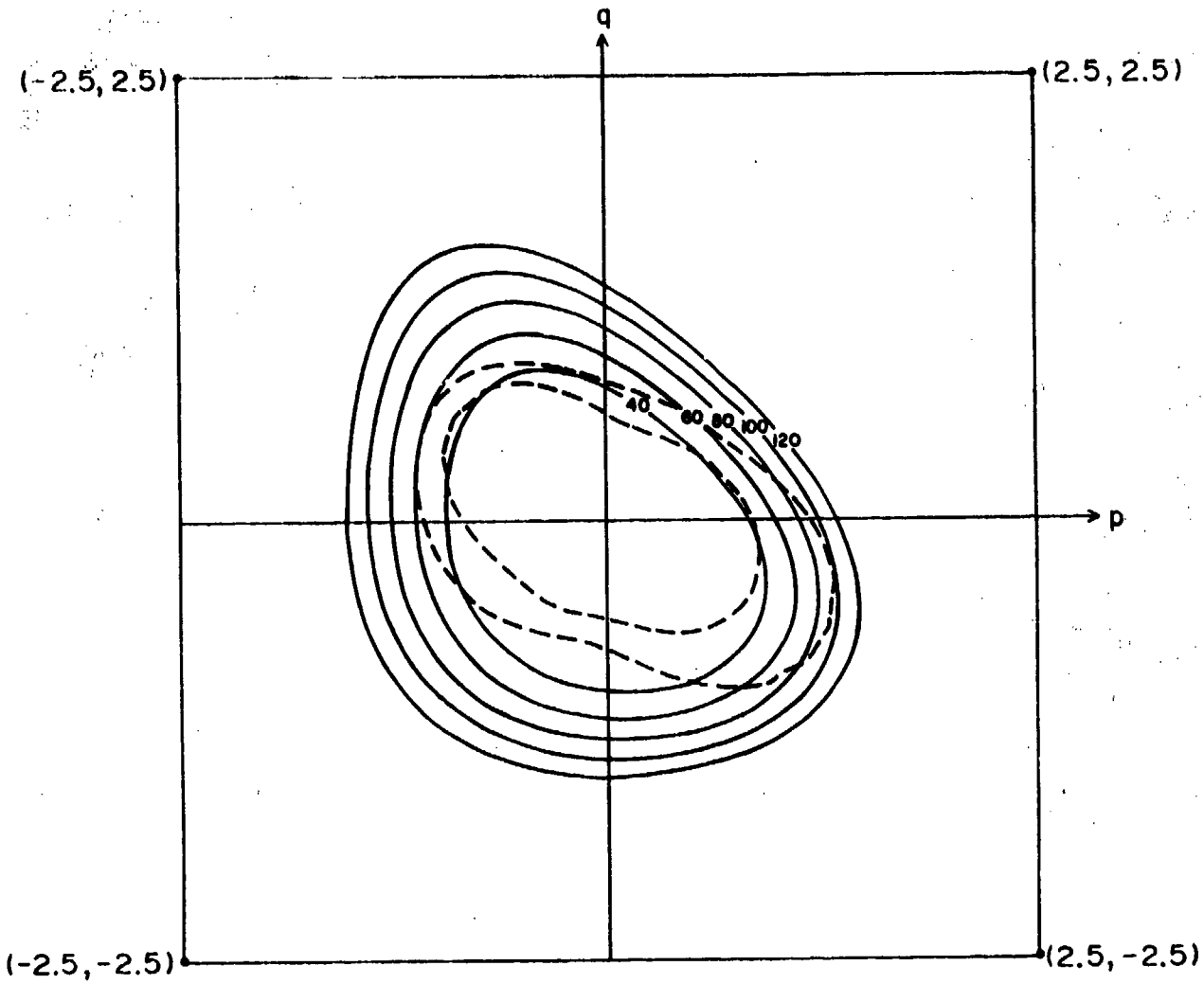

Fig. 4.14 Constant resistive force (moment), in Newtons (Newton-Meters), contour map on the modified joint axis system, in radians, for subject No. 3. The maximal voluntary hip complex sinus (inner dashed) and the maximal forced sinus (outer dashed) are also indicated.

3. In the two front quadrants ($\pi < \phi < 2\pi$), no real discomfort was observed due to adduction of the upper leg into the opposite leg or the torso. In this region, the maximal forced sinus is based on the θ values reached as far as possible during constant-ϕ sweeps for the force (moment) levels which were applied.

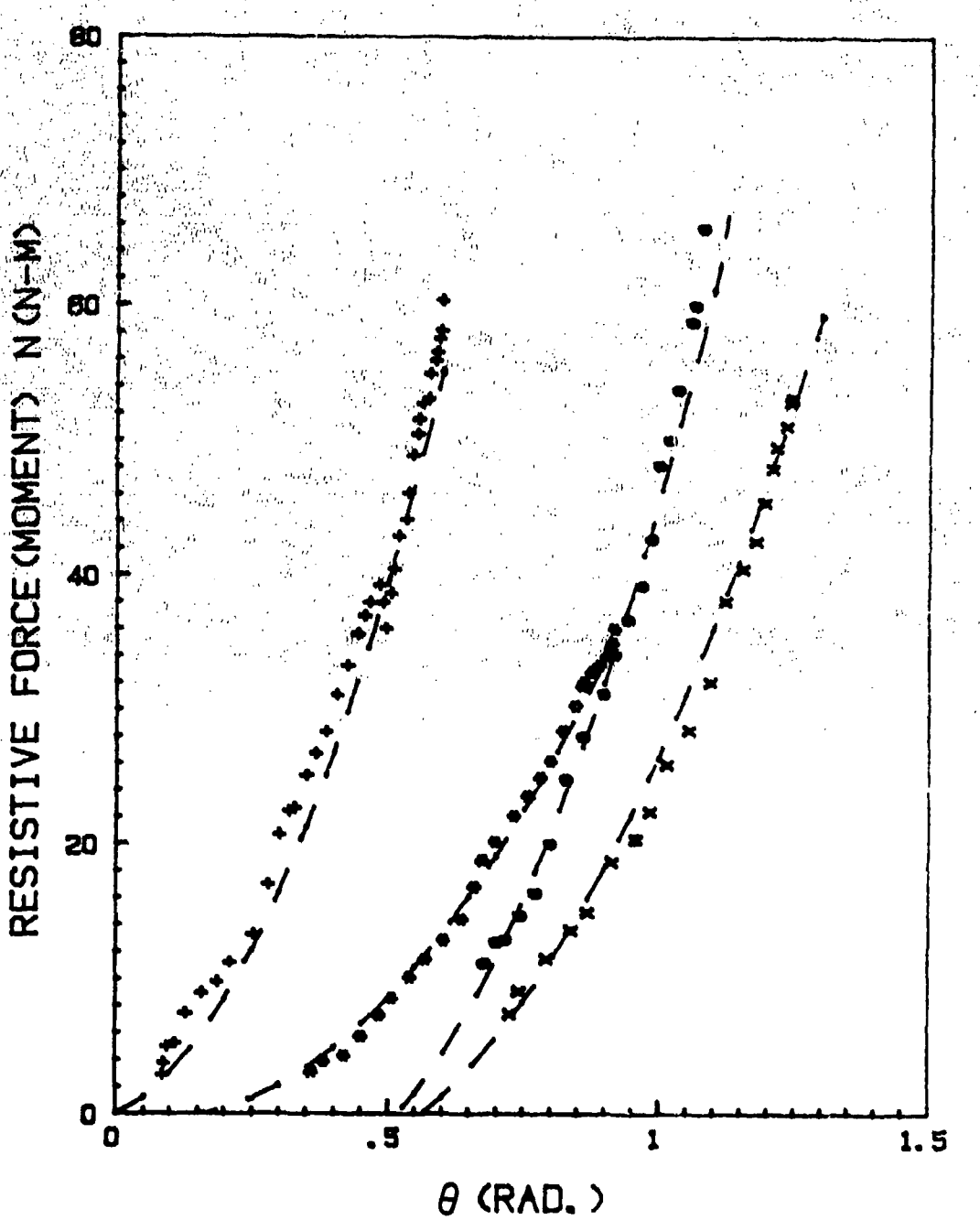

Fig. 4.15 Raw data and the fitted curves (drawn from Fig. 4.12) for several constant-ϕ sweeps.

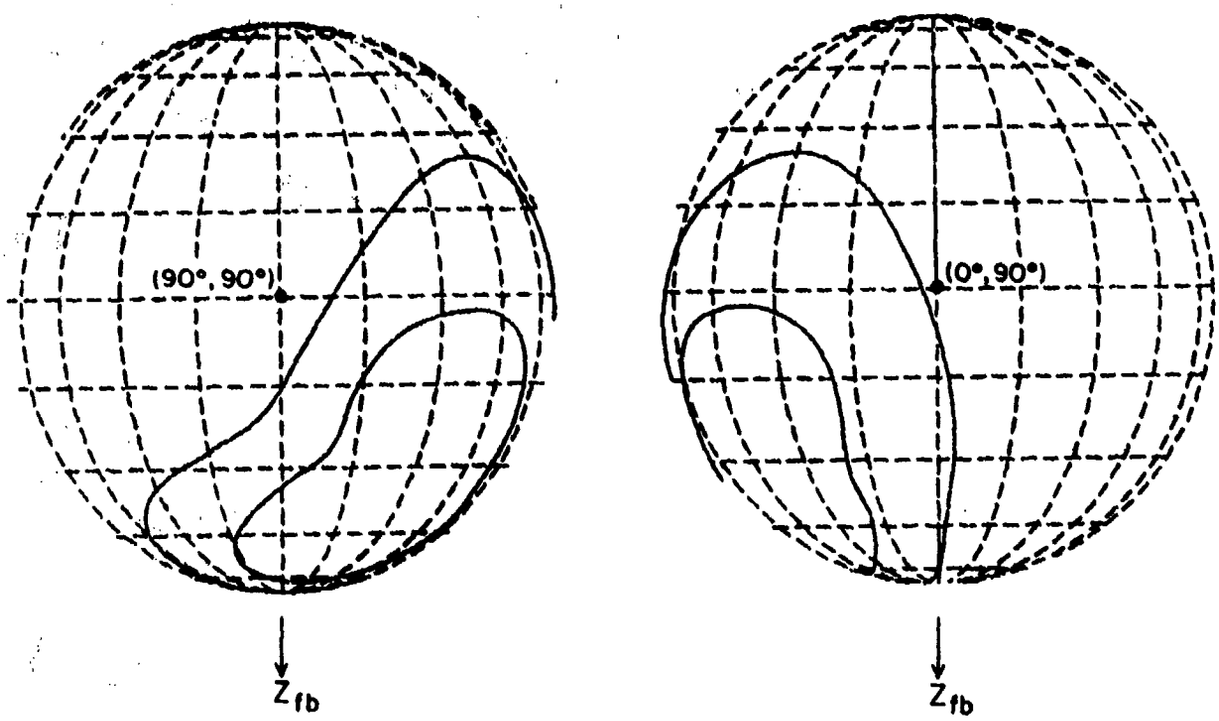

Fig. 4.16 Globographic representations of the maximal voluntary (inner curve) and forced (outer curve) sinuses for subject No. 1.

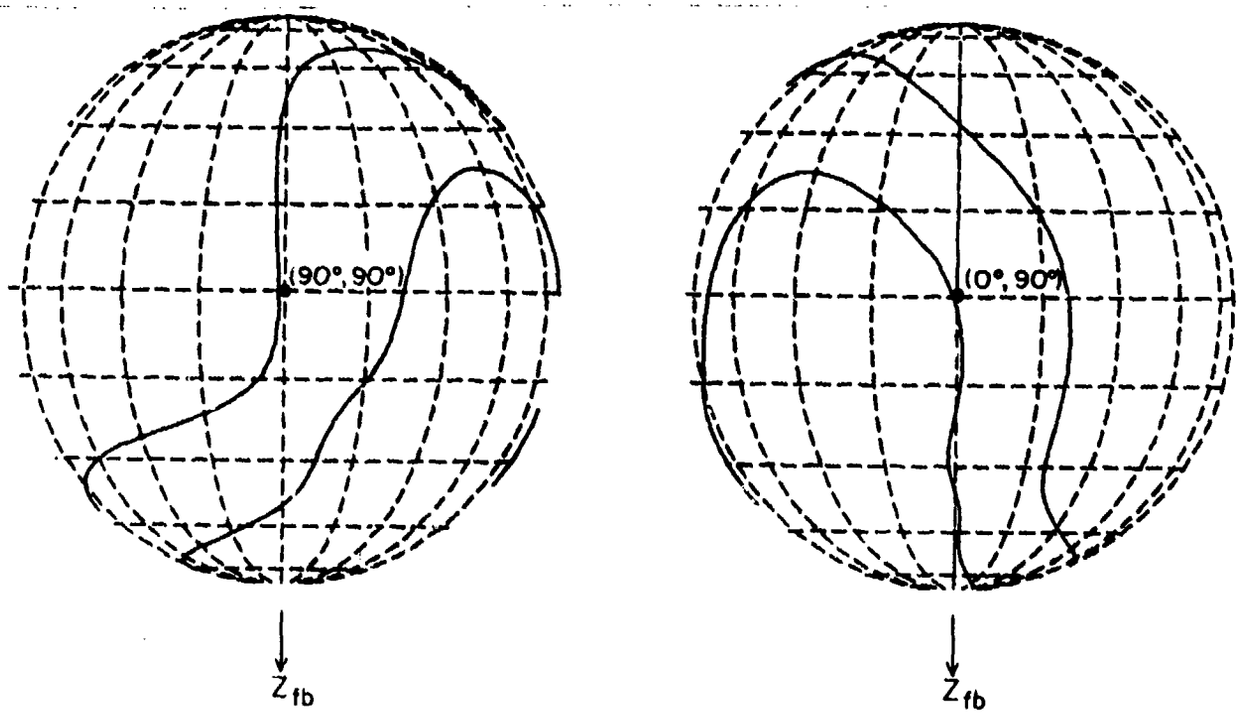

Fig. 4.17 Globographic representations of the maximal voluntary (inner curve) and forced (outer curve) sinuses for subject No. 2.

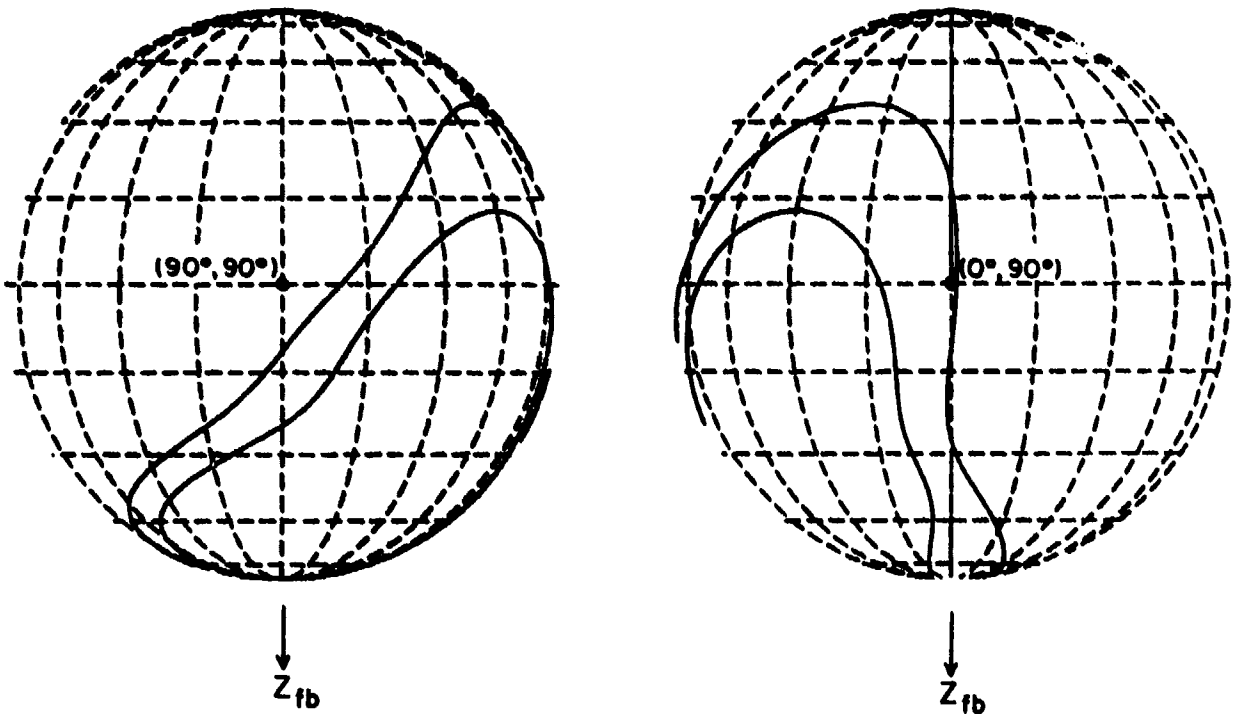

Fig. 4.18 Globographic representations of the maximal voluntary (inner curve) and forced (outer curve) sinuses for subject No. 3.

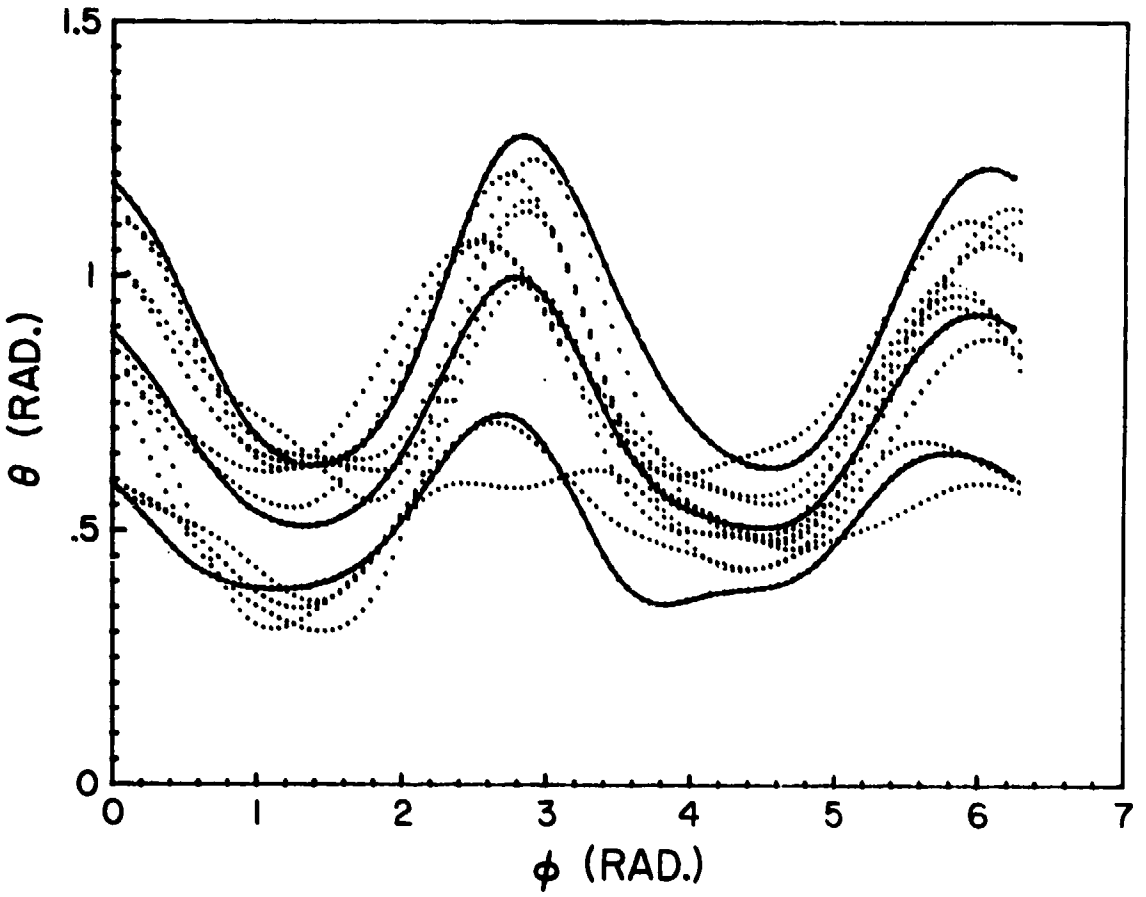

Fig. 4.19 Hip complex sinuses for all ten subjects (dotted curves). Solid curves are for $\bar{\theta}$ and $\bar{\theta} \pm s_{\theta}$.

Table 4.2 Expansion coefficients of the hip complex sinuses for all ten subjects

COEFFICIENTS		C_1	C_2	C_3	C_4	C_5	C_6	C_7	C_8	C_9	C_{10}
SUBJ. NO.	1	0.39571	-0.08703	-0.00428	-0.11163	0.56715	-0.02082	-0.00608	-0.55837	-0.13548	0.13040
	2	0.41498	-0.03727	-0.03586	-0.15646	0.26460	0.25202	0.02128	0.15108	-0.08600	-0.31333
	3	0.66374	-0.01989	0.01311	-0.14792	0.33131	0.04340	0.00400	-0.43214	0.03317	0.19523
	4	0.64836	0.05747	-0.09878	-0.27652	0.38494	0.01268	0.09635	-0.13057	-0.15474	-0.00942
	5	0.41728	-0.03587	-0.01455	-0.21832	0.38268	-0.02453	0.00890	-0.00675	-0.19582	0.14766
	6	0.57179	0.05677	0.13936	-0.10665	0.25711	-0.42213	-0.09643	-0.26946	-0.23603	0.77554
	7	0.58089	0.01795	-0.11139	-0.23718	0.52750	0.06738	0.11461	-0.22175	-0.26809	0.02208
	8	0.56665	0.07304	0.07290	-0.04798	0.21822	-0.11714	-0.08476	-0.30503	0.35835	0.29331
	9	0.42387	-0.04199	-0.11612	-0.13343	0.28786	-0.21253	0.09007	-0.27206	0.16308	0.37762
	10	0.54724	0.04135	0.18203	0.05549	0.31620	-0.01822	-0.17311	-0.52484	0.16224	0.21174
Sample Mean		0.52305	0.00245	0.00264	-0.13806	0.35376	-0.04399	-0.00252	-0.25699	0.01127	0.18308
Sample Variance		0.01029	0.00292	0.01057	0.00924	0.01327	0.03213	0.00861	0.04915	0.04409	0.07949

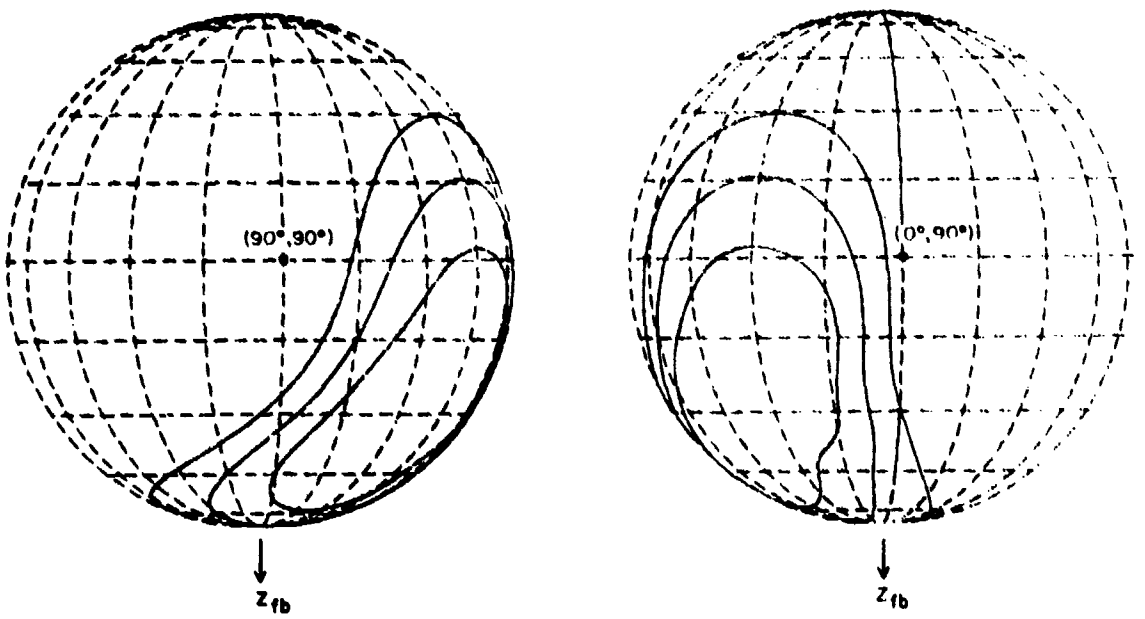

Fig. 4.20 Globographic representations of $\bar{\theta}$ and $\bar{\theta} \pm S_\theta$.

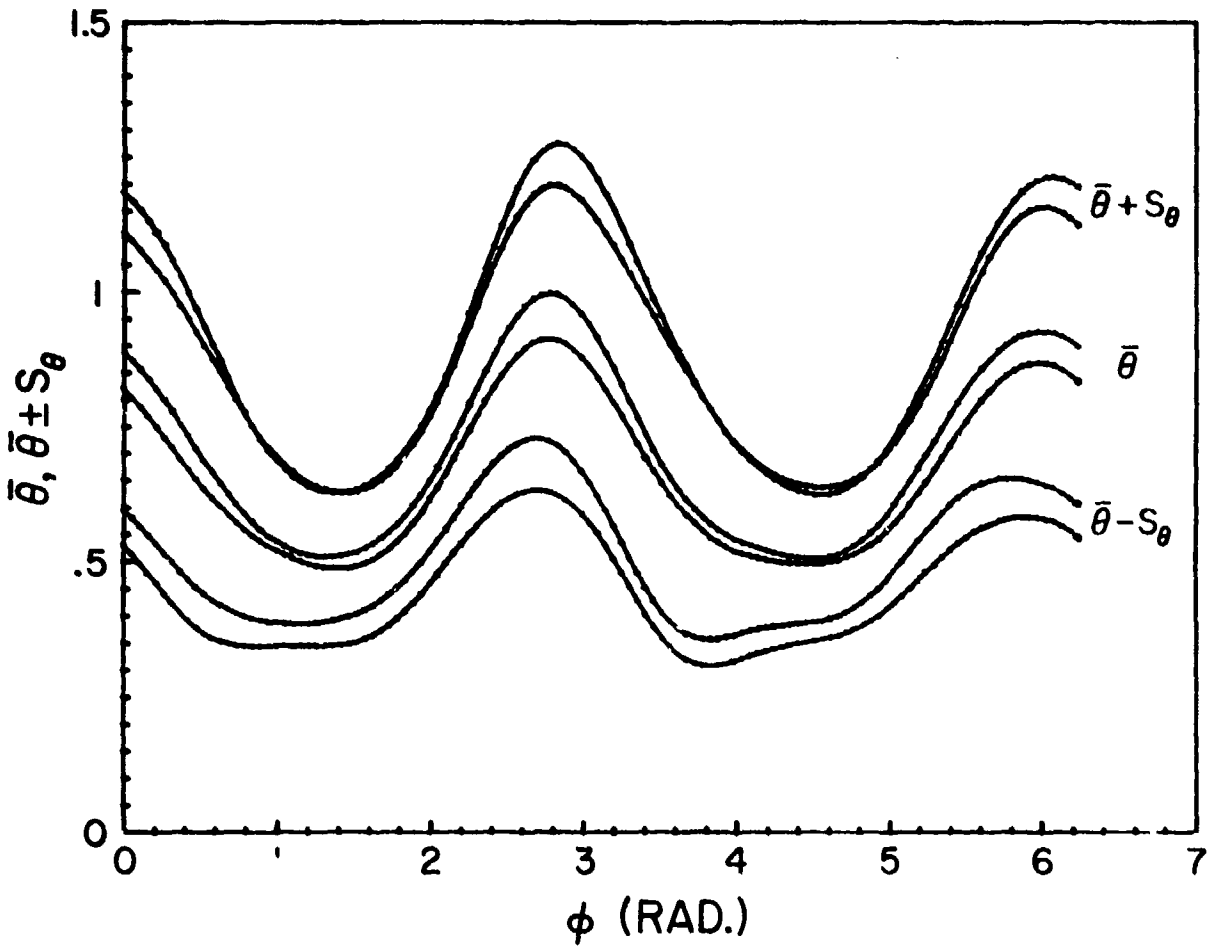

Fig. 4.21 $\bar{\theta}$ and $\bar{\theta} \pm S_\theta$ for two different runs.

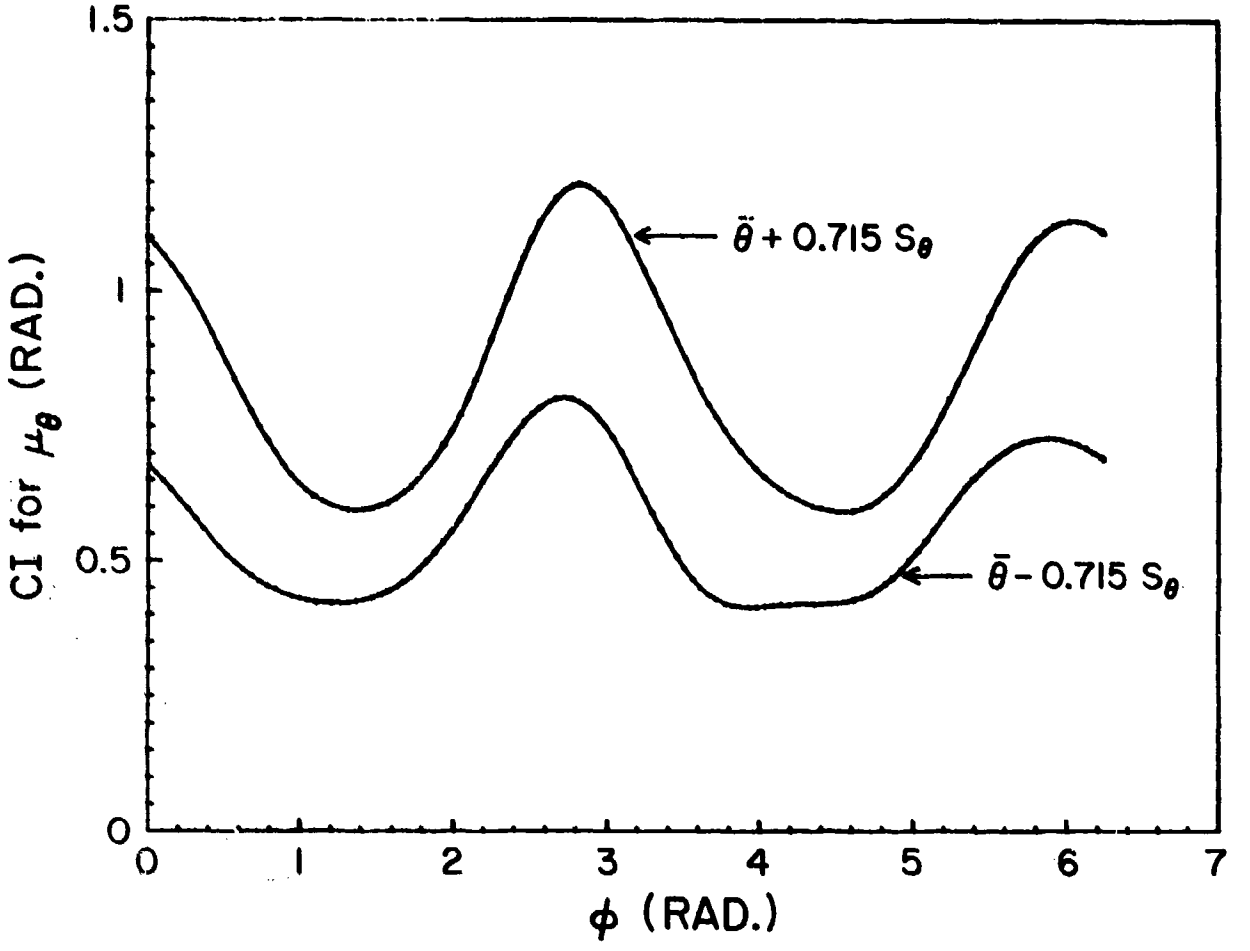

Fig. 4.22 Confidence Interval (CI) for the population mean, μ_θ.

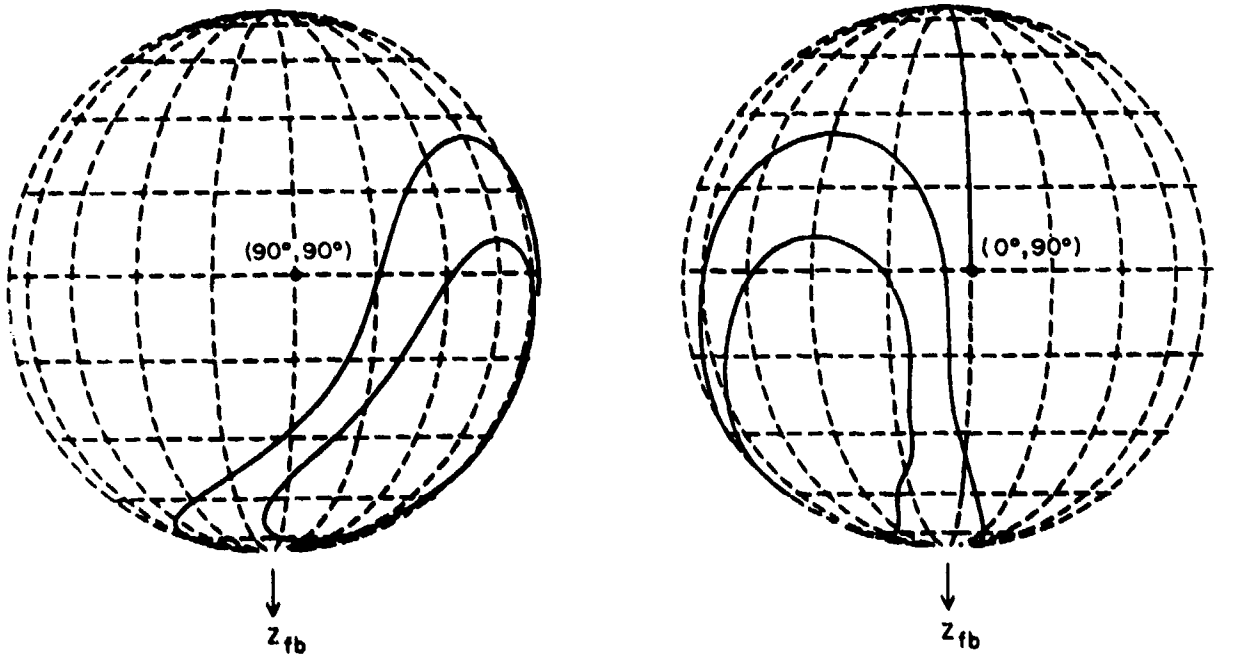

Fig. 4.23 Globographic representation of the Confidence Interval for the population mean.

Table 4.3 Expansion coefficients of the passive resistive force (moment) data for all ten subjects.

COEFFICIENTS		C_1	C_2	C_3	C_4	C_5	C_6	C_7	C_8	C_9	C_{10}
SUBJ. NO.	1	-4.93	-1.37	15.12	59.24	94.97	143.89	-7.94	-3.70	16.63	-11.34
	2	-8.67	-7.68	57.96	59.73	49.13	87.61	5.85	18.72	18.19	-14.19
	3	-9.11	-6.55	12.47	50.23	40.16	75.25	-2.09	-5.58	13.33	18.98
	4	-7.13	-0.64	14.65	83.48	69.25	81.22	-2.24	-23.48	-29.01	-24.03
	5	-14.45	7.85	34.81	66.84	60.81	106.39	3.81	14.80	11.74	-13.59
	6	-2.18	-2.84	20.29	45.56	46.48	89.29	1.30	-20.55	-27.34	-14.46
	7	-17.84	5.44	18.03	72.58	39.33	73.49	2.92	14.38	22.40	-4.73
	8	-1.49	-7.80	11.03	39.68	47.88	79.22	2.56	5.13	10.72	-10.57
	9	-12.48	3.12	17.87	63.94	71.45	102.09	2.17	9.04	15.20	-13.51
	10	-5.86	-6.18	20.78	53.17	54.48	112.70	1.28	-19.82	-26.17	-18.85
Sample Mean		-8.41	-1.66	22.32	59.44	57.39	95.11	0.76	-1.11	2.57	-10.63
Sample Variance		27.72	31.61	200.61	170.33	296.83	473.58	15.39	253.70	442.067	133.73

Table 4.4 Expansion coefficients of the maximum forced sinuses

COEFFICIENTS		C_1	C_2	C_3	C_4	C_5	C_6	C_7	C_8	C_9	C_{10}
SUBJ. NO.	1	0.86022	-0.29444	0.43908	-0.89108	-0.01064	0.37849	-0.53381	0.60123	0.37733	-0.35817
	2	0.87910	-0.16396	0.21117	-0.61168	0.02493	-0.03323	-0.28160	0.29654	0.07114	0.03164
	3	0.95953	-0.30142	0.37933	-0.52935	0.12908	0.16419	-0.33168	0.35897	0.00000	0.00000
	4	0.95015	-0.06743	0.02830	-0.46765	0.20000	-0.16934	-0.07731	0.12608	0.00000	0.00000
	5	0.79477	-0.11009	-0.01419	-0.36841	0.30207	0.22030	0.15289	-0.05182	0.12805	-0.26038
	6	0.96264	-0.00587	0.17370	-0.45350	0.81117	0.50267	-0.02478	-0.50541	-0.22958	-0.07306
	7	0.76140	0.02475	0.01770	-0.30282	0.67457	-0.10819	0.03962	-0.27926	-0.30765	-0.17010
	8	0.82154	-0.05859	0.43567	-0.62290	0.30109	-0.45838	-0.31269	0.42118	-0.00489	0.31648
	9	0.61995	-0.17743	0.36143	-0.61903	0.70729	-0.34451	-0.49297	0.38546	-0.27602	0.37877
	10	1.05702	0.01582	0.33113	-0.14915	0.34016	0.67845	-0.43865	-0.33994	-0.18280	-1.04720
Sample Mean		0.86663	-0.11387	0.23633	-0.50156	0.34797	0.08304	-0.23010	0.20238	-0.06805	-0.11820
Sample Variance		0.01560	0.01414	0.03159	0.04200	0.08416	0.13700	0.05662	0.10691	0.04161	0.15910

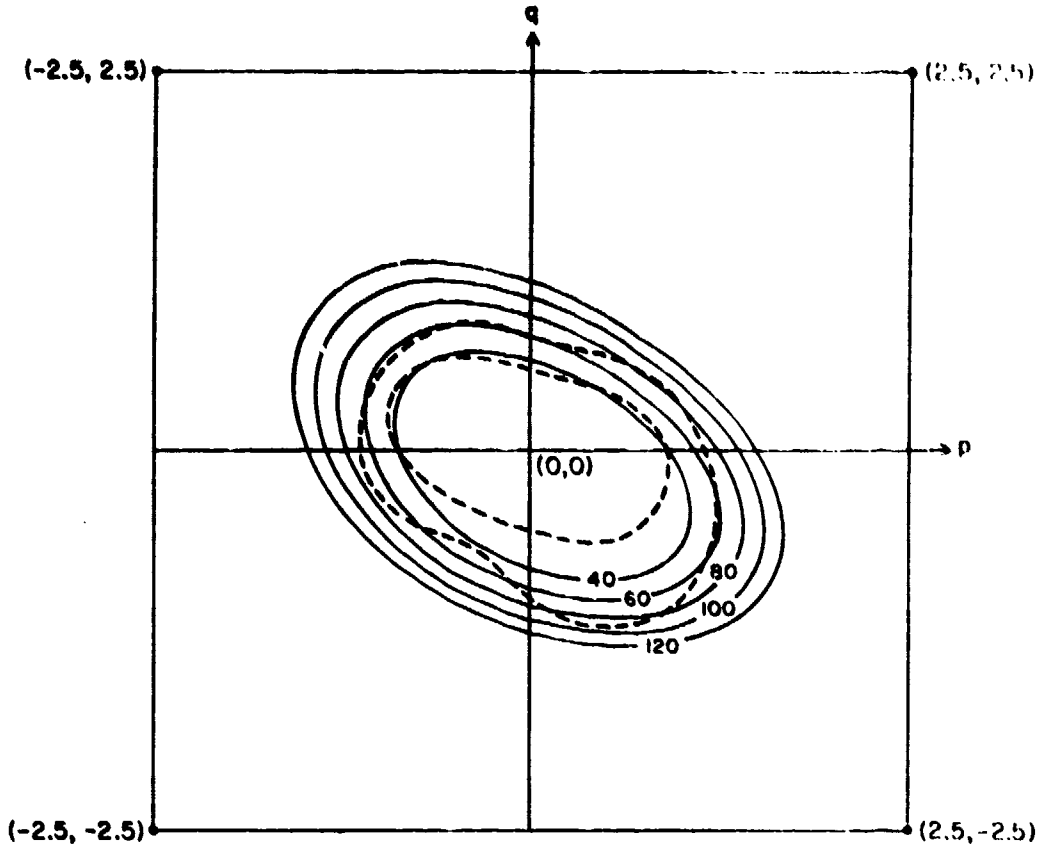

Fig. 4.24 Sample means of the passive resistive property, maximum voluntary sinus (inner dashed), and maximum forced sinus (outer dashed).

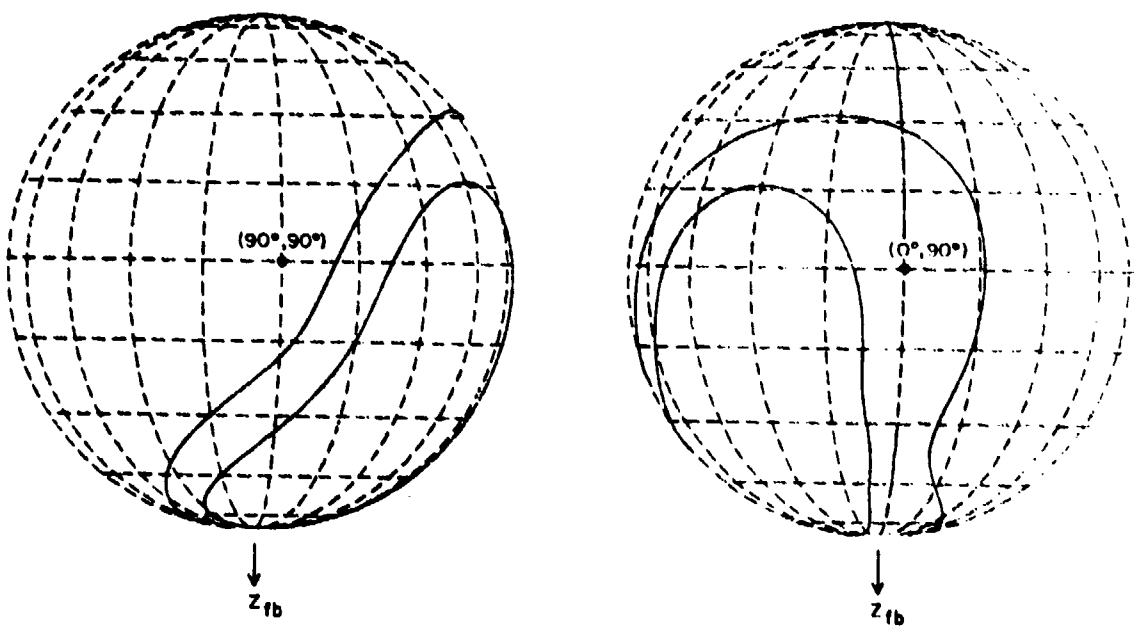

Fig. 4.25 Globographic representations of the sample means of the maximum voluntary and forced sinuses.

5. BIOMECHANICAL PROPERTIES OF THE HUMAN HUMERO-ELBOW COMPLEX

5.1 Introduction

Two types of data are considered in this chapter: (1) the maximum voluntary humero-elbow complex sinus, or, the angular range of the extreme allowable motion of the lower arm with respect to the upper arm whose axial rotation is permitted, and (2) the passive resistive properties beyond the full elbow extension with the lower arm in pronation.

The elbow complex is composed of three articulations: the humeroradial, the humeroulnar, and the superior radioulnar; it has been modeled as a trochoginglymus joint possessing two rotational degrees of freedom (flexion-extension and pronation-supination) by most investigators (Dempster, 1955; Steindler, 1973; Youm et al., 1979). By utilizing the inserted Kirschner wires for defining coordinate axes and biplanar radiographs, Chao and Morrey (1979) were able to accurately isolate the three-dimensional rotation of cadaver forearms under passive elbow motion; the translatory components of the joint motion were ignored by assuming that the tight ligamentous constraints would limit such motion to small magnitudes. The additional component of rotation is referred to as the carrying angle (or abduction-adduction). Chao et al. (1980) also developed a device similar to the electrogoniometer for determining the three-dimensional angular motion occurring at living normal subject's elbow joint while performing different daily functions. The carrying angle normally disappears when the lower arm is pronated with the elbow in full extension. Due to the articular check (between the olecranon process and fossa) and the ligamentous constraints, excessive elbow extension beyond the maximum voluntary range may cause serious injuries.

5.2 Determination of the Humero-Elbow Complex Sinus

Both kinematic and force application tests for the elbow joint are shown in Fig. 5.1. This figure also shows the upper arm restraint fixture. The fixed longitudinal axis of the upper arm with respect to the torso is chosen to coincide with the z-axis of the statistical mean joint axis system established for the shoulder complex in Section 3.2.

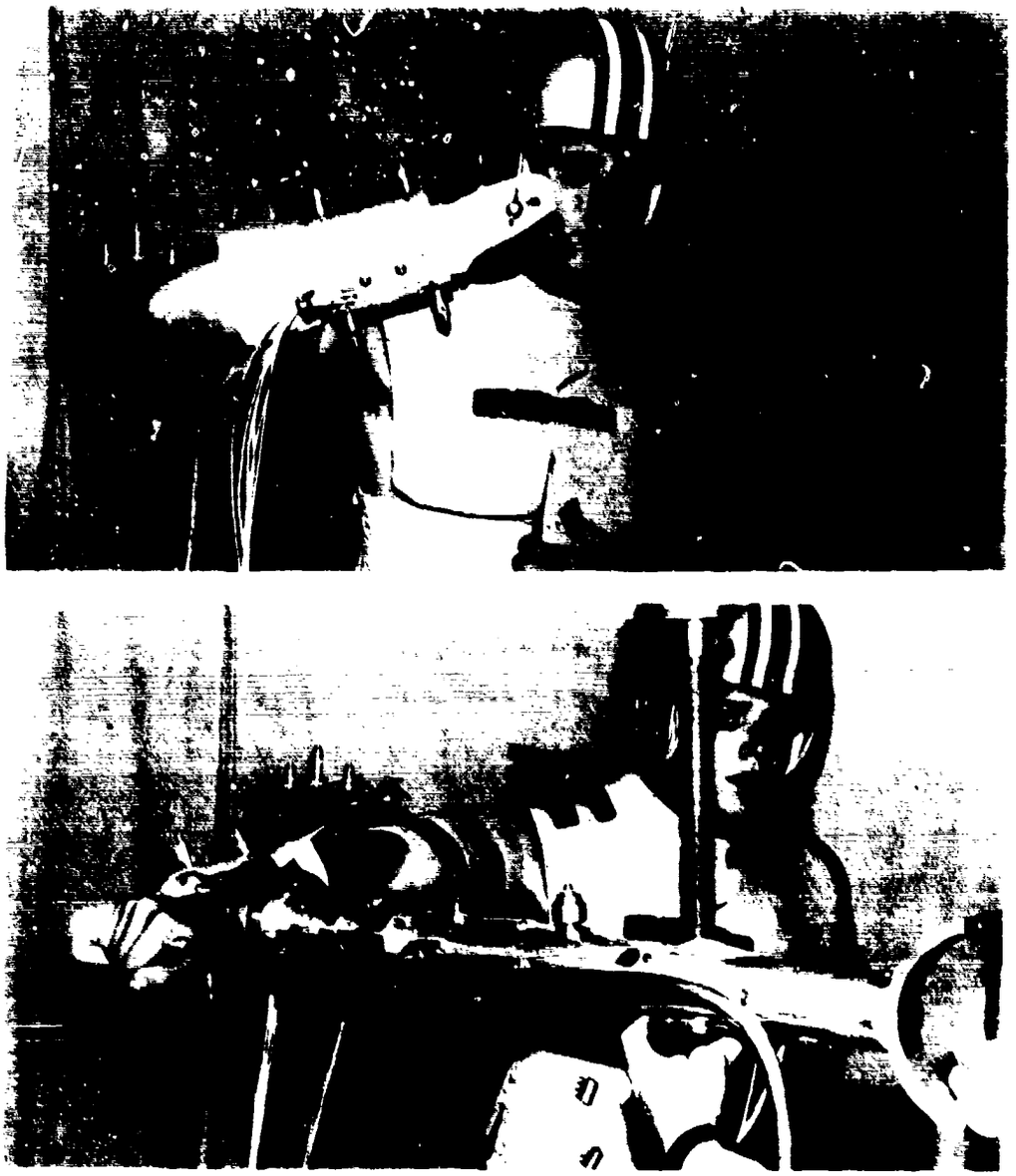

Fig. 5.1 Kinematic and force application tests for the elbow complex.

In the author's opinion, by positioning the upper arm in this orientation, the shoulder complex is in a state of maximum laxity. As shown in Fig. 5.2, the mean joint axis system is uniquely obtained by first rotating the torso axis system by the mean angle ϕ_m (= 59°) about the z_{ts}-axis and then rotating the intermediate (primed) axis system by the mean angle θ_m (= 79°) about the y'-axis. In this study, this mean joint axis system is also naturally selected as the fixed reference frame (fixed-body axis system) for performing the kinematic analyses of the forearm; the origin of this fixed-body axis system is conveniently chosen to be the center of the humeral head.

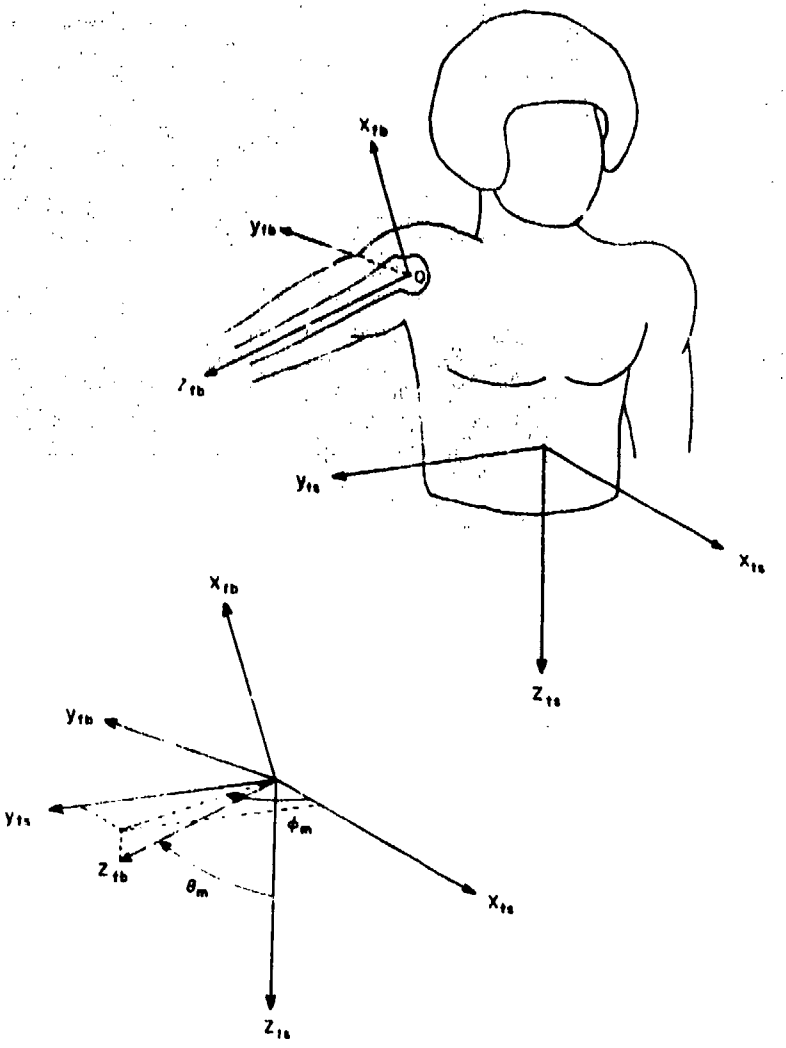

Fig. 5.2 Relative orientation of the mean joint axis system, or the fixed-body axis system, (x_{fb}, y_{fb}, z_{fb}) and the torso axis system, (x_{ts}, y_{ts}, z_{ts}).

Since the upper arm is only permitted to rotate about its longitudinal (long-bone) axis, its translational degrees of freedom are prohibited by the shoulder part of the torso restraint shell, and the other two rotational degrees of freedom are eliminated by fastening the upper arm onto a rigid fixture (whose direction, of course, is along the z_{fb}-axis of the fixed reference frame) with three Velcro straps.

An orthotic brace made of heat-moldable orthoplast is used in order to mount the six sonic emitters on the lower arm to monitor its rigid-

body kinematics. Two Velcro straps are used to hold the brace on the lower arm. In addition, by letting the hand hold a pole which extends from the brace, the wrist complex is fixed so that the forearm muscles are held in a stable configuration. This orthotic device thus eliminates the relative shifting motion between the forearm and the brace. The forearm cuff with six emitters affixed to it is then rigidly attached to the brace by two screws. The forearm cuff is made of a rigid, cylindrical, plastic shell which extends about three-quarters of the way around the lower arm. It is believed that this orthotic configuration comes as close as possible to rigid body conditions, and provides for accurate measurement of forearm kinematics.

The procedure for quantitative determination of the humero-elbow complex sinus consists of the following steps: (1) immobilizing the torso and upper arm, and defining the fixed body axis system as described before (also refer to Fig. 5.2), (2) having the subject move his forearm along the maximum voluntary range of motion and continuously monitoring, with respect to the fixed-body axis system, the 3-D coordinates of a distal point on the moving body segment; this point (to be referred to as the wrist joint reference point) is selected as being on the longitudinal axis of the forearm at the level of the styloid process, (3) fitting the wrist joint reference point coordinates to a sphere using the least-squares method, thus establishing a center for the best-fitted sphere and an idealized link length (radius of the sphere), (4) fitting a plane to the same wrist joint reference point coordinates using the least-squares method; the normal to this plane (specified by the spherical coordinates (ϕ_n, θ_n) as shown in Fig. 5.3) establishes the pole (z_{jt}-axis) of a local joint axis system (for the humero-elbow complex) with respect to which the humero-elbow complex sinus, designated by the spherical coordinates (ϕ, θ) of the vector connecting the center of the best-fitted sphere with the wrist joint reference point, can be expressed as a single-valued functional relationship, i.e., $\theta = \theta(\phi)$.

Since only the wrist joint reference point is monitored, the same initialization procedure as that used for the hip complex is employed.

Before the humero-elbow complex sinus test, the subject was instructed to move his forearm along its maximum voluntary range of motion in a counter-clockwise direction as viewed from the sensor

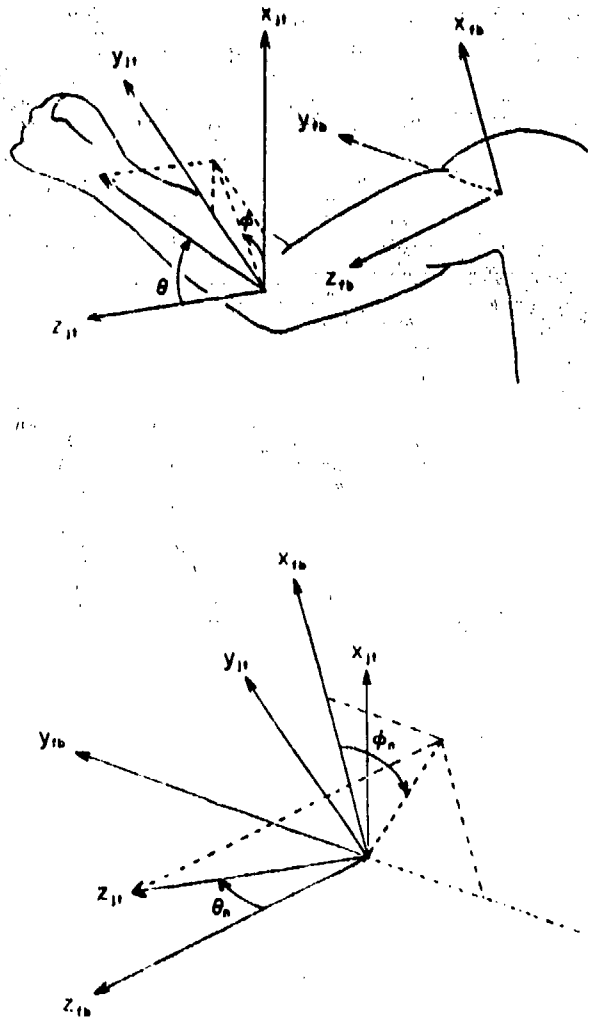

Fig. 5.3 Relative orientation of the fixed-body (x_{fb}, y_{fb}, z_{fb}) and the locally-defined joint (x_{jt}, y_{jt}, z_{jt}) axis systems.

assembly. Preferred rotation of the forearm about its longitudinal axis was left up to the discretion of the subject in obtaining the maximum sinus. Several sweeps of this type were practiced before data were collected so that the subject could experiment with obtaining the largest possible range of motion. In order to help maintain a constant

rate of motion during data collection, a large clock with an easily visible second hand was placed in front of the subject. The subject was instructed to imagine his forearm as the second hand, and to synchronize his circumscription with the clock's 60 second sweep. The firing rate of the sonic emitters was set at seven data records per second (as used for the shoulder and hip complexes) so that a total of 420 wrist joint reference points was collected for each complete humero-elbow complex sinus.

Table 5.1 lists the centers and radii of the best-fitted spheres and (ϕ_n, θ_n) values of the best-fitted planes for all ten subjects. With respect to each individual local joint axis system designated by (ϕ_n, θ_n), Figs. 5.4-5.6 show both the raw data and least-squares fitted values of the single-valued functional relationship, i.e., $\theta = \vartheta(\phi)$ of the humero-elbow complex sinus for three subjects. In these figures, only 72 raw data points (approximately equally spaced) were plotted and used for curve-fitting of the functional expansion, Eq. (3.2.1). Figs. 5.7-5.9 display the globographic representations of these three functional expansion sinuses with respect to the fixed-body axis system.

5.3 Determination of the Passive Resistive Properties Beyond the Full Elbow Extension

Since the force applicator is constrained to motion in a level horizontal plane by a track-mounted trolley system located overhead, it is necessary to tilt the torso, while sitting, $11°$ $(= 90° - \theta_m)$ about x_{ts}-axis so that the upper arm is also parallel to the ground. The subject was first instructed to pronate his forearm to face the ground and to fully extend it. The force applicator was then positioned vertically at the same level as the subject's forearm, and the transducer front was positioned near the wrist joint. The subject's forearm was next forced beyond its full extension in a quasi-static manner until the subject started experiencing discomfort. During the entire course of the test, the subject was instructed to let his forearm hang limply and not to actively (muscularly) resist the motion of the test.

The data collected according to the foregoing procedure were analyzed as follows. First, the force $(\vec{F})$ and moment $(\vec{M})$ vectors obtained from the force applicator transducer were used to calculate a

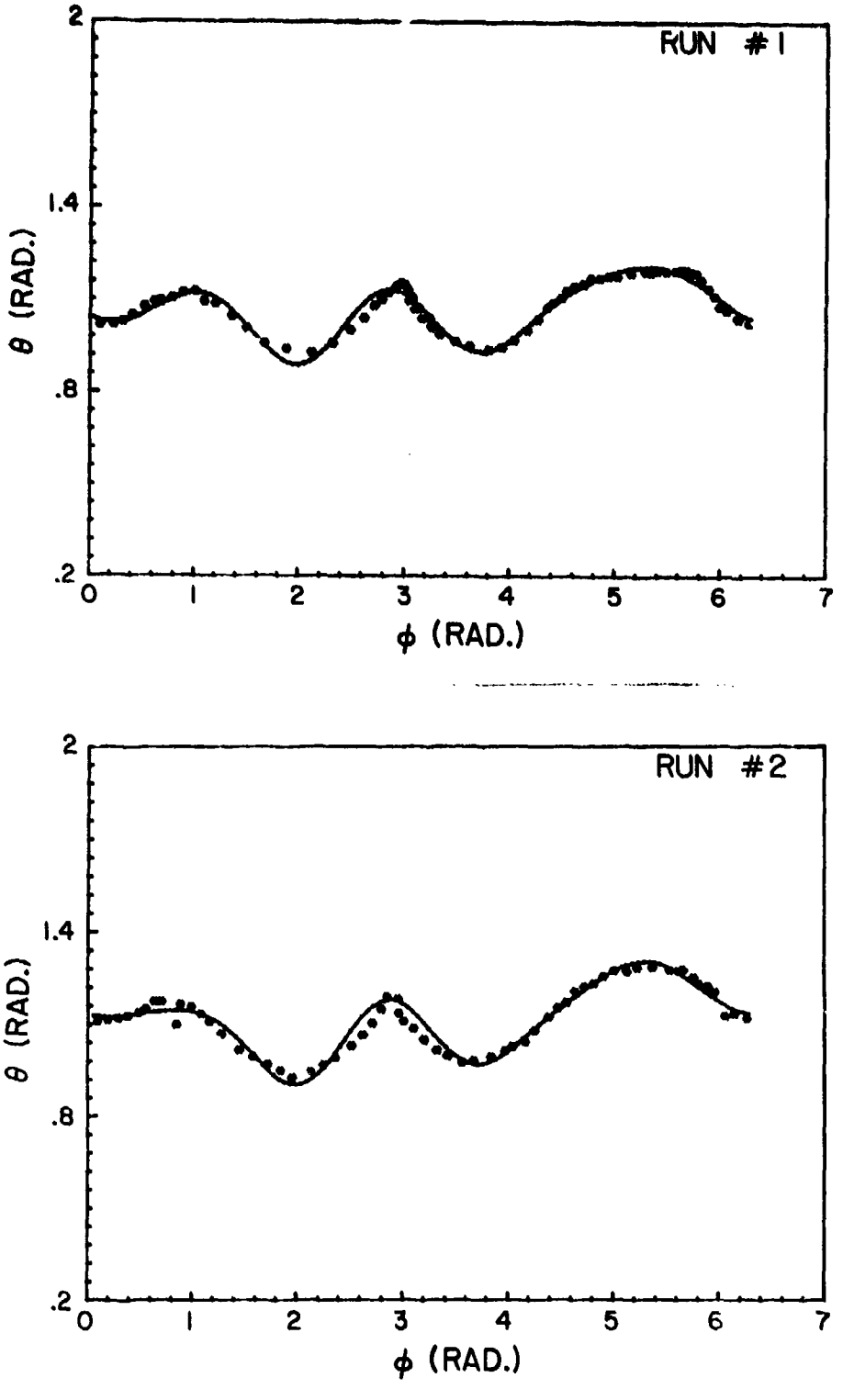

Fig. 5.4 Raw data and the functional expansions of the humero-elbow complex sinus for subject No. 1.

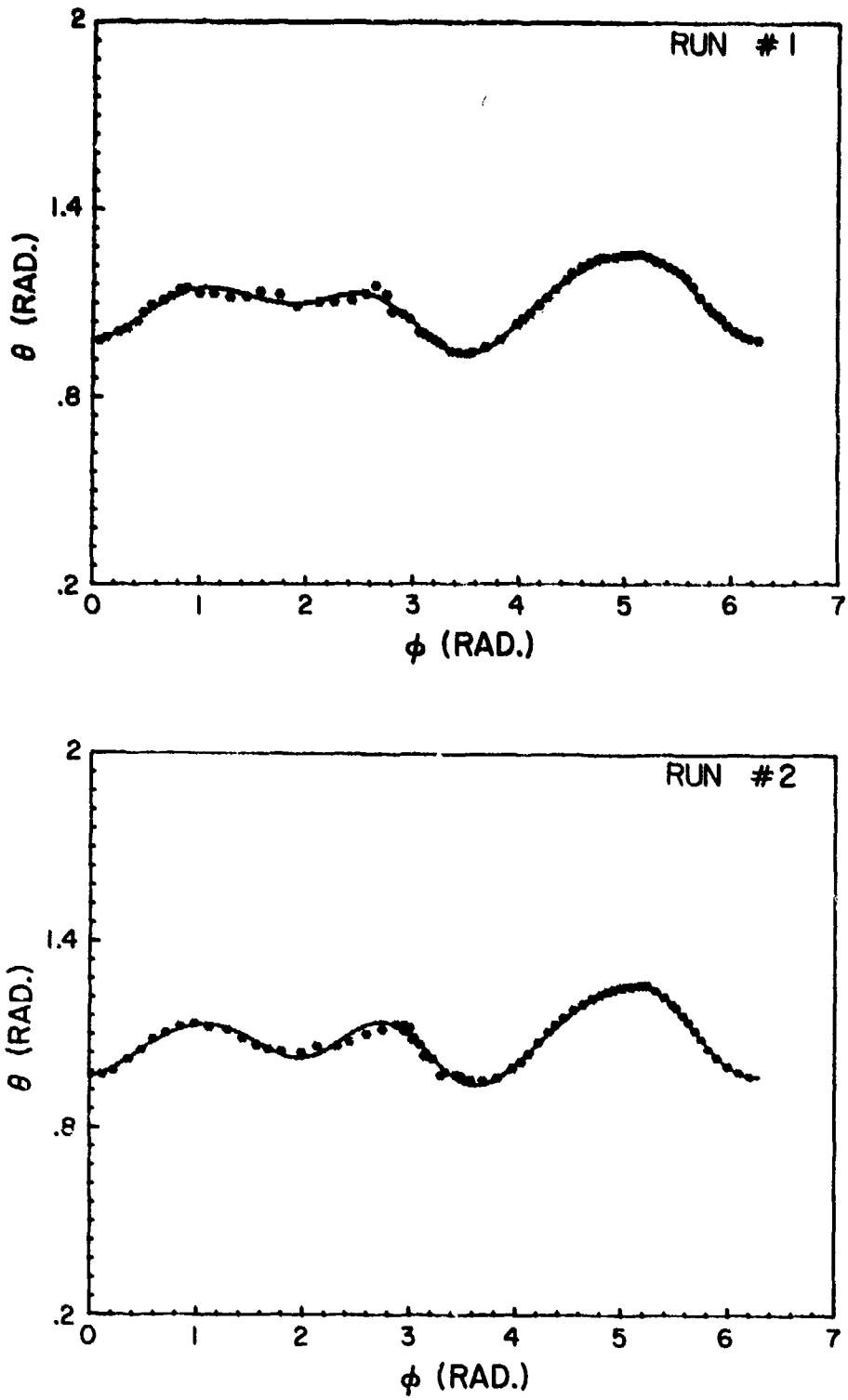

Fig. 5.5 Raw data and the functional expansions of the humero-elbow complex sinus for subject No. 2.

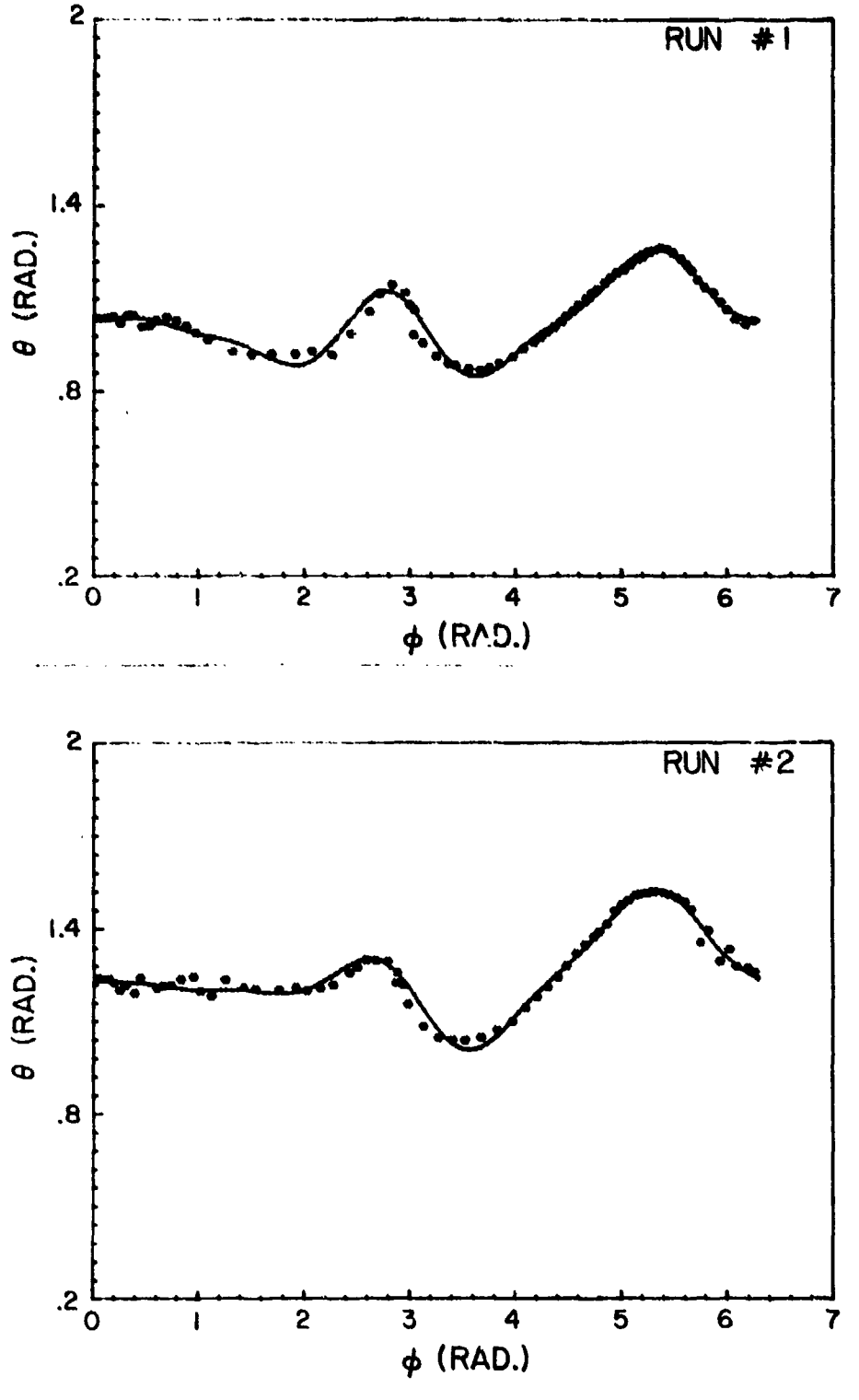

Fig. 5.6 Raw data and the functional expansions of the humero-elbow complex sinus for subject No. 3.

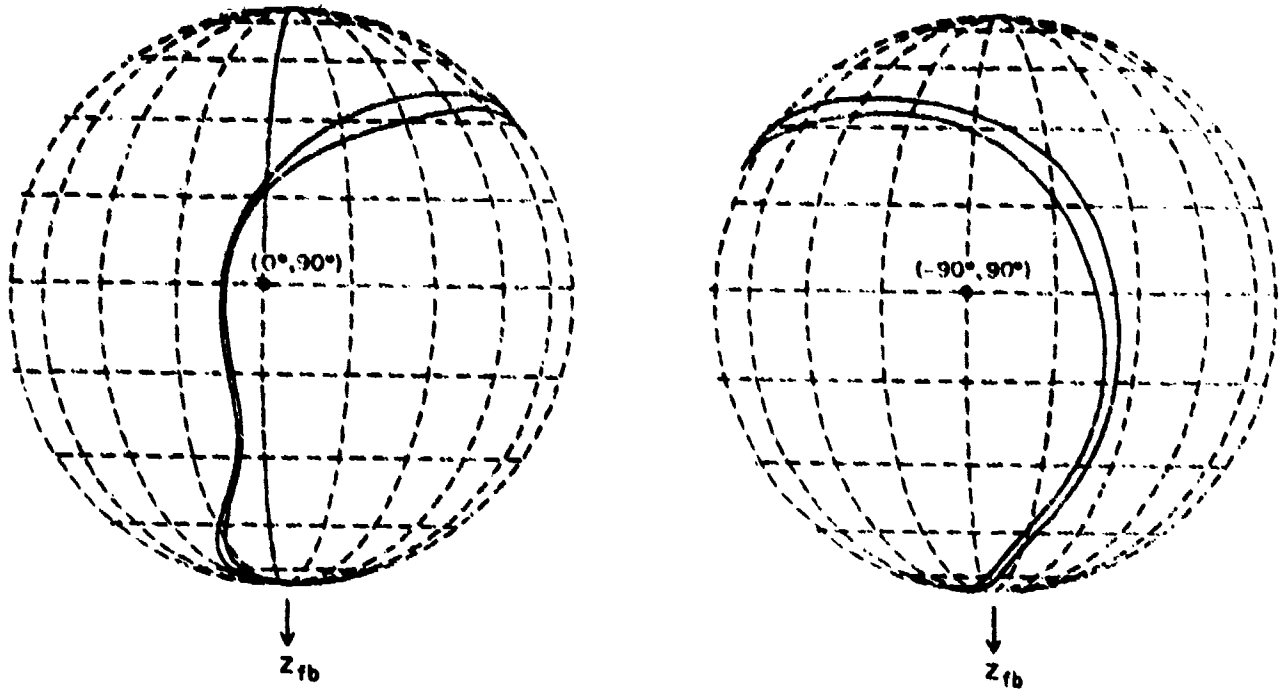

Fig. 5.7 Globographic representation of Fig. 5.4.

total moment vector with respect to the center of the best-fitted sphere (described in Section 5.2):

$$\vec{M}_{total} = \vec{M} + \vec{r} \times \vec{F}$$

where $\vec{r}$ is the moment arm vector from the center of the best-fitted sphere to the point of force application. Next, the total moment vector was resolved into components along and perpendicular to the moment arm vector. The component along the moment arm vector was then discarded, since it does not serve to restore the forearm towards its full extension position. Finally, a "normalized" moment arm vector of unit length, i.e., one meter, along the moment arm vector was used together with the remaining moment component (the passive resistive moment vector) to calculate the passive resistive force vector. Since the moment arm is normalized to unit length, the magnitude of the resistive force vector is the same as that of the resistive moment vector. We shall refer to this magnitude as the passive resistive force (moment) property, which is

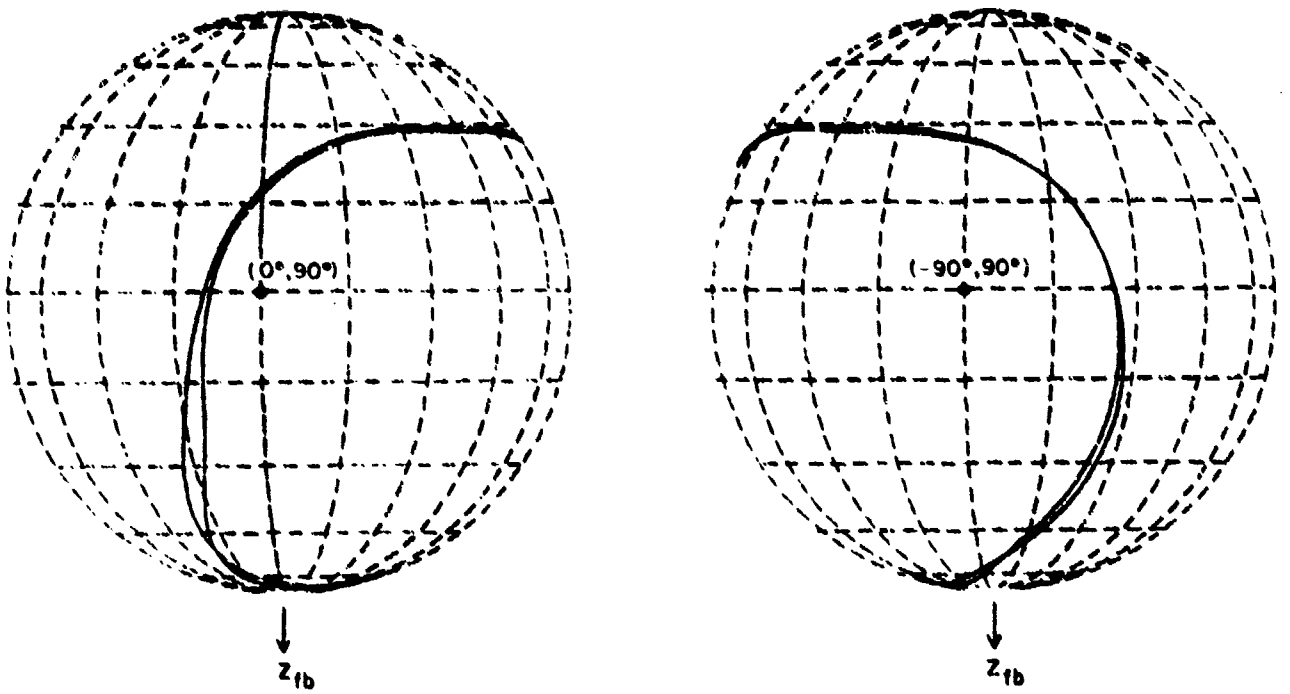

Fig. 5.8 Globographic representation of Fig. 5.5.

expressed as a function of α, or the angular displacement from the full elbow extension. In calculating this angle, the line connecting the center of the best-fitted sphere and the distal wrist joint reference point is used as the longitudinal axis of the forearm.

Figs. 5.10-5.12 show two runs of both the raw data and the curve-fitted function values of the passive resistive force (moment) properties for three subjects. The expansion function used is of the following polynomial form:

$$f(\alpha) = C_1 + C_2\alpha + C_3\alpha^2 + C_4\alpha^3 \qquad (5.3.1)$$

5.4 Statistical Data Base for the Biomechanical Properties of the Human Humero-Elbow Complex

Since the functional expansion used for the humero-elbow complex sinus is the same as that used for the shoulder complex sinus, the statistical procedure is the same as discussed in Section 3.6. Table 5.2

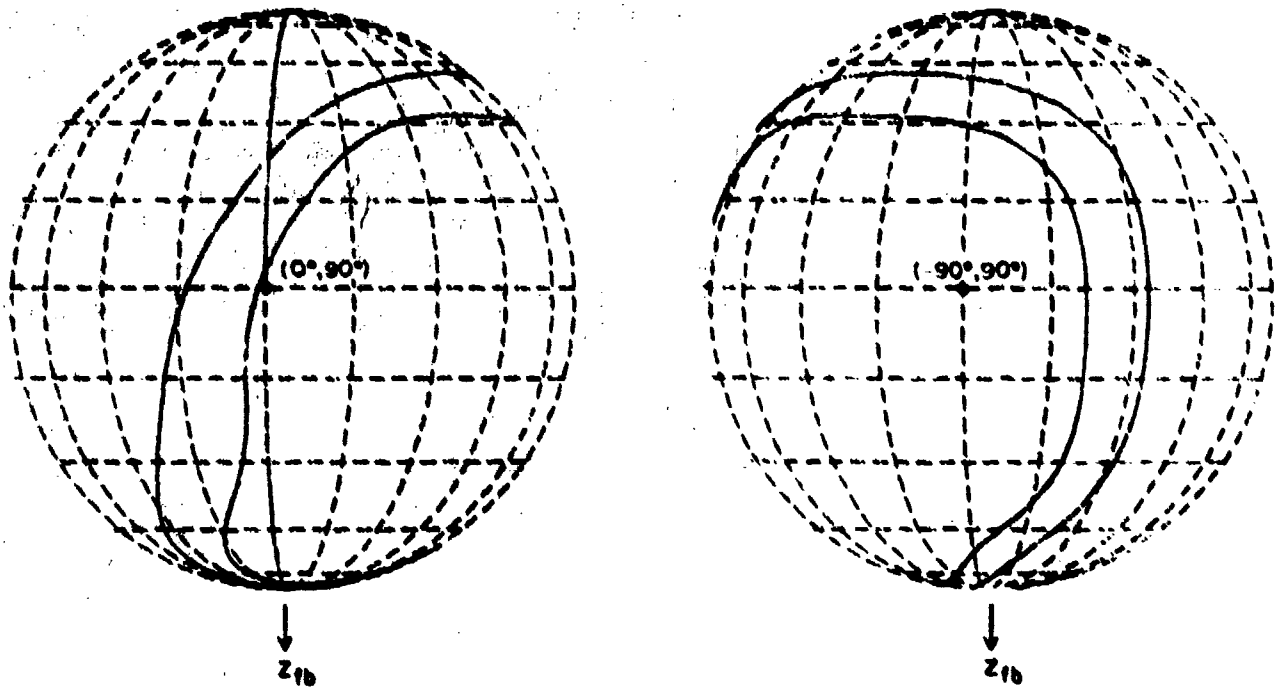

Fig. 5.9 Globographic representation of Fig. 5.6.

lists the expansion coefficients of the humero-elbow complex sinuses for all ten subjects. Fig. 5.13 shows the ten sinuses as well as their sample mean, $\bar{\theta}(\phi)$, and $\bar{\theta}(\phi) \pm s_\theta(\phi)$. Fig. 5.14 displays the globographic representations of $\bar{\theta}$ and $\bar{\theta} \pm s_\theta$ in the fixed-body axis system. Finally, Fig. 5.15 shows the $\bar{\theta}$ and $\bar{\theta} \pm s_\theta$ curves for two different runs. Good repeatability is observed.

Table 5.3 lists the expansion coefficients of the passive resistive properties beyond the full elbow extension for all ten subjects. From Eqs. (5.3.1), (3.4.6), and (3.4.7), one obtains the sample mean,

$$\bar{f}(\alpha) = \bar{c}_1 + \bar{c}_2\alpha + \bar{c}_3\alpha^2 + \bar{c}_4\alpha^3 \tag{5.3.2}$$

and the unbiased sample variance,

$$s_f^2(\alpha) = s_{c_1}^2 + s_{c_2}^2\,\alpha^2 + s_{c_3}^2\,\alpha^4 + s_{c_4}^2\,\alpha^6 \tag{5.3.3}$$

Fig. 5.16 shows $f(\alpha)$ for all ten subjects as well as their sample mean $\bar{f}$ and $\bar{f} \pm s_f$.

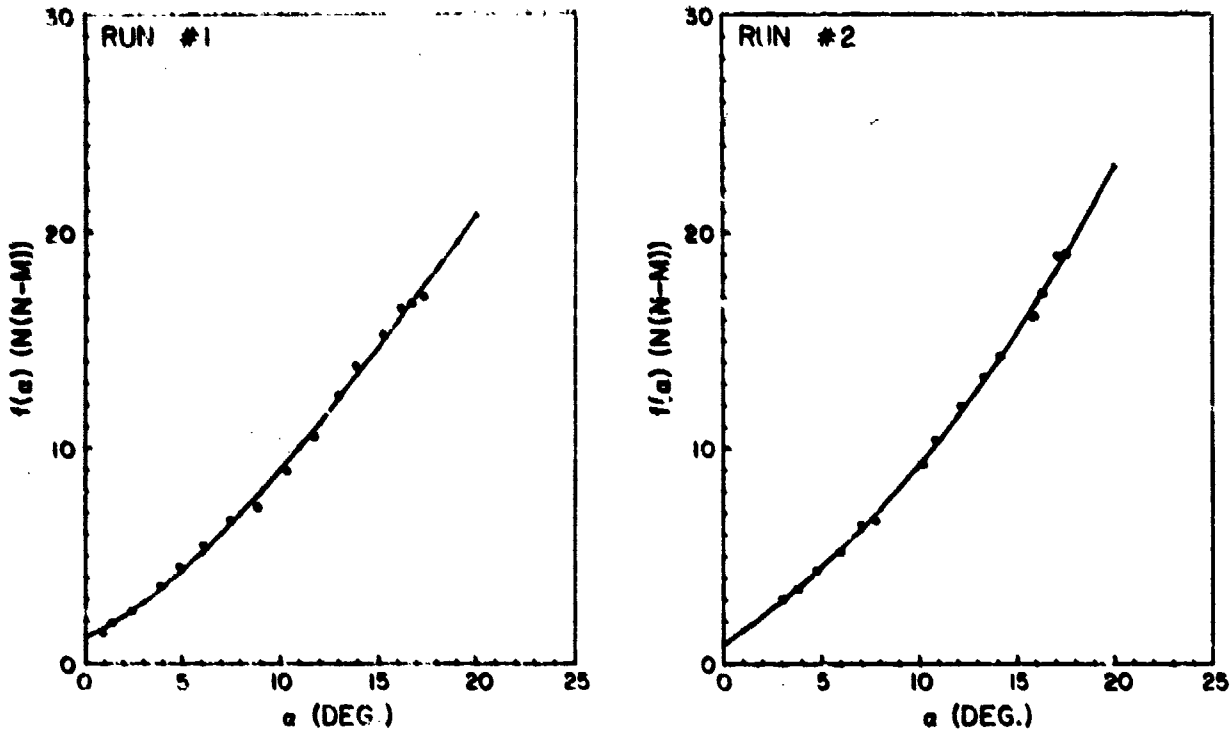

Fig. 5.10 Raw data and functional expansions of the passive resistive property for subject No. 1.

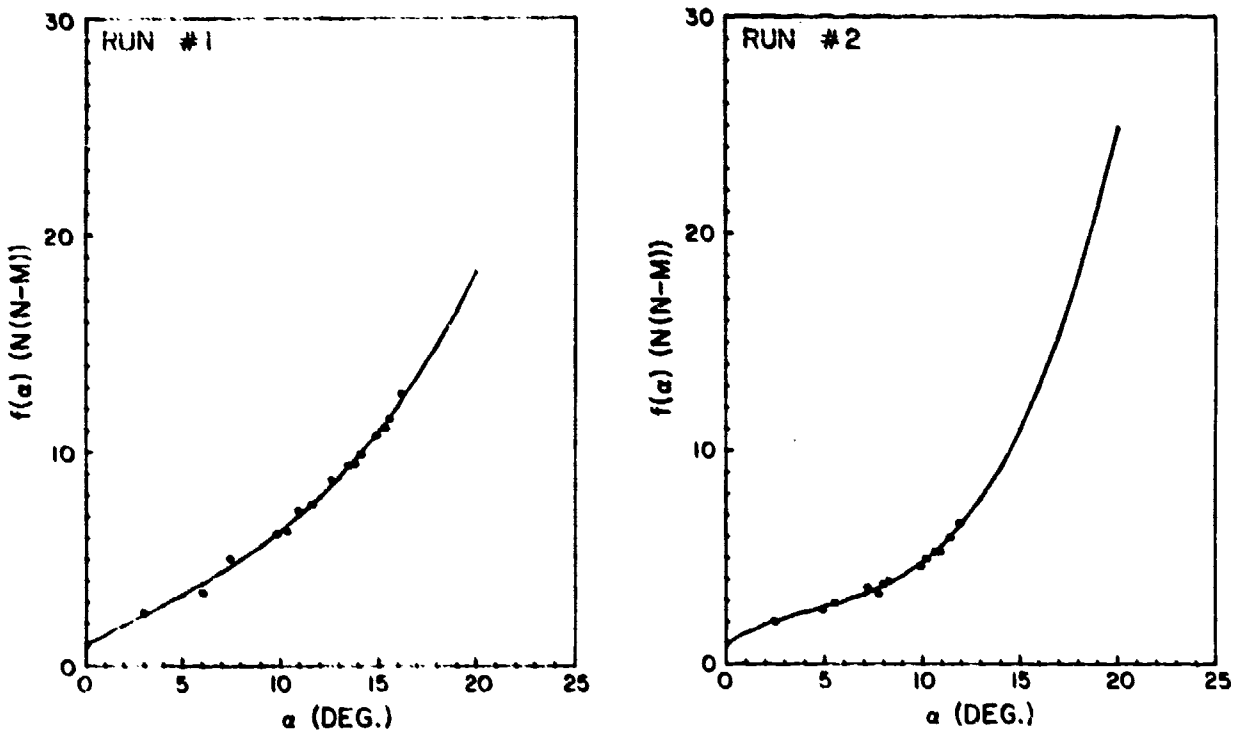

Fig. 5.11 Raw data and functional expansions of the passive resistive property for subject No. 2.

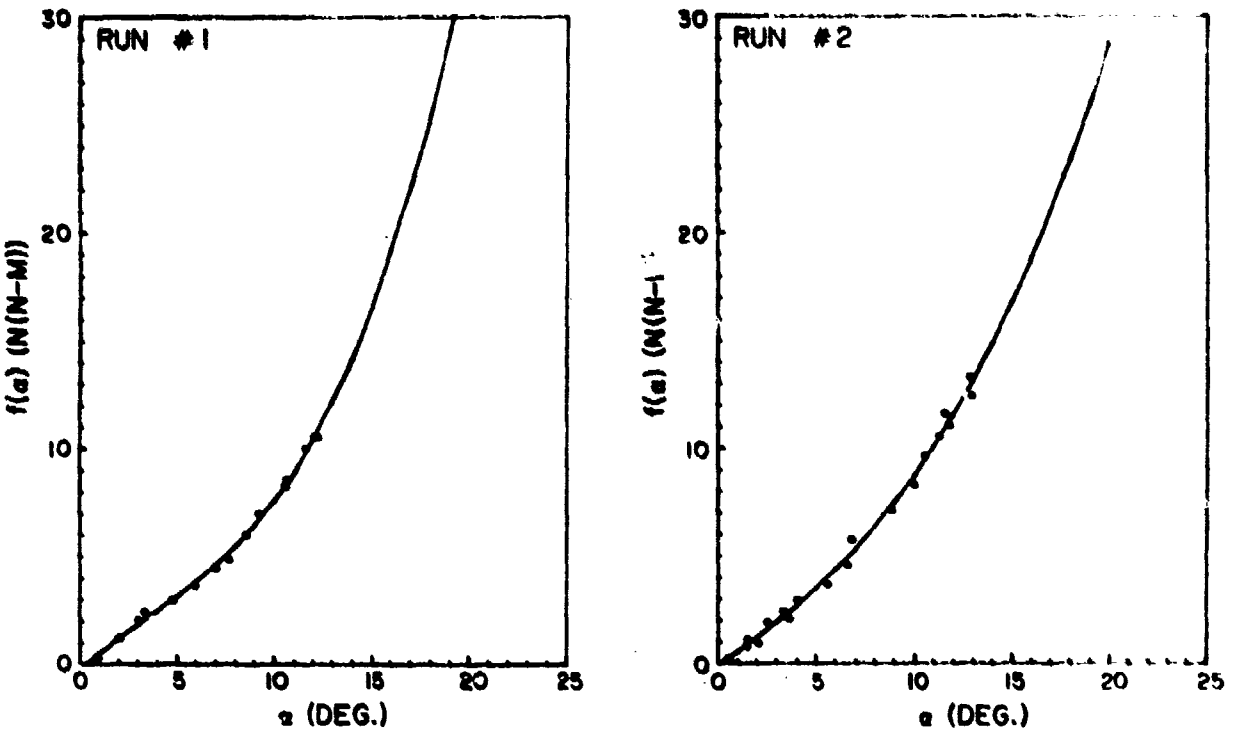

Fig. 5.12 Raw data and functional expansions of the passive resistive property for subject No. 3.

The fast-increasing feature of the passive resistive property reveals the characteristic of the articular check occurring at the elbow joint. Human tolerance beyond the full elbow extension, based on the ten subjects tested, is found to be about 10 to 15 N(N-M) at about 10 to 15 degrees of hyperextension.

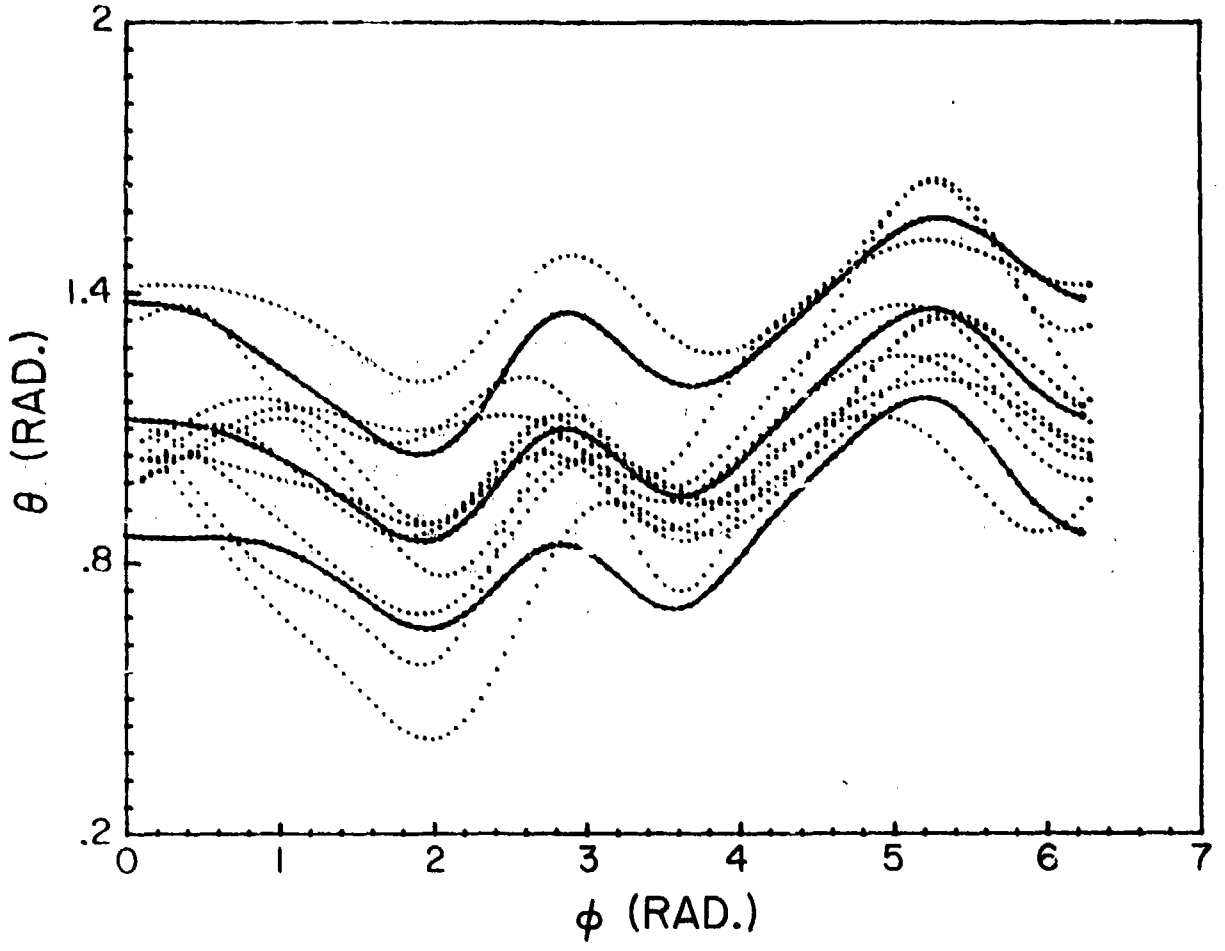

Fig. 5.13 Humero-elbow complex sinuses for all ten subjects. Solid curves are for $\bar{\theta}$ and $\bar{\theta} \pm S_\theta$.

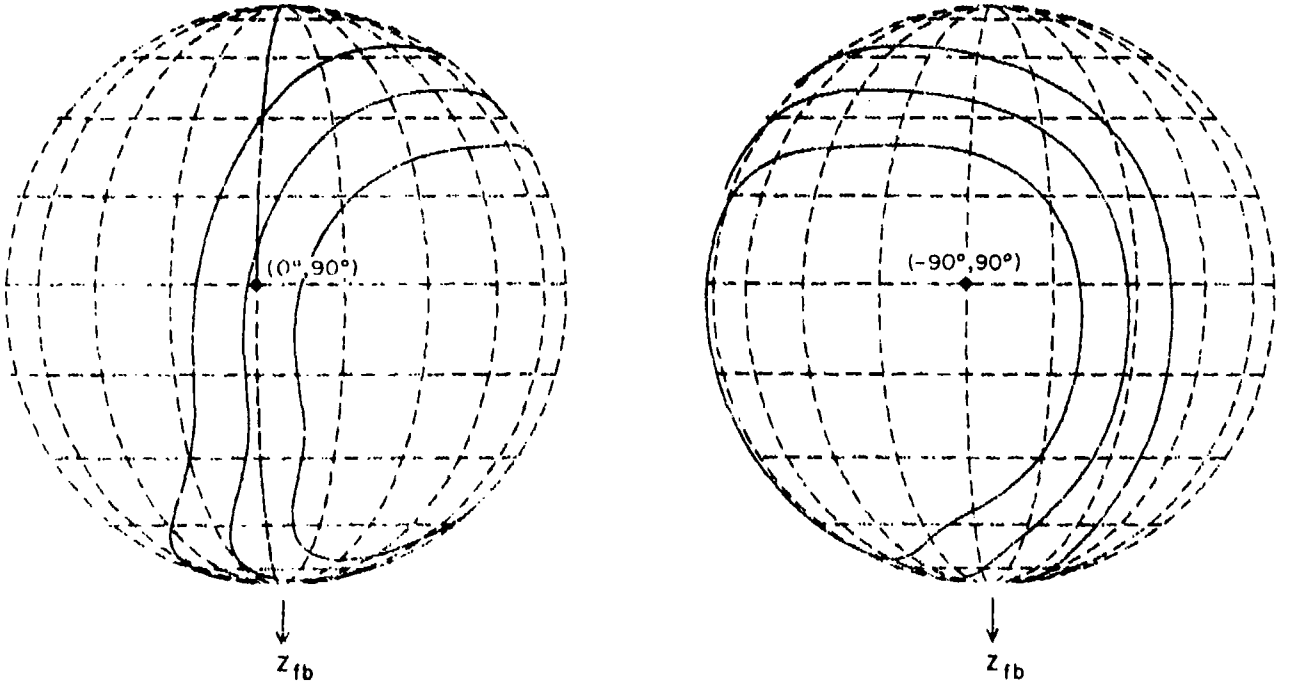

Fig. 5.14 Globographic representations of $\bar{\theta}$ and $\bar{\theta} \pm S_\theta$.

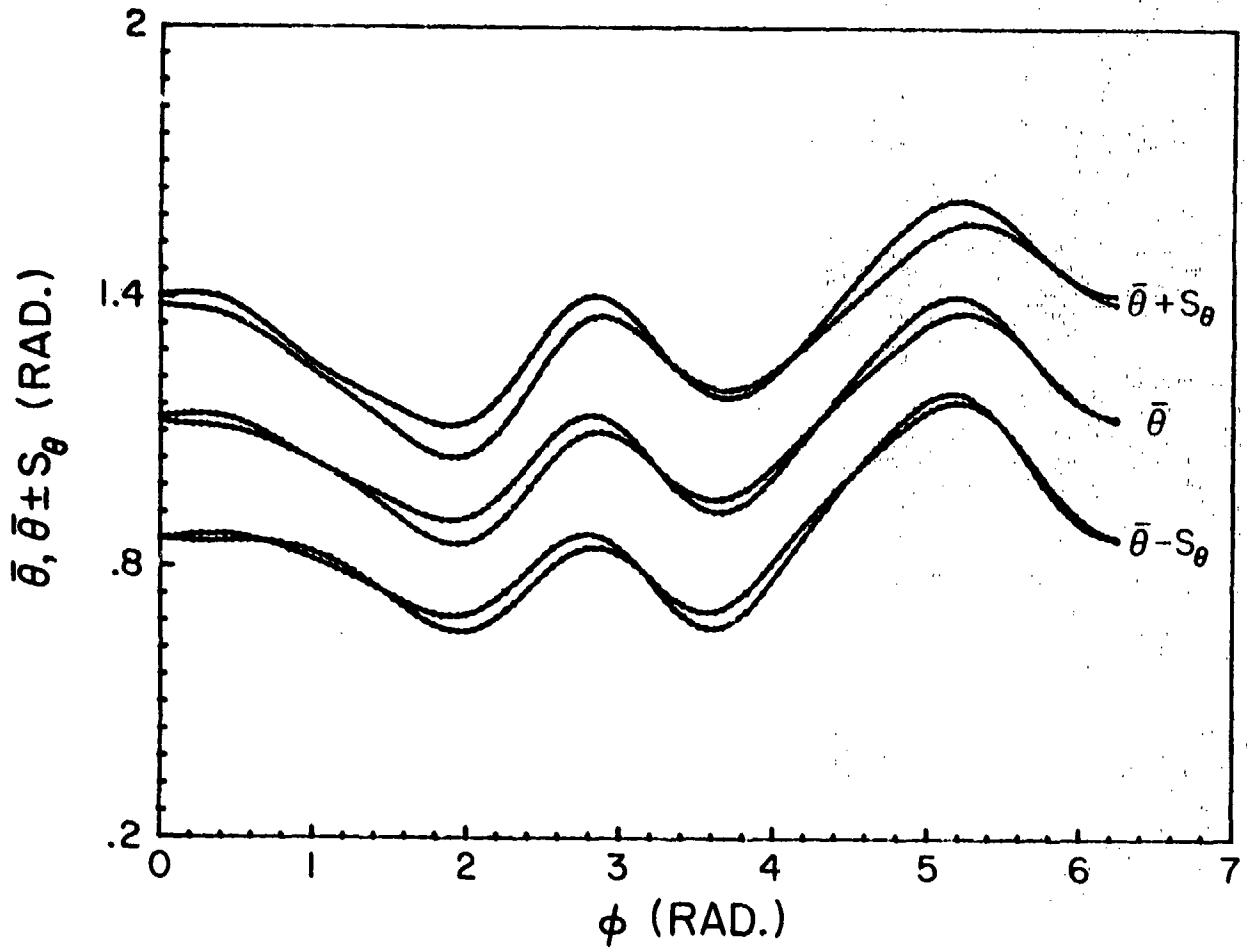

Fig. 5.15 $\bar{\theta}$ and $\bar{\theta} \pm S_\theta$ for two runs.

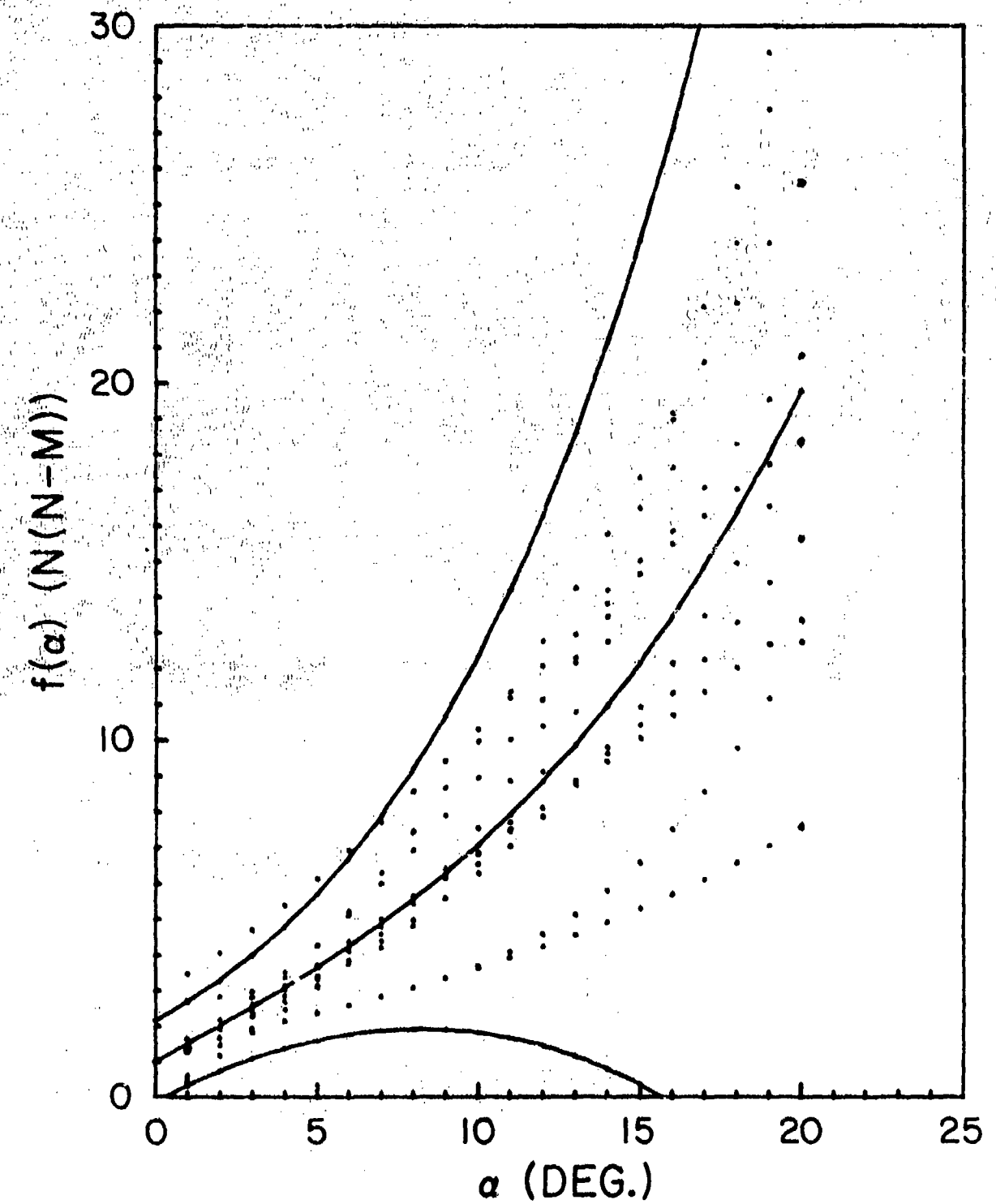

Fig. 5.16 $f(\alpha)$ for all ten subjects. Solid curves are for $\bar{f}$ and $\bar{f} \pm s_f$.

Table 5.1 Centers and radii of the best-fitted spheres and (ϕ_n, θ_n) for all ten subjects.

SUBJECT No.	CENTER (cm) x_{fb}	y_{fb}	z_{fb}	RADIUS (cm)	ϕ_n (deg.)	θ_n (deg.)
1	-0.06	0.19	28.76	29.58	-57.25	74.47
2	0.43	0.12	25.90	29.62	-40.57	71.42
3	0.69	0.96	27.11	29.72	-57.51	70.92
4	1.62	-0.20	28.14	31.12	-43.44	70.21
5	-1.22	-0.30	22.09	28.38	-67.33	58.75
6	-0.72	-1.51	25.00	29.93	-55.06	66.69
7	-0.77	0.88	26.79	30.96	-42.73	75.45
8	-0.43	0.66	27.73	30.24	-53.74	68.01
9	-1.27	1.01	26.90	29.39	-37.92	73.99
10	-1.10	0.21	26.51	28.69	-55.70	59.94
Sample Mean	-0.42	0.20	26.49	29.76	-51.14	68.98
Sample St. Dev.	0.89	0.76	1.88	0.87	9.46	5.78

Table 5.2 Expansion coefficients of the humero-elbow complex sinuses for all ten subjects.

COEFFICIENTS		C_1	C_2	C_3	C_4	C_5	C_6	C_7	C_8	C_9	C_{10}
SUBJ. NO.	1	0.94660	-0.20931	0.35965	-0.11399	0.09762	-0.03984	-0.30936	-0.02223	0.04501	0.16160
	2	1.00298	-0.11922	0.11995	0.05758	0.04369	0.15991	-0.12879	-0.03236	-0.09795	0.31772
	3	1.06830	-0.09237	0.27826	0.10650	-0.02804	0.06418	-0.29654	-0.34261	0.01997	0.11073
	4	1.35042	-0.09649	0.23392	0.00335	-0.00341	0.05962	-0.24854	-0.15328	0.08454	0.17398
	5	0.83271	-0.33242	0.40520	-0.05891	-0.01626	-0.08224	-0.31606	-0.11071	0.20727	0.20206
	6	1.19426	-0.27498	0.40907	0.03315	0.14440	-0.28925	-0.24968	-0.03632	-0.17170	0.70481
	7	1.20455	-0.13006	0.51425	-0.05006	0.02719	0.18983	-0.15035	-0.15804	-0.16461	0.13516
	8	1.17002	-0.05783	0.13041	-0.03689	-0.04236	0.08745	-0.13670	-0.10281	-0.13730	0.11914
	9	1.01306	-0.08750	0.23569	-0.06580	0.08852	-0.17986	-0.22606	-0.19725	-0.08117	0.51515
	10	1.03835	-0.38860	0.46054	-0.15291	-0.10472	-0.16720	-0.36231	-0.40137	0.13013	0.66868
Sample Mean		1.08213	-0.17788	0.27869	-0.02780	-0.02066	-0.01974	-0.24244	-0.15570	-0.01658	0.31150
Sample Variance		0.02233	0.01364	0.01546	0.00623	0.00560	0.02504	0.00668	0.01657	0.01759	0.05377

Table 5.3 Expansion coefficients of the passive resistive properties beyond the full elbow extension for all ten subjects.

COEFFI-CIENTS		C_1	C_2	C_3	C_4
SUBJ. NO.	1	-0.29505	0.97641	-0.04239	0.00167
	2	2.62520	0.12251	-0.01258	0.00397
	3	1.21570	0.41974	0.04335	-0.00077
	4	0.99568	0.36091	0.06439	-0.00104
	5	0.97960	0.40776	-0.03570	0.00224
	6	2.99000	0.47401	0.03703	-0.00111
	7	-0.38531	0.81571	-0.01229	0.00029
	8	1.00290	0.48261	-0.00950	0.00143
	9	-0.28201	0.81601	-0.04942	0.00465
	10	1.25800	0.22501	-0.00158	0.00031
Sample Mean		1.01047	0.51007	-0.00187	0.00116
Sample Variance		1.32818	0.07543	0.00148	0.00000

6. CONCLUDING REMARKS

In biomechanics research, many random variables associated with the human body are either normally distributed or have approximately normal distributions. Therefore, a sample of size ten utilized in this research is expected to provide reasonably good statistical estimations from the analyses presented herein. All the results were presented in a compact format and can thus be easily incorporated into the joint complex regions of the currently existing multisegmented models of the total human body.

From a safety design point of view, the maximal forced sinus data presented in this work can be considered as a prelude towards establishment of a criterion for the impending injury on the joint complexes studied. Any support/restraint or protective device should have the capability of restricting the range of motion of the moving body segment below the maximal forced sinus under most types of external loading conditions.

In conclusion, it is important to point out that biological materials, especially soft tissues, display nonlinear viscoelastic behavior. If we assume that the passive resistive response of the soft tissues in the joint complexes can be modeled similar to the Kelvin viscoelastic material, i.e., elastic and viscous forces are additive, results presented in this work can lead one to the determination of the elastic component of the passive resistive force (moment) on a particular soft tissue. Thus, the next important research endeavor should be the determination of the velocity-dependent viscous component of the passive resistive force (moment) properties.

APPENDIX A: SELECTED ANTHROPOMETRIC MEASUREMENTS OF TEN SUBJECTS

Subject No. / DIMENSIONS (cm)	1	2	3	4	5	6	7	8	9	10
Weight (Newtons)	800	778	889	689	832	734	801	734	734	690
Stature	179.2	188	179.2	183	173	182	183	180	184	187.6
Shoulder circumference	126.5	127	123.8	113	120.6	114.3	119.5	106.7	111	104.1
Waist circumference	93	86	89	73.7	94	79	88	83.8	81	73.7
Wrist circumference	16.8	18.4	18.9	17.8	17.8	17.8	17.8	17.8	17.8	17.8
Lower arm circumference	31.2	29.9	31.3	26.7	29.8	27.9	28.5	27.9	26.7	24.1
Biceps circumference	33.4	34.3	36.5	26.7	34.9	30.5	30.5	27.9	26.7	25.4
Thigh, upper circumference	61.3	58	56	53.3	58.4	53.3	60	56.6	52	50.8
Thigh, lower circumference	42.5	42	44	38.1	43.2	43.2	47	38.1	39	39.4
Calf circumference	39.8	37	39.5	34.9	40.6	40.6	42	39.4	36.5	35.6
Ankle circumference	25.4	26.3	26.7	26.7	25.4	26.7	27	25.4	28	25.4
Forearm - wrist length	20.5	23	20.5	25.4	24.1	24	25.4	23.9	25.4	22.9
Shoulder - elbow length	36	40	35.5	33	27.9	34	37	38.1	35.5	37
Shoulder - height, sitting	60	63	59.5	66	62	60	70	58.4	66	64
Shoulder breadth	51	50	50	44	46	45	44	42	46	43
Chest breadth	32	34.5	31	33	33	32	34	33	34	31
Chest depth	28	27	26	24	25	24	26	24	21	18
Waist depth	27	24.5	25	20	24	18	24	21	21	18
Buttock - knee length	61	65.5	61	56	57	60	58	61	59	61
Buttock - popliteal length	49	54	50	55	50	50	52	50	56	57
Knee height, sitting	54	67	55.7	57	53	56	55	58	56	57
Elbow-to-elbow breadth	47	46	50.5	44	51	45	45	43	44	39
Hip breadth, sitting	39	37	38	37	39	35	41	38	37	34
Knee-to-knee breadth, sitting	25	22.5	23	20	23	25	23	23	22	19

APPENDIX B: COMPUTER PROGRAMS FOR DATA ACQUISITION AND ANALYSIS

The following computer programs were used for the data acquisition and the associated data analysis described in this research work. They are derived from their prototypes used for studying the shoulder complex (Engin and Peindl, 1985), and can be used to study any joint complex as discussed in Chapter 2. Fig. B.1 shows the flowchart for executing these

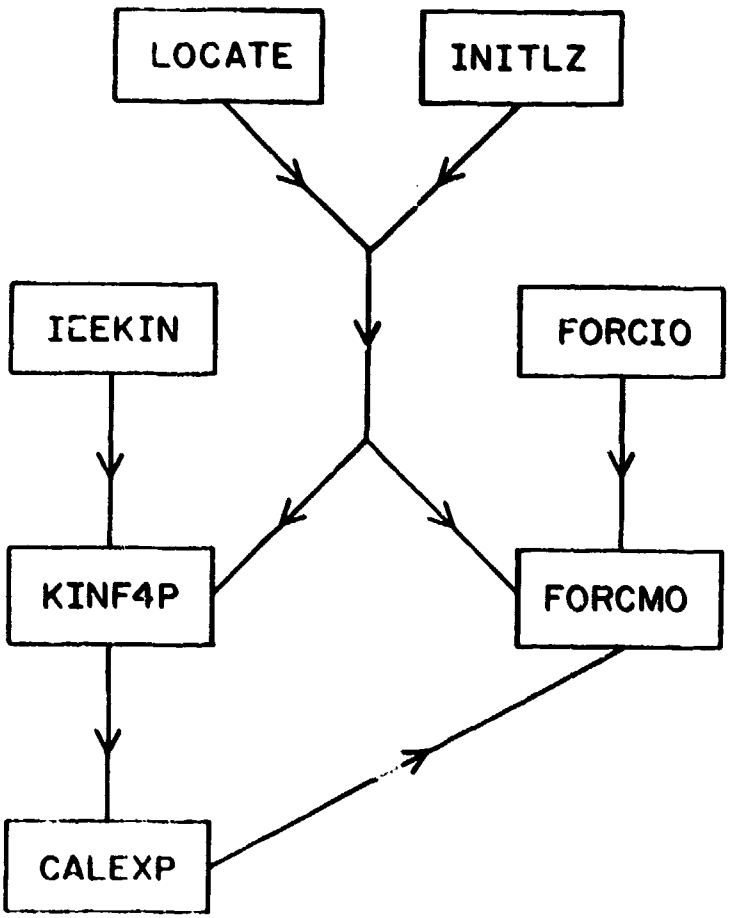

Fig. B.1 Flowchart for data acquisition and associated data analysis.

programs. Data acquisition programs include LOCATE, INITLZ, IEEKIN, and FORCIO; data analysis programs include KINF4P, FORCMO, and CALEXP. A brief description for each program is provided below.

LOCATE: Calculates the direction cosine matrix and origin of the RALD axis system in terms of the sensor assembly axis system. Output from this program is used for determining the fixed-body axis system by both KINF4P and FORCMO.

INITLZ: Performs the initialization procedure as described in Section 2.2 for the interrelationships between the moving-body axis system and the six emitters on the moving body segment. Output from this program is used for selection of the "most accurate" system by both KINF4P and FORCMO.

IEEKIN: Collects slant range data from the six emitters on the moving-body segment. This program is used for the joint complex sinus tests in this work, and can also be applied to collect any kind of kinematic data. Data from this program are analyzed by KINF4P.

FORCIO: Collects slant range data from the six emitters on the moving-body segment and the three emitters on the force applicator. It also collects digital data from the force/moment transducer by means of a FORTRAN-callable macro subroutine OSUATD which exercises the Data Translation DT-1712 Analog-to-Digit converter. Data from this program are analyzed by FORCMO.

KINF4F: Analyzes the kinematics of a moving-body segment with respect to a fixed-body segment by selecting the "most accurate" axis system on the moving-body segment.

FORCMO: Analyzes the kinematics (sweeping-type) of the moving-body segment with respect to the fixed-body segment and calculates the passive resistive forces (moments). It requires the input of the coordinates of the best-fitted sphere center obtained by CALEXP.

CALEXP: Calculates the center and radius of the best-fitted sphere to the joint complex sinus by least-squares method. It also calculates the best-fitted plane to the sinus and then transforms the sinus data into functional relationship with respect to the local joint axis system. Finally, the functional expansion of Eq. (3.2.1) is used to obtain the expansion coefficients for the joint complex sinus.

```
      PROGRAM LOCATE
C
C     THIS PROGRAM USES EMITTER DATA FROM THE 'RALD' TO
C     CALCULATE THE DIRECTION COSINE MATRIX AND ORIGIN OF
C     AN AXIS SYSTEM IN SPACE WITH RESPECT TO THE SENSOR BOARD
C     AXIS SYSTEM
C
      LOGICAL*1 RECDAT(88,5),TEMP(88)
      LOGICAL*1 FINAME(13)
      DIMENSION RECRD(20),POINT(4,3),PTAVG(4,3),DEV(4,3)
      DIMENSION AVGPT(4,3),PT1(3),PT2(3),PT3(3),PT4(3),RALDAX(3,3)
      DIMENSION CNTPT(3),OUTPUT(24),V(6,3),A(3),B(3)
      REAL L1,L2
      INTEGER IPARAM(6,5),DSW,IOST(2),IOSB(2),PRLA(6),CMDA(2)
      COMMON /AC/ L1,L2
      DATA IREC/1/CMDA/'_?','XP'/N/0/KDIV/1/PTAVG/12*0.0/
      DATA AVGPT/12*0.0/
C
C     CREATE & OPEN OUTPUT FILE
C
      WRITE(5,5)
      READ(5,10) (FINAME(I),I=1,13)
      CALL ASSIGN (1,FINAME,13)
      DEFINE FILE 1 (2,48,U,IREC)
C
C     GET THE BUFFER ADDRESSES
C
      CALL GETADR(IPARAM(1,1),RECDAT(1,1))
      CALL GETADR(IPARAM(1,2),RECDAT(1,2))
      CALL GETADR(IPARAM(1,3),RECDAT(1,3))
      CALL GETADR(IPARAM(1,4),RECDAT(1,4))
      CALL GETADR(IPARAM(1,5),RECDAT(1,5))
      IPARAM(2,1)=88
      IPARAM(2,2)=88
      IPARAM(2,3)=88
      IPARAM(2,4)=88
      IPARAM(2,5)=88
C
C     ATTACH IEEE BUS
C
      CALL WTQIO (*1420,2,1,,IOST,,DSW)
      IF(DSW.NE.1)TYPE *,' IEEE BUS WILL NOT PICK YOU UP TODAY!'
      IF(DSW.NE.1) GO TO 2000
      IF(IOST(1).NE.1)TYPE *,' IEEE BUS WILL NOT PICK YOU UP TODAY!'
      IF(IOST(1).NE.1) GO TO 2000
      CALL GETADR (PRLA(1),CMDA(1))
      PRLA(2)=4
C
C     SET UP DIGITIZER AS TALKER
C
      CALL WTQIO (*420,2,1,,IOST,PRLA,DSW)
      IF(DSW.NE.1)TYPE *,' IEEE BUS IS NOT TALKING TODAY!'
      IF(DSW.NE.1) GO TO 2000
```

```
      IF(IOST(1).NE.1)TYPE *,' IEEE BUS IS NOT TALKING TODAY!'
      IF(IOST(1).NE.1) GO TO 2000
C
C     READ FIVE SETS OF POINT VALUES
C
      KOUNT=1
      GO TO 30
20    CALL WAITFR(10)
30    CALL QIO('1000,2,10,,IOSB(1),IPARAM(1,KOUNT),DSW)
      KOUNT=KOUNT+1
      IF(KOUNT.EQ.6) GO TO 50
      GO TO 20
50    CALL WAITFR(10)
      CALL WTQIO('2000,2,1,,IOST,,DSW)
      CALL CLREF(10)
C
C     CALCULATE THE AVERAGE VALUES FOR THE FOUR POINTS
C
55    DO 100 KNT=1,5
      KDIV=KNT-N
      DO 60 II=1,88
      TEMP(II)=RECDAT(II,KNT)
60    CONTINUE
      DECODE (88,300,TEMP) (RECRD(KK),KK=1,20)
      IF(K.GT.1) GO TO 65
      TYPE *,'SLANT RANGE VALUES FOR FIRST RECORD:'
      WRITE(5,900)(RECRD(LK),LK=1,20)
65    CALL COORD(RECRD,POINT,KNT)
      DO 70 JK=1,4
      IF(POINT(JK,1).NE.0.0)GO TO 70
      WRITE(5,560)KNT
      N=N+1
      IF(N.EQ.2) TYPE *,' TWO RECORDS CONTAIN ZERO VALUES. '
     *   ,'JOB FAILED!'
      IF(N.EQ.2)GO TO 3000
      GO TO 100
70    CONTINUE
      DO 90 J=1,4
      DO 80 I=1,3
      PTAVG(J,I)=PTAVG(J,I)+POINT(J,I)
      AVGPT(J,I)=PTAVG(J,I)/KDIV
      DEV(J,I)=ABS(AVGPT(J,I)-POINT(J,I))
      IF(DEV(J,I).LT.0.25) GO TO 80
      WRITE(5,540)
80    CONTINUE
90    CONTINUE
100   CONTINUE
      DO 110 JJ=1,3
      PT1(JJ)=AVGPT(1,JJ)
      PT2(JJ)=AVGPT(2,JJ)
      PT3(JJ)=AVGPT(3,JJ)
      PT4(JJ)=AVGPT(4,JJ)
110   CONTINUE
```

```
      DO 111 I=1,3
      V(1,I)=PT2(I)-PT1(I)
      V(2,I)=PT3(I)-PT1(I)
      V(5,I)=PT4(I)-PT1(I)
      V(4,I)=PT3(I)-PT2(I)
      V(3,I)=PT4(I)-PT3(I)
      V(6,I)=PT2(I)-PT4(I)
111   CONTINUE
      DO 112 I=1,6
      V(I,1)=V(I,1)**2+V(I,2)**2+V(I,3)**2
      V(I,1)=SQRT(V(I,1))
112   CONTINUE
C
C     CALCULATE THE AXIS SYSTEM (RALDAX) AND ORIGIN (CNTPT)
C
      DO 120 I=1,3
      A(I)=PT4(I)-PT2(I)
      B(I)=PT3(I)-PT2(I)
120   CONTINUE
      CALL DRCMAT(A,B,RALDAX)
      DO 130 J=1,3
      CNTPT(J)=PT1(J)-8.491*RALDAX(1,J)
130   CONTINUE
      DO 140 K=1,3
      OUTPUT(K)=PT1(K)
      OUTPUT(K+3)=RALDAX(1,K)
      OUTPUT(K+6)=CNTPT(K)
      OUTPUT(K+9)=PT2(K)
      OUTPUT(K+12)=RALDAX(2,K)
      OUTPUT(K+15)=PT3(K)
      OUTPUT(K+18)=RALDAX(3,K)
      OUTPUT(K+21)=PT4(K)
140   CONTINUE
C
C     PLACE INFORMATION IN DATA FILE
C
      WRITE(5,580)
      WRITE(5,600) (OUTPUT(I),I=1,9)
      WRITE(5,700) (OUTPUT(I), I=10,15)
      WRITE(5,700) (OUTPUT(I), I=16,21)
      WRITE(5,800) (OUTPUT(I), I=22,24)
      WRITE(5,820)
      WRITE(5,840)V(1,1),V(4,1),V(2,1),V(5,1),V(3,1),V(6,1)
      WRITE (1'REC) (OUTPUT(I),I=1,24)
      CLOSE (UNIT=1)
      CALL CLREF(10)
9     FORMAT('$','Enter the name to be given to the data
     $file [S-13]:')
10    FORMAT(13A1)
500   FORMAT(4(F1.0,4F5.2,1X))
540   FORMAT('0','INACCURATE COORDINATE--DEV. EXCEEDS .25CM')
560   FORMAT('0','RECORD NUMBER: ',I5,' CONTAINED ZERO VALUES AND
     $ HAS BEEN DELETED.')
```

```
580   FORMAT('0',T14,'POINT  COORDINATES',T52,'PLATFORM AXES w.r.t.
     $BOARD',T96,'CENTERPOINT (BASE)',/)
600   FORMAT(' ',T10,3(F8.2),T50,3(F9.4),T92,3(F8.2))
700   FORMAT(' ',T10,3(F8.2),T50,3(F9.4))
800   FORMAT(' ',T10,3(F8.2))
820   FORMAT('0',T14,'DIMENSIONAL CHECK'//T5,'LGTH (1-2,1-3,1-4)=4.
     $83cm',T40,'LGTH (2-3,3-4,4-2)=7.67cm',/)
840   FORMAT(' ',T10,'LGTH12=',T18,F5.2,T45,'LGTH23=',T53,F5.2/
     $T10,'LGTH13=',T18,F5.2,T45,'LGTH34=',T53,F5.2/
     $T10,'LGTH14=',T18,F5.2,T45,'LGTH42=',T53,F5.2)
900   FORMAT('0',4(F3.0,4F7.2,4X))
2000  STOP
      END
C
C
      SUBROUTINE DRCMAT(A,B,C)
C
C     THIS SUBROUTINE CALCULATES THE DIRECTION COSINE MATRIX
C     FOR AN AXIS SYSTEM BASED ON TWO COPLANAR VECTORS (A and B).
C     THE RESULTING MATRIX, C, IS ORTHOGONAL AND UNITARY.
C
      DIMENSION A(3),B(3),C(3,3)
      AMAG=SQRT(A(1)**2+A(2)**2+A(3)**2)
      BMAG=SQRT(B(1)**2+B(2)**2+B(3)**2)
      C(2,1)=A(1)/AMAG
      C(2,2)=A(2)/AMAG
      C(2,3)=A(3)/AMAG
      C(3,1)=B(1)/BMAG
      C(3,2)=B(2)/BMAG
      C(3,3)=B(3)/BMAG
      C(1,1)=(C(2,2)*C(3,3))-(C(3,2)*C(2,3))
      C(1,2)=(C(3,1)*C(2,3))-(C(2,1)*C(3,3))
      C(1,3)=(C(2,1)*C(3,2))-(C(3,1)*C(2,2))
      C(3,1)=(C(1,2)*C(2,3))-(C(2,2)*C(1,3))
      C(3,2)=(C(2,1)*C(1,3))-(C(1,1)*C(2,3))
      C(3,3)=(C(1,1)*C(2,2))-(C(2,1)*C(1,2))
      DO 10 J=1,3
      CMAG=SQRT(C(J,1)**2+C(J,2)**2+C(J,3)**2)
      DO 5 I=1,3
      C(J,I)=C(J,I)/CMAG
5     CONTINUE
10    CONTINUE
      RETURN
      END
C
C
      SUBROUTINE COORD(RC2DAT,POINT,KNT)
C
C     THIS SUBROUTINE COMPUTES THE X,Y,Z COORDINATES FOR THE SPARK
C     GAPS IN THE BOARD REFERENCE SYSTEM BY PERFORMING CALCULATIONS
C     ON THE SLANT RANGE DATA FROM THE FOUR CORNER MICROPHONES
C
      DIMENSION RC2DAT(20),POINT(4,3)
```

```
      INTEGER CASE,KNT,SW
      REAL L1,L2,K1
      DATA L1/167.75/, L2/111.60/, K1/3.90/
      CASE=0
      J=1
      DO 110 I=1,16,5
      SW=1
      KK=1
      IF(RC2DAT(I+1) .EQ. 0.0) KK=KK+1
      IF(RC2DAT(I+2) .EQ. 0.0) KK=KK+1
      IF(RC2DAT(I+3) .EQ. 0.0) KK=KK+1
      IF(RC2DAT(I+4) .EQ. 0.0) KK=KK+1
      IF(KK.GT.2) GO TO 115
      PA=RC2DAT(I+1)
      PB=RC2DAT(I+2)
      PC=RC2DAT(I+3)
      PD=RC2DAT(I+4)
      IF(PD.GE.PA.AND.PD.GE.PB.AND.PD.GE.PC) CASE=1
      IF(PC.GE.PA.AND.PC.GE.PB.AND.PC.GE.PD) CASE=2
      IF(PB.GE.PA.AND.PB.GE.PC.AND.PB.GE.PD) CASE=3
      IF(PA.GE.PB.AND.PA.GE.PC.AND.PA.GE.PD) CASE=4
      IF(PD .EQ. 0.0) CASE=1
      IF(PC .EQ. 0.0) CASE=2
      IF(PB .EQ. 0.0) CASE=3
      IF(PA .EQ. 0.0) CASE=4
      GO TO (60,70,80,90),CASE
60    XC=((PA+K1)**2-((PB+K1)**2)+L1**2)/(2.0*L1)
      IF(ABS(XC).GT.ABS(PA+K1)) GO TO 114
      YC=((PA+K1)**2-((PC+K1)**2)+L2**2)/(2.0*L2)
      PP=SQRT((PA+K1)**2-XC**2)
      IF(ABS(YC).GT.PP) GO TO 114
      ZC=SQRT((PP)**2-YC**2)
      GO TO 100
70    XC=((PA+K1)**2-((PB+K1)**2)+L1**2)/(2.0*L1)
      IF(ABS(XC).GT.ABS(PA+K1)) GO TO 114
      YC=((PB+K1)**2-((PD+K1)**2)+L2**2)/(2.0*L2)
      PP=SQRT((PA+K1)**2-XC**2)
      IF(ABS(YC).GT.PP) GO TO 114
      ZC=SQRT((PP)**2-YC**2)
      GO TO 100
80    XC=((PC+K1)**2-((PD+K1)**2)+L1**2)/(2.0*L1)
      IF(ABS(XC).GT.ABS(PC+K1)) GO TO 114
      YC=((PA+K1)**2-((PC+K1)**2)+L2**2)/(2.0*L2)
      PP=SQRT((PC+K1)**2-XC**2)
      YCOMP=L.-YC
      IF(ABS(YCOMP).GT.PP) GO TO 114
      ZC=SQRT((PP)**2-YCOMP**2)
      GO TO 100
90    XC=((PC+K1)**2-((PD+K1)**2)+L1**2)/(2.0*L1)
      IF(ABS(XC).GT.ABS(PC+K1)) GO TO 114
      YC=((PB+K1)**2-((PD+K1)**2)+L2**2)/(2.0*L2)
      PP=SQRT((PC+K1)**2-XC**2)
      YCOMP=L2-YC
```

```
      IF(ABS(YCOMP).GT.PP) GO TO 114
      ZC=SQRT((PP)**2-YCOMP**2)
  100 POINT(J,1)=XC
      POINT(J,2)=YC
      POINT(J,3)=ZC
      J=J+1
      GO TO 110
  114 SW=-1
      WRITE(5,200)J,KNT
  200 FORMAT('0','SPARKER',I4,' IN REC.',I3,' INVALID')
  115 POINT(J,1)=0.0
      POINT(J,2)=0.0
      POINT(J,3)=0.0
      J=J+1
      IF(SW .EQ. -1)GO TO 110
      WRITE(5,130)J,KNT
  130 FORMAT('0','SPARKER',I4,' IN REC.',I3,' IS ZERO')
  110 CONTINUE
      RETURN
      END
```

```
      PROGRAM INITLZ
C
C     THIS PROGRAM SPECIFIES THE INITIAL POSITIONING OF THE ARM
C     CUFF WITH RESPECT TO THE HUMERUS. IT CALCULATES THE JOINT
C     CENTER, LONG BONE AXIS, AND HUMERAL AXIS SYSTEM WITH RESPECT
C     TO ALL THE AXIS SYSTEMS WHICH CAN BE OBTAINED BY THE VARIOUS
C     COMBINATIONS OF THREE CUFF EMITTERS.  IT ALSO ESTABLISHES A
C     CRITERION FOR THE CHOICE OF THE THREE POINTS BY MEANS OF
C     INTER-EMITTER DISTANCES AND AXIS SYSTEM SKEW ANGLES.
C
      LOGICAL*1 RECDAT(198,5),TEMP(198)
      LOGICAL*1 FINAME(13)
      DIMENSION RECRD(45),POINT(9,3),PTAVG(9,3),DEV(9,3)
      DIMENSION AVGPT(9,3),VECMAG(15),COSMAT(60,3)
      DIMENSION DRCOS(3,3),NVEC(20,4),LBVEC(3),JNTVEC(20,3)
      DIMENSION JTVEC(5,3),H1(3),H2(3),H3(3),HUMAX(3,3),HUMDRC(60,3)
      DIMENSION TEMP2(3,3),F1(3),G1(3),V(5,4)
      REAL LBVEC,JTVEC,JNTVEC,LBMAG,L1,L2
      INTEGER IPARAM(6,5),DSW,IOST(2),IOSB(2),PRLA(6),CMDA(2)
      DATA IREC/1/CMDA/'.T','&F'/N/0/KDIV/1/PTAVG/2740.0/
      DATA AVGPT/2740.0/JTVEC/1540.0/
      DATA NVEC/1,1,1,1,2,2,2,3,3,4,6,6,6,7,7,8,10,10,11,13,6,7,8,9
     &,10,11,12,13,14,15,10,11,12,13,14,15,13,14,15,15,2,3,4,5,3,4,5,
     &4,5,5,7,8,9,8,9,9,11,12,13,14,2,2,2,2,3,3,3,4,4,5,3,3,3,4,4,5,4
     &,4,5,5/
      COMMON /AC/ VEC(15,3)
C
C     CREATE & OPEN OUTPUT FILE
C
      WRITE(5,5)
      READ(5,10) (FINAME(I),I=1,13)
      CALL ASSIGN (1,FINAME,13)
      DEFINE FILE 1 (876,2,U,IREC)
C
C     GET THE BUFFER ADDRESSES
C
      CALL GETADR(IPARAM(1,1),RECDAT(1,1))
      CALL GETADR(IPARAM(1,2),RECDAT(1,2))
      CALL GETADR(IPARAM(1,3),RECDAT(1,3))
      CALL GETADR(IPARAM(1,4),RECDAT(1,4))
      CALL GETADR(IPARAM(1,5),RECDAT(1,5))
      IPARAM(2,1)=198
      IPARAM(2,2)=198
      IPARAM(2,3)=198
      IPARAM(2,4)=198
      IPARAM(2,5)=198
C
C     ATTACH IEEE BUS
C
      CALL WTQIO (%1420,2,1,,IOST,,DSW)
      IF(DSW.NE.1)TYPE *,' IEEE BUS IS NOT ATTACHED!'
      IF(DSW.NE.1) GO TO 2000
      IF(IOST(1).NE.1)TYPE *,' IEEE BUS IS NOT ATTACHED!'
```

```
      IF(IOST(1).NE.1) GO TO 2000
      CALL GETADR (PRLA(1),CMDA(1))
      PRLA(2)=4
C
C     SET UP DIGITIZER AS TALKER
C
      CALL WTQIO (%420,2,1,,IOST,PRLA,DSW)
      IF(DSW.NE.1)TYPE 4,' DIGITIZER IS NOT TALKING!'
      IF(DSW.NE.1) GO TO 2000
      IF(IOST(1).NE.1)TYPE 4,' DIGITIZER IS NOT TALKING!'
      IF(IOST(1).NE.1) GO TO 2000
C
C     READ FIVE SETS OF NINE POINT VALUES
C
      KOUNT=1
      GO TO 30
20    CALL WAITFR(10)
30    CALL QIO(%1000,2,10,,IOSB(1),IPARAM(1,KOUNT),DSW)
      KOUNT=KOUNT+1
      IF(KOUNT.EQ.6) GO TO 50
      GO TO 20
50    CALL WAITFR(10)
      CALL WTQIO(%2000,2,1,,IOST,,DSW)
      CALL CLREF(10)
C
C     CALCULATE THE AVERAGE VALUES FOR THE NINE POINTS
C
55    DO 100 KNT=1,5
      KDIV=KNT-N
      DO 60 II=1,198
      TEMP(II)=RECDAT(II,KNT)
60    CONTINUE
      DECODE (198,300,TEMP) (RECRD(KK),KK=1,45)
      WRITE(5,1003) KNT,(RECRD(KK),KK=1,20)
      WRITE(5,1004)(RECRD(KK),KK=21,45)
      CALL COORD(RECRD,POINT,SW,KNT)
      DO 70 JK=1,9
      IF(POINT(JK,1).NE.0.0) GO TO 70
      WRITE(5,560) KNT
      N=N+1
      IF(N.EQ.2)TYPE 4,' TWO SWEEPS CONTAIN ZERO VALUES, JOB FAILED!'
      IF(N.EQ.2) GO TO 2000
      GO TO 100
70    CONTINUE
      DO 90 J=1,9
      DO 80 I=1,3
      PTAVG(J,I)=PTAVG(J,I)+POINT(J,I)
      AVGPT(J,I)=PTAVG(J,I)/KDIV
      DEV(J,I)=ABS(AVGPT(J,I)-POINT(J,I))
      IF(DEV(J,I).LT.0.25) GO TO 80
      WRITE(5,540)
80    CONTINUE
90    CONTINUE
```

```
100  CONTINUE
     WRITE(5,3)
3    FORMAT('0')
     TYPE *,' AVERAGE COORDINATES W.R.T. SENSOR BOARD:'
     TYPE *,'                          X              Y              Z'
     TYPE *,' '
     DO 101 I=1,9
     TYPE *,' SPARKER #',I,(AVGPT(I,J), J=1,3)
101  CONTINUE
     DO 1001 I=1,3
     V(1,I)=AVGPT(2,I)-AVGPT(1,I)
     V(2,I)=AVGPT(4,I)-AVGPT(3,I)
     V(3,I)=AVGPT(6,I)-AVGPT(5,I)
     V(4,I)=AVGPT(8,I)-AVGPT(7,I)
     V(5,I)=AVGPT(9,I)-AVGPT(8,I)
1001 CONTINUE
     DO 1002 I=1,5
     V(I,4)=SQRT(V(I,1)**2+V(I,2)**2+V(I,3)**2)
1002 CONTINUE
     WRITE(5,800)
     WRITE(5,801)V(1,4),V(2,4),V(3,4),V(4,4),V(5,4)
C
C    CALCULATE THE 20 POSSIBLE VECTOR TRIADS FOR THE
C    VARIOUS COMBINATIONS OF 3 CUFF EMITTERS
C    1ST, CALCULATE ALL THE VECTORS
C
     KK=1
     L=1
102  JJ=L+1
     DO 104 M=JJ,6
     VEC(KK,1)=AVGPT(M,1)-AVGPT(L,1)
     VEC(KK,2)=AVGPT(M,2)-AVGPT(L,2)
     VEC(KK,3)=AVGPT(M,3)-AVGPT(L,3)
     KK=KK+1
104  CONTINUE
     L=L+1
     IF(L.LT.6)GO TO 102
C
C
     DO 105 I=1,15
     VECMAG(I)=VEC(I,1)**2+VEC(I,2)**2+VEC(I,3)**2
     VECMAG(I)=SQRT(VECMAG(I))
105  CONTINUE
     DO 109 I=1,15
     DO 108 J=1,3
     VEC(I,J)=VEC(I,J)/VECMAG(I)
108  CONTINUE
109  CONTINUE
C
C    CALCULATE THE POSSIBLE AXIS SYSTEMS
C
     KK=0
     DO 150 M=1,20
```

```
      K=NVEC(M,1)
      L=NVEC(M,2)
      CALL DRCMAT(K,L,DRCOS)
      DO 140 J=1,3
      DO 130 N=1,3
      COSMAT(KK+J,N)=DRCOS(J,N)
  130 CONTINUE
  140 CONTINUE
      KK=KK+3
  150 CONTINUE
C
C     CALCULATE THE JOINT CENTER, WHICH IS LOCATED AT
C     THE CENTER OF SPARKER 7 & 8, AND STORE IT IN AVGPT(7,I)
C
      DO 145 I=1,3
  145 AVGPT(7,I)=(AVGPT(7,I)+AVGPT(8,I))/2.0
C
C     CALCULATE THE VECTORS FROM THE ORIGINS OF THE VARIOUS
C     AXIS SYSTEMS TO THE JOINT CENTER
C
      DO 180 I=2,5
      JTVEC(I,1)=AVGPT(7,1)-AVGPT(I,1)
      JTVEC(I,2)=AVGPT(7,2)-AVGPT(I,2)
      JTVEC(I,3)=AVGPT(7,3)-AVGPT(I,3)
  180 CONTINUE
C
C     CALCULATE THE HUMERAL AXIS SYSTEM
C
      DO 181 I=1,3
      H3(I)=AVGPT(9,1)-AVGPT(7,I)
      H2(I)=AVGPT(8,1)-AVGPT(7,I)
  181 CONTINUE
      CALL CROS(H2,H3,H1)
      DO 182 I=1,3
      HUMAX(1,I)=H1(I)
      HUMAX(2,I)=H2(I)
  182 HUMAX(3,I)=H3(I)
C
C     CALCULATE EACH JOINT CENTER AND HUMERAL AXIS SYSTEM IN TERMS
C     OF EACH LOCAL AXIS SYSTEM
C
      K=0
      CALL MINV(HUMAX,3,D,F1,G1)
      DO 190 I=1,20
      DO 185 J=1,3
      DRCOS(J,1)=COSMAT(K+J,1)
      DRCOS(J,2)=COSMAT(K+J,2)
      DRCOS(J,3)=COSMAT(K+J,3)
  185 CONTINUE
      L=NVEC(I,4)
      JNTVEC(I,1)=DRCOS(1,1)*JTVEC(L,1)+DRCOS(1,2)*JTVEC(L,2)+
     *DRCOS(1,3)*JTVEC(L,3)
      JNTVEC(I,2)=DRCOS(2,1)*JTVEC(L,1)+DRCOS(2,2)*JTVEC(L,2)+
```

```
     &DRCOS(2,3)&JTVEC(L,3)
     JNTVEC(I,3)=DRCOS(3,1)&JTVEC(L,1)+DRCOS(3,2)&JTVEC(L,2)+
     &DRCOS(3,3)&JTVEC(L,3)
     CALL GMPRD(DRCOS,HUMAX,TEMP2,3,3,3)
     DO 187 J=1,3
     HUMDRC(K+1,J)=TEMP2(J,1)
     HUMDRC(K+2,J)=TEMP2(J,2)
187  HUMDRC(K+3,J)=TEMP2(J,3)
     K=K+3
190  CONTINUE
C
C    WRITE DATA TO DATA FILE
C
     DO 750 I=1,6
     DO 749 J=1,3
     WRITE(1'IREC)AVGPT(I,J)
749  CONTINUE
750  CONTINUE
     DO 760 I=1,60
     DO 759 J=1,3
     WRITE(1'IREC)COSMAT(I,J)
759  CONTINUE
760  CONTINUE
     DO 780 I=1,20
     DO 779 J=1,3
     WRITE(1'IREC)JNTVEC(I,J)
779  CONTINUE
780  CONTINUE
     DO 790 I=1,60
     DO 789 J=1,3
     WRITE(1'IREC)HUMDRC(I,J)
789  CONTINUE
790  CONTINUE
C
C
     CLOSE (UNIT=1)
C
C
C
     CALL CLREF(10)
5    FORMAT('$','Enter the name to be given to the data
     $file [S-13]:')
10   FORMAT(13A1)
300  FORMAT(9(F1.0,4F5.2,1X))
540  FORMAT('0','INACCURATE COORDINATE--DEV. EXCEEDS .25CM')
560  FORMAT('0','RECORD NUMBER: ',I5,' CONTAINED ZERO VALUES AND
     $ HAS BEEN DELETED.')
800  FORMAT('0','DIMENSIONAL CHECK--LGTH(1-2)=9.48cm',T50,'LGTH
     &(3-4)=9.58cm',T80,'LGTH(5-6)=9.52cm',T110,'LGTH(7-8)=21.92CM',
     &T140,'LGTH(8-9)=15.10CM')
801  FORMAT('0',T5,'CALCULATED LENGTHS:=',T30,F5.2,T59,F5.2,T89,
     &F5.2,T120-F5.2,T150,F5.2)
1003 FORMAT('0','RECORD(SWEEP) NO.',I2/1X,4(F3.0,4F7.2,2X))
```

```
1004 FORMAT(' ',5(F3.0,4F7.2,2X))
2000 STOP
     END
C
C
     SUBROUTINE COORD(RC2DAT,POINT,SW,KOUNT)
C
C    THIS SUBROUTINE COMPUTES THE X,Y,Z COORDINATES FOR THE SPARK
C    GAPS IN THE ROOM REFERENCE SYSTEM BY PERFORMING CALCULATIONS
C    ON THE SLANT RANGE DATA FROM THE FOUR CORNER MICROPHONES
C
     DIMENSION RC2DAT(45),POINT(9,3)
     INTEGER CASE,KOUNT,SW
     REAL L1,L2,K1
     DATA L1/167.75/, L2/111.80/, K1/3.90/
     CASE=0
     J=1
     DO 110 I=1,41,5
     SW=1
     KK=1
     IF(RC2DAT(I+1) .EQ. 0.0) KK=KK+1
     IF(RC2DAT(I+2) .EQ. 0.0) KK=KK+1
     IF(RC2DAT(I+3) .EQ. 0.0) KK=KK+1
     IF(RC2DAT(I+4) .EQ. 0.0) KK=KK+1
     IF(KK.GT.2) GO TO 115
     PA=RC2DAT(I+1)
     PB=RC2DAT(I+2)
     PC=RC2DAT(I+3)
     PD=RC2DAT(I+4)
     IF(PD.GE.PA.AND.PD.GE.PB.AND.PD.GE.PC) CASE=1
     IF(PC.GE.PA.AND.PC.GE.PB.AND.PC.GE.PD) CASE=2
     IF(PB.GE.PA.AND.PB.GE.PC.AND.PB.GE.PD) CASE=3
     IF(PA.GE.PB.AND.PA.GE.PC.AND.PA.GE.PD) CASE=4
     IF(PD .EQ. 0.0) CASE=1
     IF(PC .EQ. 0.0) CASE=2
     IF(PB .EQ. 0.0) CASE=3
     IF(PA .EQ. 0.0) CASE=4
     GO TO (60,70,80,90),CASE
60   XC=((PA+K1)**2-((PB+K1)**2)+L1**2)/(2.0*L1)
     IF(ABS(XC).GT.ABS(PA+K1)) GO TO 114
     YC=((PA+K1)**2-((PC+K1)**2)+L2**2)/(2.0*L2)
     PP=SQRT((PA+K1)**2-XC**2)
     IF(ABS(YC).GT.PP) GO TO 114
     ZC=SQRT((PP)**2-YC**2)
     GO TO 100
70   XC=((PA+K1)**2-((PB+K1)**2)+L1**2)/(2.0*L1)
     IF(ABS(XC).GT.ABS(PA+K1)) GO TO 114
     YC=((PB+K1)**2-((PD+K1)**2)+L2**2)/(2.0*L2)
     PP=SQRT((PA+K1)**2-XC**2)
     IF(ABS(YC).GT.PP) GO TO 114
     ZC=SQRT((PP)**2-YC**2)
     GO TO 100
80   XC=((PC+K1)**2-((PD+K1)**2)+L1**2)/(2.0*L1)
```

```
      IF(ABS(XC).GT.ABS(PC+R1)) GO TO 114
      YC=((PA+R1)**2-((PC+R1)**2)+L2**2)/(2.0*L2)
      PP=SQRT((PC+R1)**2-XC**2)
      YCCOMP=L2-YC
      IF(ABS(YCCOMP).GT.PP) GO TO 114
      ZC=SQRT((PP)**2-YCCOMP**2)
      GO TO 100
   90 XC=((PC+R1)**2-((PD+R1)**2)+L1**2)/(2.0*L1)
      IF(ABS(XC).GT.ABS(PC+R1)) GO TO 114
      YC=((PB+R1)**2-((PD+R1)**2)+L2**2)/(2.0*L2)
      PP=SQRT((PC+R1)**2-XC**2)
      YCCOMP=L2-YC
      IF(ABS(YCCOMP).GT.PP) GO TO 114
      ZC=SQRT((PP)**2-YCCOMP**2)
  100 POINT(J,1)=XC
      POINT(J,2)=YC
      POINT(J,3)=ZC
      GO TO 117
  114 SW=-1
      WRITE(5,200)RC2DAT(I),KOUNT
  200 FORMAT('0','SPARKER',F3.0,' IN REC.',I3,' INVALID')
  115 POINT(J,1)=0.0
      POINT(J,2)=0.0
      POINT(J,3)=0.0
      IF(SW .EQ. -1)GO TO 117
      WRITE(5,130)RC2DAT(I),KOUNT
  130 FORMAT('0','SPARKER',F3.0,' IN REC.',I3,' IS ZERO')
  117 J=J+1
  110 CONTINUE
      RETURN
      END
C
      SUBROUTINE CROS(A,B,C)
C
C     THIS SUBROUTINE CALCULATES A UNIT VECTOR (C) WHICH IS PERPEN-
C     DICULAR TO THE PLANE CONTAINING THE VECTORS A AND B.  NOTE
C     THAT THE VECTORS A AND B ARE RETURNED AS UNIT VECTORS!
C
      DIMENSION A(3),B(3),C(3)
      AMAG=SQRT(A(1)**2+A(2)**2+A(3)**2)
      BMAG=SQRT(B(1)**2+B(2)**2+B(3)**2)
      A(1)=A(1)/AMAG
      A(2)=A(2)/AMAG
      A(3)=A(3)/AMAG
      B(1)=B(1)/BMAG
      B(2)=B(2)/BMAG
      B(3)=B(3)/BMAG
      C(1)=(A(2)*B(3))-(B(2)*A(3))
      C(2)=(A(3)*B(1))-(B(3)*A(1))
      C(3)=(A(1)*B(2))-(B(1)*A(2))
      RETURN
      END
C
```

```
      SUBROUTINE DRCMAT(K,L,C)
C
C     THIS SUBROUTINE CALCULATES THE DIRECTION COSINE MATRIX
C     FOR AN AXIS SYSTEM BASED ON TWO COPLANAR VECTORS (SPECIFIED
C     BY K and L).  THE RESULTING MATRIX, C, IS ORTHOGONAL AND
C     UNITARY.
C
      DIMENSION A(3),B(3),C(3,3)
         INTEGER K,L
      COMMON /AC/ VEC(15,3)
C
      DO 2 I=1,3
      A(I)=VEC(K,I)
      B(I)=VEC(L,I)
2     CONTINUE
      AMAG=SQRT(A(1)**2+A(2)**2+A(3)**2)
      BMAG=SQRT(B(1)**2+B(2)**2+B(3)**2)
      C(1,1)=A(1)/AMAG
      C(1,2)=A(2)/AMAG
      C(1,3)=A(3)/AMAG
      C(2,1)=B(1)/BMAG
      C(2,2)=B(2)/BMAG
      C(2,3)=B(3)/BMAG
      C(3,1)=(C(1,2)*C(2,3))-(C(2,2)*C(1,3))
      C(3,2)=(C(1,3)*C(2,1))-(C(2,3)*C(1,1))
      C(3,3)=(C(1,1)*C(2,2))-(C(2,1)*C(1,2))
      C(2,1)=(C(3,2)*C(1,3))-(C(1,2)*C(3,3))
      C(2,2)=(C(3,3)*C(1,1))-(C(3,1)*C(1,3))
      C(2,3)=(C(3,1)*C(1,2))-(C(1,1)*C(3,2))
      DO 10 J=1,3
      CMAG=SQRT(C(J,1)**2+C(J,2)**2+C(J,3)**2)
      DO 5 I=1,3
      C(J,I)=C(J,I)/CMAG
5     CONTINUE
10    CONTINUE
      RETURN
      END
```

```
      PROGRAM IEEEIN
C
C     THIS PROGRAM COLLECTS THE SLANT RANGE VALUES FROM THE SONIC
C     DIGITIZER FOR SIX EMITTERS USING THE IEE-488 INTERFACE.  THIS
C     DATA IS USED FOR KINEMATIC ANALYSIS OF THE MOVING BODY SEGMENT.
C
      DIMENSION OUTPUT(5,30),RECORD(24)
      DIMENSION ONEREC(30)
      VIRTUAL BIGBUF(1000,24)
      LOGICAL*1 TRANS(660)
      LOGICAL*1 RECDAT(660,2)
      LOGICAL*1 FNAME(13)
      INTEGER IPARAM(6,2),IOSB(2,2),PRLA(6),CHECK2
      INTEGER IPARM(6),IOSTOP(2),DSW,CMDA(2)
      INTEGER COLUMN,TEST(1),CHECK,SW,KOUNT,IOST(2)
      DATA TEST/-1/CHECK/0/COLUMN/1/KOUNT/0/
      DATA CMDA/'_P','UP'/
      DATA MODE/1/LMODE/2/NREC/1/
C
C     INPUT DATA FILENAME AND # OF RECORDS
C
      WRITE(5,4)
      WRITE(5,5)
      READ(5,10) (FNAME(I),I=1,13)
      WRITE(5,15)
      READ (5,20) NREC
      NDIV=NREC/5
C
C     OPEN TEMPORARY DATA FILE FOR INCOMING SLANT RANGE DATA
C
      OPEN (UNIT=1,TYPE='SCRATCH',FORM='UNFORMATTED')
C
C     GET THE BUFFER ADDRESSES
C
      CALL GETADR(IPARAM(1,1),RECDAT(1,1))
      CALL GETADR(IPARAM(1,2),RECDAT(1,2))
      IPARAM(2,1)=660
      IPARAM(2,2)=660
      CALL GETADR(IPARM(1),TEST(1))
      IPARM(2)=1
C
C     ATTACH IEEE BUS
C
      CALL WTQIO ('1420,2,1,,IOST,,DSW)
      IF(DSW.NE.1) TYPE *,' IEEE BUS WILL NOT PICK YOU UP TODAY! '
      IF(DSW.NE.1) GO TO 2000
      IF(IOST(1).NE.1) TYPE *,' IEEE BUS WILL NOT PICK YOU UP TODAY! '
      IF(IOST(1).NE.1) GO TO 2000
      CALL GETADR (PRLA(1),CMDA(1))
      PRLA(3)=4
C
C     SET UP DIGITIZER AS TALKER
C
```

```
      CALL WTQIO ('420,2,1,,IOST,PRLA,DSW)
      IF(DSW.NE.1) TYPE 4,' IEEE BUS IS NOT TALKING TODAY! '
      IF(DSW.NE.1) GO TO 2000
      IF(IOST(1).NE.1) TYPE 4,' IEEE BUS IS NOT TALKING TODAY! '
      IF(IOST(1).NE.1) GO TO 2000
C
C     QUEUE THE FIRST I/O
C
      CALL QIO('1000,2,10,,IOSB(1,1),IPARAM(1,1),DSW)
C
C     INITIALIZE THE NUMBER OF RECORDS TRANSFERRED
C
100   NNODE=MODE
      MODE=LMODE
      LMODE=NNODE
C
C     WAIT FOR THE BUFFER TO FILL
C
      CALL WAITFR(10)
      CALL QIO('1000,2,10,,IOSB(1,MODE),IPARAM(1,MODE),DSW)
      IF(CHECK .EQ. NDIV)GO TO 1200
      WRITE(1)(RECDAT(I,LMODE),I=1,660)
C
C     INCREMENT THE NUMBER OF RECORDS
C
      COLUMN=COLUMN+1
      CHECK=COLUMN-1
      GOTO 100
1200  CHECK2=CHECK*5
      WRITE(5,45)CHECK2
C
C     READ SLANT RANGE DATA FROM DISK AND CONVERT TO
C     X,Y,Z COORDINATES
C
      REWIND 1
C
      DO 980 K=1,CHECK
      READ(1)(TRANS(I),I=1,660)
      DECODE (660,530,TRANS)((OUTPUT(J,KK),KK=1,30),J=1,5)
      IF(K.NE.CHECK) GO TO 901
      TYPE 4,'SLANT RANGE DATA FOR FINAL RECORD:'
      WRITE(5,1010)(OUTPUT(5,LL),LL=1,15)
      WRITE(5,1015)(OUTPUT(5,LL),LL=16,30)
901   IF(K.GT.1) GO TO 902
      TYPE 4,'SLANT RANGE DATA FOR FIRST RECORD:'
      WRITE(5,1010)(OUTPUT(1,LL),LL=1,15)
      WRITE(5,1015)(OUTPUT(1,LL),LL=16,30)
902   DO 960 II=1,5
      DO 910 JJ=1,30
      ONEREC(JJ)=OUTPUT(II,JJ)
910   CONTINUE
            CALL COORD(ONEREC,RECORD,SW,NOUNT)
            IF(NOUNT .GT. 0) GOTO 920
```

```
            WRITE(5,535) (FNAME(I),I=1,13)
            WRITE(5,540) (RECORD(I),I=1,20)
            WRITE(5,545) (RECORD(I),I=21,24)
920   DO 930 J=1,24
      BIGBUF((KOUNT+1),J)=RECORD(J)
930   CONTINUE
            DO 940 I=1,30
                  INCREC(I)=0.0
940         CONTINUE
            DO 950 I=1,24
            RECORD(I)=0.0
950         CONTINUE
            KOUNT=KOUNT+1
960   CONTINUE
            DO 970 I=1,660
                  TRANS(I)=' '
970         CONTINUE
980   CONTINUE
1500  CLOSE (UNIT=1)
C
C     OPEN DATA FILE FOR CONVERTED DATA AND WRITE
C     EMITTER COORDINATE DATA TO DISK
C
      CALL ASSIGN (1,FNAME,13)
      DEFINE FILE 1 (NREC,48,U,KREC)
      DO 1550 I=1,NREC
      WRITE(1'KREC)(BIGBUF(I,J),J=1,24)
1550  CONTINUE
      CLOSE (UNIT=1)
      CALL WTQIO('2000,2,1,,IOST,,DSW)
      WRITE(5,555) (FNAME(I),I=1,13),KOUNT
      CALL CLREF(10)
4     FORMAT('0','NOTE: Maximum allowable # of records is 1000!
     & (approx. 10M seconds)',/,' Records must be allocated in
     & increments of 5!',//)
5     FORMAT('$','Enter the name to be given to the data file [8-13]: ')
10    FORMAT(13A1)
15    FORMAT('$','Enter the number of records (digitizer sweeps) to b
     $e allocated to the data file [N-5]: ')
20    FORMAT(I5)
45    FORMAT('0','SUCCESS. ',I6,' SWEEPS RECORDED IN TEMPORARY FILE.')
530   FORMAT(30(F1.0,4F5.2,1X))
535   FORMAT('0','PROCESSED DATA FOR FILE: ',13A1)
540   FORMAT('0',5(F3.0,3F7.2))
545   FORMAT('0',1(F3.0,3F7.2))
555   FORMAT('0','DATA WRITTEN TO DISK. ',13A1,'CONTAINS',I5,' RECORD
     $S.')
560   FORMAT('0 ','RECORD NUMBER:  ',I5,' CONTAINED ZERO VALUES AND
     $ HAS BEEN DELETED.')
1010  FORMAT('0',3(F3.0,4F7.2,4X))
1015  FORMAT(' ',3(F3.0,4F7.2,4X))
2000  STOP
      END
```

```
      SUBROUTINE COORD(RC2DAT,RC3DAT,SW,KOUNT)
C
C     THIS SUBROUTINE COMPUTES THE X,Y,Z COORDINATES FOR THE SPARK
C     GAPS IN THE BOARD REFERENCE SYSTEM BY PERFORMING CALCULATIONS
C     ON THE SLANT RANGE DATA FROM THE FOUR CORNER MICROPHONES
C
      DIMENSION RC2DAT(30),RC3DAT(24)
      INTEGER CASE,KOUNT,SW
      REAL L1,L2,K1
      DATA L1/167.75/, L2/111.80/, K1/3.90/
      CASE=0
      K=0
      DO 110 I=1,26,5
      SW=1
      KK=1
      IF(RC2DAT(I+1) .EQ. 0.0) KK=KK+1
      IF(RC2DAT(I+2) .EQ. 0.0) KK=KK+1
      IF(RC2DAT(I+3) .EQ. 0.0) KK=KK+1
      IF(RC2DAT(I+4) .EQ. 0.0) KK=KK+1
      IF(KK.GT.2) GO TO 115
      PA=RC2DAT(I+1)
      PB=RC2DAT(I+2)
      PC=RC2DAT(I+3)
      PD=RC2DAT(I+4)
      IF(PD.GE.PA.AND.PD.GE.PB.AND.PD.GE.PC) CASE=1
      IF(PC.GE.PA.AND.PC.GE.PB.AND.PC.GE.PD) CASE=2
      IF(PB.GE.PA.AND.PB.GE.PC.AND.PB.GE.PD) CASE=3
      IF(PA.GE.PB.AND.PA.GE.PC.AND.PA.GE.PD) CASE=4
      IF(PD .EQ. 0.0) CASE=1
      IF(PC .EQ. 0.0) CASE=2
      IF(PB .EQ. 0.0) CASE=3
      IF(PA .EQ. 0.0) CASE=4
      GO TO (60,70,80,90),CASE
60    XC=((PA+K1)**2-((PB+K1)**2)+L1**2)/(2.0*L1)
      IF(ABS(XC).GT.ABS(PA+K1)) GO TO 114
      YC=((PA+K1)**2-((PC+K1)**2)+L2**2)/(2.0*L2)
      PP=SQRT((PA+K1)**2-XC**2)
      IF(ABS(YC).GT.PP) GO TO 114
      ZC=SQRT((PP)**2-YC**2)
      GO TO 100
70    XC=((PA+K1)**2-((PB+K1)**2)+L1**2)/(2.0*L1)
      IF(ABS(XC).GT.ABS(PA+K1)) GO TO 114
      YC=((PB+K1)**2-((PD+K1)**2)+L2**2)/(2.0*L2)
      PP=SQRT((PA+K1)**2-XC**2)
      IF(ABS(YC).GT.PP) GO TO 114
      ZC=SQRT((PP)**2-YC**2)
      GO TO 100
80    XC=((PC+K1)**2-((PD+K1)**2)+L1**2)/(2.0*L1)
      IF.ABS(XC).GT.ABS(PC+K1)) GO TO 114
      YC=((PA+K1)**2-((PC+K1)**2)+L2**2)/(2.0*L2)
      PP=SQRT((PC+K1)**2-XC**2)
      YCCOMP=L2-YC
      IF(ABS(YCCOMP).GT.PP) GO TO 114
```

```
      ZC=SQRT((PP)**2-YCCOMP**2)
      GO TO 100
 70   XC=((PC+N1)**2-((PD+N1)**2)+L1**2)/(2.0*L1)
      IF(ABS(XC).GT.ABS(PC+N1)) GO TO 114
      YC=((PB+N1)**2-((PD+N1)**2)+L2**2)/(2.0*L2)
      PP=SQRT((PC+N1)**2-XC**2)
      YCCOMP=L2-YC
      IF(ABS(YCCOMP).GT.PP) GO TO 114
      ZC=SQRT((PP)**2-YCCOMP**2)
 100  RC3DAT(I-N)=RC2DAT(I)
      RC3DAT(I-N+1)=XC
      RC3DAT(I-N+2)=YC
      RC3DAT(I-N+3)=ZC
      GO TO 117
 114  SW=-1
      WRITE(5,200)RC2DAT(I),KOUNT
 200  FORMAT('0','SPARKER',F3.0,' IN REC.',I3,' INVALID')
 115  RC3DAT(I-N)=RC2DAT(I)
      RC3DAT(I-N+1)=0.0
      RC3DAT(I-N+2)=0.0
      RC3DAT(I-N+3)=0.0
      IF(SW .EQ. -1)GO TO 117
      WRITE(5,130)RC3DAT(I-N),KOUNT
 130  FORMAT('0','SPARKER',F3.0,' IN REC.',I3,' IS ZERO')
 117  N=N+1
 110  CONTINUE
      RETURN
      END
>
```

```
      PROGRAM FORCIO
C
C     THIS PROGRAM COLLECTS THE SLANT RANGE VALUES FROM THE SONIC
C     DIGITIZER AND SIX CHANNELS FROM THE A-TO-D BOARD AND USES
C        THE IEEE-488 INTERFACE.  THIS DATA IS USED FOR FORCED
C        KINEMATIC ANALYSIS OF THE MOVING BODY SEGMENT.
C
      DIMENSION OUTPUT(45),RECORD(33)
      VIRTUAL BIGBUF(198,156),ATDDAT(6,156)
      LOGICAL*1 BIGBUF,TRANS(198)
      LOGICAL*1 RECDAT(198,2)
      LOGICAL*1 FNAME(13)
      INTEGER IPARAM(6,2),IOSB(2,2),PRLA(6),CHANNL
      INTEGER IPARM(6),IOSTOP(2),DSW,CMDA(2)
      DIMENSION SUM(6,2),ATDOUT(6)
      INTEGER COLUMN,TEST(1),CHECK,SW,KOUNT,IOST(2)
      DATA TEST/-1/CHECK/0/COLUMN/1/KOUNT/0/
      DATA IREC/1/CMDA/'_?','%P'/
      DATA MODE/1/LMODE/2/
C
C     CREATE & OPEN OUTPUT FILE
C
      TYPE *,'NOTE: the maximum number of records allowable is 155.'
      TYPE *,'       this is approx. 19.5 seconds.'
      WRITE(5,5)
      READ(5,10) (FNAME(I),I=1,13)
      WRITE(5,15)
      READ (5,20) NREC
      NREC=NREC*2
      CALL ASSIGN (1,FNAME,13)
      DEFINE FILE 1 (nREC,66,U,IREC)
C
C     GET THE BUFFER ADDRESSES
C
      CALL GETADR(IPARAM(1,1),RECDAT(1,1))
      CALL GETADR(IPARAM(1,2),RECDAT(1,2))
      IPARAM(2,1)=198
      IPARAM(2,2)=198
      CALL GETADR(IPARM(1),TEST(1))
      IPARM(2)=1
C
C     ATTACH IEEE BUS
C
      CALL WTQIO ('1420,2,1,,IOST,,DSW)
      IF(DSW.NE.1) TYPE *,' IEEE BUS WILL NOT PICK YOU UP TODAY! '
      IF(DSW.NE.1) GO TO 2000
      IF(IOST(1).NE.1) TYPE *,' IEEE BUS WILL NOT PICK YOU UP TODAY! '
      IF(IOST(1).NE.1) GO TO 2000
      CALL GETADR (PRLA(1),CMDA(1))
      PRLA(2)=4
C
C     SET UP DIGITIZER AS TALKER
C
```

```
      CALL WTQIO (%420,2,1,,IOST,PRLA,DSW)
      IF(DSW.NE.1) TYPE *,' IEEE BUS IS NOT TALKING TODAY! '
      IF(DSW.NE.1) GO TO 2000
      IF(IOST(1).NE.1) TYPE *,' IEEE BUS IS NOT TALKING TODAY! '
      IF(IOST(1).NE.1) GO TO 2000
C
C     QUEUE THE FIRST I/O
C
      CALL QIO(%1000,2,10,,IOSB(1,1),IPARAM(1,1),DSW)
      DO 25 I=1,12
      DO 25 J=32,37
            K=J-31
            CALL DSUATD(J,0,IDATA,ISTAT)
            DATA=IDATA*0.00030571578
            SUM(K,1)=SUM(K,1)+DATA
25    CONTINUE
C
C     INITIALIZE THE NUMBER OF RECORDS TRANSFERRED
C
100   NMODE=MODE
      MODE=LMODE
      LMODE=NMODE
C
C     WAIT FOR THE BUFFER TO FILL
C
      CALL WAITFR(10)
      CALL QIO(%1000,2,10,,IOSB(1,MODE),IPARAM(1,MODE),DSW)
1     DO 90 I=1,198
            BIGBUF(I,COLUMN)=RECDAT(I,LMODE)
90    CONTINUE
      DO 30 I=1,12
      DO 30 J=32,37
            K=J-31
            CALL DSUATD(J,0,IDATA,ISTAT)
            DATA=IDATA*0.00030571578
            SUM(K,MODE)=SUM(K,MODE)+DATA
30    CONTINUE
2     DO 35 I=1,6
            ATDDAT(I,COLUMN)=SUM(I,LMODE)
            SUM(I,LMODE)=0.0
35    CONTINUE
      IF(CHECK .EQ. NREC+1)GOTO 1200
C
C     INCREMENT THE NUMBER OF RECORDS
C
      COLUMN=COLUMN+1
      CHECK=COLUMN-1
      GOTO 100
1200  CHKMN1=CHECK-1
      WRITE(5,45)CHKMN1
      DO 999 K=1,CHECK
            DO 998 I=1,198
                  TRANS(I)=BIGBUF(I,K)
```

```
998         CONTINUE
C
C    DELETE 1ST RECORD FOR SETTLING PURPOSES
C
     IF(K.EQ.1)GO TO 3
C
C
            DECODE (198,530,TRANS) (OUTPUT(J),J=1,45)
            DO 997 I=1,6
                   ATDOUT(I)=ATDDAT(I,K)
                   RECORD(27+I)=ATDOUT(I)*0.083333
997         CONTINUE
            CALL COORD(OUTPUT,RECORD,SW,KOUNT)
            IF(KOUNT .GT. 0) GOTO 993
994         WRITE(5,535) (FNAME(I),I=1,13)
            WRITE(5,540) (RECORD(I),I=1,15)
            WRITE(5,545) (RECORD(I),I=16,27)
            WRITE(5,550) (RECORD(I),I=28,33)
993         WRITE(1'IREC) (RECORD(I),I=1,33)
            DO 899 I=1,45
                   OUTPUT(I)=0.0
899         CONTINUE
            DO 886 I=1,6
                   ATDOUT(I)=0.0
886         CONTINUE
            DO 300 I=1,33
            RECORD(I)=0.0
300         CONTINUE
            DO 887 I=1,198
                   TRANS(I)=' '
887         CONTINUE
            KOUNT=KOUNT+1
3    CONTINUE
999  CONTINUE
1500 CLOSE (UNIT=1)
     CALL WTQIO('2000,2,1,,IOST,DSW)
     WRITE(5,555) (FNAME(I),I=1,13),KOUNT
     CALL CLREF(10)
5    FORMAT('$','Enter the name to be given to the data file [S-13]: ')
10   FORMAT(13A1)
15   FORMAT('$','Enter the number of records (digitizer sweeps) to b
     $e allocated to the data file [N-5]: ')
20   FORMAT(I5)
45   FORMAT('0','SUCCESS.',I6,' SWEEPS RECORDED.')
530  FORMAT(9(F1.0,4F5.2,1X))
535  FORMAT('0','PROCESSED DATA FOR FILE: ',13A1)
540  FORMAT('0',5(3F7.2))
545  FORMAT('0',4(3F7.2))
550  FORMAT('0',6F17.9)
555  FORMAT('0','DATA WRITTEN TO DISK. ',13A1,'CONTAINS',I5,' RECORD
     $S.')
560  FORMAT(' ','RECORD NUMBER: ',I5,' CONTAINED ZERO VALUES AND
     $ HAS BEEN DELETED.')
```

```
2000 STOP
     END
     SUBROUTINE COORD(RC2DAT,RC3DAT,SW,KOUNT)
C
C    THIS SUBROUTINE COMPUTES THE X,Y,Z COORDINATES FOR THE SPARK
C    GAPS IN THE BOARD REFERENCE SYSTEM BY PERFORMING CALCULATIONS
C    ON THE SLANT RANGE DATA FROM THE FOUR CORNER MICROPHONES
C
     DIMENSION RC2DAT(45),RC3DAT(33)
     INTEGER CASE,KOUNT,SW
     REAL L1,L2,K1
     DATA L1/167.75/, L2/111.80/, K1/3.90/
     CASE=0
     J=0
     DO 110 I=1,41,5
     SW=1
     KK=1
     IF(RC2DAT(I+1) .EQ. 0.0) KK=KK+1
     IF(RC2DAT(I+2) .EQ. 0.0) KK=KK+1
     IF(RC2DAT(I+3) .EQ. 0.0) KK=KK+1
     IF(RC2DAT(I+4) .EQ. 0.0) KK=KK+1
     IF(KK.GT.2) GO TO 115
     PA=RC2DAT(I+1)
     PB=RC2DAT(I+2)
     PC=RC2DAT(I+3)
     PD=RC2DAT(I+4)
     IF(PD.GE.PA.AND.PD.GE.PB.AND.PD.GE.PC) CASE=1
     IF(PC.GE.PA.AND.PC.GE.PB.AND.PC.GE.PD) CASE=2
     IF(PB.GE.PA.AND.PB.GE.PC.AND.PB.GE.PD) CASE=3
     IF(PA.GE.PB.AND.PA.GE.PC.AND.PA.GE.PD) CASE=4
     IF(PD .EQ. 0.0) CASE=1
     IF(PC .EQ. 0.0) CASE=2
     IF(PB .EQ. 0.0) CASE=3
     IF(PA .EQ. 0.0) CASE=4
     GO TO (60,70,80,90),CASE
60   XC=((PA+K1)**2-((PB+K1)**2)+L1**2)/(2.0*L1)
     IF(ABS(XC).GT.ABS(PA+K1)) GO TO 114
     YC=((PA+K1)**2-((PC+K1)**2)+L2**2)/(2.0*L2)
     PP=SQRT((PA+K1)**2-XC**2)
     IF(ABS(YC).GT.PP) GO TO 114
     ZC=SQRT((PP)**2-YC**2)
     GO TO 100
70   XC=((PA+K1)**2-((PB+K1)**2)+L1**2)/(2.0*L1)
     IF(ABS(XC).GT.ABS(PA+K1)) GO TO 114
     YC=((PB+K1)**2-((PD+K1)**2)+L2**2)/(2.0*L2)
     PP=SQRT((PA+K1)**2-XC**2)
     IF(ABS(YC).GT.PP) GO TO 114
     ZC=SQRT((PP)**2-YC**2)
     GO TO 100
80   XC=((PC+K1)**2-((PD+K1)**2)+L1**2)/(2.0*L1)
     IF(ABS(XC).GT.ABS(PC+K1)) GO TO 114
     YC=((PA+K1)**2-((PC+K1)**2)+L2**2)/(2.0*L2)
     PP=SQRT((PC+K1)**2-XC**2)
```

```
      YCCOMP=L2-YC
      IF(ABS(YCCOMP).GT.PP) GO TO 114
      ZC=SQRT((PP)**2-YCCOMP**2)
      GO TO 100
90    XC=((PC+K1)**2-((PD+K1)**2)+L1**2)/(2.0*L1)
      IF(ABS(XC).GT.ABS(PC+K1)) GO TO 114
      YC=((PB+K1)**2-((PD+K1)**2)+L2**2)/(2.0*L2)
      PP=SQRT((PC+K1)**2-XC**2)
      YCCOMP=L2-YC
      IF(ABS(YCCOMP).GT.PP) GO TO 114
      ZC=SQRT((PP)**2-YCCOMP**2)
100   RC3DAT(J+1)=XC
      RC3DAT(J+2)=YC
      RC3DAT(J+3)=ZC
      GO TO 117
114   SW=-1
      WRITE(5,200)RC2DAT(I),KOUNT
200   FORMAT('0','SPARKER',F3.0,' IN REC.',I3,' INVALID')
115   RC3DAT(J+1)=0.0
      RC3DAT(J+2)=0.0
      RC3DAT(J+3)=0.0
      IF(SW .EQ. -1)GO TO 117
      WRITE(5,130)RC2DAT(I),KOUNT
130   FORMAT('0','SPARKER',F3.0,' IN REC.',I3,' IS ZERO')
117   J=J+3
110   CONTINUE
      RETURN
      END
```

```
      PROGRAM KINF4P
C
C     THIS PROGRAM ANALIZES THE KINEMATICS OF A MOVING BODY RELATIVE
C     TO A FIXED BODY.  IT REQUIRES THE INPUT OF A LOCATOR FILE (FOR
C     THE FIXED BODY), AN INITIALIZNG FILE (FOR THE MOVING BODY) AND
C     A KINEMATIC DATA FILE.
C
C       DECLARE & TYPE VARIABLES; DIMENSION ARRAYS; INITIALIZE CONSTANTS
C
      DIMENSION SHLJNT(4),EBOWJT(4),ANGOUT(4)
      DIMENSION CTLOC(3),RC2DAT(24),PNTK(6,3)
      DIMENSION RC1DAT(24),VEC1(3),VEC2(3),VEC3(3)
      DIMENSION F1(3),ERRTOT(20,3),ELBJNT(3),ELBCNT(3),CSMAT(3,3)
      DIMENSION G1(3),TMAT(3,3),CVEC(3),HUMDRC(60,3),HUM(3,3)
      DIMENSION LBVEC(3),CNTVEC(3),T2(3,3),T1(3,3),T21(3,3),FBCNT(3)
      DIMENSION LOCOGN(3),JTCNT(3),ANGS(3),LGBVEC(3),JNTCNT(3)
      DIMENSION LBVEC1(3),LBVEC2(3),LGVEC1(3),LGVEC2(3)
      LOGICAL*1 JTNAME(9),SNAME(25),MESS(80),F1NAME(13),F2NAME(13)
      LOGICAL*1 F3NAME(13),DAY(9),HOUR(8),F4NAME(13),F5NAME(13)
      LOGICAL*1 F6NAME(13)
      INTEGER ANS,Y,N,IPT(20),TRIAD,CASE,ANS2
      REAL JNTVEC,LBVEC,LOCOGN,JTCNT,LGBVEC
      REAL JNTCNT,LBVEC1,LBVEC2,LGVEC1,LGVEC2
      COMMON /AC/ PNTI(6,3),COSMAT(60,3),COSTRN(60,3),DRCOS(60,3),
     $DRCTRN(60,3),TRIAD(20,3),JNTVEC(20,3)
      DATA IREC/1/JREC/1/KREC/1/'Y'/'Y'/N/'N'/KOUNT/1/
      DATA LMREC/1/LREC/1/MREC/1/
C
C     PROMPT FOR DIMENSIONS, DATA FILES AND OUTPUT INFORMATION
C
505   WRITE(5,5)
      READ(5,10,ERR=505) (JTNAME(I),I=1,9)
510   WRITE(5,15)
      READ(5,20,ERR=510) (SNAME(I),I=1,25)
515   WRITE(5,25)
      READ (5,30,ERR=515) (MESS(I),I=1,80)
520   WRITE(5,35)
      READ (5,40,ERR=520) (F1NAME(I),I=1,13)
525   WRITE(5,45)
      READ (5,50,ERR=525) NREC
527   WRITE(5,51)
      READ(5,40,ERR=527)(F2NAME(I),I=1,13)
555   WRITE(5,85)
      READ(5,40,ERR=555)(F3NAME(I),I=1,13)
534   WRITE(5,431)
      READ(5,432,ERR=534)NANS
530   WRITE(5,55)
535   WRITE(5,60)
      READ(5,65,ERR=535)CTLOC(1)
540   WRITE(5,70)
      READ(5,65,ERR=540)CTLOC(2)
545   WRITE(5,75)
      READ(5,65,ERR=545)CTLOC(3)
```

```
550   WRITE(5,80)
      DO 601 I=1,3
      DO 602 J=1,3
603   WRITE(5,604)I,J
      READ(5,66,ERR=603)T2(I,J)
602   CONTINUE
601   CONTINUE
557   WRITE(5,885)
      READ(5,40,ERR=557)(F5NAME(I),I=1,13)
566   WRITE(5,896)
      READ(5,40,ERR=568)(F6NAME(I),I=1,13)
C
C     LOCATE, IDENTIFY AND ACCESS THE LOCATOR DATA FILE
C
      CALL ASSIGN (1,F2NAME,13)
      DEFINE FILE 1 (1,48,U,IREC)
C
C     READ LOCATOR DATA FILE
C
      READ (1'IREC,ERR=3000)(RC2DAT(I),I=1,24)
C
C     ASSIGN DATA TO VARIABLES
C
      DO 87 I=1,3
      T1(1,I)=RC2DAT(3+I)
      T1(2,I)=RC2DAT(12+I)
      T1(3,I)=RC2DAT(18+I)
      LOCOGN(I)=RC2DAT(6+I)
87    CONTINUE
      CLOSE (UNIT=1)
C
C     LOCATE, IDENTIFY AND ACCESS THE INITIALIZING DATA FILE
C
      CALL ASSIGN (1,F3NAME,13)
      DEFINE FILE 1 (876,2,U,JREC)
      DO 90 I=1,6
      DO 89 J=1,3
      READ(1'JREC,ERR=3500)PNTI(I,J)
89    CONTINUE
90    CONTINUE
      DO 93 I=1,60
      DO 92 J=1,3
      READ(1'JREC,ERR=3500)COSHAT(I,J)
92    CONTINUE
93    CONTINUE
      DO 96 I=1,20
      DO 94 J=1,3
      READ(1'JREC,ERR=3500)(JNTVEC(I,J))
94    CONTINUE
96    CONTINUE
      DO 98 I=1,60
      DO 97 J=1,3
      READ(1'JREC,ERR=3500)(NUMDRC(I,J))
```

```
97    CONTINUE
98    CONTINUE
      CLOSE (UNIT=1)
C
C     CALCULATE THE TRANSPOSES FOR THE VARIOUS AXIS SYSTEM DIRECTION
C     COSINE MATRICES.
C
      DO 152 N=1,20
      M=(N-1)*3
      DO 151 J=1,3
      COSTRN(M+J,1)=COSMAT(M+1,J)
      COSTRN(M+J,2)=COSMAT(M+2,J)
      COSTRN(M+J,3)=COSMAT(M+3,J)
151   CONTINUE
152   CONTINUE
C
C     CALCULATE THE LOCATION OF THE FIXED BODY CENTER W.R.T. THE
C     BOARD.
      CALL GMFRD(T2,T1,T21,3,3,3)
      CALL MINV(T1,3,D,F1,G1)
      CALL GMFRD(T1,CTLOC,FBCNT,3,3,1)
      DO 920 I=1,3
      FBCNT(I)=FBCNT(I)+LOCOGN(I)
920   CONTINUE
C
C     OUTPUT HEADER INFORMATION
C
2000  CALL DATE(DAY)
      CALL TIME(HOUR)
      WRITE (5,200)
      WRITE(5,100) (JINAME(I),I=1,9)
      WRITE(5,205)
      WRITE(5,105) DAY,HOUR,(SNAME(I),I=1,25)
      WRITE(5,110) (FINAME(I),I=1,13),NREC,(MESS(I),I=1,80)
      WRITE(5,205)
C
C     LOCATE, IDENTIFY AND ACCESS THE MAIN DATA FILE
C
      CALL ASSIGN (1,FINAME,13)
      DEFINE FILE 1 (NREC,46,U,KREC)
      CALL ASSIGN (3,FSNAME,13)
      DEFINE FILE 3 (NREC,8,U,MREC)
      CALL ASSIGN (4,FSNAME,13)
      DEFINE FILE 4 (NREC,8,U,LMREC)
C
C     READ ONE RECORD
C
 500  READ (1'KREC,ERR=4000) (RCIDAT(I),I=1,24)
C
C     ASSIGN DATA TO VARIABLES
C
      DO 499 I=1,3
             FNTK(I,1)=RCIDAT(I+1)
```

```
            PNTK(2,I)=RC1DAT(I+5)
            PNTK(3,I)=RC1DAT(I+9)
            PNTK(4,I)=RC1DAT(I+13)
            PNTK(5,I)=RC1DAT(I+17)
            PNTK(6,I)=RC1DAT(I+21)
499   CONTINUE
501   KK=0
      DO 805 I=1,6
      IF(PNTK(I,1).NE.0.0) GO TO 805
      KK=KK+1
805   CONTINUE
      IF(KK.GE.4) GO TO 3700
      N=1
      DO 840 J=1,4
      DO 830 K=J+1,5
      DO 820 L=K+1,6
      TRIAD(N,1)=J
      TRIAD(N,2)=K
      TRIAD(N,3)=L
      IF(PNTK(K,1).NE.0.0.AND.PNTK(J,1).NE.0.0.AND.PNTK(L,1).NE.
     &0.0) GO TO 850
      II=((N-1)*3)+1
      DO 845 JJ=1,3
      DRCOS(II,JJ)=0.0
      DRCOS(II+1,JJ)=0.0
      DRCOS(II+2,JJ)=0.0
      DRCTRN(II,JJ)=0.0
      DRCTRN(II+1,JJ)=0.0
      DRCTRN(II+2,JJ)=0.0
845   CONTINUE
      IPT(N)=K
      N=N+1
      GO TO 820
850   DO 800 M=1,3
      VEC1(M)=PNTK(K,M)-PNTK(J,M)
      VEC2(M)=PNTK(L,M)-PNTK(K,M)
800   CONTINUE
      IPT(N)=K
      CALL DRCMAT(VEC1,VEC2,CSMAT)
      I=((N-1)*3)
      DO 810 JJ=1,3
      DRCOS(I+1,JJ)=CSMAT(1,JJ)
      DRCOS(I+2,JJ)=CSMAT(2,JJ)
      DRCOS(I+3,JJ)=CSMAT(3,JJ)
      DRCTRN(I+JJ,1)=CSMAT(1,JJ)
      DRCTRN(I+JJ,2)=CSMAT(2,JJ)
      DRCTRN(I+JJ,3)=CSMAT(3,JJ)
810   CONTINUE
      N=N+1
820   CONTINUE
830   CONTINUE
840   CONTINUE
      CALL LOCAXS(PNTK,CASE,ERRTOT)
```

```
C
C     CALCULATE THE JOINT CENTER W.R.T. THE FIXED BODY CENTER
C
      I=((CASE-1)*3)+1
      DO 900 J=1,3
      TMAT(1,J)=DRCTRN(I,J)
      TMAT(2,J)=DRCTRN(I+1,J)
      TMAT(3,J)=DRCTRN(I+2,J)
      HUM(1,J)=HUMDRC(I,J)
      HUM(2,J)=HUMDRC(I+1,J)
      HUM(3,J)=HUMDRC(I+2,J)
      CVEC(J)=JNTVEC(CASE,J)
900   CONTINUE
      DO 339 J=1,3
      LBVEC(J)=HUM(3,J)
      LBVEC1(J)=HUM(1,J)
      LBVEC2(J)=HUM(2,J)
339   CONTINUE
      CALL GMPRD(TMAT,CVEC,CNTVEC,3,3,1)
      CALL GMPRD(TMAT,LBVEC,LGBVEC,3,3,1)
      CALL GMPRD(TMAT,LBVEC1,LGVEC1,3,3,1)
      CALL GMPRD(TMAT,LBVEC2,LGVEC2,3,3,1)
      CALL UNITVR(LGBVEC)
      CALL UNITVR(LGVEC1)
      CALL UNITVR(LGVEC2)
      N=IPT(CASE)
      DO 910 I=1,3
      ELBJNT(I)=PNTS(N,I)+CNTVEC(I)
910   CONTINUE
      DO 930 I=1,3
      ELBJNT(I)=ELBJNT(I)-FBCNT(I)
930   CONTINUE
      CALL GMPRD(T21,ELBJNT,ELBCNT,3,3,1)
      DO 931 I=1,3
      EROWJT(I+1)=ELBCNT(I)
931   CONTINUE
      CALL GMPRD(T21,LGBVEC,LBVEC,3,3,1)
      CALL GMPRD(T21,LGVEC1,LBVEC1,3,3,1)
      CALL GMPRD(T21,LGVEC2,LBVEC2,3,3,1)
C
C     CALCULATE THE THETA AND PHI ANGLES OF THE LONG BONE AXIS
C     W. R. T. THE FIXED BODY AXIS SYSTEM
C
      THETA=0.00
      PHI=0.00
      CALL UNITVR(LBVEC)
      CALL UNITVR(LBVEC1)
      CALL UNITVR(LBVEC2)
      CALL SPHERE(LBVEC,THETA,PHI)
      DO 338 J=1,3
      HUM(1,J)=LBVEC1(J)
      HUM(2,J)=LBVEC2(J)
      HUM(3,J)=LBVEC(J)
```

```
 338  CONTINUE
      IF(NANS.EQ.2) GO TO 399
      CALL EULER(HUM,ANGS)
      ANGOUT(2)=ANGS(1)
      ANGOUT(3)=ANGS(2)
      ANGOUT(4)=ANGS(3)
      GO TO 699
 399  CALL EULER2(HUM,ANGS)
      ANGOUT(2)=ANGS(1)
      ANGOUT(3)=ANGS(2)
      ANGOUT(4)=ANGS(3)
C
C     WRITE DISTAL JOINT CENTER COORD.'S AND EULER ANGLES W. R. T.
C     THE FIXED BODY AXIS SYSTEM TO DISK FOR THE MOVING BODY
C
 699  CONTINUE
      EBOUJT(1)=FLOAT(KOUNT)
      WRITE(3'NREC)(EBOUJT(J),J=1,4)
      ANGOUT(1)=FLOAT(KOUNT)
      WRITE(4'LNREC)(ANGOUT(J),J=1,4)
C
C     WRITE OUT THE DATA
C
      IF(KOUNT.GT.1)GO TO 710
      WRITE(5,700)
 710  WRITE(5,720)KOUNT,THETA,PHI
     $,ANGOUT(2),ANGOUT(3),ANGOUT(4),TRIAD(CASE,1),TRIAD(CASE,2),
     $TRIAD(CASE,3),ERRTOT(CASE,1),ERRTOT(CASE,2),ELBCNT(1),
     $ELBCNT(2),ELBCNT(3)
      IF(ERRTOT(CASE,1).NE.9.999) GO TO 318
      I=TRIAD(CASE,1)
      J=TRIAD(CASE,2)
      K=TRIAD(CASE,3)
      DKMG1=SQRT((PNTK(I,1)-PNTK(J,1))**2+(PNTK(I,2)-PNTK(J,2))**2+
     $(PNTK(I,3)-PNTK(J,3))**2)
      DKMG2=SQRT((PNTK(J,1)-PNTK(K,1))**2+(PNTK(J,2)-PNTK(K,2))**2+
     $(PNTK(J,3)-PNTK(K,3))**2)
      DKMG3=SQRT((PNTK(K,1)-PNTK(I,1))**2+(PNTK(K,2)-PNTK(I,2))**2+
     $(PNTK(K,3)-PNTK(I,3))**2)
      DIMG1=SQRT((PNTI(I,1)-PNTI(J,1))**2+(PNTI(I,2)-PNTI(J,2))**2+
     $(PNTI(I,3)-PNTI(J,3))**2)
      DIMG2=SQRT((PNTI(J,1)-PNTI(K,1))**2+(PNTI(J,2)-PNTI(K,2))**2+
     $(PNTI(J,3)-PNTI(K,3))**2)
      DIMG3=SQRT((PNTI(K,1)-PNTI(I,1))**2+(PNTI(K,2)-PNTI(I,2))**2+
     $(PNTI(K,3)-PNTI(I,3))**2)
      WRITE(5,926)
      WRITE(5,927)I,J,DIMG1,J,K,DIMG2,K,I,DIMG3,I,J,DKMG1,J,K,DKMG2
     $,K,I,DKMG3
C
C     IF THERE ARE ANY MORE RECORDS, GO GET THEM!
C
 318  KOUNT=KOUNT+1
      IF(KOUNT.LE.NREC) GO TO 500
```

```
C
C     FORMAT STATEMENTS FOR PROMPTS AND RESULTS
C
5     FORMAT('$','Enter name of joint tested [S-9]: ')
10    FORMAT(9A1)
15    FORMAT('$','Enter subject name or number [S-25]: ')
20    FORMAT(25A1)
25    FORMAT('0','Enter a description of the  test [S-80] ')
30    FORMAT(80A1)
35    FORMAT('$','Enter data file name [S-13]: ')
40    FORMAT(13A1)
45    FORMAT('$','Enter number of records to be read [N-5]: ')
50    FORMAT(I5)
51    FORMAT('$','Enter the corresponding fixed body locator file na
     &me [s-13]: ')
55    FORMAT('0','Enter the distances in centimeters along the loca
     &tor axes to the desired fixed body center :')
60    FORMAT('$',T15,'Enter the X-COORDINATE [N-8]: ')
65    FORMAT(F10.5)
66    FORMAT(F8.4)
70    FORMAT('$',T15,'Enter the Y-COORDINATE [N-8]: ')
75    FORMAT('$',T15,'Enter the Z-COORDINATE [N-8]: ')
80    FORMAT('0','Input a 3x3 matrix (by rows) that defines the body
     & axis system w.r.t. the locator axis system : ')
85    FORMAT('$','Enter the corresponding initializing file name [
     &S-13]: ')
100   FORMAT('0',T78,9A1,'JOINT')
105   FORMAT('0',T5,'DATE: ',9A1,/,T5,'TIME: ',8A1,/,T5,'SUBJECT
     &NAME AND NUMBER: ',25A1)
110   FORMAT(' ',T5,'DATA FILE NAME: ',13A1,/,T5,'NUMBER OF RECORDS:
     &',I5,//,T5,'DESCRIPTION:  ',80A1)
200   FORMAT('0',165('-')/)
205   FORMAT('0',165('-')//)
206   FORMAT(' ',165('-'))
207   FORMAT('0',165('-'))
275   FORMAT('0','ERROR ON ATTEMPT TO READ LOCATOR FILE ')
280   FORMAT('0','ERROR ON ATTEMPT TO READ INITIALIZING FILE ')
285   FORMAT('0',' FOUR EMITTERS ON CUFF READ ZERO-PROCEEDING TO NEXT
     & RECORD ')
300   FORMAT('0',130,' ERROR ON ATTEMPT TO READ NEXT RECORD')
311   FORMAT('0',T20,'NOMINAL JOINT CENTER AS INITIALIZED'/)
340   FORMAT('0',//,'$','Are there other files to be processed?
     &[Y/N]: ')
345   FORMAT(A4)
420   FORMAT('$','Do you want to print out the euler angles for the
     & humerus? [Y/N]: ')
431   FORMAT('$','Do you wish type 1 (z-x-z), or type 2 (z-y-z)
     & euler angle output? [1 or 2]:')
432   FORMAT(I2)
433   FORMAT('0',118,'EULER ANGLES FOR HUMERUS',//,T5,'REC. #',T16,
     &'PRECESSION',T34,'NUTATION',T51,'SPIN',/,T20,'(PHI)',T34,'(THETA
     &)',T50,'(PSI)')
435   FORMAT(' ',T6,I3,T19,F7.2,T34,F7.2,T49,F7.2)
```

```
604  FORMAT('$',T15,'T2(',I1,',',I1,'):[N-8]: ')
700  FORMAT('0',T2,'REC.#',T13,'THETA',T23,'PHI',T32,
     &'EULER ANGLES FOR MOVING BODY',T63,'TRIAD USED',T78,'SKEW-DEV'
     &,T93,'DIST-DEV ',T110,'DISTAL JOINT CENTER',/,T35,'PREC.',4X,
     &'NUT.',4X,'SPIN',/)
720  FORMAT(' ',I5,T11,F7.2,T20,F7.2,T33,3F8.2,T62,
     &3I3,T78,F7.3,T92,F7.3,T105,3F9.3)
881  FORMAT(4F8.3)
885  FORMAT('$','Enter the output data filename for ',
     &  'THE DISTAL JOINT CENTER COORDINATES ! [S-13]:')
896  FORMAT('$','Enter the output data filename for EULER
     & ANGLES OF THE MOVING BODY [S-13]: ')
926  FORMAT(' ',T5,'INITIALIZED DISTANCES:',T63,'DISTANCES, CURRENT
     & RECORD:')
927  FORMAT(' ',3(I1,'-',I1,'= ',F5.2,'   '),T60,3(I1,'-',I1,'=',
     &F5.2,'   '))
C
C    CLOSE UP DATA FILE & THAT'S ALL FOLKS!
C
2001 CLOSE (UNIT=1)
     CLOSE (UNIT=3)
     CLOSE (UNIT=4)
     WRITE(5,207)
     WRITE(5,340)
     READ(5,345)ANS
     IF(ANS .EQ. 'N')GO TO 5000
     WRITE(5,35)
     READ(5,40) (FINAME(I),I=1,13)
     WRITE(5,45)
     READ(5,50) NREC
     WRITE(5,25)
     READ(5,30) (MESS(I),I=1,80)
     KREC=1
     KOUNT=1
     LREC=1
     MREC=1
     LMREC=1
559  WRITE(5,885)
     READ(5,40,ERR=559)(F5NAME(I),I=1,13)
560  WRITE(5,896)
     READ(5,40,ERR=560)(F6NAME(I),I=1,13)
     GO TO 2000
3000 WRITE(5,205)
     WRITE(5,275)
     GO TO 5000
3500 WRITE(5,205)
     WRITE(5,280)
     GO TO 5000
3700 WRITE(5,285)
     KOUNT=KOUNT+1
     IF(KOUNT.GT.NREC) GO TO 2001
     GO TO 500
4000 WRITE(5,205)
```

```
      WRITE(5,300)
      GOTO 2001
5000  WRITE(5,205)
      STOP
      END
      SUBROUTINE SPHERE(VEC,THETA,PHI)
C
C     SUBROUTINE TO CALCULATE THE SPHERICAL COORDINATES (THETA,PHI)
C     OF THE VECTOR 'VEC'.
C
      DIMENSION B(3),VEC(3)
      DATA PI/3.141592654/
      VECMAG=SQRT(VEC(1)**2+VEC(2)**2+VEC(3)**2)
      IF(VECMAG.LT.1.001) GO TO 10
      B(1)=VEC(1)/VECMAG
      B(2)=VEC(2)/VECMAG
      B(3)=VEC(3)/VECMAG
      GO TO 15
10    B(1)=VEC(1)
      B(2)=VEC(2)
      B(3)=VEC(3)
15    A1=SQRT(B(1)**2+B(2)**2)
      THETA=(ATAN2(A1,B(3)))*180.0/PI
      IF(THETA.LT.179.99.OR.THETA.GT.0.01) GO TO 20
      PHI=0.0
      GO TO 30
20    PHI=(ATAN2(B(2),B(1)))*180.0/PI
30    RETURN
      END
C
      SUBROUTINE UNITVR(VEC)
C
C     SUBROUTINE CALCULATES A UNIT VECTOR FOR ANY GIVEN VECTOR
C
      DIMENSION VEC(3)
      VECMAG=(VEC(1)**2)+(VEC(2)**2)+(VEC(3)**2)
      VECMAG=SQRT(VECMAG)
      IF(VECMAG.EQ.0.0) VECMAG=1.0
      DO 10 I=1,3
      VEC(I)=VEC(I)/VECMAG
10    CONTINUE
      RETURN
      END
      SUBROUTINE LOCAXS(FNIK,CASE,ERRTOT)
C
C     THIS SUBROUTINE SELECTS THE 'MOST ACCURATE' LOCAL AXIS  SYSTEM
C     BASED ON INTRA-AXIS SYSTEM DISTANCES AND RELATIVE SKEW ANGLES.
C
      DIMENSION FNIK(6,3),TIS(3,3),TISK(3,3),TJS(3,3),TJSK(3,3)
      DIMENSION TIJ(3,3),TIJK(3,3),GFN(3,3),VECI(3),VECK(3)
      DIMENSION ERRTOT(20,3),F1(3),G1(3)
      INTEGER TRIAD,CASE
      REAL JNTVEC,JTDSMG
```

```
      COMMON /AC/ PNTI(6,3),COSMAT(60,3),COSTRN(60,3),DRCOS(60,3),
     $DRCTRN(60,3),TRIAD(20,3),JNTVEC(20,3)
C
      ERRSK=0.0
      ERRDLT=0.0
C
      DO 20 MM=1,20
C
      I1=TRIAD(MM,1)
      J1=TRIAD(MM,2)
      K1=TRIAD(MM,3)
       IF(PNTK(I1,1).EQ.0.0.OR.PNTK(J1,1).EQ.0.0.OR.PNTK(K1,1).EQ.0.0)
      $ GO TO 19
C
      KK=(MM-1)*3
C
C
      DO 3 J=1,3
      TIS(1,J)=COSMAT(KK+1,J)
      TIS(2,J)=COSMAT(KK+2,J)
      TIS(3,J)=COSMAT(KK+3,J)
C
      TISK(1,J)=DRCOS(KK+1,J)
      TISK(2,J)=DRCOS(KK+2,J)
      TISK(3,J)=DRCOS(KK+3,J)
3     CONTINUE
C
      MKNT1=0
      MKNT2=0
C
      DO 10 N=1,20
      I2=TRIAD(N,1)
      J2=TRIAD(N,2)
      K2=TRIAD(N,3)
       IF(PNTK(I2,1).EQ.0.0.OR.PNTK(J2,1).EQ.0.0.OR.PNTK(K2,1).EQ.0.0)
      $ GO TO 10
      M=(N-1)*3
      IF(N.EQ.MM) GO TO 10
C
      DO 5 J=1,3
      TJS(1,J)=COSTRN(M+1,J)
      TJS(2,J)=COSTRN(M+2,J)
      TJS(3,J)=COSTRN(M+3,J)
C
      TJSK(1,J)=DRCTRN(M+1,J)
      TJSK(2,J)=DRCTRN(M+2,J)
      TJSK(3,J)=DRCTRN(M+3,J)
5     CONTINUE
C
C
      CALL GMPRD(TIS,TJS,TIJ,3,3,3)
      CALL GMPRD(TISK,TJSK,TIJK,3,3,3)
      CALL MINV(TIJK,3,D,F1,G1)
```

```
      CALL GMPRD(TIJ,TIJK,GEN,3,3,3)
      TRACE=(GEN(1,1)**2+GEN(2,2)**2+GEN(3,3)**2)
      GAM=.5*(TRACE-1.0)
      IF(GAM.GT.1.0.AND.GAM.LT.1.05) GAM=1.0
      GAM=ACOS(GAM)
      JTDSMG=SQRT((JNTVEC(N,1)**2)+(JNTVEC(N,2)**2)+(JNTVEC(N,3)
     **2))
      GAMSIN=SIN(GAM)
      DELTAS=JTDSMG*GAMSIN
      DELTAS=DELTAS**2
      ERRSK=ERRSK+DELTAS
      MKNT1=MKNT1+1
      III=TRIAD(MM,2)
      JJJ=TRIAD(N,2)
      IF(III.EQ.JJJ) GO TO 10
C
      DO 7 L=1,3
      VECI(L)=PNTI(JJJ,L)-PNTI(III,L)
      VECK(L)=PNTK(JJJ,L)-PNTK(III,L)
7     CONTINUE
C
      VECIMG=SQRT((VECI(1)**2)+(VECI(2)**2)+(VECI(3)**2))
      VECKMG=SQRT((VECK(1)**2)+(VECK(2)**2)+(VECK(3)**2))
      DELTAD=ABS(VECKMG-VECIMG)
      DELTAD=DELTAD**2
      ERRDLT=ERRDLT+DELTAD
      MKNT2=MKNT2+1
10    CONTINUE
C
      RMKNT1=FLOAT(MKNT1)
      RMKNT2=FLOAT(MKNT2)
      DIV1=RMKNT1*1.0
      DIV2=RMKNT2*1.0
      IF(MKNT1.NE.0) GO TO 11
      SKERR=9.999
      GO TO 12
11    SKERR=SQRT(ERRSK/DIV1)
12    IF(MKNT2.NE.0) GO TO 13
      DERR=9.999
      GO TO 14
13    DERR=SQRT(ERRDLT/DIV2)
14    ERRTOT(MM,1)=SKERR
      ERRTOT(MM,2)=DERR
      ERRTOT(MM,3)=SQRT((SKERR**2+DERR**2)/2.0)
C
      ERRSK=0.0
      ERRDLT=0.0
      GO TO 20
19    ERRTOT(MM,1)=25.0
      ERRTOT(MM,2)=25.0
      ERRTOT(MM,3)=50.0
      ERRSK=0.0
      ERRDLT=0.0
```

```
20    CONTINUE
C
      CASE=1
      ERTOTL=ERRTOT(1,3)
      DO 25 I=1,19
      IF(ERTOTL.LE.ERRTOT(I+1,3)) GO TO 25
      CASE=I+1
      ERTOTL=ERRTOT(I+1,3)
25    CONTINUE
      RETURN
      END
C
C
      SUBROUTINE EULER(D,ANGS)
C
C     THIS SUBROUTINE CALCULATES THE EULER ANGLES (Z-X-Z) WHICH
C     DESCRIBE THE HUMERAL AXIS SYSTEM RELATIVE TO THE FIXED BODY
C     SYSTEM.
C
      DIMENSION D(3,3),ANGS(3)
      DATA PI/3.141592654/
C
      ANGS(2)=(ACOS(D(3,3)))*180.0/PI
      IF(ANGS(2).LT.0.01) GO TO 20
      IF(ANGS(2).GT.179.99) GO TO 30
      ANGS(3)=(ATAN2(D(1,3),D(2,3)))*180.0/PI
      ANGS(1)=(ATAN2(D(3,1),-D(3,2)))*180.0/PI
      GO TO 40
20    PSIPHI=(ATAN2((D(1,2)-D(2,1)),(D(1,1)+D(2,2))))*180.0/PI
      ANGS(1)=PSIPHI
      ANGS(3)=0.0
      GO TO 40
30    PSIPHI=(ATAN2((D(1,2)+D(2,1)),(D(1,1)-D(2,2))))*180.0/PI
      ANGS(1)=PSIPHI
      ANGS(3)=0.0
40    RETURN
      END
C
C
      SUBROUTINE EULER2(D,ANGS)
C
C     THIS SUBROUTINE CALCULATES THE EULER ANGLES (Z-Y-Z) WHICH
C     DESCRIBE THE HUMERAL AXIS SYSTEM RELATIVE TO THE FIXED BODY
C     SYSTEM.
C
      DIMENSION D(3,3),ANGS(3)
      DATA PI/3.141592654/
C
      ANGS(2)=(ACOS(D(3,3)))*180.0/PI
      IF(ANGS(2).LT.0.01) GO TO 20
      IF(ANGS(2).GT.179.99) GO TO 30
      ANGS(3)=(ATAN2(D(2,3),-D(1,3)))*180.0/PI
      ANGS(1)=(ATAN2(D(3,2),D(3,1)))*180.0/PI
```

```
      GO TO 40
20    PSIPHI=(ATAN2((D(1,2)-D(2,1)),(D(1,1)+D(2,2))))*180.0/PI
      ANGS(1)=PSIPHI
      ANGS(3)=0.0
      GO TO 40
30    PSIPHI=(ATAN2((D(1,2)+D(2,1)),(D(1,1)-D(2,2))))*180.0/PI
      ANGS(1)=PSIPHI
      ANGS(3)=0.0
40    RETURN
      END
C
C
      SUBROUTINE DRCMAT(A,B,C)
C
C     THIS SUBROUTINE CALCULATES THE DIRECTION COSINE MATRIX
C     FOR AN AXIS SYSTEM BASED ON TWO COPLANAR VECTORS (A and B).
C     THE RESULTING MATRIX, C, IS ORTHOGONAL AND UNITARY.
C
      DIMENSION A(3),B(3),C(3,3)
      AMAG=SQRT(A(1)**2+A(2)**2+A(3)**2)
      BMAG=SQRT(B(1)**2+B(2)**2+B(3)**2)
      C(1,1)=A(1)/AMAG
      C(1,2)=A(2)/AMAG
      C(1,3)=A(3)/AMAG
      C(2,1)=B(1)/BMAG
      C(2,2)=B(2)/BMAG
      C(2,3)=B(3)/BMAG
      C(3,1)=(C(1,2)*C(2,3))-(C(2,2)*C(1,3))
      C(3,2)=(C(1,3)*C(2,1))-(C(2,3)*C(1,1))
      C(3,3)=(C(1,1)*C(2,2))-(C(2,1)*C(1,2))
         C(2,1)=(C(3,2)*C(1,3))-(C(1,2)*C(3,3))
         C(2,2)=(C(3,3)*C(1,1))-(C(3,1)*C(1,3))
         C(2,3)=(C(3,1)*C(1,2))-(C(1,1)*C(3,2))
      DO 10 J=1,3
      CMAG=SQRT(C(J,1)**2+C(J,2)**2+C(J,3)**2)
      DO 5 I=1,3
      C(J,I)=C(J,I)/CMAG
5     CONTINUE
10    CONTINUE
      RETURN
      END
```

```
      PROGRAM FORCMO
C
C     THIS PROGRAM ANALIZES THE KINEMATICS OF A MOVING BODY RELATIVE
C     TO A FIXED BODY FOR SITUATIONS WITH APPLIED LOADING.
C     THIS PROGRAM REQUIRES THE INPUT OF A LOCATOR FILE (FOR
C     THE FIXED BODY), AN INITIALIZNG FILE (FOR THE MOVING BODY) AND
C     A KINEMATIC DATA FILE.
C
C       DECLARE & TYPE VARIABLES; DIMENSION ARRAYS; INITIALIZE CONSTANTS
C
      DIMENSION SHLJNT(4),EBOWJT(4),ANGOUT(4),CAL(6,6),F2(6),G2(6)
      DIMENSION CTLOC(3),R(3),RC2DAT(24),PNTK(6,3),FXJTCT(3),RCNTR(3)
      DIMENSION RC1DAT(33),VEC1(3),OUTPUT(22),VEC2(3),VEC3(3)
      DIMENSION F1(3),ERRTOT(20,3),ELBJNT(3),ELBCNT(3),CSMAT(3,3)
      DIMENSION G1(3),TMAT(3,3),CVEC(3),HUMDRC(60,3),HUM(3,3)
      DIMENSION LBVEC(3),CNTVEC(3),T2(3,3),T1(3,3),T21(3,3),FBCNT(3)
      DIMENSION LOCOGN(3),JTCNT(3),ANGS(3),LGBVEC(3),JNTCNT(3)
      DIMENSION LBVEC1(3),PNTG(3,3),LBVEC2(3),LGVEC1(3),LGVEC2(3)
      DIMENSION PTAXTF(3,3),PTAPP(3),PTAXIS(3,3),PTAPB(3),OUTPT2(12)
      DIMENSION TRNAXT(3,3),X(6),UJT(3,3)
      LOGICAL*1 JTNAME(9),SNAME(25),MESS(80),F1NAME(13),F2NAME(13)
      LOGICAL*1 F3NAME(25),DAY(9),HOUR(8),F4NAME(13)
      INTEGER ANS,Y,N,IPT(20),TRIAD,CASE,ANS2,GUNSD
      REAL JNTVEC,LBVEC,LOCOGN,JTCNT,LGBVEC
      REAL JNTCNT,LBVEC1,LBVEC2,LGVEC1,LGVEC2
      COMMON /BC/ PNTI(6,3),COSMAT(60,3),COSTRN(60,3),DRCOS(60,3),
     $DRCTRN(60,3),TRIAD(20,3),JNTVEC(20,3)
      COMMON /BC/ FRCTRN(6),TRNAX(3,3)
      DATA IREC/1/,JREC/1/,KREC/1/,Y/'Y'/,N/'N'/,KOUNT/1/
      DATA A/'A'/,B/'B'/,PI/3.141592694/,LREC/1/
C
C     PROMPT FOR DIMENSIONS, DATA FILES AND OUTPUT INFORMATION
C
505   WRITE(5,5)
      READ(5,10,ERR=505) (JTNAME(I),I=1,9)
510   WRITE(5,15)
      READ(5,20,ERR=510) (SNAME(I),I=1,25)
515   WRITE(5,25)
      READ (5,30,ERR=515) (MESS(I),I=1,80)
520   WRITE(5,35)
      READ (5,40,ERR=520) (F1NAME(I),I=1,13)
525   WRITE(5,45)
      READ (5,50,ERR=525) NREC
527   WRITE(5,51)
      READ(5,40,ERR=527)(F2NAME(I),I=1,13)
555   WRITE(5,85)
      READ(5,20,ERR=555)(F3NAME(I),I=1,25)
537   WRITE(5,88)
      READ(5,345,ERR=537)GUNSD
530   WRITE(5,55)
535   WRITE(5,60)
      READ(5,65,ERR=535)CTLOC(1)
540   WRITE(5,70)
```

```
      READ(5,65,ERR=540)CTLOC(2)
545   WRITE(5,75)
      READ(5,65,ERR=545)CTLOC(3)
      WRITE(5,76)
546   WRITE(5,77)
      READ(5,65,ERR=546)FXJTCT(1)
547   WRITE(5,78)
      READ(5,65,ERR=547)FXJTCT(2)
548   WRITE(5,79)
      READ(5,65,ERR=548)FXJTCT(3)
721   WRITE(5,731)
      WRITE(5,734)
      READ(5,65,ERR=721)THATU
722   WRITE(5,732)
      READ(5,65,ERR=722)PHIU
550   WRITE(5,80)
      DO 601 I=1,3
      DO 602 J=1,3
603   WRITE(5,804)I,J
      READ(5,66,ERR=603)T2(I,J)
602   CONTINUE
601   CONTINUE
625   WRITE(5,626)
      READ(5,65,ERR=625)HHDIS
630   WRITE(5,631)
      READ(5,65,ERR=630)HYDIS
627   WRITE(5,628)
      READ(5,65,ERR=627)EJDIS
556   WRITE(5,884)
      READ(5,40,ERR=556)(F4NAME(I),I=1,13)
C
C     LOCATE, IDENTIFY AND ACCESS THE INITIALIZING DATA FILE
C
      CALL ASSIGN (1,F3NAME,25)
      DEFINE FILE 1 (876,2,U,JREC)
      DO 90 I=1,6
      DO 89 J=1,3
      READ(1'JREC,ERR=3500)PNTI(I,J)
89    CONTINUE
90    CONTINUE
      DO 93 I=1,60
      DO 92 J=1,3
      READ(1'JREC,ERR=3500)COSMAT(I,J)
92    CONTINUE
93    CONTINUE
      DO 96 I=1,20
      DO 94 J=1,3
      READ(1'JREC,ERR=3500)(JNTVEC(I,J))
94    CONTINUE
96    CONTINUE
      DO 98 I=1,60
      DO 97 J=1,3
      READ(1'JREC,ERR=3500)(NUMDRC(I,J))
```

```
 97   CONTINUE
 98   CONTINUE
      CLOSE (UNIT=1)
C
C     CALCULATE THE TRANSPOSES FOR THE VARIOUS AXIS SYSTEM DIRECTION
C     COSINE MATRICES.
C
      DO 152 N=1,20
      M=(N-1)*3
      DO 151 J=1,3
      COSTRN(M+J,1)=COSMAT(M+1,J)
      COSTRN(M+J,2)=COSMAT(M+2,J)
      COSTRN(M+J,3)=COSMAT(M+3,J)
151   CONTINUE
152   CONTINUE
C
C     FILL THE TRANSDUCER CALIBRATION MATRIX
C
      CALL ASSIGN (1,'[7,1]CAL.DAT')
      DEFINE FILE 1 (2,72,U,LREC)
      READ(1'LREC,ERR=3800)((CAL(I,J),J=1,6),I=1,6)
      CLOSE (UNIT=1)
      CALL MINV(CAL,6,D,F2,G2)
C
C     LOCATE, IDENTIFY AND ACCESS THE LOCATOR DATA FILE
C
2000  CALL ASSIGN (1,F2NAME,13)
      DEFINE FILE 1 (1,48,U,IREC)
C
C     READ LOCATOR DATA FILE
C
      READ (1'IREC,ERR=3000)(RC2DAT(I),I=1,24)
C
C     ASSIGN DATA TO VARIABLES
C
      DO 87 I=1,3
      T1(1,I)=RC2DAT(3+I)
      T1(2,I)=RC2DAT(12+I)
      T1(3,I)=RC2DAT(18+I)
      LOCOGN(I)=RC2DAT(6+I)
87    CONTINUE
      CLOSE (UNIT=1)
C
C     CALCULATE THE LOCATION OF THE FIXED BODY CENTER W.R.T. THE
C     BOARD.
      CALL GMPRD(T2,T1,T21,3,3,3)
      CALL MINV(T1,3,D,F1,G1)
      CALL GMPRD(T1,CTLOC,FBCNT,3,3,1)
      DO 920 I=1,3
      FBCNT(I)=FBCNT(I)+LOCOGN(I)
920   CONTINUE
C
C     OUTPUT HEADER INFORMATION
```

```
C
      CALL DATE(DAY)
      CALL TIME(HOUR)
      WRITE (5,200)
      WRITE(5,100) (JTNAME(I),I=1,9)
      WRITE(5,205)
      WRITE(5,105) DAY,HOUR,(SNAME(I),I=1,25)
      WRITE(5,110) (FINAME(I),I=1,13),NREC,(MESS(I),I=1,80)
      WRITE(5,205)
D     WRITE(5,700)
D     WRITE(5,701)
C
C     LOCATE, IDENTIFY AND ACCESS THE MAIN DATA FILE
C     OPEN ANY OUTPUT DATA FILES
C
      CALL ASSIGN (1,FINAME,13)
      DEFINE FILE 1 (NREC,66,U,KREC)
      CALL ASSIGN (2,F4NAME,13)
C
C     READ ONE RECORD
C
  500 READ (1'KREC,ERR=4000) (RC1DAT(I),I=1,33)
C
C     ASSIGN DATA TO VARIABLES
C
      DO 499 I=1,3
              PNTK(1,I)=RC1DAT(I)
              PNTK(2,I)=RC1DAT(I+3)
              PNTK(3,I)=RC1DAT(I+6)
              PNTK(4,I)=RC1DAT(I+9)
              PNTK(5,I)=RC1DAT(I+12)
              PNTK(6,I)=RC1DAT(I+15)
      PNTG(1,I)=RC1DAT(I+18)
      PNTG(2,I)=RC1DAT(I+21)
      PNTG(3,I)=RC1DAT(I+24)
C
C     CONVERT TRANSDUCER FORCE AND MOMENT DATA TO
C     NEWTONS AND NEWTON-METERS
C
              FRCTRN(1)=RC1DAT(28)*4.448
              FRCTRN(2)=RC1DAT(29)*4.448
              FRCTRN(3)=RC1DAT(30)*4.448
              FRCTRN(4)=RC1DAT(31)*0.11298
              FRCTRN(5)=RC1DAT(32)*0.11298
              FRCTRN(6)=RC1DAT(33)*0.11298
  499 CONTINUE
      DO 689 I=1,3
      IF(PNTG(I,1).NE.0.0) GO TO 689
      GO TO 3900
  689 CONTINUE
  501 N=0
      DO 805 I=1,6
      IF(PNTK(I,1).NE.0.0) GO TO 805
```

```
      KK=KK+1
  805 CONTINUE
      IF(KK.GE.4) GO TO 3700
      N=1
      DO 840 J=1,4
      DO 830 K=J+1,5
      DO 820 L=K+1,6
      TRIAD(N,1)=J
      TRIAD(N,2)=K
      TRIAD(N,3)=L
      IF(PNTK(K,1).NE.0.0.AND.PNTK(J,1).NE.0.0.AND.PNTK(L,1).NE.
      &0.0) GO TO 850
      II=((N-1)&3)+1
      DO 845 JJ=1,3
      DRCOS(II,JJ)=0.0
      DRCOS(II+1,JJ)=0.0
      DRCOS(II+2,JJ)=0.0
      DRCTRN(II,JJ)=0.0
      DRCTRN(II+1,JJ)=0.0
      DRCTRN(II+2,JJ)=0.0
  845 CONTINUE
      IPT(N)=K
      N=N+1
      GO TO 820
  850 DO 800 M=1,3
      VEC1(M)=PNTK(K,M)-PNTK(J,M)
      VEC2(M)=PNTK(L,M)-PNTK(K,M)
  800 CONTINUE
      IPT(N)=K
      CALL DRCMAT(VEC1,VEC2,CSMAT)
      I=((N-1)&3)
      DO 810 JJ=1,3
      DRCOS(I+1,JJ)=CSMAT(1,JJ)
      DRCOS(I+2,JJ)=CSMAT(2,JJ)
      DRCOS(I+3,JJ)=CSMAT(3,JJ)
      DRCTRN(I+JJ,1)=CSMAT(1,JJ)
      DRCTRN(I+JJ,2)=CSMAT(2,JJ)
      DRCTRN(I+JJ,3)=CSMAT(3,JJ)
  810 CONTINUE
      N=N+1
  820 CONTINUE
  830 CONTINUE
  840 CONTINUE
C
C     SELECT 'MOST-ACCURATE' TRIAD OF EMITTERS
C
      CALL LOCAXS(PNTK,CASE,ERRTOT)
C
C     MULTIPLY THE TRANSDUCER VALUES BY THE CALIBRATION MATRIX
C     TO GET THE FORCES.
C
      CALL GMPRD(CAL,FRCTRN,X,6,6,1)
      DO 492 I=1,6
```

```
      FRCTRN(I)=X(I)
  492 CONTINUE
C
C     CALCULATE THE POINT OF FORCE APPLICATION AND THE AXIS SYSTEM
C     OF THE FORCE TRANSDUCER W.R.T. THE FIXED BODY CENTER
C     IN ADDITION, CHECK THE ACCURACY OF THE F-A EMITTERS
C
      CALL FORPT(PNTG,GUNSD,PTAPP,PTAXIS)
      DO 503 I=1,3
      PTAPP(I)=PTAPP(I)-FRCNT(I)
  503 CONTINUE
      CALL GMPRD(T21,PTAPP,PTAPB,3,3,1)
      DO 509 I=1,3
      PTAXTP(I,1)=PTAXIS(1,I)
      PTAXTP(I,2)=PTAXIS(2,I)
      PTAXTP(I,3)=PTAXIS(3,I)
  509 CONTINUE
      CALL GMPRD(T21,PTAXTP,TRNAXT,3,3,3)
      DO 511 I=1,3
      TRNAX(I,1)=TRNAXT(1,I)
      TRNAX(I,2)=TRNAXT(2,I)
      TRNAX(I,3)=TRNAXT(3,I)
  511 CONTINUE
C
C     CALCULATE THE JOINT CENTER W.R.T. THE FIXED BODY CENTER
C
      I=((CASE-1)*3)+1
      DO 900 J=1,3
      TMAT(1,J)=DRCTRN(I,J)
      TMAT(2,J)=DRCTRN(I+1,J)
      TMAT(3,J)=DRCTRN(I+2,J)
      HUM(1,J)=HUMDRC(I,J)
      HUM(2,J)=HUMDRC(I+1,J)
      HUM(3,J)=HUMDRC(I+2,J)
      CVEC(J)=JNTVEC(CASE,J)
  900 CONTINUE
      DO 339 J=1,3
      LBVEC(J)=HUM(3,J)
      LBVEC1(J)=HUM(1,J)
      LBVEC2(J)=HUM(2,J)
  339 CONTINUE
      CALL GMPRD(TMAT,CVEC,CNTVEC,3,3,1)
      CALL GMPRD(TMAT,LBVEC,LGBVEC,3,3,1)
      CALL GMPRD(TMAT,LBVEC1,LGVEC1,3,3,1)
      CALL GMPRD(TMAT,LBVEC2,LGVEC2,3,3,1)
      CALL UNITVR(LGBVEC)
      CALL UNITVR(LGVEC1)
      CALL UNITVR(LGVEC2)
      K=IPT(CASE)
      DO 910 I=1,3
      JNTCNT(I)=PNTK(K,I)+CNTVEC(I)+HHDIS*LGBVEC(I)-HYDIS*LGVEC2(I)
      ELBJNT(I)=JNTCNT(I)+EJDIS*LGBVEC(I)
  910 CONTINUE
```

```
      DO 930 I=1,3
      JNTCNT(I)=JNTCNT(I)-FBCNT(I)
      ELBJNT(I)=ELBJNT(I)-FBCNT(I)
  930 CONTINUE
      CALL GMPRD(T21,JNTCNT,JTCNT,3,3,1)
      CALL GMPRD(T21,ELBJNT,ELBCNT,3,3,1)
      DO 931 I=1,3
      SHLJNT(I+1)=JTCNT(I)
      EBOWJT(I+1)=ELBCNT(I)
      OUTPUT(16+I)=JTCNT(I)
      OUTPUT(19+I)=ELBCNT(I)
  931 CONTINUE
      CALL GMPRD(T21,LGBVEC,LBVEC,3,3,1)
      CALL GMPRD(T21,LGVEC1,LBVEC1,3,3,1)
      CALL GMPRD(T21,LGVEC2,LBVEC2,3,3,1)
C
C     CALCULATE THE THETA AND PHI ANGLES OF THE LONG BONE AXIS
C
      THETA=0.00
      PHI=0.00
      CALL UNITVR(LBVEC)
      CALL UNITVR(LBVEC1)
      CALL UNITVR(LBVEC2)
      CALL SPHERE(LBVEC,THETA,PHI)
      DO 338 J=1,3
      HUM(1,J)=LBVEC1(J)
      HUM(2,J)=LBVEC2(J)
      HUM(3,J)=LBVEC(J)
      RCNTR(J)=ELBCNT(J)-FXJTCT(J)
  338 CONTINUE
      CALL SPHERE(RCNTR,THA2,PHI2)
      OUTPUT(2)=ERRTOT(CASE,1)
      OUTPUT(3)=ERRTOT(CASE,2)
      OUTPUT(4)=THA2
      OUTPUT(5)=PHI2
C
C     MULTIPLY RxF AND CALCULATE THE FORCES AND MOMENTS AT THE
C     JOINT CENTER
C
      R(1)=(PTAPB(1)-FXJTCT(1))/100.0
      R(2)=(PTAPB(2)-FXJTCT(2))/100.0
      R(3)=(PTAPB(3)-FXJTCT(3))/100.0
      CALL RESULT(R,OUTPUT)
      OUTPUT(1)=FLOAT(KOUNT)
      OUTPT2(1)=FLOAT(KOUNT)
C
C     TRANSFORM THETA & PHI COORDINATES OF R VECTOR INTO
C     JOINT SYSTEM COORDINATES
C
      VO=THA2*PI/180.0
      HO=PHI2*PI/180.0
      VC=THATO*PI/180.0
      HC=PHIO*PI/180.0
```

```
      ARG1=(SIN(VO)*SIN(HO-HC))
      ARG2=(SIN(VO)*COS(VC)*COS(HO-HC)-COS(VO)*SIN(VC))
      ARG3=(COS(VO)*COS(VC)+SIN(VO)*SIN(VC)*COS(HO-HC))
      HT=ATAN2(ARG1,ARG2)
      IF(HT.GT.0.0) GO TO 337
      HT=2.0*PI-ABS(HT)
  337 VT=ACOS(.,RG3)
      OUTPT2(2)=VT*(180.00/PI)
      OUTPT2(3)=HT*(180.00/PI)
C
C     PERFORM ANALYSIS OF FORCES AND MOMENTS IN THE JOINT
C     AXIS SYSTEM
C
      IF(KOUNT.GT.1) GO TO 608
      PHIX=PHIO*PI/180.0
      THAX=(THATO+90.0)*PI/180.0
      PHIZ=PHIO*PI/180.0
      THATZ=THATO*PI/180.0
      UJT(1,1)=COS(PHIX)*SIN(THAX)
      UJT(1,2)=SIN(PHIX)*SIN(THAX)
      UJT(1,3)=COS(THAX)
      UJT(3,1)=SIN(THATZ)*COS(PHIZ)
      UJT(3,2)=SIN(THATZ)*SIN(PHIZ)
      UJT(3,3)=COS(THATZ)
      UJT(2,1)=(UJT(3,2)*UJT(1,3)-UJT(1,2)*UJT(3,3))
      UJT(2,2)=-(UJT(3,1)*UJT(1,3)-UJT(1,1)*UJT(3,3))
      UJT(2,3)=(UJT(3,1)*UJT(1,2)-UJT(1,1)*UJT(3,2))
  608 CALL MOANAL(OUTPUT,VT,HT,UJT,OUTPT2)
C
C     WRITE OUT THE DATA
C
      WRITE(5,702)(OUTPUT(I),I=1,16)
      WRITE(5,703)(OUTPUT(I),I=17,22),(OUTPT2(J),J=2,12)
      WRITE(2,704)(OUTPT2(J),J=1,12)
      DO 818 I=1,22
      OUTPUT(I)=0.00
  818 CONTINUE
      DO 1010 I=1,11
      OUTPT2(I)=0.0
 1010 CONTINUE
      DO 819 I=1,33
      MODAT(I)=0.00
  819 CONTINUE
      IF(ERRTOT(CASE,1).NE.9.999) GO TO 318
      I=TRIAD(CASE,1)
      J=TRIAD(CASE,2)
      K=TRIAD(CASE,3)
      DKMG1=SQRT((PNTK(I,1)-PNTK(J,1))**2+(PNTK(I,2)-PNTK(J,2))**2+
     &(PNTK(I,3)-PNTK(J,3))**2)
      DKMG2=SQRT((PNTK(J,1)-PNTK(K,1))**2+(PNTK(J,2)-PNTK(K,2))**2+
     &(PNTK(J,3)-PNTK(K,3))**2)
      DKMG3=SQRT((PNTK(K,1)-PNTK(I,1))**2+(PNTK(K,2)-PNTK(I,2))**2+
     &(PNTK(K,3)-PNTK(I,3))**2)
```

```
      DIMG1=SQRT((PNTI(I,1)-PNTI(J,1))**2+(PNTI(I,2)-PNTI(J,2))**2+
     &(PNTI(I,3)-PNTI(J,3))**2)
      DIMG2=SQRT((PNTI(J,1)-PNTI(K,1))**2+(PNTI(J,2)-PNTI(K,2))**2+
     &(PNTI(J,3)-PNTI(K,3))**2)
      DIMG3=SQRT((PNTI(K,1)-PNTI(I,1))**2+(PNTI(K,2)-PNTI(I,2))**2+
     &(PNTI(K,3)-PNTI(I,3))**2)
      WRITE(5,926)
      WRITE(5,927)I,J,DIMG1,J,K,DIMG2,K,I,DIMG3,I,J,DKMG1,J,K,DKMG2
     &,K,I,DKMG3
C
C     IF THERE ARE ANY MORE RECORDS, GO GET THEM!
C
318   KOUNT=KOUNT+1
      IF(KOUNT.LE.NREC) GO TO 500
C
C     FORMAT STATEMENTS FOR PROMPTS AND RESULTS
C
5     FORMAT('$','Enter name of joint tested [S-9]: ')
10    FORMAT(9A1)
15    FORMAT('$','Enter subject name or number [S-25]: ')
20    FORMAT(25A1)
25    FORMAT('0','Enter a description of the  test [S-80] ')
30    FORMAT(80A1)
35    FORMAT('$','Enter data file name [S-13]: ')
40    FORMAT(13A1)
45    FORMAT('$','Enter number of records to be read [N-5]: ')
50    FORMAT(I5)
51    FORMAT('$','Enter the corresponding fixed body locator file na
     &me [s-13]: ')
55    FORMAT('0','Enter the distances in centimeters along the loca
     &tor axes to the desired fixed body center :')
60    FORMAT('$',T15,'Enter the X-COORDINATE [N-8]: ')
65    FORMAT(F10.5)
66    FORMAT(F8.4)
70    FORMAT('$',T15,'Enter the Y-COORDINATE [N-8]: ')
75    FORMAT('$',T15,'Enter the Z-COORDINATE [N-8]: ')
76    FORMAT('0','Enter the coordinates of the fixed joint center
     & w.r.t. the fixed-body system:')
77    FORMAT('$','Enter the joint x-coordinate:  ')
78    FORMAT('$','Enter the joint y-coordinate:  ')
79    FORMAT('$','Enter the joint z-coordinate:  ')
80    FORMAT('0','Input a 3x3 matrix (by rows) that defines the body
     & axis system w.r.t. the locator axis system : ')
85    FORMAT('$','Enter the corresponding initializing file name [
     &S-25]: ')
88    FORMAT('$','Enter which side of the force applicator
     & faced the sensor assembly during the test [A or B]:')
100   FORMAT('0',T78,9A1,'JOINT')
105   FORMAT('0',T5,'DATE: ',9A1,/,T5,'TIME: ',8A1,/,T5,'SUBJECT
     &NAME AND NUMBER: ',25A1)
110   FORMAT(' ',T5,'DATA FILE NAME: ',13A1,/,T5,'NUMBER OF RECORDS:
     & ',I5,//,T5,'DESCRIPTION:  ',80A1)
200   FORMAT('0',165('-')/)
```

```
205  FORMAT('0',165('-'),/)
206  FORMAT(' ',165('-'),
207  FORMAT('0',165(','))
275  FORMAT('0','ERROR ON ATTEMPT TO READ LOCATOR FILE ')
280  FORMAT('0','ERROR ON ATTEMPT TO READ INITIALIZING FILE ')
285  FORMAT('0','FOUR EMITTERS ON CUFF READ ZERO-PROCEEDING TO NEXT
     & RECORD ')
287  FORMAT('0','ERROR ON ATTEMPT TO READ TRANSDUCER CALIBRATION
     & MATRIX DATA FILE!')
300  FORMAT( 0',T30,'ERROR ON ATTEMPT TO READ NEXT RECORD')
311  FORMAT('0',T20,'NOMINAL JOINT CENTER AS INITIALIZED'/)
340  FORMAT('0',/'$','Are there other files to be processed?
     $[Y/N]: ')
345  FORMAT(A4)
432  FORMAT(I2)
604  FORMAT('$',T15,'T.C(',I1,',',I1,'):[N-8]: ')
626  FORMAT('$','Enter the distance from the acromion-based emitter
     $ to the center of the humeral head [N-8]:')
628  FORMAT('$','Enter the distance from the center of the humeral
     $ head to the center of the elbow joint [N-8]:')
631  FORMAT('$','Enter the lateral distance to the long bone axis
     & [N-8]:')
702  FORMAT(1F9.1,4F9.2,11F10.2,/)
703  FORMAT(9F9.2,8F10.2,/)
704  FORMAT(12F10.2)
731  FORMAT(' ','Enter values for the nominal humeral axis orientation:')
734  FORMAT('$','Theta Nominal:  ')
732  FORMAT('$','Phi Nominal:  ')
733  FORMAT('$','Enter the "Best-Fit" sphere radius:  ')
750  FORMAT('0','F-A EMITTER IS ZERO, PROCEEDING TO NEXT RECORD!')
881  FORMAT(4F8.3)
884  FORMAT('$','Enter the output data filename for restoring
     & forces and moments [S-13]: ')
920  FORMAT(' ',T5,'INITIALIZED DISTANCES:',T63,'DISTANCES, CURRENT
     & RECORD:')
927  FORMAT(' ',3(I1,'-',I1,'=',F5.2,'    '),T60,3(I1,'-',I1,'=',
     &F5.2,'    '))
C
C    CLOSE UP DATA FILE & THAT'S ALL FOLKS!
C
2001 CLOSE (UNIT=1)
     CLOSE (UNIT=2)
     WRITE(5,207)
     WRITE(5,340)
     READ(5,345)ANS
     IF(ANS .EQ. 'N')GO TO 5000
     WRITE(5,35)
     READ(5,40) (FINAME(I),I=1,13)
     WRITE(5,45)
     READ(5,50) NREC
     WRITE(5,25)
     READ(5,30) (MESS(I),I=1,80)
     IREC=1
```

```
      NREC=1
      KOUNT=1
  557 WRITE(5,51)
      READ(5,40,ERR=557)(F2NAME(I),I=1,13)
  558 WRITE(5,884)
      READ(5,40,ERR=558)(F4NAME(I),I=1,13)
      GO TO 2000
 3000 WRITE(5,205)
      WRITE(5,275)
      GO TO 5000
 3500 WRITE(5,205)
      WRITE(5,280)
      GO TO 5000
 3700 WRITE(5,285)
      KOUNT=KOUNT+1
      IF(KOUNT.GT.NREC) GO TO 2001
      GO TO 500
 3800 WRITE(5,287)
      GO TO 500
 3900 WRITE(5,750)
      KOUNT=KOUNT+1
      GO TO 500
 4000 WRITE(5,205)
      WRITE(5,300)
      GOTO 20
 5000 WRITE(5,205)
      STOP
      END
C
C
      SUBROUTINE SPHERE(VEC,THETA,PHI)
C
C     SUBROUTINE TO CALCULATE THE SPHERICAL COORDINATES (THETA,PHI)
C     OF THE VECTOR 'VEC'.
C
      DIMENSION B(3),VEC(3)
      DATA PI/3.141592654/
      VECMAG=SQRT(VEC(1)**2+VEC(2)**2+VEC(3)**2)
      IF(VECMAG.LT.1.001) GO TO 10
      B(1)=VEC(1)/VECMAG
      B(2)=VEC(2)/VECMAG
      B(3)=VEC(3)/VECMAG
      GO TO 15
   10 B(1)=VEC(1)
      B(2)=VEC(2)
      B(3)=VEC(3)
   15 A1=SQRT(B(1)**2+B(2)**2)
      THETA=(ATAN2(A1,B(3)))*180.0/PI
      IF(THETA.LT.179.99.OR.THETA.GT.0.01) GO TO 20
      PHI=0.0
      GO TO 30
   20 PHI=(ATAN2(B(2),B(1)))*180.0/PI
   30 RETURN
```

```
      END
C
      SUBROUTINE UNITVR(VEC)
C
C     SUBROUTINE CALCULATES A UNIT VECTOR FOR ANY GIVEN VECTOR
C
      DIMENSION VEC(3)
      VECMAG=(VEC(1)**2)+(VEC(2)**2)+(VEC(3)**2)
      VECMAG=SQRT(VECMAG)
      IF(VECMAG.EQ.0.0) VECMAG=1.0
      DO 10 I=1,3
      VEC(I)=VEC(I)/VECMAG
10    CONTINUE
      RETURN
      END
C
      SUBROUTINE LOCAXS(PNTK,CASE,ERRTOT)
C
C     THIS SUBROUTINE SELECTS THE 'MOST ACCURATE' LOCAL AXIS  SYSTEM
C     BASED ON INTRA-AXIS SYSTEM DISTANCES AND RELATIVE SKEW ANGLES.
C
      DIMENSION PNTK(6,3),TIS(3,3),TISK(3,3),TJS(3,3),TJSK(3,3)
      DIMENSION TIJ(3,3),TIJK(3,3),GEN(3,3),VECI(3),VECK(3)
      DIMENSION ERRTOT(20,3),F1(3),G1(3)
      INTEGER TRIAD,CASE
      REAL JNTVEC,JTDSMG
      COMMON /AC/ PNTI(6,3),COSMAT(60,3),COSTRN(60,3),DRCOS(60,3),
     $DRCTRN(60,3),TRIAD(20,3),JNTVEC(20,3)
C
      ERRSK=0.0
      ERRDLT=0.0
C
      DO 20 MM=1,20
C
      I1=TRIAD(MM,1)
      J1=TRIAD(MM,2)
      K1=TRIAD(MM,3)
       IF(PNTK(I1,1).EQ.0.0.OR.PNTK(J1,1).EQ.0.0.OR.PNTK(K1,1).EQ.0.0)
     $ GO TO 19
C
      NN=(MM-1)*3
C
C
      DO 3 J=1,3
      TIS(1,J)=COSMAT(NN+1,J)
      TIS(2,J)=COSMAT(NN+2,J)
      TIS(3,J)=COSMAT(NN+3,J)
C
      TISK(1,J)=DRCOS(NN+1,J)
      TISK(2,J)=DRCOS(NN+2,J)
      TISK(3,J)=DRCOS(NN+3,J)
3     CONTINUE
C
```

```
      MKNT1=0
      MKNT2=0
C
      DO 10 N=1,20
      I2=TRIAD(N,1)
      J2=TRIAD(N,2)
      K2=TRIAD(N,3)
       IF(PNTK(I2,1).EQ.0.0.OR.PNTK(J2,1).EQ.0.0.OR.PNTK(K2,1).EQ.0.0)
      $ GO TO 10
      M=(N-1)*3
      IF(N.EQ.MM) GO TO 10
C
      DO 5 J=1,3
      TJS(1,J)=COSTRN(M+1,J)
      TJS(2,J)=COSTRN(M+2,J)
      TJS(3,J)=COSTRN(M+3,J)
C
      TJSK(1,J)=DRCTRN(M+1,J)
      TJSK(2,J)=DRCTRN(M+2,J)
      TJSK(3,J)=DRCTRN(M+3,J)
5     CONTINUE
C
C
      CALL GMPRD(TIS,TJS,TIJ,3,3,3)
      CALL GMPRD(TISK,TJSK,TIJK,3,3,3)
      CALL MINV(TIJK,3,D,F1,G1)
      CALL GMPRD(TIJ,TIJK,GEN,3,3,3)
      TRACE=(GEN(1,1)**2+GEN(2,2)**2+GEN(3,3)**2)
      GAM=.5*(TRACE-1.0)
      IF(GAM.GT.1.0.AND.GAM.LT.1.05) GAM=1.0
      GAM=ACOS(GAM)
      JTDSMG=SQRT((JNTVEC(N,1)**2)+(JNTVEC(N,2)**2)+(JNTVEC(N,3)
      1**2))
      GAMSIN=SIN(GAM)
      DELTAS=JTDSMG*GAMSIN
      DELTAS=DELTAS**2
      ERRSK=ERRSK+DELTAS
      MKNT1=MKNT1+1
      III=TRIAD(MM,2)
      JJJ=TRIAD(N,2)
      IF(III.EQ.JJJ) GO TO 10
C
      DO 7 L=1,3
      VECI(L)=PNTI(JJJ,L)-PNTI(III,L)
      VECK(L)=PNTK(JJJ,L)-PNTK(III,L)
7     CONTINUE
C
      VECIMG=SQRT((VECI(1)**2)+(VECI(2)**2)+(VECI(3)**2))
      VECKMG=SQRT((VECK(1)**2)+(VECK(2)**2)+(VECK(3)**2))
      DELTAD=ABS(VECKMG-VECIMG)
      DELTAD=DELTAD**2
      ERRDLT=ERRDLT+DELTAD
      MKNT2=MKNT2+1
```

```
 10   CONTINUE
C
      RMKNT1=FLOAT(MKNT1)
      RMKNT2=FLOAT(MKNT2)
      DIV1=RMKNT1*1.0
      DIV2=RMKNT2*1.0
      IF(MKNT1.NE.0) GO TO 11
      SKERR=9.999
      GO TO 12
 11   SKERR=SQRT(ERRSK/DIV1)
 12   IF(MKNT2.NE.0) GO TO 13
      DERR=9.999
      GO TO 14
 13   DERR=SQRT(ERRDLT/DIV2)
 14   ERRTOT(MM,1)=SKERR
      ERRTOT(MM,2)=DERR
      ERRTOT(MM,3)=SQRT((SKERR**2+DERR**2)/2.0)
C
      ERRSK=0.0
      ERRDLT=0.0
      GO TO 20
 19   ERRTOT(MM,1)=25.0
      ERRTOT(MM,2)=25.0
      ERRTOT(MM,3)=50.0
      ERRSK=0.0
      ERRDLT=0.0
 20   CONTINUE
C
      CASE=1
      ERTOTL=ERRTOT(1,3)
      DO 25 I=1,19
      IF(ERTOTL.LE.ERRTOT(I+1,3)) GO TO 25
      CASE=I+1
      ERTOTL=ERRTOT(I+1,3)
 25   CONTINUE
      RETURN
      END
C
C
      SUBROUTINE MOANAL(OUTPUT,VT,HT,UJT,OUTPT2)
C
      DIMENSION OUTPUT(22),OUTPT2(12),UJT(3,3),MFB(3),MJTT(3),URJT(3)
      DIMENSION FJTR(3),MJTR(3)
      REAL MFB,MJTT,MJTR,MJTRMG,MURMAG
      DATA PI/3.141592694/
C
C     CALCULATE TOTAL RESTORING MOMENT, TRANSFORM INTO JOINT SYSTEM,
C     AND FACTOR OUT COMPONENT ALONG R VECTOR
C
      MFB(1)=OUTPUT(10)+OUTPUT(13)
      MFB(2)=OUTPUT(11)+OUTPUT(14)
      MFB(3)=OUTPUT(12)+OUTPUT(15)
      CALL GMFRD(UJT,MFB,MJTT,3,3,1)
```

```
      URJT(1)=SIN(VT)*COS(HT)
      URJT(2)=SIN(VT)*SIN(HT)
      URJT(3)=COS(VT)
      CALL UNITVR(URJT)
      MURMAG=(MJTT(1)*URJT(1)+MJTT(2)*URJT(2)+MJTT(3)*URJT(3))
      OUTPT2(4)=MURMAG
      MJTR(1)=MJTT(1)-(MURMAG*URJT(1))
      MJTR(2)=MJTT(2)-(MURMAG*URJT(2))
      MJTR(3)=MJTT(3)-(MURMAG*URJT(3))
      MJTRMG=SQRT(MJTR(1)**2+MJTR(2)**2+MJTR(3)**2)
      OUTPT2(9)=MJTR(1)
      OUTPT2(10)=MJTR(2)
      OUTPT2(11)=MJTR(3)
      OUTPT2(12)=MJTRMG
      CALL UNITVR(MJTR)
      FJTR(1)=(MJTR(2)*URJT(3)-URJT(2)*MJTR(3))*(MJTRMG/1.0)
      FJTR(2)=-(MJTR(1)*URJT(3)-URJT(1)*MJTR(3))*(MJTRMG/1.0)
      FJTR(3)=(MJTR(1)*URJT(2)-URJT(1)*MJTR(2))*(MJTRMG/1.0)
      FJTRMG=SQRT(FJTR(1)**2+FJTR(2)**2+FJTR(3)**2)
      OUTPT2(5)=FJTR(1)
      OUTPT2(6)=FJTR(2)
      OUTPT2(7)=FJTR(3)
      OUTPT2(8)=FJTRMG
      RETURN
      END
C
C
      SUBROUTINE DRCMAT(A,B,C)
C
C     THIS SUBROUTINE CALCULATES THE DIRECTION COSINE MATRIX
C     FOR AN AXIS SYSTEM BASED ON TWO COPLANAR VECTORS (A and B).
C     THE RESULTING MATRIX, C, IS ORTHOGONAL AND UNITARY.
C
      DIMENSION A(3),B(3),C(3,3)
      AMAG=SQRT(A(1)**2+A(2)**2+A(3)**2)
      BMAG=SQRT(B(1)**2+B(2)**2+B(3)**2)
      C(1,1)=A(1)/AMAG
      C(1,2)=A(2)/AMAG
      C(1,3)=A(3)/AMAG
      C(2,1)=B(1)/BMAG
      C(2,2)=B(2)/BMAG
      C(2,3)=B(3)/BMAG
      C(3,1)=(C(1,2)*C(2,3))-(C(2,2)*C(1,3))
      C(3,2)=(C(1,3)*C(2,1))-(C(2,3)*C(1,1))
      C(3,3)=(C(1,1)*C(2,2))-(C(2,1)*C(1,2))
         C(2,1)=(C(3,2)*C(1,3))-(C(1,2)*C(3,3))
         C(2,2)=(C(3,3)*C(1,1))-(C(3,1)*C(1,3))
         C(2,3)=(C(3,1)*C(1,2))-(C(1,1)*C(3,2))
      DO 10 J=1,3
      CMAG=SQRT(C(J,1)**2+C(J,2)**2+C(J,3)**2)
      DO 5 I=1,3
      C(J,I)=C(J,I)/CMAG
5     CONTINUE
```

```
10    CONTINUE
      RETURN
      END
C
      SUBROUTINE RESULT(R,OUTPUT)
C
C
      DIMENSION R(3),X(3),Y(3),Z(3),MOMXTR(3),MOMYTR(3),MOMZTR(3)
      DIMENSION FRCBD(3),PMOMBD(3),MOMBD(3),MOMTBD(3),OUTPUT(22)
      REAL MOMXTR,MOMYTR,MOMZTR,MOMBD,MOMTBD
      COMMON /BC/ FRCTRN(6),TRNAX(3,3)
      DO 7 J=1,3
      X(J)=FRCTRN(1)*TRNAX(1,J)
      Y(J)=FRCTRN(2)*TRNAX(2,J)
      Z(J)=FRCTRN(3)*TRNAX(3,J)
      MOMXTR(J)=FRCTRN(4)*TRNAX(1,J)
      MOMYTR(J)=FRCTRN(5)*TRNAX(2,J)
      MOMZTR(J)=FRCTRN(6)*TRNAX(3,J)
7     CONTINUE
      DO 8 I=1,3
      FRCBD(I)=X(I)+Y(I)+Z(I)
      OUTPUT(5+I)=FRCBD(I)
      PMOMBD(I)=MOMXTR(I)+MOMYTR(I)+MOMZTR(I)
      OUTPUT(9+I)=PMOMBD(I)
8     CONTINUE
      CALL CRSPRD(R,FRCBD,MOMBD)
      DO 9 I=1,3
      MOMTBD(I)=PMOMBD(I)+MOMBD(I)
      OUTPUT(12+I)=MOMBD(I)
9     CONTINUE
      OUTPUT(9)=SQRT((FRCBD(1)**2)+(FRCBD(2)**2)+(FRCBD(3)**2))
      OUTPUT(16)=SQRT((MOMTBD(1)**2)+(MOMTBD(2)**2)+(MOMTBD(3)**2))
      RETURN
      END
C
C
      SUBROUTINE CRSPRD(R,F,OUT)
C
      DIMENSION R(3),F(3),OUT(3)
      OUT(1)=(R(2)*F(3))-(R(3)*F(2))
      OUT(2)=(R(3)*F(1))-(R(1)*F(3))
      OUT(3)=(R(1)*F(2))-(R(2)*F(1))
      RETURN
      END
C
C
      SUBROUTINE FORPT(PNTG,GUNSD,PTAPP,PTAXIS)
C
C     SUBROUTINE TO CALCULATE THE POINT OF FORCE APPLICATION
C     AND THE AXIS SYSTEM OF THE FORCE APPLICATOR
C
      DIMENSION PTAPP(3),NORMAL(3),PT1PT2(3),PT2PT3(3)
      DIMENSION PTAXIS(3,3),X(3),Y(3),PNTG(3,3)
```

```
      REAL NORMAL,NORLEN
      INTEGER GUNSD
      DO 10 I=1,3
              PT1PT2(I)=PNTG(2,I)-PNTG(1,I)
              PT2PT3(I)=PNTG(3,I)-PNTG(2,I)
10    CONTINUE
      P12MAG=SQRT(PT1PT2(1)**2+PT1PT2(2)**2+PT1PT2(3)**2)
      P23MAG=SQRT(PT2PT3(1)**2+PT2PT3(2)**2+PT2PT3(3)**2)
      P12DIF=ABS(P12MAG-12.90)
      P23DIF=ABS(P23MAG-9.10)
      DOT123=PT1PT2(1)*PT2PT3(1)+PT1PT2(2)*PT2PT3(2)+PT1PT2(3)*
     *PT2PT3(3)
      THA=(ACOS(DOT123/(P12MAG*P23MAG)))*57.2958
      THADIF=ABS(90-THA)
      IF(P12DIF.GT.0.30) WRITE(5,40)P12DIF
      IF(P23DIF.GT.0.30) WRITE(5,45)P23DIF
      IF(THADIF.GT.5.0) WRITE(5,50)THADIF
      CALL CRSPRD(PT1PT2,PT2PT3,NORMAL)
      IF(GUNSD .EQ. 'A')GOTO 15
      NORMAL(1)=-1.0*NORMAL(1)
      NORMAL(2)=-1.0*NORMAL(2)
      NORMAL(3)=-1.0*NORMAL(3)
15    NORLEN=SQRT(PT2PT3(1)**2+PT2PT3(2)**2+PT2PT3(3)**2)*0.5
      CALL UNITVR(NORMAL)
      DO 20 I=1,3
              NORMAL(I)=NORMAL(I)*NORLEN
              PT2PT3(I)=PT2PT3(I)*0.5+PNTG(2,I)
              PTAPP(I)=NORMAL(I)+PT2PT3(I)
              X(I)=PNTG(2,I)-PTAPP(I)
              Y(I)=PNTG(3,I)-PTAPP(1)
20    CONTINUE
      CALL UNITVR(PT1PT2)
      CALL UNITVR(X)
      CALL UNITVR(Y)
      IF(GUNSD.EQ.'B') GO TO 25
      DO 23 I=1,3
      Y(I)=-1.0*Y(I)
23    CONTINUE
25    DO 30 I=1,3
              PTAPP(I)=PTAPP(I)+PT1PT2(I)*30.0
              PTAXIS(1,I)=-X(I)
              PTAXIS(2,I)=Y(I)
              PTAXIS(3,I)=-PT1PT2(I)
30    CONTINUE
40    FORMAT('0','P12 discrepancy is:',F6.3)
45    FORMAT('0','P23 discrepancy is:',F6.3)
50    FORMAT('0','Cross product discrepancy is:',F6.3,'degrees')
      RETURN
      END
C
```

```
      PROGRAM CALEXP
C
C     THIS PROGRAM USES JOINT ENVELOPE DATA TO CALCULATE THE JOINT
C     SINUS EXPANSION IN THE SAME FORM AS FOUND IN THE CALSPAN ATB
C     MODEL. THE SAME PROCEDURE IS FOLLOWED AS IN THE BAYLOR BIO-
C     STEREOMETRIC LABORATORY REPORT.
C
      EXTERNAL FFCT
      DIMENSION JINAME(9),OUTDAT(120,2),DATA(72,4)
      DIMENSION PTMAT(72,3),U1(4),U2(3),PTS(72,3),ANG(72,2)
      DIMENSION WORK(66),P(11),DATI(72,2),COEF(10)
      INTEGER YES,ANS1,ANS2,ANS3,ANS4,ANS5
      LOGICAL*1 SNAME(25),MESS(80),FNAME(25),F2NAME(13),F3NAME(13)
        LOGICAL*1 F4NAME(25)
      DOUBLE PRECISION DATI,WORK,PI,P,WGT,HTRAD,VTRAD,COEF
      DOUBLE PRECISION DARG1,DARG2,DARG3,DARG4
      DATA IREC/1/PI/3.14159265358979310D0/COEF/10*0.0D0/
      DATA YES/'Y'/N/'N'/JREC/1/F/11*0.0D0/WORK/66*0.0D0/
C
510   WRITE(5,15)
      READ(5,20,ERR=510) (SNAME(I),I=1,25)
515   WRITE(5,25)
      READ(5,30,ERR=515) (MESS(I),I=1,80)
520   WRITE(5,35)
      READ(5,20,ERR=520) (FNAME(I),I=1,25)
521   WRITE(5,220)
      READ(5,221,ERR=521)EPS
      IF(EPS.EQ.0.0) EPS=0.0005
522   WRITE(5,230)
      READ(5,221,ERR=522)ETA
      IF(ETA.EQ.0.0) ETA=0.0005
      WRITE(5,1)
1     FORMAT('$ENTER X-TRANSLATION FOR THE F. B. C. ! [F9.6]:')
      READ(5,221) XTRANS
      WRITE(5,2)
2     FORMAT('$ENTER Y-TRANSLATION FOR THE F. B. C. ! [F9.6]:')
      READ(5,221) YTRANS
      WRITE(5,3)
3     FORMAT('$ENTER Z-TRANSLATION FOR THE F. B. C. ! [F9.6]:')
      READ(5,221) ZTRANS
523   WRITE(5,241)
      READ(5,242,ERR=523)ANS1
600   WRITE(5,300)
      READ(5,242,ERR=600)ANS2
      IF(ANS2.NE.YES) GO TO 620
610   WRITE(5,310)
      READ(5,40,ERR=610)(F2NAME(I),I=1,13)
620   WRITE(5,320)
      READ(5,242,ERR=620)ANS3
      IF(ANS3.NE.YES) GO TO 640
630   WRITE(5,330)
      READ(5,40,ERR=630)(F3NAME(I),I=1,13)
640    WRITE(5,340)
```

```
340   FORMAT('$','DO YOU WISH TO CREATE A DATA FILE CONTAINING EXPANSIO
     +N COEFFICIENTS? [Y/N]:')
      READ(5,242,ERR=640) ANS4
      IF(ANS4.NE.YES) GOTO 42
650   WRITE(5,350)
350   FORMAT('$','ENTER THE OUTPUT FILE NAME FOR EXPANSION COEFFICIENTS
     +! [S-25]:')
      READ(5,20,ERR=650) (F4NAME(I),I=1,25)
C
C     LOCATE, IDENTIFY, AND ACCESS THE DATA FILE
C
42    CALL ASSIGN(1,FNAME,25)
      KN=0
      DO 50 I=1,72
      READ(1,820,END=51,ERR=525)(DATA(I,J),J=1,4)
      IF(DATA(I,1).EQ.0.0) GO TO 50
      KN=KN+1
      PTMAT(KN,1)=DATA(I,2)-XTRANS
      PTMAT(KN,2)=DATA(I,3)-YTRANS
      PTMAT(KN,3)=DATA(I,4)-ZTRANS
50    CONTINUE
51    CLOSE (UNIT=1)
      GO TO 52
525   WRITE(5,2000)
      GO TO 2001
C
C     FIT THE DATA TO A 'BEST-FIT' SPHERE IN SPACE.
C
52    CALL SPHFIT(PTMAT,U1,ANG,PTS,KN)
C
C     USE THE JOINT SINUS OUTLINE ON THE SPHERE TO CALCULATE THE
C     NORMAL (DEFINED BY THETA AND PHI) OF THE 'BEST-FIT' PLANE TO
C     THESE POINTS.
C
      CALL PLAFIT(PTS,U2,KN,THETA,PHI)
C
C     FROM THIS NORMAL, CALCULATE RELATIVE THETA AND PHI ANGLES FOR
C     THE SINUS OUTLINE POINTS.
C
      VC=THETA
      HC=PHI
      VCRAD=VC*PI/180.00
      HCRAD=HC*PI/180.00
      DO 100 I=1,KN
      VO=ANG(I,1)
      HO=ANG(I,2)
      IF(HO.LT.-170.0) HO=HO+360.00
      VORAD=VO*PI/180.00
      HORAD=HO*PI/180.00
      ARG1=(SIN(VORAD)*SIN(HORAD-HCRAD))
      ARG2=(SIN(VORAD)*COS(VCRAD)*COS(HORAD-HCRAD)-COS(VORAD)*
     *SIN(VCRAD))
      ARG3=(COS(VORAD)*COS(VCRAD)+SIN(VORAD)*SIN(VCRAD)*COS(HORAD
```

```
     &-HCRAD))
      DARG1=DBLE(ARG1)
      DARG2=DBLE(ARG2)
      DARG3=DBLE(ARG3)
      HTRAD=ATAN2(DARG1,DARG2)
      DARG4=DSQRT(DARG1**2+DARG2**2)
      VTRAD=ATAN2(DARG4,DARG3)
      DATI(I,2)=VTRAD
      IF(HTRAD.LT.0.000) HTRAD=HTRAD+2.0D0*PI
      DATI(I,1)=HTRAD
  100 CONTINUE
C
C     COMPUTE THE EXPANSION COEFFICIENTS FOR THE JOINT SINUS.
C
      CALL DAFLL(FFCT,KN,10,F,WORK,DATI,IER)
      CALL DAPFS(WORK,10,IRES,-1,EPS,ETA,IER)
D     DO 104 I=1,KN
D104  DATI(I,1)=DATI(I,1)*180.00/PI
      NN=IRES-1
      M=NN*(NN+1)/2
      DO 105 I=1,IRES
105   COEF(I)=WORK(M+I)
C
C     WRITE THE OUTPUT DATA TO DISK
C
      IF(ANS2.NE.YES)GO TO 109
      CALL ASSIGN (1,F2NAME,13)
      CALL OUTPUT(COEF,OUTDAT,KN)
      DO 106 I=1,120
      WRITE (1,700)OUTDAT(I,1),OUTDAT(I,2)
D     TYPE *,'PHI,THETA(CALC.)=',OUTDAT(I,1),OUTDAT(I,2)
106   CONTINUE
      CLOSE (UNIT=1)
C
C     WRITE RHO-GAMMA DATA TO DISK
C
109    IF(ANS3.NE.YES) GOTO 111
      CALL ASSIGN(1,F3NAME,13)
      DO 107 I=1,KN
      WRITE(1,700)DATI(I,1),DATI(I,2)
107   CONTINUE
      CLOSE (UNIT=1)
      WRITE(5,146) KN,(F3NAME(IJ),IJ=1,13)
146   FORMAT('0',I5,'  RECORDS OF (PHI,THETA) RAW DATA',
     1          ' WERE OUTPUT TO FILE',5X,13A1)
111    IF(ANS4.NE.YES) GOTO 108
       CALL ASSIGN(1,F4NAME,25)
       WRITE(1,701) (COEF(J),J=1,10)
701    FORMAT(2E20.10)
       CLOSE (UNIT=1)
C
C     WRITE OUT THE DESIRED DATA
C
```

```
108   WRITE(5,110)SNAME
      WRITE(5,115)MESS
      WRITE(5,118)
118   FORMAT('0','  F. B. C. TRANSLATIONS:')
      WRITE(5,125) XTRANS,YTRANS,ZTRANS
      WRITE(5,120)
      WRITE(5,125)U1(1),U1(2),U1(3),U1(4)
      WRITE(5,130)VC,HC
      WRITE(5,133)IER
      WRITE(5,135)IRES,EPS,ETA
      WRITE(5,140)(COEF(I),I=1,10)
      IF(ANS1.NE.YES) GO TO 2001
      WRITE(5,145)
      WRITE(5,150)(ANG(I,1),ANG(I,2),DATI(I,1)
     &,DATI(I,2),I=1,NN)
C
C     FORMAT STATEMENTS FOR PROMPTS AND RESULTS
C
5     FORMAT('$','Enter the name of the Joint tested. [S-9]:')
10    FORMAT(9A1)
15    FORMAT('$','Enter the subject name or number. [S-25]:')
20    FORMAT(25A1)
25    FORMAT('$','Comments on, or description of test. [S-80]:')
30    FORMAT(80A1)
35    FORMAT('$','Enter the input data file name. [S-25]:')
40    FORMAT(13A1)
241   FORMAT('$','Do you want sinus data in terms of theta-phi and
     & rho-gamma coordinates issued as output? [Y/N]:')
242   FORMAT(A4)
110   FORMAT('0','Shoulder Joint Sinus Analysis for Subject:',25A1)
115   FORMAT(' ','Comments:',80A1//165('_'))
120   FORMAT('0  Joint Center Coordinates:',T50,'Sphere Avg. Radius')
125   FORMAT(1X,F7.3,2F9.3,T54,F8.3)
130   FORMAT('0','Orientation of Normal for "Best-Fit" Plane'/T16,
     &'Theta',T27,'Phi'/T14,F7.2,T24,F7.2)
133   FORMAT('0','"IER"=',T9,I2)
135   FORMAT('0','Expansion Coefficients for "Ires"=',I38,I3,
     &T48,'EPS=',T53,E9.2,T68,'ETA=',T73,E9.2/T11,'A1',
     &T28,'A2',T44,'A3',T60,'A4',T76,'A5',T92,'A6',T108,'A7',T124,'A
     &8',T140,'A9',T156,'A10'/)
140   FORMAT(10E16.5)
145   FORMAT('0','Sinus Data in terms of Theta-Phi Coordinates and
     & 2-D Coordinates:'/T10,'Theta-Phi W.R.T. Body',
     & T60,'Joint System Coords.'/)
150   FORMAT(T11,2F8.2,T60,2F8.2)
220   FORMAT('$','Select EPS (between 1.E-3 and 1.E-6) [F9.6]:')
221   FORMAT(F9.6)
230   FORMAT('$','Select ETA (between 1.E0 and 1.E-6) [F9.6]:')
300   FORMAT('$','Do you wish to create an output data file ',
     +   'FOR THE BEST-FIT FUNCTION VALUES? [Y/N]:')
310   FORMAT('$','Enter the output data file name! [S-13]:')
320   FORMAT('$','Do you wish to create a data file containing
     & rho-gamma coordinates? [Y/N]:')
```

```
330   FORMAT('$','Enter the output file name for rho-seams data!
     & [S-13]:')
700   FORMAT(F10.5,',',F10.5)
820   FORMAT(4F8.3)
2000  FORMAT('$','ERROR ON ATTEMPT TO READ DATA FILE!')
2001  WRITE(5,99)
99    FORMAT('$ARE THERE OTHER FILES TO BE PROCESSED ! [Y/N]:')
      READ(5,242) ANSS
      IF(ANSS.EQ.YES) GO TO 510
      STOP
      END
C
C
C
      SUBROUTINE SPHFIT(PTMAT,U,ANG,PTS,KN)
C
C     THIS SUBROUTINE CALCULATES THE "BEST FIT" SPHERE TO A SET
C     OF DATA POINTS AND THEN OUTPUTS INFORMATION ON THE SPHERE
C     AND ON THE REVISED DATA SET.
C
      DIMENSION PTMAT(72,3),P(72),U(4),PTS(72,3)
      DIMENSION ANG(72,2),PVEC(3),GIG(4,4),F1(4),GI(4)
      DIMENSION G(72,4),GI(4,72),GG(4,72),MIN(3)
      DATA P/72*1.0/
C
C
      XMIN=PTMAT(1,1)
      YMIN=PTMAT(1,2)
      ZMIN=PTMAT(1,3)
      DO 50 I=1,KN
      IF(PTMAT(I,1).LT.XMIN) XMIN=PTMAT(I,1)
      IF(PTMAT(I,2).LT.YMIN) YMIN=PTMAT(I,2)
      IF(PTMAT(I,3).LT.ZMIN) ZMIN=PTMAT(I,3)
50    CONTINUE
      MIN(1)=ABS(XMIN)+1.0
      MIN(2)=ABS(YMIN)+1.0
      MIN(3)=ABS(ZMIN)+1.0
      DO 75 J=1,KN
      PTS(J,1)=PTMAT(J,1)+MIN(1)
      PTS(J,2)=PTMAT(J,2)+MIN(2)
      PTS(J,3)=PTMAT(J,3)+MIN(3)
      DIV1=((PTS(J,1)**2)+(PTS(J,2)**2)+(PTS(J,3)**2))
      G(J,1)=(2.0*PTS(J,1))/DIV1
      G(J,2)=(2.0*PTS(J,2))/DIV1
      G(J,3)=(2.0*PTS(J,3))/DIV1
      G(J,4)=(-1.0)/DIV1
      GI(1,J)=G(J,1)
      GI(2,J)=G(J,2)
      GI(3,J)=G(J,3)
      GI(4,J)=G(J,4)
75    CONTINUE
      DO 80 I=1,4
      DO 80 K=1,4
```

```
      GTG(I,K)=0.0
      GTGN=0.0
      DO 10 J=1,KN
      GTGN=GTG(I,J)*G(J,K)
      GTG(I,K)=GTG(I,K)+GTGN
   10 CONTINUE
   20 CONTINUE
   30 CONTINUE
      CALL MINV(GTG,4,D,IP,GI)
      DO 130 I=1,4
      DO 120 K=1,KN
      GG(I,K)=0.0
      GGN=0.0
      DO 110 J=1,4
      GGN=GTG(I,J)*GI(J,K)
      GG(I,K)=GG(I,K)+GGN
  110 CONTINUE
  120 CONTINUE
  130 CONTINUE
      DO 230 I=1,4
      U(I)=0.0
      UN=0.0
      DO 220 J=1,KN
      UN=GG(I,J)*P(J)
      U(I)=U(I)+UN
  220 CONTINUE
  230 CONTINUE
      R=SQRT(((U(1)**2)+(U(2)**2)+(U(3)**2))-U(4))
C     TYPE *,'R=',R
      DO 80 I=1,KN
      PTS(I,1)=PTS(I,1)-U(1)
      PTS(I,2)=PTS(I,2)-U(2)
      PTS(I,3)=PTS(I,3)-U(3)
      PTMAG=SQRT((PTS(I,1)**2)+(PTS(I,2)**2)+(PTS(I,3)**2))
      PVEC(1)=PTS(I,1)/PTMAG
      PVEC(2)=PTS(I,2)/PTMAG
      PVEC(3)=PTS(I,3)/PTMAG
      CALL SPHERE(PVEC,THETA,PHI)
      ANG(I,1)=THETA
      ANG(I,2)=PHI
      PTS(I,1)=PVEC(1)*R
      PTS(I,2)=PVEC(2)*R
      PTS(I,3)=PVEC(3)*R
   80 CONTINUE
      DO 85 I=1,KN
C     TYPE *,'THETA-PHI=',ANG(I,1),ANG(I,2)
   85 CONTINUE
      U(1)=U(1)-MIN(1)
      U(2)=U(2)-MIN(2)
      U(3)=U(3)-MIN(3)
      U(4)=R
C     TYPE *,'U=',U(1),U(2),U(3),U(4)
      RETURN
```

```
      END
C
C
C
      SUBROUTINE PLAFIT(PTS,D,KN,THETA,PHI)
C
C     THIS SUBROUTINE CALCULATES THE "BEST FIT" PLANE TO A SET OF
C     DATA POINTS AND THEN OUTPUTS INFORMATION ON THE OUTWARD
C     NORMAL TO THAT PLANE.
C
      DIMENSION PTS(72,2),GTG(3,3),D(3),F(72)
      DIMENSION G(72,3),GT(3,72),F1(3),G1(3),GG(3,72)
      DATA F/72*1.0/
C
      XMIN=PTS(1,1)
      YMIN=PTS(1,2)
      ZMIN=PTS(1,3)
      DO 100 I=1,KN
      IF(PTS(I,1).LT.XMIN) XMIN=PTS(I,1)
      IF(PTS(I,2).LT.YMIN) YMIN=PTS(I,2)
      IF(PTS(I,3).LT.ZMIN) ZMIN=PTS(I,3)
100   CONTINUE
      DO 125 J=1,KN
      G(J,1)=PTS(J,1)+ABS(XMIN)+1.0
      G(J,2)=PTS(J,2)+ABS(YMIN)+1.0
      G(J,3)=PTS(J,3)+ABS(ZMIN)+1.0
      GT(1,J)=G(J,1)
      GT(2,J)=G(J,2)
      GT(3,J)=G(J,3)
125   CONTINUE
      DO 30 I=1,3
      DO 20 K=1,3
      GTG(I,K)=0.0
      GTGN=0.0
      DO 10 J=1,KN
      GTGN=GT(I,J)*G(J,K)
      GTG(I,K)=GTG(I,K)+GTGN
10    CONTINUE
20    CONTINUE
30    CONTINUE
      CALL MINV(GTG,3,D,F1,G1)
      DO 130  I=1,3
      DO 120 K=1,KN
      GG(I,K)=0.0
      GGN=0.0
      DO 110 J=1,3
      GGN=GTG(I,J)*GT(J,K)
      GG(I,K)=GG(I,K)+GGN
110   CONTINUE
120   CONTINUE
130   CONTINUE
      DO 250 I=1,3
      D(I)=0.0
```

```
      UN=0.0
      DO 220 J=1,NN
      UN=UG(I,J)*F(J)
      U(I)=U(I)+UN
  220 CONTINUE
  230 CONTINUE
      DIV2=SQRT((U(1)**2)+(U(2)**2)+(U(3)**2))
      U(1)=U(1)/DIV2
      U(2)=U(2)/DIV2
      U(3)=U(3)/DIV2
    2 TYPE *,'U PLANE NORMAL=',U(1),U(2),U(3)
      CALL SPHERE(U,THETA,PHI)
      RETURN
      END
C
C
C
      SUBROUTINE FFCT(I,N,IP,F,DATI,WGT,IER)
C
C     THIS SUBROUTINE DEFINES THE BASIS FUNCTIONS FOR THE JOINT
C     SINUS EXPANSION, AND CALCULATES THEIR VALUES FOR GIVEN
C     VALUES OF 'GAMMA'.
C
      DIMENSION F(11),DATI(72,2),IER(1)
      DOUBLE PRECISION DATI,WGT,F,GAM
C
C             CHECK FOR FORMAL ERRORS IN SPECIFIED DIMENSIONS
      IF(N)10,10,1
    1 IF(N.GT.72) GO TO 10
      IF(IP)10,10,2
    2 IF(IP.GT.10) GO TO 10
C
      IER(1)=0
      WGT=1.D0
      GAM=DATI(I,1)
      F(1)=1.D0
      F(2)=DSIN(GAM)
      F(3)=DCOS(GAM)
      F(4)=(DSIN(GAM))*(DCOS(GAM))
      F(5)=(DCOS(GAM))**2
      F(6)=(DSIN(GAM))*((DCOS(GAM))**2)
      F(7)=(DCOS(GAM))**3
      F(8)=(DSIN(GAM))*((DCOS(GAM))**3)
      F(9)=(DCOS(GAM))**4
      F(10)=(DSIN(GAM))*((DCOS(GAM))**4)
      F(11)=DATI(I,2)
      GO TO 15
   10 IER(1)=1
   15 RETURN
      END
C
C
C
```

```
      SUBROUTINE SPHERE(B,THETA,PHI)
C
C     SUBROUTINE TO CALCULATE THE SPHERICAL COORDINATES (THETA,PHI)
C     OF THE UNIT VECTOR B.
C
      DIMENSION B(3)
      DATA PI/3.141592654/
      A1=SQRT(B(1)**2+B(2)**2)
      THETA=(ATAN2(A1,B(3)))*180.0/PI
      IF(THETA.LT.179.99.OR.THETA.GT.0.01) GO TO 10
      PHI=0.0
      GO TO 20
10    PHI=(ATAN2(B(2),B(1)))*180.0/PI
20    RETURN
      END
C
C
      SUBROUTINE OUTPUT(COEF,OUTDAT,KN)
C
      DIMENSION COEF(10),OUTDAT(120,2),R(10)
      INTEGER EX(10,2)
      DOUBLE PRECISION COEF,PI,DEG2,R,GAM,RT,RX,RY
      DATA PI/3.14159265358979310/
      DATA EX/0,1,0,1,0,1,0,1,0,1,0,0,1,1,2,2,3,3,4,4/
      DEG3=3.0D0*(PI/180.0D0)
      GAM=0.0D0
      DO 35 J=1,120
      GAM=GAM+DEG3
      DO 15 I=1,10
      N=EX(I,1)
      M=EX(I,2)
      R(I)=COEF(I)*(DSIN(GAM)**N)*(DCOS(GAM)**M)
15    CONTINUE
      RT=R(1)+R(2)+R(3)+R(4)+R(5)+R(6)+R(7)+R(8)+R(9)+R(10)
      OUTDAT(J,1)=SNGL(GAM)
      OUTDAT(J,2)=SNGL(RT)
35    CONTINUE
      RETURN
      END
```

REFERENCES

Beckett, R. and Chang, K. (1968) An Evaluation of the Kinematics of Gait by Energy. Journal of Biomechanics, Vol. 1, pp. 147-159.

Berzteiss, A.T. (1964) "Least-Squares Fitting of Polynomials to Irregularly Spaced Data," SIAM Review, Vol. 6, No. 3, pp. 203-227.

Chao, E.Y.S., et al. (1970) The Application of 4 x 4 Matrix Methods to the Correction of the Measurements of Hip Joint Rotations. Journal of Biomechanics, Vol. 2, pp. 459-471.

Chao, E.Y. and Morrey, B.F. (1978) Three-Dimensional Rotation of the Elbow. Journal of Biomechanics, Vol. 11, pp. 57-73.

Chao, E.Y., An, K.N., Askew, L.J., and Morrey, B.F. (1980) Electrogoniometer for the Measurement of Human Elbow Joint Rotation. Journal of Biomechanical Engineering, Vol. 102, pp. 301-310.

Clayson, S.J., et al. (1966) Goniometer Adaptation for Measuring Hip Extension. Archives of Physical Medicine, Vol. 47, pp. 255-261.

Dempster, S.T. (1955) The Anthropometry of Body Motion. Annals New York Academy of Sciences, Vol. 63, pp. 559-585.

Dempster, S.T. (1965) Mechanism of Shoulder Movement. Arch. Phys. Med. Rehab. (46), pp. 49-70.

Engin, A.E. (1980) On the Biomechanics of the Shoulder Complex. Journal of Biomechanics, Vol. 13, No. 7, pp. 575-590.

Engin, A.E. (1984) On the Damping Properties of the Shoulder Complex. Journal of Biomechanical Engineering, Vol. 106, pp. 360-363.

Engin, A.E., Peindl, R.D., Berme, N., and Kaleps, I. (1984a) Kinematic and Force Data Collection in Biomechanics by Means of Sonic Emitters - I: Kinematic Data Collection Methodology. Journal of Biomechanical Engineering, Vol. 106, pp. 204-211.

Engin, A.E., Peindl, R.D., Berme, N., and Kaleps, I. (1984b) Kinematic and Force Data Collection in Biomechanics by Means of Sonic Emitters - II: Force Data Collection and Application to the Human Shoulder Complex. Journal of Biomechanical Engineering, Vol. 106, pp. 212-219.

Engin, A.E. and Peindl, R.D. (1985) "Passive Resistive and Damping Properties of Human Shoulder Complex," AFAMRL-TR-84-051.

Engin, A.E. and Peindl, R.D. (1986) On the Biomechanics of Human Shoulder Complex - I: Kinematics for Determination of the Shoulder Complex Sinus. Journal of Biomechanics, Vol. 19, (in print).

Fleck, J.T. (1975) Calspan 3-D Crash Victim Simulation Program. Proceedings Symposium on Aircraft Crashworthiness, University Press of Virginia, Charlottesville.

Gray's Anatomy (1973) 35th British edition (edited by Warwick, R. and Williams, P.L.), W.B. Saunders, Philadelphia.

Hatze, H. (1980) A Mathematical Model for the Computational Determination of Parameter Values of Anthropomorphic Segments. Journal of Biomechanics, Vol. 13, No. 10, pp. 833-843.

Herron, R.E. (1974) Experimental Determination of Mechanical Features of Children and Adults. D.O.T. Report, No. DOT-HS-231-2-397.

Huston, R.L., Hessel, R.E., and Passerello, C.E. (1974) A Three-Dimensional Vehicle-Man Model for Collision and High Acceleration Studies. SEA Paper No. 740275.

Johnston, R.C. and Smidt, G.L. (1969) Measurement of Hip Joint Motion during Motion Walking. The Journal of Bone and Joint Surgery, Vol. 51-A, pp. 1083-1094.

King, A.I. and Chou, C.C. (1976) Mathematical Modeling, Simulation and Experimental Testing of Biomechanical System Crash Response. Journal of Biomechanics, Vol. 9, pp. 301-317.

Kreyszig, E., (1972) Advanced Engineering Mathematics, 3rd Edition, John Wiley and Sons, Inc.

Lamoreux, L.W. (1971) Kinematic Measurements in the Study of Human Walking. Bulletin of Prosthetics Research, pp. 3-84.

McConville, J.T., Churchill, T.D., Kaleps, I., Clauser, C.E., and Cuzzi, J., (1980) "Anthropometric Relationships of Body Segments and Body Segment Moments of Inertia." AFAMRL Report, No. TR-80-119, December 1980.

Neter, J., Wasserman, W., and Kutner, M.H. (1985) Applied Linear Statistical Models. Second Edition, Richard D. Irwin, Inc., Homewood, Illinois.

Norkin, C.C. and Levangie, P.K. (1983) Joint Structure and Function: A Comprehensive Analysis, F.A. Davis Company, Philadelphia.

Paul, J.P. (1965) Forces Transmitted by Joints in the Human Body. Proceedings of the Institution of Mechanical Engineers, Vol. 181, pp. 369-380.

Robbins, D.H., Bennett, R.O., and Bowman, B.M. (1972) User-Oriented Mathematical Crash Victim Simulator. Proceedings of the 16th Strapp Car Crash Conference, pp. 128-148.

SAS User's Guide, 1982 Edition. SAS Institute Inc., Cary, North Carolina.

Saunders, J.B., Inman, V.T., and Eberhart, H.D., (1953) The Major Determination in Normal and Pathological Gait. The Journal of Bone and Joint Surgery, Vol. 35-A, pp. 75-96.

Steindler, A. (1973) Kinesiology of the Human Body. Publisher: Charles C. Thomas, Springfield, Illinois.

Suh, C.H. and Radcliffe, C.W. (1978) Kinematics and Mechanisms Design. John Wiley and Sons, Inc.

Youm, Y., Dryer, R.F., Thambyrajah, K., Flatt, A.E., and Sprague, B.L. (1979) Biomechanical Analyses of Forearm Pronation - Supination and Elbow Flexion-Extension. Journal of Biomechanics, Vol. 12, pp. 245-255.

Young, R.D. (1970) A Three-Dimensional Mathematical Model of an Automobile Passenger. Texas Transportation Institute Research Report 140-2.

U.S. GOVERNMENT PRINTING OFFICE 1987 - 748-001/60749